frontiers | Research Topics

# Recent advances in pheochromocytoma and paraganglioma: molecular pathogenesis, clinical impacts, and therapeutic perspective, volume II

**Edited by**
Farhadul Islam, Ichiro Abe and Suja Pillai

**Published in**
Frontiers in Endocrinology

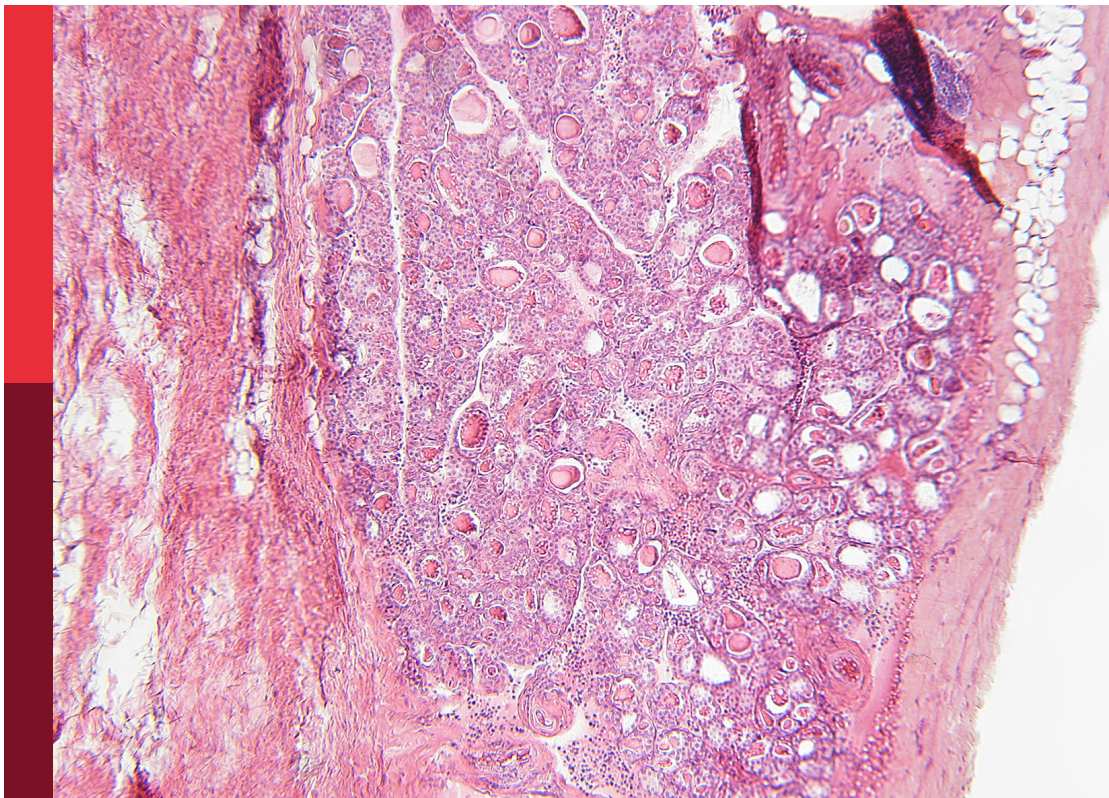

FRONTIERS EBOOK COPYRIGHT STATEMENT

The copyright in the text of individual articles in this ebook is the property of their respective authors or their respective institutions or funders. The copyright in graphics and images within each article may be subject to copyright of other parties. In both cases this is subject to a license granted to Frontiers.

The compilation of articles constituting this ebook is the property of Frontiers.

Each article within this ebook, and the ebook itself, are published under the most recent version of the Creative Commons CC-BY licence. The version current at the date of publication of this ebook is CC-BY 4.0. If the CC-BY licence is updated, the licence granted by Frontiers is automatically updated to the new version.

When exercising any right under the CC-BY licence, Frontiers must be attributed as the original publisher of the article or ebook, as applicable.

Authors have the responsibility of ensuring that any graphics or other materials which are the property of others may be included in the CC-BY licence, but this should be checked before relying on the CC-BY licence to reproduce those materials. Any copyright notices relating to those materials must be complied with.

Copyright and source acknowledgement notices may not be removed and must be displayed in any copy, derivative work or partial copy which includes the elements in question.

All copyright, and all rights therein, are protected by national and international copyright laws. The above represents a summary only. For further information please read Frontiers' Conditions for Website Use and Copyright Statement, and the applicable CC-BY licence.

ISSN 1664-8714
ISBN 978-2-8325-6347-2
DOI 10.3389/978-2-8325-6347-2

## About Frontiers

Frontiers is more than just an open access publisher of scholarly articles: it is a pioneering approach to the world of academia, radically improving the way scholarly research is managed. The grand vision of Frontiers is a world where all people have an equal opportunity to seek, share and generate knowledge. Frontiers provides immediate and permanent online open access to all its publications, but this alone is not enough to realize our grand goals.

## Frontiers journal series

The Frontiers journal series is a multi-tier and interdisciplinary set of open-access, online journals, promising a paradigm shift from the current review, selection and dissemination processes in academic publishing. All Frontiers journals are driven by researchers for researchers; therefore, they constitute a service to the scholarly community. At the same time, the *Frontiers journal series* operates on a revolutionary invention, the tiered publishing system, initially addressing specific communities of scholars, and gradually climbing up to broader public understanding, thus serving the interests of the lay society, too.

## Dedication to quality

Each Frontiers article is a landmark of the highest quality, thanks to genuinely collaborative interactions between authors and review editors, who include some of the world's best academicians. Research must be certified by peers before entering a stream of knowledge that may eventually reach the public - and shape society; therefore, Frontiers only applies the most rigorous and unbiased reviews. Frontiers revolutionizes research publishing by freely delivering the most outstanding research, evaluated with no bias from both the academic and social point of view. By applying the most advanced information technologies, Frontiers is catapulting scholarly publishing into a new generation.

## What are Frontiers Research Topics?

Frontiers Research Topics are very popular trademarks of the *Frontiers journals series*: they are collections of at least ten articles, all centered on a particular subject. With their unique mix of varied contributions from Original Research to Review Articles, Frontiers Research Topics unify the most influential researchers, the latest key findings and historical advances in a hot research area.

Find out more on how to host your own Frontiers Research Topic or contribute to one as an author by contacting the Frontiers editorial office: frontiersin.org/about/contact

# Recent advances in pheochromocytoma and paraganglioma: molecular pathogenesis, clinical impacts, and therapeutic perspective, volume II

**Topic editors**

Farhadul Islam — University of Rajshahi, Bangladesh

Ichiro Abe — Fukuoka University Chikushi Hospital, Japan

Suja Pillai — The University of Queensland, Australia

**Citation**

Islam, F., Abe, I., Pillai, S., eds. (2025). *Recent advances in pheochromocytoma and paraganglioma: molecular pathogenesis, clinical impacts, and therapeutic perspective, volume II*. Lausanne: Frontiers Media SA.

doi: 10.3389/978-2-8325-6347-2

# Table of contents

frontiers | Frontiers in Endocrinology

TYPE Editorial
PUBLISHED 02 May 2025
DOI 10.3389/fendo.2025.1605189

Check for updates

OPEN ACCESS

EDITED AND REVIEWED BY
Hubert Vaudry,
Université de Rouen, France

*CORRESPONDENCE
Ichiro Abe
abe1ro@fukuoka-u.ac.jp

RECEIVED 02 April 2025
ACCEPTED 11 April 2025
PUBLISHED 02 May 2025

CITATION
Abe I, Islam F and Pillai S (2025) Editorial: Recent advances in pheochromocytoma and paraganglioma: molecular pathogenesis, clinical impacts, and therapeutic perspective, volume II. *Front. Endocrinol.* 16:1605189. doi: 10.3389/fendo.2025.1605189

COPYRIGHT
© 2025 Abe, Islam and Pillai. This is an open-access article distributed under the terms of the Creative Commons Attribution License (CC BY). The use, distribution or reproduction in other forums is permitted, provided the original author(s) and the copyright owner(s) are credited and that the original publication in this journal is cited, in accordance with accepted academic practice. No use, distribution or reproduction is permitted which does not comply with these terms.

# Editorial: Recent advances in pheochromocytoma and paraganglioma: molecular pathogenesis, clinical impacts, and therapeutic perspective, volume II

Ichiro Abe[1]*, Farhadul Islam[2] and Suja Pillai[3]

[1]Department of Endocrinology and Diabetes Mellitus, Fukuoka University Chikushi Hospital, Chikushino, Fukuoka, Japan, [2]Department of Biochemistry and Molecular Biology, University of Rajshahi, Rajshahi, Bangladesh, [3]School of Biomedical Sciences, Faculty of Medicine, University of Queensland, Saint Lucia, QLD, Australia

KEYWORDS

**pheochromocytoma, paraganglioma, molecular pathogenesis, clinical impacts, therapeutic perspective**

Editorial on the Research Topic

Recent advances in pheochromocytoma and paraganglioma: molecular pathogenesis, clinical impacts, and therapeutic perspective, volume II

This Research Topic encompasses current perspectives on the molecular mechanisms, genetics, clinical manifestations, and novel therapeutic management of Pheochromocytomas and Paragangliomas (PPGLs). In the previous Research Topic, Recent Advances in Pheochromocytoma and Paraganglioma: Molecular Pathogenesis, Clinical Impacts, and Therapeutic Perspective, *i.e.* knowledge of the molecular and genetic spectrum, mechanisms of complications, and novel therapeutic options of PPGLs were illustrated. The knowledge of PPGLs has been advancing; thus, in this Research Topic, we have updated the current understanding of PPGLs.

PPGLs are relatively rare neuroendocrine tumors derived from chromaffin cells in the adrenal medulla and/or autonomic nervous system ganglia. Their clinical importance, including various associated complications, is due to catecholamine excess (1, 2). Moreover, PPGLs could lead to pheochromocytoma multisystem crisis (PMC), which is a life-threatening endocrine emergency with reported mortality as high as 85-90% (3). Thus, updated knowledge of management of PPGLs, especially based on the molecular mechanisms and genetics, is necessary. Meanwhile, according to the WHO's classification in 2017, all pheochromocytomas could have metastatic potential and no histological system to assess the biological aggressiveness. Hence, "Malignant pheochromocytoma" in the 2004 WHO classification was replaced with "Metastatic pheochromocytoma" in the 2017 WHO classification (4). Considering the above, an

updated understanding of clinicopathological advances and the management of PPGLs, mainly based on molecular mechanisms and genetics, is necessary (2, 4–7).

In this Research Topic, Saavedra et al. reviewed the clinical presentation, management, and treatment of patients with PPGLs. In this review article, early diagnosis, combined with an understanding of the genetic landscapes and comprehensive treatment strategies, was described as necessary to improve outcomes for patients with PPGLs. Nevertheless, surgery is the mainstay of treatment for patients with PPGLs. The utilization of Da Vinci robot-assisted laparoscopic surgery contributed to a favorable prognosis for a patient. In addition, Yang et al. reported a case of paraganglioma with a newly detected *EPAS1* mutation, which may be the primary driver of the disease.

Some therapeutic options in patients who could not receive surgery and/or have metastatic PPGLs have been reported in this Research Topic. For example, Cyclophosphamide-Vincristine-Dacarbazine (CVD) chemotherapy is a conventional therapeutic option and was reported to be the first-line treatment for PPGLs with *SDHB*-mutation previously (8). Zhang et al. performed CVD chemotherapy for a patient with metastatic paraganglioma having *SDHB*-mutation and treated it very effectively.

Recently, radiotherapy for metastatic PPGLs has evolved. Gubbi et al. performed a phase 2 trial of [$^{177}$Lu]Lu-DOTA-TATE therapy of somatostatin receptor (SSTR)-2+ on patients with inoperable/metastatic PPGLs and evaluated the abnormalities in the immediate post-treatment period. This study indicates that [$^{177}$Lu]Lu-DOTA-TATE therapy is associated with alterations in endocrine function likely from radiation exposure to SSTR2+ endocrine tissues, and these could cause clinically significant endocrinopathies. The information from this investigation should be important for the patients who receive [$^{177}$Lu]Lu-DOTA-TATE therapy.

Furthermore, the advances of molecular mechanisms and genetics with PPGLs have led to novel therapeutic management, such as tyrosine kinase inhibitors, as reviewed by Saavedra et al. In addition, the relationship between PPGLs and other diseases has been reported. In this topic, Dai et al. reported a patient with pheochromocytoma and Langerhans cell histiocytosis (LCH), who had *EPAS1* mutation (pheochromocytoma) and *RAD54B* mutation (LCH). Wang et al. also reported a patient with paraganglioma and higher IL-6 value, who had *KIF1B* mutation. Moreover, Li et al. reported a patient with metastatic pheochromocytoma and without typical symptoms of catecholamine excess, who had *DLST* mutation. Thus, it is unclear whether the gene mutation is the cause of the phenotype/complication/co-existing disease. Future advances might explain the mechanism.

Besides, Małgorzata et al. investigated a patient with pheochromocytoma, whose ACTH and cortisol values were elevated. Previously, ACTH-producing pheochromocytomas were reported (9, 10). However, the patient described by Małgorzata et al. was negative for ACTH (and CRH). Hence, they described that catecholamine excess could activate the hypothalamic-pituitary-adrenal (HPA) axis. Considering the various complications of PPGLs, the phenotype of this case should be taken into consideration.

In conclusion, the information presented in this Research Topic provides updated perspectives of the molecular mechanisms and genetics of PPGLs and their unveiled clinicopathological implications. These enrich the perspectives of PPGLs, which could lead to improved clinical outcomes for patients with PPGLs.

## Author contributions

IA: Conceptualization, Formal analysis, Investigation, Methodology, Project administration, Resources, Supervision, Validation, Writing – original draft. FI: Conceptualization, Formal analysis, Investigation, Methodology, Project administration, Resources, Supervision, Validation, Writing – review & editing. SP: Conceptualization, Formal analysis, Investigation, Methodology, Project administration, Resources, Supervision, Validation, Writing – review & editing.

## Conflict of interest

The authors declare that the research was conducted in the absence of any commercial or financial relationships that could be construed as a potential conflict of interest.

The author(s) declared that they were an editorial board member of Frontiers, at the time of submission. This had no impact on the peer review process and the final decision.

## Generative AI statement

The author(s) declare that no Generative AI was used in the creation of this manuscript.

## Publisher's note

All claims expressed in this article are solely those of the authors and do not necessarily represent those of their affiliated organizations, or those of the publisher, the editors and the reviewers. Any product that may be evaluated in this article, or claim that may be made by its manufacturer, is not guaranteed or endorsed by the publisher.

# References

1. Aygun N, Uludag M. Pheochromocytoma and paraganglioma: from clinical findings to diagnosis. *Sisli Etfal Hastan Tip Bul*. (2020) 54:271–80. doi: 10.14744/SEMB.2020.14826

2. Abe I, Islam F, Lo CY, Liew V, Pillai S, Lam AK. VEGF-A/VEGF-B/VEGF-C expressions in non-hereditary, non-metastatic phaeochromocytoma. *Histol Histopathol*. (2021) 18:18329. doi: 10.14670/HH-18-329

3. Abe I, Nomura M, Watanabe M, Shimada S, Kohno M, Matsuda Y, et al. Pheochromocytoma crisis caused by Campylobacter fetus. *Int J Urol*. (2012) 19:465–7. doi: 10.1111/j.1442-2042.2011.02950.x

4. Lloyd RV, Osamura RY, Kloppel G, Rosai J. *WHO classification of tumors: pathology and genetics of tumors of endocrine organs. 4th ed*. Lyon: IARC (2017).

5. Dahia PL. Pheochromocytoma and paraganglioma pathogenesis: learning from genetic heterogeneity. *Nat Rev Cancer*. (2014) 14:108–19. doi: 10.1038/nrc3648

6. Pillai S, Gopalan V, Smith RA, Lam AK. Updates on the genetics and the clinical impacts on phaeochromocytoma and paraganglioma in the new era. *Crit Rev Oncol Hematol*. (2016) 100:190–208. doi: 10.1016/j.critrevonc.2016.01.022

7. Islam F, Pillai S, Gopalan V, Lam AK. Identification of novel mutations and expressions of EPAS1 in phaeochromocytomas and paragangliomas. *Genes (Basel)*. (2020) 11:1254. doi: 10.3390/genes11111254

8. Jawed I, Velarde M, Därr R, Wolf KI, Adams K, Venkatesan AM, et al. Continued tumor reduction of metastatic pheochromocytoma/paraganglioma harboring succinate dehydrogenase subunit B mutations with cyclical chemotherapy. *Cell Mol Neurobiol*. (2018) 38:1099–106. doi: 10.1007/s10571-018-0579-4

9. Soto-Montes Z, Medina-Julio D, Solis-Coronado OD, Mendoza-García JG, Tenorio-Aguirre EK, Martínez-Sánchez FD. Ectopic ACTH-secreting pheochromocytoma without typical signs of Cushing syndrome. *Oxf Med Case Rep*. (2025) 28:omaf005. doi: 10.1093/omcr/omaf005

10. Kishlyansky D, Leung AA, Pasieka JL, Mahajan A, Kline GA. Cushing syndrome from an ACTH-producing pheochromocytoma or paraganglioma: structured review of 94 cases. *Endocr Relat Cancer*. (2024) 14:e240029. doi: 10.1530/ERC-24-0029

frontiers | Frontiers in Endocrinology

TYPE Case Report
PUBLISHED 28 July 2023
DOI 10.3389/fendo.2023.1180091

Check for updates

OPEN ACCESS

EDITED BY
Farhadul Islam,
University of Rajshahi, Bangladesh

REVIEWED BY
Matthew Nazari,
National Institutes of Health (NIH), United States
Sergei Tevosian,
University of Florida, United States

*CORRESPONDENCE
Kai Liu
liukaicardiology@163.com
Liming Zhao
ermine1048@163.com

†These authors have contributed equally to this work and share first authorship

RECEIVED 28 April 2023
ACCEPTED 10 July 2023
PUBLISHED 28 July 2023

CITATION
Yang H, Chen Y, Liu K and Zhao L (2023) Case Report: A novel *EPAS1* mutation in a case of paraganglioma complicated with polycythemia and atrial septal defect. *Front. Endocrinol.* 14:1180091. doi: 10.3389/fendo.2023.1180091

COPYRIGHT
© 2023 Yang, Chen, Liu and Zhao. This is an open-access article distributed under the terms of the Creative Commons Attribution License (CC BY). The use, distribution or reproduction in other forums is permitted, provided the original author(s) and the copyright owner(s) are credited and that the original publication in this journal is cited, in accordance with accepted academic practice. No use, distribution or reproduction is permitted which does not comply with these terms.

# Case Report: A novel *EPAS1* mutation in a case of paraganglioma complicated with polycythemia and atrial septal defect

Haiyan Yang[1,2†], Yue Chen[3,4†], Kai Liu[1*] and Liming Zhao[5*]

[1]Department of Cardiology, West China Hospital, Sichuan University, Chengdu, Sichuan, China, [2]Department of Geriatrics, Chongqing General Hospital, Chongqing, China, [3]Department of Clinical Medicine, West China Hospital, Sichuan University, Chengdu, Sichuan, China, [4]Department of Pharmacy, West China Tianfu Hospital, Sichuan University, Chengdu, Sichuan, China, [5]Department of Cardiology, Hospital of Chengdu Office of People's Government of Tibetan Autonomous Region, Chengdu, Sichuan, China

**Background:** Paraganglioma is a rare neuroendocrine tumor and is highly associated with hereditary susceptibility genes, often occurring as part of a genetic syndrome. The genetic heterogeneity of paraganglioma poses challenges in diagnosis, counseling, and clinical management.

**Case summary:** We present the case of a 60-year-old woman with hypertension, atrial septal defect, and polycythemia, who experienced paroxysmal palpitations, sweating, headache, abdominal pain, nausea, and vomiting. Her blood pressure was severely unstable. Blood laboratory tests revealed elevated catecholamine levels, contrast-enhanced CT of her whole abdomen showed a round retroperitoneal mass with soft tissue density, and somatostatin receptor imaging (68Ga PET-CT) indicated a retroperitoneal mass with abnormally increased expression of somatostatin receptor. It is interesting to note that whole exome sequencing (WES) analyses on both blood and tumor samples revealed a novel *EPAS1* mutation, specifically the c.2501A > G; p.Tyr834Cys variant, which has never been reported. The patient was diagnosed with paraganglioma and underwent successful Da Vinci robot-assisted laparoscopic resection of the retroperitoneal tumor. During a 3-month follow-up period, her blood pressure stabilized, and her symptoms significantly improved.

**Conclusion:** This case reveals that the *EPSA1* mutation may be the primary driver of paraganglioma complicated by atrial septal defect and polycythemia. Additionally, the utilization of Da Vinci robot-assisted laparoscopic surgery contributed to a favorable prognosis for the patient.

KEYWORDS

**paraganglioma, EPAS1, hypertension, atrial septal defect, polycythemia**

# 1 Introduction

Paraganglioma is a rare neuroendocrine tumor arising from chromaffin tissues in the extra-adrenal sympathetic and parasympathetic nervous systems outside the adrenal glands (1, 2). The clinical signs of paraganglioma often lack specificity and occur intermittently, including intermittent palpitations, hypertension, and metabolic abnormalities, leading to diagnostic delays. Catecholamine crisis and catecholamine-induced cardiomyopathy (CICMP) secondary to paraganglioma may be life-threatening. Paraganglioma is strongly associated with hereditary susceptibility genes, and it constitutes a part of a genetic syndrome in approximately one-third to one-half of cases (3). Therefore, prevailing guidelines recommend the consideration of genetic testing for all patients suffering from paraganglioma by accredited laboratories (4, 5). The genetic heterogeneity of paraganglioma poses considerable challenges in genetic diagnosis, counseling, and clinical monitoring of patients with this condition (6). In this article, we present an uncommon and critical case of paraganglioma complicated with polycythemia and atrial septal defect. The patient exhibited symptoms of abnormally fluctuating hypertension and heart failure and subsequently developed secondary catecholamine cardiomyopathy. A novel mutation of *EPAS1*, not previously reported, was detected in her blood and tumor samples. Catecholamine cardiomyopathy was significantly improved after the surgical removal of the paraganglioma.

# 2 Case presentation

A 60-year-old woman presented at our institution with paroxysmal palpitations, sweating, headache, abdominal pain, nausea, and emesis. Approximately a decade prior, she experienced recurrent paroxysmal palpitations and diaphoresis without apparent etiology, which showed limited improvement with symptomatic management. One month ago, her palpitations and diaphoresis intensified, accompanied by headache, abdominal pain, nausea, and vomiting, without chest pain or syncope. Transthoracic echocardiography (TTE) performed at a local hospital revealed an atrial septal defect, prompting her admission to our facility. Throughout her hospitalization, her blood pressure exhibited severe instability, with the highest recorded reading reaching 251/168 mmHg and the lowest recorded reading dropping to 70/43 mmHg. Her medical history included a 2-year diagnosis of hypertension, managed with controlled-release nifedipine and irbesartan hydrochlorothiazide tablets, as well as a 1-year use of Tibetan medicine for diabetes and previous surgical treatment for gallstones. The patient is a non-smoker and does not consume alcohol. Her older brother had a history of atrial septal defect, and her parents passed away due to undisclosed causes.

During the physical examination, the patient exhibited a body temperature of 36°C, a heart rate of 114 beats per minute (bpm), a blood pressure of 163/115 mmHg, a respiratory rate of 20 breaths per minute, and a body mass index of 18.7 kg/m$^2$. No evidence of hepatojugular reflux with jugular venous distension was observed, and there were no signs of moist rales or wheezing in either lung field. A cardiac examination revealed tachycardia with a regular rhythm and no audible cardiac murmurs. The abdomen exhibited softness, and the presence of a mass was scarcely palpable. Furthermore, there was no evidence of edema in the lower extremities.

Blood laboratory tests revealed a notable elevation in catecholamine levels, including epinephrine at 7,241.6 pmol/L (normal range, 0–605.4 pmol/L), norepinephrine at 69,645 pmol/L (normal range, 414–4,435.5 pmol/L), dopamine at 575.3 pmol/L (normal range, 0–195.7 pmol/L), metanephrine at 3.01 nmol/L (normal range, 0–0.5 nmol/L), and normetanephrine exceeding 20.56 nmol/L (normal range, 0–0.9 nmol/L). At the same time, the resin–angiotensin–aldosterone system (RAAS), adrenocorticotropic hormone, cortisol, and dehydroepiandrosterone sulfate exhibited normal values. Urinary measurements demonstrated elevated levels of epinephrine at 123.03 nmol/24 h (normal range, 4.31–61.6 nmol/24 h) and norepinephrine at 2,488.95 nmol/24 h (normal range, 60–352 nmol/24 h), while dopamine remained within normal limits. Additionally, Troponin-T levels were elevated at 245.8 pg/ml (normal range, 0–14 pg/ml), CK-MB at 5.74 ng/ml (normal range, 0–2.88 ng/ml), and N-terminal prob-type natriuretic peptide (NT-proBNP) at 11,411 pg/ml (normal range, 0–450 pg/ml). Hematocrit levels in the blood routine indicated 56.7%, with a hemoglobin level of 195 g/L.

The 12-lead electrocardiogram demonstrated sinus rhythm (Figure 1A). TTE revealed the presence of an atrial septal defect, a thickened ventricular septum measuring 13 mm, mild mitral and tricuspid regurgitation, reduced left ventricular systolic function, and an ejection fraction (EF) of 46% (Figure 1B). Contrast-enhanced CT of the entire abdominal region showed a round retroperitoneal mass with soft tissue density, measuring approximately 4.5×2.5 cm, exhibiting notable heterogeneous enhancement. Considering these findings, the possibility of a neurogenic tumor was considered (Figure 1C). To better assess the mass's relationship with adjacent structures, a three-dimensional reconstruction of the retroperitoneal mass in the abdomen was performed, revealing its proximity to the inferior vena cava, aorta, portal vein, right renal artery, and left renal artery (Figure 1D). Somatostatin receptor imaging (68Ga PET-CT) indicated abnormally increased expression of somatostatin receptor in the retroperitoneal mass, consistent with the appearance of paraganglioma, and no evidence of tumor metastasis elsewhere in the body (Figure 2).

Upon admission, the patient's symptoms and examination results led to the diagnosis of paraganglioma, catecholamine cardiomyopathy, hypertensive crisis, atrial septal defect, and diabetes. Treatment was initiated with nifedipine controlled-release tablets, phenoxybenzamine, metoprolol sustained-release tablets, and immediate restoration of circulating volume. Subsequently, the frequency of symptoms such as palpitations, sweating, and headache notably decreased. Additionally, there was a significant improvement in cardiac function, evidenced by a decrease in NT-proBNP from a maximum of 18,128 pg/ml to 187.6 pg/ml, a reduction in Troponin-T from a maximum of 320 pg/ml to 17.6 pg/ml, heart rate fluctuations within the range of 60–70 bpm, and blood pressure maintained below 140/90 mmHg. Following evaluations by cardiologists and urologists, the patient underwent Da Vinci robot-assisted laparoscopic resection of the retroperitoneal tumor. During the operation, the grayish-white tumor measuring 4.0 cm × 3.0 cm was successfully removed with intact encapsulation.

10.3389/fendo.2023.1180091

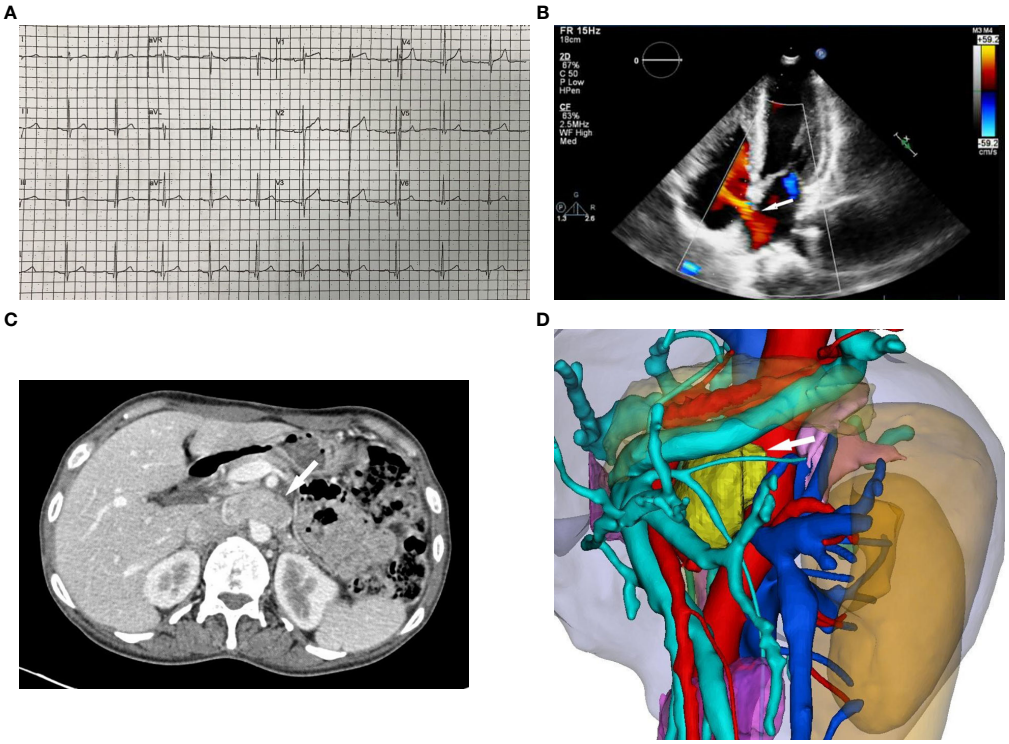


FIGURE 1
**(A)** 12-lead electrocardiogram shows sinus rhythm, and no significant ST-T changes. **(B)** Transthoracic echocardiography shows the white arrow indicate the atrial septal defect, which shows a discontinuity in the continuity of the middle atrial septum and a shunt from left to right. **(C)** Abdomen contrast-enhanced CT shows the white arrow indicate a round retroperitoneal mass with soft tissue density (about 4.5×2.5cm in size) and marked heterogeneous enhancement. **(D)** 3D reconstruction of the retroperitoneal mass shows the yellow mass indicated by the white arrow is the retroperitoneal mass, the red is the artery, the blue is the vein, and the sky blue is the portal vein. The retroperitoneal mass is closely adjacent to the inferior vena cava, aorta, portal vein, right renal artery and left renal artery.

Hematoxylin–eosin staining of tumor tissue showed characteristic "Zellballen" architecture of tumor cells. Postoperative pathological examination confirmed the diagnosis of paraganglioma (Figure 3).

Owing to the significant association between paragangliomas and hereditary susceptibility genes, whole exome sequencing (WES) was performed on venous whole blood and tumor samples of the patient. All suspicious mutations were identified in both sample types and thus considered as germline ones, and no additional potential somatic mutations associated with pheochromocytomas and paragangliomas were identified with a frequency higher than 5%. This analysis successfully detected germline *EPAS1* mutations, specifically identifying the c.2501A > G; p.Tyr834Cys mutation in the 16th exon of the *EPAS1* gene. Additionally, the patient presented with germline *ACTN2* (c.971G > A; p.Arg3244Gln) and *DSC2* (c.898A > G; p.Thr300Ala) mutations. Concurrently, the patient's brother provided oral epithelial cells through a buccal swab for WES, revealing consistent gene mutation sites with the patient. We predicted the protein structures of the *EPAS1* wild type and mutant shown on the 3D model (Figure 4).

We conducted a 3-month follow-up after the surgery to assess the therapeutic outcomes. Throughout this period, the patient did not experience any episodes of paroxysmal palpitations, diaphoresis, or headaches. The treatment consisting of nifedipine controlled-release tablets, phenoxybenzamine, metoprolol sustained-release tablets, and sacubitril valsartan was continued, resulting in blood pressure control within the range of 125–150/78–95 mmHg, while the heart rate fluctuated between 70 and 85 bpm. Following the resection of paraganglioma, a repeat TTE demonstrated that the interventricular septal thickness had decreased from 13 mm to 12 mm, and the EF had increased from 46% to 63%. These findings indicated a significant improvement in cardiac function following the administered treatment.

## 3 Discussion

Pheochromocytoma and paraganglioma are rare catecholamine-producing neural crest tumors derived from neuroendocrine chromaffin cells. According to a study conducted in Canada, the overall incidence of pheochromocytoma or paraganglioma was 0.66 cases per 100,000 people per year. The prevalence of pheochromocytoma and paraganglioma increased with age, with the highest occurrence observed among individuals aged 60–79 years (7). Most paragangliomas are located in the thoracic and abdominal sympathetic nerves, and retroperitoneal paragangliomas account for more than 50% of all cases, with functional paragangliomas comprising 15%–24% of cases (8). Paragangliomas primarily secrete catecholamines, including epinephrine, norepinephrine, and dopamine. The typical clinical manifestations of paraganglioma are paroxysmal palpitation, headache, sweating,

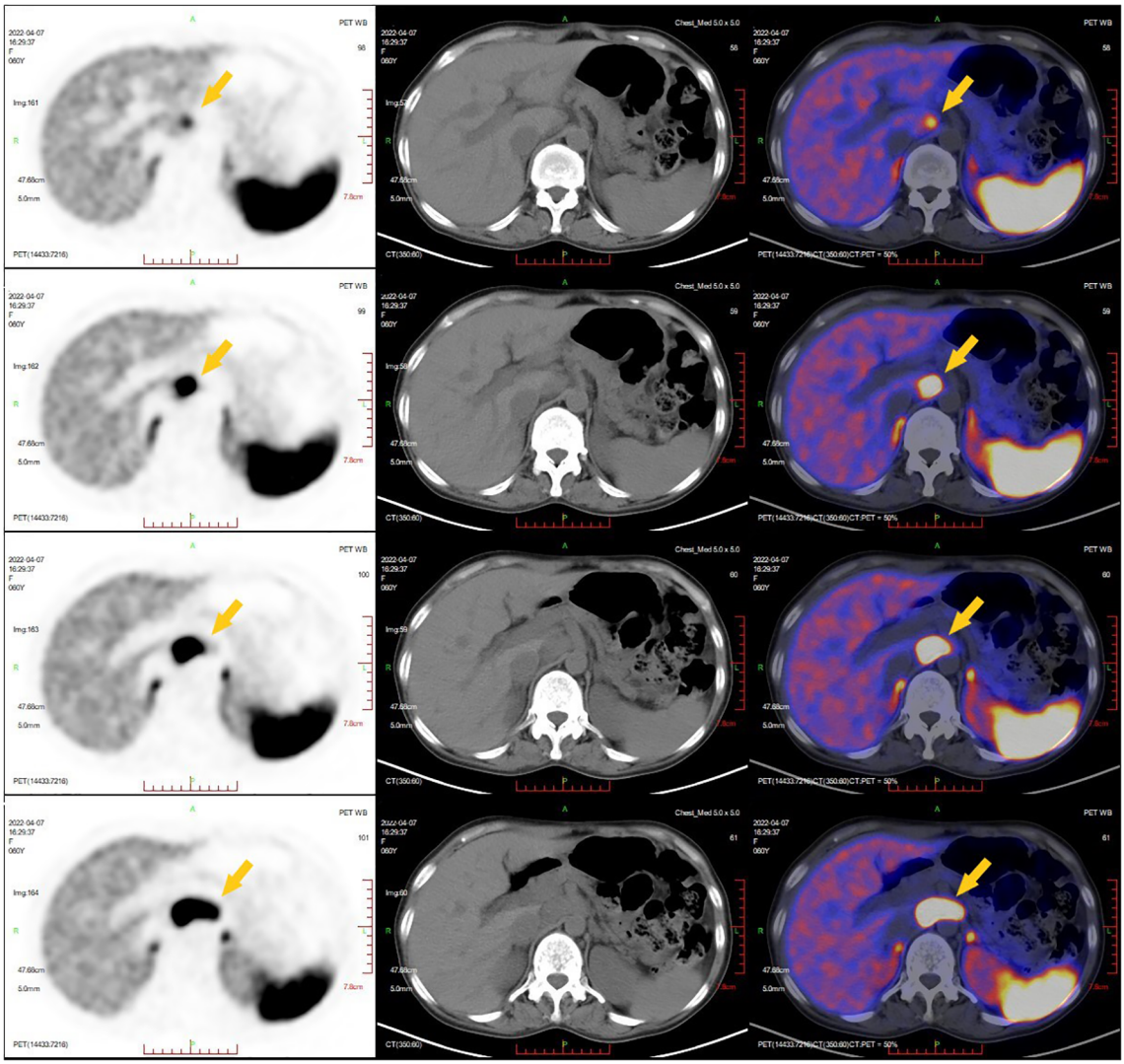

FIGURE 2
Somatostatin receptor imaging (68Ga PET-CT). The yellow arrow indicated a retroperitoneal mass with abnormal increased expression of somatostatin receptor was consistent with the appearance of paraganglioma.

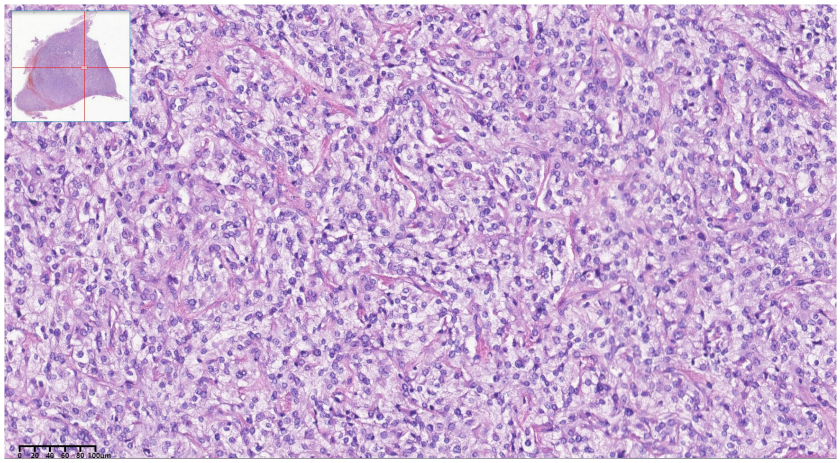

FIGURE 3
Histopathologic pictures of the retroperitoneal mass. Hematoxylin-eosin staining showed characteristic 'Zellballen' architecture of tumor cells.

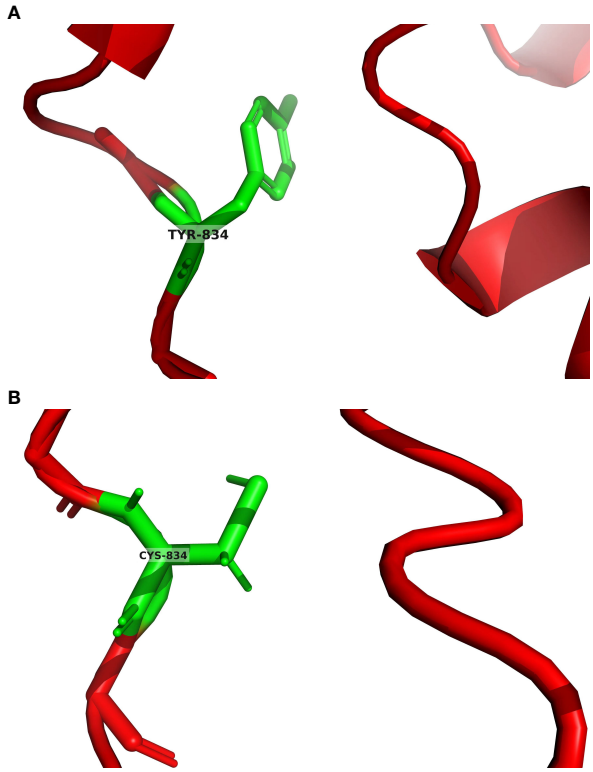


FIGURE 4
**(A)** EPAS1 wild type was predicted by AlphaFold2. The green color in the figure represents the tyrosine at position 834 of the EPAS1 wild type encoded protein. **(B)** EPAS1 mutant was predicted by tFold. The green color in the figure represents the cysteine at position 834 of the EPAS1 mutant encoded protein.

pallor, tremors, and anxiety, often accompanied by episodic or sustained hypertension (9, 10). Neuroendocrine paragangliomas may exhibit atypical symptoms or remain asymptomatic, leading to delayed diagnoses. However, in the case of this patient, the presence of characteristic symptoms such as palpitation, headache, and hypertension, along with significantly elevated catecholamine levels and the identification of a retroperitoneal mass, raised strong suspicion of a functional paraganglioma, facilitating an expeditious confirmation of the diagnosis.

The majority of hereditary paragangliomas are caused by pathogenic variants in genes such as *SDHD*, *SDHB*, *SDHC*, *VHL*, and *NF1* (2). Therefore, patients diagnosed with paraganglioma should undergo *SDHx* mutation testing, while those with metastatic disease should undergo *SDHB* mutation testing. *EPAS1* mutations have been reported in human congenital heart disease and polycythemia (11). Recently, genetic and constitutional mutations of *EPAS1* have been discovered to be connected to the pathogenesis of pheochromocytoma and paraganglioma (12). Gene sequencing of tumor tissue in paraganglioma patients with paraganglioma has revealed that approximately 7% of cases exhibit *EPAS1* mutations, particularly the c.1091A>T (p.Lys364Met) variant. Notably, these mutations were detected in tumor tissues but not in non-neoplastic adrenal tissues. Additionally, mutations of *EPAS1* may contribute to the progression of this group of tumors ascribed to the association of the mutations with high tumor weight and larger tumor size (6). Another study reported a gain-of-function somatic pathogenic variant of *EPAS1* in four of five patients (80%) with pheochromocytoma and paraganglioma who presented with cyanotic congenital heart disease; one of the four patients had paraganglioma with c.1592C>G (p.Pro531Arg) mutation (13). Based on previous studies, the presence of the *EPAS1* mutation in this patient suggests a potential association with paraganglioma, polycythemia, and atrial septal defect. It is encouraging that this variant represents a novel mutation site that has not been reported before.

It is noteworthy that the patient and her brother exhibit two additional genetic variants: *ACTN2* and *DSC2*. These genes are implicated in cardiac abnormalities such as hypertrophic cardiomyopathy, dilated cardiomyopathy, and arrhythmias. Therefore, it is not certain whether they are involved in the mechanism of atrial septal defect formation. However, *ACTN2* and *DSC2* mutations have not been reported to be associated with paraganglioma, atrial septal defect, or polycythemia. This further strengthens our suspicion that the *EPSA1* mutation may be the primary driver of the disease in this patient.

Our case does have certain limitations. The patient's brother, who also carries the same heterozygous mutation sites and has atrial septal defect without polycythemia, has not exhibited similar paraganglioma symptoms and has not undergone abdominal CT to date. It is unknown whether he possesses a nonfunctional paraganglioma. Consequently, the precise association between the novel *EPAS1* mutation and paraganglioma complicated by polycythemia and atrial septal defect remains inconclusive. Further follow-up is essential to elucidate the clinical significance of this novel mutation site.

Surgical resection of the tumor is the primary treatment for paraganglioma. However, it is crucial to stabilize blood pressure with α adrenoceptor blockers and subsequently introduce β adrenoceptor blockers to stabilize tachycardia before surgery to avoid inducing catecholamine crisis (5). Phenoxybenzamine is often preferred due to its long half-life, compared to phentolamine, which can be started once hemodynamic stability has been achieved. Angiotensin receptor neprilysin inhibitor (ARNI) may also play a role in managing heart failure and hypertension in patients with pheochromocytoma or paraganglioma, as it has been reported to be effective in the follow-up of patients without pheochromocytoma resection (14). Excellent preoperative management strategies combined with optimal surgical methods can minimize surgical complications and improve the prognosis of patients. In this particular case, considering the challenging location of the tumor due to its proximity to the surrounding blood vessels, the urologist choose the Da Vinci robot-assisted laparoscopic surgery. During the procedure, the robotic arm enabled easy access to the tumor. Moreover, the three-dimensional vision clearly delineated the vascular anatomy surrounding the tumor. Compared to standard laparoscopic procedures, Da Vinci robot-assisted laparoscopic surgery offers greater precision, reduced invasiveness, and faster postoperative recovery. It is worth noting that there are limited

reports regarding the use of this surgical modality in the treatment of paragangliomas.

## 4 Conclusions

Paraganglioma is a rare neuroendocrine tumor and highly associated with hereditary susceptibility genes. In this case, we have identified a novel *EPAS1* mutation in patients with paraganglioma, which may have significant implications in the pathogenesis of the disease, particularly in cases complicated by atrial septal defect and polycythemia. This finding adds to the growing body of knowledge regarding the genetic basis of paragangliomas. Furthermore, the utilization of Da Vinci robot-assisted laparoscopic surgery has demonstrated its potential to contribute to favorable outcomes in the management of paragangliomas. Although the application of this technique in paraganglioma treatment is relatively limited, it shows promise as an effective surgical modality. Continued follow-up and further research are necessary to better understand the clinical significance of the novel *EPAS1* mutation and its association with paraganglioma, atrial septal defect, and polycythemia.

## Data availability statement

The raw data supporting the conclusions of this article will be made available by the authors, without undue reservation.

## Ethics statement

Written informed consent was obtained from the participant/patient(s) for the publication of this case report.

## Author contributions

HY contributed to writing the original draft. KL contributed to reviewing and editing. LZ and YC contributed to data collection. KL and LZ contributed to conceptualization, resources, and supervision. HY and YC contributed equally to this work and share first authorship. KL and LZ share corresponding authorship. All authors have read and agreed to the published version of the manuscript.

## Funding

This study was supported by the Major Science & Technology Pillar Program in Tibet Autonomous Region, China (grant no. XZ202201ZD0001G01), the Science & Technology Pillar Program in Sichuan Province, China (grant no. 2022YFS0356), and Medical Research Projects of Chongqing Science and Technology Commission and Chongqing Health Committee (grant no. 2021MSXM066).

## Acknowledgments

All authors sincerely thank Professor Yuchun Zhu of Urology Department, West China Hospital, Sichuan University, for his wonderful Da Vinci robot-assisted laparoscopic surgery. The authors appreciate the Departments of Pathology, Ultrasound, Radiology, and Nuclear Medicine for their technical support.

## Conflict of interest

The authors declare that the research was conducted in the absence of any commercial or financial relationships that could be construed as a potential conflict of interest.

## Publisher's note

All claims expressed in this article are solely those of the authors and do not necessarily represent those of their affiliated organizations, or those of the publisher, the editors and the reviewers. Any product that may be evaluated in this article, or claim that may be made by its manufacturer, is not guaranteed or endorsed by the publisher.

## References

1. Lenders JW, Duh QY, Eisenhofer G, Gimenez-Roqueplo AP, Grebe SK, Murad MH, et al. Pheochromocytoma and paraganglioma: an endocrine society clinical practice guideline. *J Clin Endocrinol Metab* (2014) 99(6):1915–42. doi: 10.1210/jc.2014-1498

2. Neumann HPH, Young WF, Eng C. Pheochromocytoma and paraganglioma. *New Engl J Med* (2019) 381(6):552–65. doi: 10.1056/NEJMra1806651

3. Drovdlic CM, Myers EN, Peters JA, Baysal BE, Brackmann DE, Slattery WH3rd, et al. Proportion of heritable paraganglioma cases and associated clinical characteristics. *Laryngoscope* (2001) 111(10):1822–7. doi: 10.1097/00005537-200110000-00029

4. Wachtel H, Fishbein L. Genetics of pheochromocytoma and paraganglioma. *Curr Opin endocrinol diabetes Obes* (2021) 28(3):283–90. doi: 10.1097/MED.0000000000000634

5. Garcia-Carbonero R, Matute Teresa F, Mercader-Cidoncha E, Mitjavila-Casanovas M, Robledo M, Tena I, et al. Multidisciplinary practice guidelines for the diagnosis, genetic counseling and treatment of pheochromocytomas and paragangliomas. *Clin Trans Oncol* (2021) 23(10):1995–2019. doi: 10.1007/s12094-021-02622-9

6. Islam F, Pillai S, Gopalan V, Lam AK. Identification of novel mutations and expressions of EPAS1 in phaeochromocytomas and paragangliomas. *Genes* (2020) 11 (11):1254. doi: 10.3390/genes11111254

7. Leung AA, Pasieka JL, Hyrcza MD, Pacaud D, Dong Y, Boyd JM, et al. Epidemiology of pheochromocytoma and paraganglioma: population-based cohort study. *Eur J Endocrinol* (2021) 184(1):19–28. doi: 10.1530/EJE-20-0628

8. Li P, Zhao D. A rare case of retroperitoneal paraganglioma-case report and literature review. *Trans Gastroenterol Hepatol* (2016) 1:58. doi: 10.21037/tgh.2016.06.01

9. Y-Hassan S, Falhammar H. Clinical features, complications, and outcomes of exogenous and endogenous catecholamine-triggered Takotsubo syndrome: A systematic review and meta-analysis of 156 published cases. *Clin Cardiol* (2020) 43 (5):459–67. doi: 10.1002/clc.23352

10. Falhammar H, Kjellman M, Calissendorff J. Initial clinical presentation and spectrum of pheochromocytoma: a study of 94 cases from a single center. *Endoc connections* (2018) 7(1):186–92. doi: 10.1530/EC-17-0321

11. Pillai S, Gopalan V, Smith RA, Lam AK. Updates on the genetics and the clinical impacts on phaeochromocytoma and paraganglioma in the new era. *Crit Rev oncology/ hematol* (2016) 100:190–208. doi: 10.1016/j.critrevonc.2016.01.022

12. Buffet A, Burnichon N, Favier J, Gimenez-Roqueplo AP. An overview of 20 years of genetic studies in pheochromocytoma and paraganglioma. *Best Pract Res Clin Endocrinol Metab* (2020) 34(2):101416. doi: 10.1016/j.beem.2020.101416

13. Vaidya A, Flores SK, Cheng ZM, Nicolas M, Deng Y, Opotowsky AR, et al. EPAS1 mutations and paragangliomas in cyanotic congenital heart disease. *New Engl J Med* (2018) 378(13):1259–61. doi: 10.1056/NEJMc1716652

14. Yu M, Du B, Yao S, Ma J, Yang P. Von Hippel-Lindau syndrome with a rare complication of dilated cardiomyopathy: a case report. *BMC Cardiovasc Disord* (2022) 22(1):489. doi: 10.1186/s12872-022-02913-1

frontiers | Frontiers in Endocrinology

TYPE Case Report
PUBLISHED 14 September 2023
DOI 10.3389/fendo.2023.1226468

Check for updates

OPEN ACCESS

EDITED BY
Suja Pillai,
The University of Queensland, Australia

REVIEWED BY
Shetty Ravi Dyavar,
Adicet Bio, Inc., United States
Hiroshi Nagasaki,
Fujita Health University, Japan

*CORRESPONDENCE
Can Cui
cuican1972x@163.com

RECEIVED 21 May 2023
ACCEPTED 23 August 2023
PUBLISHED 14 September 2023

CITATION
Wang C, Guan M, Zhang S and Cui C (2023) Case Report: A 65-year-old man with paraganglioma accompanied by elevated interleukin-6 levels and KIF1B single gene mutation.
*Front. Endocrinol.* 14:1226468.
doi: 10.3389/fendo.2023.1226468

COPYRIGHT
© 2023 Wang, Guan, Zhang and Cui. This is an open-access article distributed under the terms of the Creative Commons Attribution License (CC BY). The use, distribution or reproduction in other forums is permitted, provided the original author(s) and the copyright owner(s) are credited and that the original publication in this journal is cited, in accordance with accepted academic practice. No use, distribution or reproduction is permitted which does not comply with these terms.

# Case Report: A 65-year-old man with paraganglioma accompanied by elevated interleukin-6 levels and KIF1B single gene mutation

Chi Wang, Ming Guan, Shuang Zhang and Can Cui*

Department of Endocrinology and Metabolism, The Second Affiliated Hospital of Harbin Medical University, Harbin, Heilongjiang, China

Paraganglioma is a less prevalent disease, and paraganglioma with only secreting interleukin-6 (IL-6) has not been previously reported. A 64-year-old male patient came to the hospital with the chief complaints of fever and palpitations. The peak body temperature was 38.7°C (101.66°F). Heart rate was 110 bpm, while blood pressure was in the normal range. Antibiotics and antiviral therapies were ineffective. The levels of blood IL-6, C-reactive protein (CRP), alkaline phosphatase (ALP), platelets (PLT), glutamyltransferase (GGT), fibrinogen, and D-dimer were all elevated. Infectious diseases, auto-immune diseases, and hematological malignancy were all excluded. Nearly 10 years ago, a large retroperitoneal mass of the patient was detected by accident. Fortunately, there have been no special symptoms for the past 10 years after regular follow-up. After admission this time, PET-CT was performed. A large confounding density mass at the upper part of the abdominal and retroperitoneal area was seen, and the possibility of paraganglioma was considered. However, biochemical assays for blood and urine catecholamine and their metabolites including adrenaline, norepinephrine, 3-methoxytyramine, methoxyepinephrine, methoxynorepinephrine, and vanillylmandelic acid were all in normal range in spite of mild elevated dopamine with no significance. The whole-exome capture and sequencing of the genomic DNA of the patient showed a heterozygous mutation in the coding site of KIF1B gene (Coding: NM_015047.3:c.4660G>C, Mutation: p.Val1554Leu; chromosomal location was chr1: 10428570). The mutation at this locus of KIF1B has not been reported previously. The patient refused the surgical treatment. Because the mass burdens several important organs including the pancreas, the risk of surgery was high. Doxazosin was then administered to the patient. After taking doxazosin, the symptoms disappeared rapidly. Body temperature returned to normal range in 3 days. Heart rate decreased to approximately 90 bpm. In the following days, the levels of IL-6, CPR, ALP, platelets, GGT fibrinogen, and D-dimer continued to decrease. After 63 days of taking doxazosin, IL-6 level was completely normal. After 190 days of medication, hemoglobin (Hb) and GGT levels also returned to the normal range. After 1 year onset, the patient again underwent a blood test. Almost all blood indexes were in the normal range including IL-6.

KEYWORDS

**paraganglioma, interleukin-6, fever, KIF1B gene, single gene mutation**

## Introduction

Paraganglioma and pheochromocytoma were a family of rare neuroendocrine tumors. They arise from the sympathetic/parasympathetic neural ganglia and chromaffin cells of the adrenal medulla, respectively. The clinical manifestations include hypertension, headache, and palpitations, but owing to different loci, the manifestations are heterogeneous (1–4). Paraganglioma not only diversified its symptoms, but also occurs in various locations. It can appear in the retroperitoneum, duodenum, and even the middle ear (5). In previous case reports, despite the variety of symptoms and different locations of paraganglioma, patients would have a significant increase in catecholamines or their metabolites, along with an elevation of cytokines, including IL-1, IL-6, and TNF-α (6). However, we diagnosed a patient with retroperitoneal paraganglioma with only an increase in serum IL-6 levels without elevated levels of catecholamines and their derivatives. The patient presented only with a monogenic mutation in KIF1B. This patient had only fever and palpitations as the main symptoms, without hypertension and headache. After treatment with doxazosin, the symptoms disappeared and abnormal indicators returned to normal levels in this case report.

## Case presentation

A 65-year-old male patient presented to our hospital due to fever, palpitations, and fatigue in February 2022. The peak body temperature of the patient was 38.7°C. There is no hypertension but tachycardia was present during physical examination at admission time. Blood routine test showed that neutrophilic granulocyte was slightly higher than the normal range. To rule out infectious diseases, bacteria blood cultures, hepatitis, HIV, syphilis, *Brucella*, and COVID-19-related indexes were tested. Chest CT scanning did not give any evidence of respiratory infectious disease. Even high-throughput DNA and RNA sequencing of pathogenic microorganisms was also checked, but no positive results were obtained. Rheumatic and autoimmune diseases were also excluded.

The patient had anemia, and the hemoglobin level was very low. The blood routine showed microcytic hypochromic anemia: 70 g/L↓ (reference range: 110–160 g/L), red blood cell level 2.96 × $10^{12}$/L↓ (reference range: 2.5–5.5 × $10^{12}$/L), MCV 79.8 fl↓ (reference range: 80–100 fl), MCH 24.2 pg↓ (reference range: 27–34 pg), and MCHC 304 g/L↓ (reference range: 320–360 g/L). Therefore, after further improving the inspection, it was found that the iron level was 2.5 μmol/L↓ (reference range: 10.6–36.7 μmol/L) and the ferritin level was 472 ng/ml↑ (reference range: 21.81–274.66 ng/ml). Bone marrow image analysis showed proliferative anemia, decreased iron in iron staining, negative bone marrow culture, and no abnormal cells such as plasma cells and hemophagocytic cells, suggesting that the anemia was only caused by chronic wasting disease. Therefore, anemia and fever caused by rare blood diseases such as Castleman disease and HLH were excluded. We also found that the patient's CRP was significantly elevated: 117 mg/L↑ (reference range: 0–6 mg/L). We tried to give the patient a variety of antibiotics such as cephalosporins, carbapenems, and antiviral drugs, but the patient's fever did not improve.

The patient's abdominal ultrasound revealed a large mass in the abdominal cavity. Reviewing the patient's medical history, because of the routine physical examination, the patient indicated a huge abdominal mass by CT in December 2012, whose size was approximately 105 mm × 68 mm. The patient was hospitalized in the oncology department and interventional department of our hospital in January 2013, and the improved three-dimensional enhanced CT imaging of the abdomen suggested space-occupying lesions in the right abdominal cavity and retroperitoneal area with rich blood supply. The possibility of paraganglioma or vascular lesions was considered. The size was approximately 100 × 140 mm, which seemed to have unclear boundary with the inferior vena cava. The surrounding tissues were compressed and displaced, and there was no indication of lymphadenopathy. At this time, the blood routine, coagulation, and liver function of the patient were normal, and there were no symptoms of fever and palpitation. The patient's gastroscopy showed that there were nodular bulges in the gastric body, surface erosion, rigidity of the surrounding mucosa, easy bleeding when touching, and narrow gastric cavity in the lesion area. However, pathological examination at the gastric bulge only suggested gastric fundus gland polyps. Because the patient had no obvious discomfort, the paraganglioma volume was very large, multiple organs were compressed, and the operation was high risk, the patient and his family members did not agree to the operation.

In September 2021, the patient was hospitalized in the dermatology department due to a large area of eczema. After treatment with betamethasone injection, he developed systemic edema, dyspnea, and palpitations. Then, the patient was transferred to the cardiology department for diagnosis and treatment. Cardiac color ultrasound suggested that the right chamber of the right atrium was significantly enlarged, with lax tricuspid closure with severe regurgitation. The main pulmonary artery and branches were wider, with pulmonary hypertension (severe). The systolic pressure of pulmonary artery was approximately 96 mmHg, and the right heart function was reduced. The patient's heart rate was 96 bpm. The blood gas analysis showed a $pO_2$ level of 54 mmHg (reference range: 80–100 mmHg) and a $pCO_2$ level of 34 mmHg (reference range: 35–45 mmHg), which was type I respiratory failure. Blood findings indicated anemia, unprompted infection, increased platelet count, abnormal liver function, and increased CRP levels. Right heart catheterization was performed, with a measured pulmonary artery pressure of 44/22/31 mmHg, a total pulmonary resistance of 5.0 wood units, and a pulmonary vascular resistance of 3.06 wood units. The pulmonary angiography indicated that bilateral pulmonary artery blood flow slowed down, venous reflux slowed down, and distal occlusion of the right pulmonary artery was A10.

After discharge from the cardiology department, the patient continued oral rivaroxaban 10 mg daily for anticoagulation and polysaccharide iron complex 0.3 g daily to correct anemia. However, in January 2022, the patient had a hemoglobin level of 93 g/L↓ and had no significant improvement in anemia, and coagulation suggested a plasma fibrinogen level of 5.3 g/L↑ (2–5 g/L). The patient's alkaline phosphatase was 516 U/L↑ (reference

range: 45–125 U/L) and glutamyltransferase was 112 U/L↑ (reference range: 0–60 U/L). One month after, the patient had spontaneously discontinued the iron polysaccharide complex. The reexamination found that the anemia was significantly aggravated, including hemoglobin: 73 g/L↓ (reference range: 60–110 g/L), RBC count: 3.15 × $10^9$/L↓ (reference range: 3.5–5.5 × $10^9$/L), blood cell ratio measurement: 24.9%↓ (reference range: 37%–50%), MCV: 79 fl (reference range: 80–100 fl), MCH: 23.8pg↓ (reference range: 27–34 pg), and MCHC: 301 g/L↓ (reference range: 320–360 g/L), indicating small cell hypochromic anemia.

In February 2022, the patient was hospitalized again due to fever, palpitations, and fatigue. Considering the patient's previous medical history, the relevant examinations were given. Then, the patient underwent PET-CT examination. 18F-fluorodeoxyglucose (FDG) positron emission tomography/PET-CT showed increased uptake of FDG in the abdominal and retroperitoneal (liver and pancreatic) mass without metastases; the possibility of paraganglioma, and its internal calcification, was considered. The interface size of the mass was about 148mm*100mm, and the upper and lower diameter was about 155mm (Figure 1). The demarcation of the mass from the surrounding tissue was unclear, and the surrounding tissue (including: gallbladder, pancreas, stomach, intestinal tube) was pressure-displaced. The patient had the retroperitoneal lymph nodes enlargement which radioactive uptake increased, and the largest lymph node was about 22mm*15mm. The IL-6 and CRP levels were significantly increased, but they showed no abnormalities in IL-1, TNF-α, sCD25, and VEGF. Plasma dopamine was mildly elevated, which is 253.6 pmol/L↑ (reference range: ≤195.7 pmol/L), and this abnormal level may be affected by factors such as food or stress. It did not exceed the normal value twice, so it was not considered as a meaningful clinical change. The urinary dopamine was also not elevated. There were no abnormalities in adrenaline, norepinephrine, 3-methoxytyramine, methoxyepinephrine, methoxynorepinephrine, and Vanillylmandelic acid in peripheral blood and 24-h urine specimens (Table 1). At this time, fibrinogen, D-dimer, ALP, GGT, and other indicators were significantly increased (Figure 2). Whole exome capture and sequencing of genomic DNA indicated that it was the KIF1B gene mutation, and the chromosomal location was chr1: 10428570, which was a heterozygous gene. This is a mutation at a single-gene rare locus.

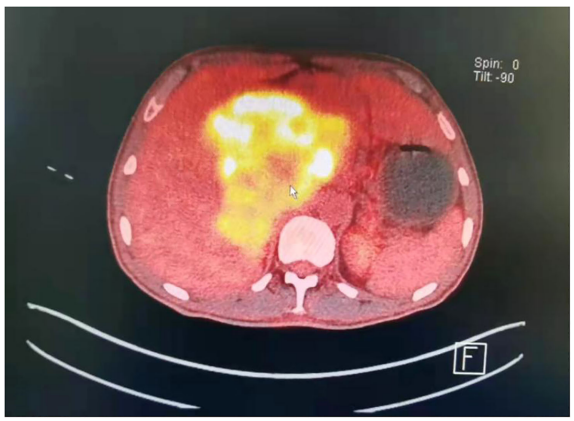


FIGURE 1
PET-CT, The paraganglioma was in the abdominal and retroperitoneal (liver and pancreatic) area. The interface size of the mass was approximately 148 mm * 100 mm, and the upper and lower diameter was approximately 155 mm.

Because the patient and his family refused surgery, doxazosin was administered at 4 mg daily for treatment. The anti-inflammatory and antiviral treatment was stopped. The patient's temperature gradually decreased and returned to normal after 3 days. After 7 days, the levels of IL-6, CPR, ALP, platelets, and GGT decreased significantly, and even fibrinogen and D-dimer returned to normal levels. After 63 days of doxazosin treatment, IL-6 levels became completely normal, albumin (ALB) returned to normal, and anemia was greatly improved. After 190 days of medication, IL-6 continued to have normal levels, and hemoglobin and GGT indicators returned to normal. Meanwhile, the patient's CRP, ALP, and platelets continued to decline and the patient's symptoms of fever and palpitations did not reappear. After about 1 year, the patient's blood indicators were examined again, and all the indicators were normal including IL-6 (Figure 2).

## Diagnosis

The patient was febrile due to the increased IL-6 levels caused by the retroperitoneal paraganglioma, but both catecholamines and their metabolites were normal. The patient had a rare single-gene mutation: the KIF1B gene.

## Treatment and outcome

Antibiotic and antiviral therapy were stopped. The patient was given doxazosin 4 mg daily since 4 February 2022. After 3 days of taking doxazosin, the body temperature of the patient gradually decreased and returned to normal range. The heart rate decreased to approximately 90 bpm. After 7 days, the levels of IL-6, CPR, ALP, platelets, and GGT decreased significantly, and even fibrinogen and D-dimer returned to normal levels. After 63 days of doxazosin treatment, IL-6 level was completely normal, albumin returned to normal levels, and anemia was greatly improved. After 190 days of medication, IL-6 continued to have normal levels, and hemoglobin and GGT indicators returned to normal. Meanwhile, the patient's CRP, ALP, and platelets continued to decline and the patient's symptoms of fever and palpitations did not reappear. Several days ago, after 1 year onset, the patient again underwent a blood test. Almost all blood indexes were in the normal range including IL-6 (Figure 2).

## Discussion

Pheochromocytoma (PCC) and paraganglioma (PGL) occur in 2 to 8 per million people (1). Paragangliomas (PGLs) are rare neuroendocrine tumors that arise from chromaffin cells of extra-adrenal paraganglia usually with persistent or intermittent hypertension accompanied by headache and/or palpitations (1). This case had symptoms of fever and palpitations, without

10.3389/fendo.2023.1226468

TABLE 1 Levels of cytokine, related proteins, serum, and urinary catecholamine before treatment by doxazosin.

| | Normal values | Before treatment |
|---|---|---|
| IL-6 (pg/ml)(≤5.9) | ≤5.9 | 32.4↑; |
| IL-1β (pg/m) | ≤5.0 | ≤5.0 |
| TNF-α (pg/m) | ≤8.1 | 7.89 |
| CD-25 (pg/m) | ≤6,400 | 1,896 |
| VEGF(pg/m) | ≤160.00 | 112.11 |
| **Plasm** | | |
| Dopamine (pmol/L) | ≤195.7 | 253.6↑ |
| Epinephrine (pmol/L) | ≤605.4 | ≤55.5 |
| Norepinephrine (pmol/L) | 414.0–4,435.5 | 2,864.9 |
| 3-Mexoxytyramine (nmol/L) | ≤0.18 | ≤0.08 |
| Metanephrine (pmol/L) | ≤0.50 | ≤0.08 |
| Normetanephrine (pmol/L) | ≤0.90 | 0.35 |
| **Urine** | | |
| Dopamine (nmol/24 ) | 655.0–3,425.0 | 1,788.54 |
| Epinephrine (nmol/24 ) | 8.45–102 | ≤16.0 |
| Norepinephrine (nmol/24 ) | 68.9–378.0 | 179.08 |
| 3-Mexoxytyramine (nmol/24 ) | ≤216 | 28 |
| Metanephrine (nmol/24 ) | ≤312 | 85 |
| Normetanephrine (nmol/24 ) | ≤382 | 102 |
| Vanillylmandelic acid (mg/24 ) | ≤12.0 | 4.8 |

↑ indicates that the patient's IL-6 and dopamine levels were above the normal values before treatment with doxazosin.

hypertension. Cases of paraganglioma presenting with unexplained fever as the main symptom were very rare. In addition to secreting large amounts of catecholamines, paragangliomas can also secrete a variety of cytokines including IL-6 that mediates inflammatory response and induces the production of acute phase proteins such as CRP and fibrinogen (7). The reasons for the increase in IL-6 levels might be indirect results of high levels of circulating norepinephrine, and sometimes rarely secreted by the tumor (8). In our case, a significant increase in IL-6 was only seen from biochemical assays, while blood and urine catecholamines or their metabolites were in the normal range. The increase in IL-6 was secreted by the tumor directly. Long-term IL-6 secretion resulted in changes in laboratory

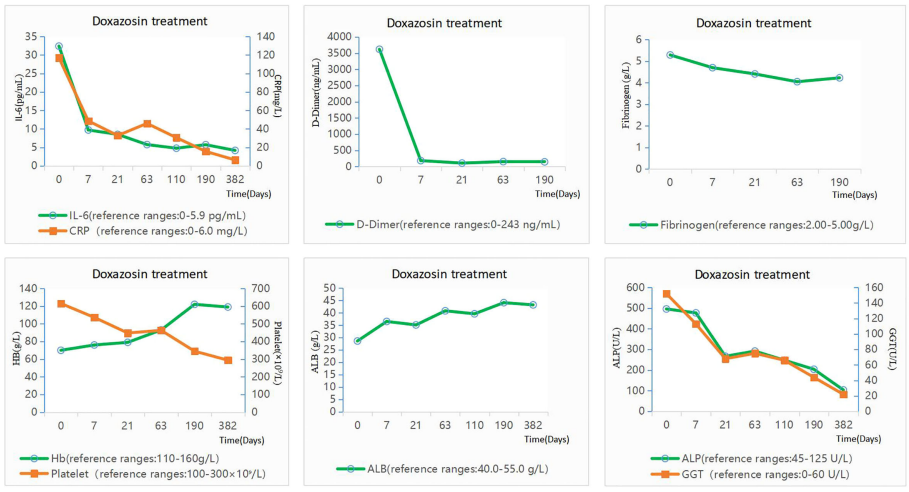


FIGURE 2
Changes in laboratory data before and after doxazosin treatment. The patient was given doxazosin 4 mg daily.

tests (CRP, fibrinogen, D-dimer, platelets, ALP, and GGT) and symptoms (fever, palpitation, fatigue, and anemia) in our case. We considered that elevated IL-6 may be associated with retroperitoneal paraganglioma secreting with IL-6 for the patients. A total of 42 cases of pheochromocytoma or paraganglioma with elevated IL-6 have been reported (9). As in our case, only IL-6 was elevated, and no abnormalities in catecholamine and its metabolites have not been reported.

The 5-year survival rate of PPGL is as high as 50% to 70% (10), which means the disease can be considered a chronic disease in some conditions. Moreover, regardless of PPGL type (benign or malignant), long-term survival could not be achieved even after surgical resection, and the recurrence rate is high (11). For some tumors that cannot be safely removed completely, other treatments, such as oral drugs, are required besides surgery to control bio-active substance secretion and the progressive growth of tumor. In our case, the large tumor lying in the abdominal cavity and retroperitoneum invaded peripheral tissues including pancreas and intestines. After assessing the risk of operation and having no significant changes in the size of the mass by comparing with CT images 10 years ago, oral drugs were the first and safest choice for the patients. Doxazosin was selected for the patients because alpha-blockers are currently the most common oral drugs before and after surgery for paraganglioma.

Different types of gene mutations in PPGL patients are directly related to the mass location, and possibly to metastasis and the variety of clinical manifestations. To date, over 20 gene mutations, including EGLN1/PHD2, KIF1B, and IDH1 genes, are thought to potentially contribute to the pathogenesis of PPGL (1). KIF1B gene mutation was noticed in recent reports, which suggested that KIF1B was the second most frequently mutated gene and often combined with other gene mutations in PPGL cases (12). To date, only two cases with KIF1B single gene mutation in PPGL were reported (in 2017 and 2022), both with elevated levels of blood and urine epinephrine and norepinephrine (12, 13). The whole-exome capture and sequencing of the genomic DNA of our patient only showed a heterozygous mutation in the coding site of KIF1B gene (Coding: NM_015047.3:c.4660G >C, Mutation: p.Val1554Leu; chromosomal location was chr1: 10428570). The single mutation at this locus of KIF 1 B has not been previously reported.

There is the question that the tumor had been existing silently over 10 years. What then triggered the eruption of the "silent volcano"? Reviewing the history carefully, we found that the patients had been treated with betamethasone for a large area of eczema 4 months starting in September 2021, which was 4 months before the appearance of fever in February 2022. Corticosteroids are one of the reasons that could cause the paraganglioma to "awaken" from its silent state (1, 4).

## Conclusions

This case reports a rare case of retroperitoneal paraganglioma, which suddenly presented with unexplained fever after 10 years of tumor silence. The case only showed a significant increase in the level of IL-6, and there were no clinically meaningful increases in other catecholamines and metabolites. After the patient was treated with the alpha-blocker doxazosin, the level of IL-6 dropped significantly, the body temperature returned to normal, and the heart rate also improved. Paraganglioma that only secretes IL-6 as the main manifestation is extremely rare at present, which suggests that clinicians should understand the secretion mode of this rare paraganglioma and the clinical symptoms of patients, and should make a differential diagnosis in patients with unexplained fever, as well as consider the possibility of the existence of paraganglioma. The application of doxazosin may become a long-term and effective non-surgical means of treating paraganglioma, and provide a new therapeutic direction for the treatment of paraganglioma. In the gene exon sequencing of this case, it was found that the patient had a rare KIF1B single-gene mutation. Although we could not clearly prove its pathogenicity, we provided some evidence for future clinical and genetic data, which may be helpful for future pathogenicity studies of this gene in PPGL disease.

## Data availability statement

The datasets presented in this study can be found in online repositories. The names of the repository/repositories and accession number(s) can be found in the article/supplementary material.

## Ethics statement

The studies involving humans were approved by The Medical Ethics Committee of the Second Affiliated Hospital of Harbin Medical University. The studies were conducted in accordance with the local legislation and institutional requirements. The participants provided their written informed consent to participate in this study. Written informed consent was obtained from the individual(s) for the publication of any potentially identifiable images or data included in this article. Written informed consent was obtained from the participant/patient(s) for the publication of this case report.

## Author contributions

CW is responsible for data collection, collation, literature review and article writing, the conception of the article, and participated in the whole treatment process of the patients. CC is the corresponding author of this case report. CC was responsible for the diagnosis and treatment of the case, and the conception of this article. CC and CW have discussed the article repeatedly. MG is responsible for caring for the patients in the case and observing the patient's condition changes. SZ is responsible for the format proofreading of this paper. All authors contributed to the article and approved the submitted version.

## Conflict of interest

The authors declare that the research was conducted in the absence of any commercial or financial relationships that could be construed as a potential conflict of interest.

## Publisher's note

All claims expressed in this article are solely those of the authors and do not necessarily represent those of their affiliated organizations, or those of the publisher, the editors and the reviewers. Any product that may be evaluated in this article, or claim that may be made by its manufacturer, is not guaranteed or endorsed by the publisher.

## References

1. Garcia-Carbonero R, Matute Teresa F, Mercader-Cidoncha E, Mitjavila-Casanovas M, Robledo M, Tena I, et al. Multidisciplinary practice guidelines for the diagnosis, genetic counseling and treatment of pheochromocytomas and paragangliomas. *Clin Transl Oncol* (2021) 23(10):1995–2019. doi: 10.1007/s12094-021-02622-9

2. Geroula A, Deutschbein T, Langton K, Masjkur J, Pamporaki C, Peitzsch M, et al. Pheochromocytoma and paraganglioma: clinical feature-based disease probability in relation to catecholamine biochemistry and reason for disease suspicion. *Eur J Endocrinol* (2019) 181:409–20. doi: 10.1530/EJE-19-0159

3. Whalen RK, Althausen AF, Daniels GH. Extra-adrenal pheochromocytoma. *J Urol.* (1992) 147:1–10. doi: 10.1016/s0022-5347(17)37119-7

4. Lenders JW, Duh QY, Eisenhofer G, Gimenez-Roqueplo AP, Grebe SK, Murad MH, et al. Pheochromocytoma and paraganglioma: an endocrine society clinical practice guideline. *J Clin Endocrinol Metab* (2014) 99:1915–42. doi: 10.1210/jc.2014-1498

5. Kawanabe S, Katabami T, Oshima R, Yanagisawa N, Sone M, Kimura N. A rare case of multiple paragangliomas in the head and neck, retroperitoneum and duodenum: A case report and review of the literature. *Front Endocrinol (Lausanne)* (2023) 13:1054468. doi: 10.3389/fendo.2022.1054468

6. Ciacciarelli M, Bellini D, Laghi A, Polidoro A, Pacelli A, Giulia Bottaccioli A, et al. IL-6-producing, noncatecholamines secreting pheochromocytoma presenting as fever of unknown origin. *Case Rep Med* (2016) 2016:3489046. doi: 10.1155/2016/3489046

7. Shimizu C, Kubo M, Takano K, Takano A, Kijima H, Saji H, et al. Interleukin-6 (IL-6) producing phaeochromocytoma: direct IL-6 suppression by non-steroidal anti-inflammatory drugs. *Clin Endocrinol* (2001) 54(3):405–10. doi: 10.1046/j.1365-2265.2001.01082.x

8. Yarman S, Soyluk O, Altunoglu E, Tanakol R. Interleukin-6-producing pheochromocytoma presenting with fever of unknown origin. *Clinics (Sao Paulo)* (2011) 66(10):1843–5. doi: 10.1590/s1807-59322011001000028

9. Meijs AC, Schroijen MA, Snel M, Corssmit EPM. Interleukin-6 producing pheochromocytoma/paraganglioma: case series from a tertiary referral centre for pheochromocytomas and paragangliomas. *J Endocrinol Invest* (2021) 44(10):2253–9. doi: 10.1007/s40618-021-01532-5

10. Fishbein L, Del Rivero J, Else T, Howe JR, Asa SL, Cohen DL, et al. The north american neuroendocrine tumor society consensus guidelines for surveillance and management of metastatic and/or unresectable pheochromocytoma and paraganglioma. *Pancreas.* (2021) 50(4):469–93. doi: 10.1097/MPA.0000000000001792

11. Amar L, Servais A, Gimenez-Roqueplo A-P, Zinzindohoue F, Chatellier G, Plouin Pierre-François. Year of diagnosis, features at presentation, and risk of recurrence in patients with pheochromocytoma or secreting paraganglioma. *J Clin Endocrinol Metab* (2005) 90(4):2110–6. doi: 10.1210/jc.2004-1398

12. Evenepoel L, Helaers R, Vroonen L, Aydin S, Hamoir M, Maiter D, et al. KIF1B and NF1 are the most frequently mutated genes in paraganglioma and pheochromocytoma tumors. *Endocr Relat Cancer* (2017) 24(8):L57–61. doi: 10.1530/ERC-17-0061

13. Nezu M, Hirotsu Y, Amemiya K, Katsumata M, Watanabe T, Takizawa S, et al. A case of juvenile-onset pheochromocytoma with KIF1B p.V1529M germline mutation. *Endocr J* (2022) 69(6):705–16. doi: 10.1507/endocrj.EJ21-0475

frontiers | Frontiers in Endocrinology

TYPE Review
PUBLISHED 05 October 2023
DOI 10.3389/fendo.2023.1274239

Check for updates

OPEN ACCESS

EDITED BY
Ichiro Abe,
Fukuoka University Chikushi Hospital, Japan

REVIEWED BY
Yuto Yamazaki,
Tohoku University, Japan
Alice Helena Dutra Violante,
Federal University of Rio de Janeiro, Brazil

*CORRESPONDENCE
Yishu Wang
wangys@jlu.edu.cn
Honglan Zhou
hlzhou@jlu.edu.cn

RECEIVED 08 August 2023
ACCEPTED 25 September 2023
PUBLISHED 05 October 2023

CITATION
Wang Y, Liu B, Li F, Zhang Y, Gao X, Wang Y and Zhou H (2023) The connection between tricarboxylic acid cycle enzyme mutations and pseudohypoxic signaling in pheochromocytoma and paraganglioma. *Front. Endocrinol.* 14:1274239. doi: 10.3389/fendo.2023.1274239

COPYRIGHT
© 2023 Wang, Liu, Li, Zhang, Gao, Wang and Zhou. This is an open-access article distributed under the terms of the Creative Commons Attribution License (CC BY). The use, distribution or reproduction in other forums is permitted, provided the original author(s) and the copyright owner(s) are credited and that the original publication in this journal is cited, in accordance with accepted academic practice. No use, distribution or reproduction is permitted which does not comply with these terms.

# The connection between tricarboxylic acid cycle enzyme mutations and pseudohypoxic signaling in pheochromocytoma and paraganglioma

Yuxiong Wang[1], Bin Liu[1], Faping Li[1], Yanghe Zhang[2], Xin Gao[1], Yishu Wang[2]* and Honglan Zhou[1]*

[1]Department of Urology, The First Hospital of Jilin University, Changchun, Jilin, China, [2]Key Laboratory of Pathobiology, Ministry of Education, Jilin University, Changchun, Jilin, China

Pheochromocytomas and paragangliomas (PPGLs) are rare neuroendocrine tumors originating from chromaffin cells, holding significant clinical importance due to their capacity for excessive catecholamine secretion and associated cardiovascular complications. Roughly 80% of cases are associated with genetic mutations. Based on the functionality of these mutated genes, PPGLs can be categorized into distinct molecular clusters: the pseudohypoxia signaling cluster (Cluster-1), the kinase signaling cluster (Cluster-2), and the WNT signaling cluster (Cluster-3). A pivotal factor in the pathogenesis of PPGLs is hypoxia-inducible factor-2α (HIF2α), which becomes upregulated even under normoxic conditions, activating downstream transcriptional processes associated with pseudohypoxia. This adaptation provides tumor cells with a growth advantage and enhances their ability to thrive in adverse microenvironments. Moreover, pseudohypoxia disrupts immune cell communication, leading to the development of an immunosuppressive tumor microenvironment. Within Cluster-1a, metabolic perturbations are particularly pronounced. Mutations in enzymes associated with the tricarboxylic acid (TCA) cycle, such as succinate dehydrogenase (SDHx), fumarate hydratase (FH), isocitrate dehydrogenase (IDH), and malate dehydrogenase type 2 (MDH2), result in the accumulation of critical oncogenic metabolic intermediates. Notable among these intermediates are succinate, fumarate, and 2-hydroxyglutarate (2-HG), which promote activation of the HIFs signaling pathway through various mechanisms, thus inducing pseudohypoxia and facilitating tumorigenesis. SDHx mutations are prevalent in PPGLs, disrupting mitochondrial function and causing succinate accumulation, which competitively inhibits α-ketoglutarate-dependent dioxygenases. Consequently, this leads to global hypermethylation, epigenetic changes, and activation of HIFs. In FH-deficient cells, fumarate accumulation leads to protein succination, impacting cell function. FH mutations also trigger metabolic reprogramming towards glycolysis and lactate synthesis. IDH1/2 mutations generate D-2HG, inhibiting α-ketoglutarate-dependent dioxygenases and stabilizing HIFs. Similarly, MDH2 mutations are associated with HIF stability and pseudohypoxic response. Understanding the intricate relationship between metabolic enzyme mutations in the TCA cycle and pseudohypoxic signaling is crucial for unraveling

the pathogenesis of PPGLs and developing targeted therapies. This knowledge enhances our comprehension of the pivotal role of cellular metabolism in PPGLs and holds implications for potential therapeutic advancements.

KEYWORDS

pheochromocytoma, paraganglioma, pseudohypoxia, VHL/HIF axis, genetic mutations, tricarboxylic acid cycle, metabolic reprogramming

## Introduction

Pheochromocytomas (pcc) and paragangliomas (PGL) (PPGLs) are infrequent neuroendocrine tumors deriving from chromaffin cells. Pheochromocytoma originates in the adrenal medulla, accounting for approximately 80%-85% of cases, while paraganglioma arises externally from sympathetic paraganglia dispersed throughout the body, constituting around 15%-20% of cases (1–3). Despite their low incidence rate (roughly 6.6 cases per million individuals annually) (4), these tumors bear noteworthy clinical significance due to their potential to induce excessive catecholamine secretion, precipitating perilous cardiovascular complications and myocardial degenerative alterations. In the latest World Health Organization guidelines, all PPGLs are now recommended for lifelong follow-up due to their metastatic potential, similar to epithelial neuroendocrine tumors (5–7).

Approximately 80% of PPGLs are linked to genetic mutations, often indicating a genetic predisposition (2, 8). Gene expression profiling enables the classification of PPGLs into three distinct clusters based on their molecular characteristics: the pseudohypoxia signaling cluster (Cluster-1), the kinase signaling cluster (Cluster-2), and the WNT signaling cluster (Cluster-3). Cluster-1 further divides into subclusters 1a and 1b. Cluster-1a comprises mutations in genes associated with the tricarboxylic acid cycle (SDHx, FH, MDH2, GOT2, SLC25A11, IDH, DLST, SUCLG2), while Cluster-1b encompasses mutations in genes constituting the hypoxia signaling pathway (PHD1/2, VHL, HIF2A/EPAS1) (9–11). Cluster-1 notably exhibits a significant enhancement of pseudohypoxic signaling pathways, resulting in heightened angiogenesis and metabolic anomalies during tumor development. Cluster-1a represents approximately 10%-15% of cases, while Cluster-1b accounts for approximately 15%-20% of PPGLs. Importantly, Cluster-2 within the PPGLs group demonstrates a marked increase in gene expression related to kinases. This involves critical mutations in genes associated with the PI3K/mTORC1 pathway and receptor kinase signaling, such as RET, NF1, H-RAS, K-RAS, TMEM127, and MAX, implying their potential significance in regulating tumor growth and metastasis. Cluster-2 constitutes approximately 50%-60% of PPGLs cases. Cluster-3 is characterized by the activation of the WNT signaling pathway, potentially contributing to increased cellular proliferation and invasiveness. Notably, Cluster-3 accounts for approximately 5%-10% of PPGLs cases and also includes tumors with mutations in the CSDE1 and the MAML3 fusion genes (2, 12, 13). In the three clusters, Cluster 1 exhibits the most prominent risk of metastasis (9). Additionally, among the cases in Cluster 1, there is typically an elevation in norepinephrine levels, which is associated with a deficiency in phenylethanolamine N-methyltransferase (13). This results in a tendency for such patients to have persistent high blood pressure (14). These findings underscore our continued focus on Cluster 1.

Roughly 40% of PPGLs patients carry a germline mutation in one of over 20 known susceptibility genes. In an additional 30-40% of sporadic disease patients, somatic mutations in the same genes or other genes that drive tumorigenesis can be identified (14, 15). Multiple studies indicate that Cluster 1a is almost exclusively germline-mutated (100%), while Cluster-1b has 25% of cases with germline mutations (13, 16). Among PPGLs, the top three genes with germline mutations are SDHB (10.3%), SDHD (8.9%), and VHL (7-10%), while the genes with the highest somatic mutation frequencies are VHL (10%) and HIF2A (5-7%), with germline or somatic mutations in other genes being less than 2% (15, 17–19). This highlights the significant role of germline mutations in the pathogenesis of Cluster-1 PPGLs. Clinical studies on sporadic PPGLs show a significantly higher occurrence of germline mutations associated with multiple PPGLs compared to isolated PPGLs (54% *vs.* 11.5%). Moreover, the research suggests that the risk of germline mutations in PPGLs located outside the adrenal gland is significantly higher than those within the adrenal gland (14, 20). Specifically for Cluster 1, PPGLs associated with mutations in TCA metabolic enzyme genes (Cluster-1a) are mainly located outside the adrenal gland. For example, SDHA mutations are linked to sympathetic and parasympathetic PGLs (21). SDHB and SDHC mutations are primarily observed in sympathetic/parasympathetic PGLs, but are less common in PCC (22). SDHD and SDHAF2 mutation-related PGLs are predominantly found in the head and neck region, with lower incidence in other extrarenal locations or within the adrenal gland (23, 24). Tumors associated with FH mutations are found both inside and outside the adrenal gland. In Cluster-1b, VHL mutations causing PCC result in 50% of cases being bilateral and occasionally occurring outside the adrenal gland. HIF2A/EPAS1 mutations may lead to tumors in both intra- and extra-adrenal locations (14).

The hypoxia-inducible factor-2α (HIF2α) protein gets upregulated in cells under normal oxygen conditions, culminating in the activation of downstream transcriptional processes, recognized as pseudohypoxia. Activation of the hypoxia response pathway confers advantages to tumor cell growth and adaptation to

adverse microenvironments (25). Studies have elucidated heightened pseudohypoxic signaling in hereditary renal cell carcinoma, giving rise to the upregulation of downstream signaling molecules such as glucose transporter 1 and vascular endothelial growth factor (VEGF), thereby fostering augmented energy metabolism and proliferative capacity in tumor cells (26). Pseudohypoxic signaling prompted by tumor cells modifies the communication patterns of immune cells, instigating alterations in immune cell metabolism that incline towards the attenuation of surveillance function in innate immune cells and the fostering of an immunosuppressive microenvironment (25, 27). Specimens of neuroblastoma and glioma have evinced the prevalence of elevated HIF2α expression and a concomitant display of nascent characteristics, signifying the presence of a pseudohypoxic niche in these tumors that correlates with malignancy (28). The instigation of pseudohypoxia through HIFs signaling also plays a pivotal role in non-neoplastic ailments. The buildup of reactive oxygen species (ROS) in lung tissue engenders HIFs activation in fibroblasts, disrupting the structural integrity of the extracellular matrix and exacerbating the progression of pulmonary fibrosis (29). In the course of the aging process, diminished nuclear NAD+ levels impede the activity of nuclear SIRT1, thus suppressing the pVHL ubiquitin-proteasome degradation pathway. This engenders heightened stability of HIF1α within the cell and the concomitant emergence of HIF1α-induced pseudohypoxia. The pseudohypoxic state engendered by HIF1α disrupts intracellular signaling between the nucleus and mitochondria, thereby impairing mitochondrial function and accelerating cellular senescence and demise (30).

Pseudohypoxia has been meticulously scrutinized and observed in the context of PPGLs. Notwithstanding their typical highly vascularized nature, PPGLs are characterized by a conspicuous upregulation of hypoxia signaling pathways, particularly within Cluster-1, thereby fueling the onward progression of tumors (25, 31–33). The principalstay treatment for PPGLs remains surgical intervention, as effective therapeutic modalities for metastatic tumors are presently scarce (34). A profound comprehension of the hypoxia-related signaling mechanisms underpinning PPGLs pathogenesis is imperative for the development and assessment of molecularly targeted therapies tailored to the diverse subtypes of PPGLs, encompassing the intricacies of the tumor microenvironment (TME). This comprehensive review seeks to illuminate how mutations in metabolic enzymes within Cluster 1a of the tricarboxylic acid cycle impinge upon the VHL/HIF signaling pathway, consequently contributing to the genesis of PPGLs. This dissection facilitates an enhanced understanding of the pivotal role of cellular metabolism in the realm of PPGLs, thereby engendering substantial implications for the refinement of extant therapeutic modalities.

## Dysregulation of the VHL/HIF signaling axis in PPGLs

The intricate interplay between the VHL tumor suppressor and HIFs signaling axis bears a profound relevance to the emergence of PPGLs (35, 36). Central to this dynamic is the orchestration of HIFs' stability by oxygen concentration within the microenvironment (see Figure 1). Under normoxic conditions, prolyl hydroxylation of HIF1α/HIF2α by oxygen-dependent prolyl hydroxylases (PHDs) triggers subsequent recognition by the E3 ubiquitin ligase VHL protein. This culminates in selective ubiquitination and proteasomal degradation of hydroxylated HIFα subunits. Conversely, under hypoxia, PHDs activity inhibition leads to non-hydroxylated HIFα subunit accumulation. Following nuclear translocation, heterodimerization with HIF1β ensues, facilitating transcriptional complex formation with coactivators p300/CBP (25, 37). This complex binds to hypoxia response elements, activating transcription of genes such as VEGF, platelet-derived growth factor (PDGF), and glucose transporter (GLUT) (11, 38, 39). Such adaptations promote metabolic reprogramming in hypoxic cells, characterized by elevated glucose uptake, anaerobic glycolysis, diminished mitochondrial mass, and heightened energy provisioning, thus fostering tumorigenic progression. Tumors frequently exhibit an intriguing phenomenon whereby normoxic conditions lead to an anomalous stabilization of HIFs within tumor cells. This multifaceted phenomenon results from diverse influences, ultimately culminating in the accumulation or heightened functional activity of HIFs. Consequently, this dynamic process upregulates the expression of HIFs target genes, remarkably mimicking the pathophysiological response seen in hypoxic states. Coined as "pseudo-hypoxia," this intriguing state prompts notable cellular transitions, including epithelial-mesenchymal transition, augmented tumor cell stemness, thereby effectively fueling the cascade of tumorigenic initiation, progression, and the potentiation of malignant attributes (40, 41).

The regulatory apparatus governing the VHL/HIF axis is intricate, encompassing a myriad of factors. Within the landscape of sporadic PPGLs, a significant subset, approximately 14%, manifests somatic VHL mutations (42). While the precise mechanistic underpinnings characterizing VHL dysfunction and its structural aberrations in the pathogenesis of PPGLs remain enigmatic, a discernible association between missense mutations in the VHL gene, particularly at positions 167 and 238, and the occurrence of PPGLs is evident (43). The implications of such missense mutations or reduced VHL expression are profound, manifesting in the impediment of HIFα ubiquitination and degradation. Consequently, a stabilization of HIFs transpires, subsequently engendering an augmented susceptibility to the development of PPGLs, specifically implicating Type 2 VHL disease (44–46). The landscape of HIFs genetic alterations is further nuanced, with HIF2α mutations assuming a more pronounced presence. Notably, germline mutations in HIF2A exon 9 (c.1121T>A, p.F374Y) significantly enhance the propensity for PPGLs (47). Comparatively, PHD mutations within the realm of PPGL patients present as a relatively infrequent occurrence, a notable distinction in contrast to the prominent roles of VHL and HIFα (48).

Intriguingly, PPGLs are increasingly recognized as metabolic disorders, particularly within the spectrum of cluster 1a manifestations. The manifestation of mutations within tricarboxylic acid (TCA) cycle enzymes precipitates an accumulation of pivotal metabolic intermediates. Subsequently, a

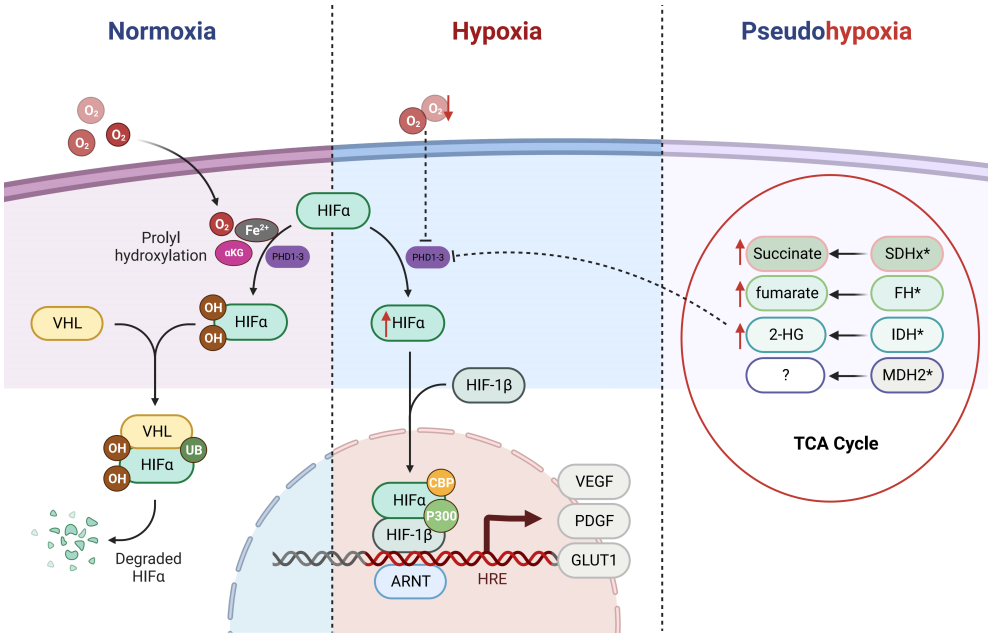


FIGURE 1
Regulation of HIFα (HIF-1α/HIF-2α) by the PHD/VHL Pathway and Impact of Tricarboxylic Acid Cycle Metabolic Mutations. HIFα (HIF-1α/HIF-2α) is primarily regulated by the PHD/VHL pathway. Under normoxic conditions, the prolyl hydroxylase domain (PHDs) proteins act upon the prolyl residues of HIFα in the presence of cofactor oxygen molecules, αKG, and $Fe^{2+}$, leading to hydroxylation. The hydroxylated HIFα is subsequently recognized and bound by E3 ubiquitin ligase VHL, followed by ubiquitination and subsequent degradation as a substrate within the proteasome. Under hypoxic conditions, the function of PHDs is inhibited, resulting in direct accumulation of HIFα. Subsequently, HIFα forms a heterodimer with HIF-1β and translocates into the nucleus, where with the assistance of p300/CBP, it activates downstream oncogenic signaling pathways. In cases of mutations in the TCA cycle metabolic enzymes (SDHx, FH, IDH, and MDH2), metabolic intermediates such as succinate, fumarate, and 2-HG accumulate. Due to their structural similarity to αKG, they competitively inhibit the αKG-assisted activation of dioxygenases (such as PHDs). As a result, under normoxic conditions, HIFα accumulates and activates downstream pathways, leading to a pseudohypoxic state.

multipronged cascade is set in motion, activating the HIFs signaling pathway via diverse mechanisms, thus engendering a pseudo-hypoxic milieu. Elevated levels of metabolites such as succinate, fumarate, or 2-hydroxyglutarate (2-HG) are indicative hallmarks within PPGLs, closely mirroring mutations inherent to TCA cycle enzymes (49–51). These metabolites, intricately interwoven with the tumorigenic context, proceed to exert their influence by modulating HIFs activity or by influencing the regulatory cascade upstream, thereby orchestrating the transduction of oncogenic signals. Within this framework, our review assumes a focal orientation, dedicated to the elucidation of the nuanced impact instigated by mutations within four pivotal TCA cycle enzymes—namely, Succinate dehydrogenase (SDHx), fumarate hydratase (FH), isocitrate dehydrogenase (IDH), and malate-dehydrogenase type 2 (MDH2)—upon the intricate VHL/HIF axis in PPGLs.

## The TCA cycle and PPGLs

A century ago, Otto Warburg's seminal investigations unveiled a noteworthy phenomenon: even under aerobic conditions, tumor cells tend to favor glycolytic pathways for energy procurement over mitochondrial respiration, positing mitochondrial dysfunction as a plausible cause, known as the Warburg effect (52). Subsequent research has illuminated that mitochondrial dysfunction isn't an obligatory trigger for tumorigenesis. Certain tumor cells adeptly generate energy through oxidative phosphorylation (OXPHOS) despite the mitochondrial milieu (53). Within this energetic landscape, the TCA cycle emerges as a pivotal conduit of mitochondrial energy metabolism. It orchestrates the oxidation of acetyl-CoA, transported to the mitochondria, into carbon dioxide, concomitantly releasing energy and reducing agents (NADH and FADH2) to facilitate subsequent OXPHOS (see Figure 2). Beyond its energy-contributing role, the TCA cycle acts as a nexus for intracellular carbohydrate, lipid, and amino acid metabolism, endowing other metabolic pathways with acetyl-CoA or diverse intermediary substrates (54, 55). Collectively, the nexus of tumorigenesis and the TCA cycle is unequivocally evident. Further probing into the intricate relationship between the TCA cycle and tumorigenesis holds the potential to unravel unique facets of tumor metabolism and unveil novel therapeutic targets.

Within the context of certain PPGLs, genetic perturbations affecting enzymes integral to the TCA cycle, such as SDH and FH, emerge as salient features (56). Since the initial discovery in 2000 of the correlation between SDHD germline mutations and familial paraganglioma, a growing compendium has cataloged mutations within at least twelve TCA cycle-related genes in the landscape of PPGLs (SDHB, SDH, SDHC, SDHD, SDHAF2, FH, IDH1, MDH2, SUCLG2, DLST, SLC25A11, and GOT2) (8, 57, 58). Among these, SDHx, FH, IDH1, and MDH2 have garnered relatively more attention, with mutations within SDHx and FH, in particular, emerging as pivotal drivers in the genesis and

10.3389/fendo.2023.1274239

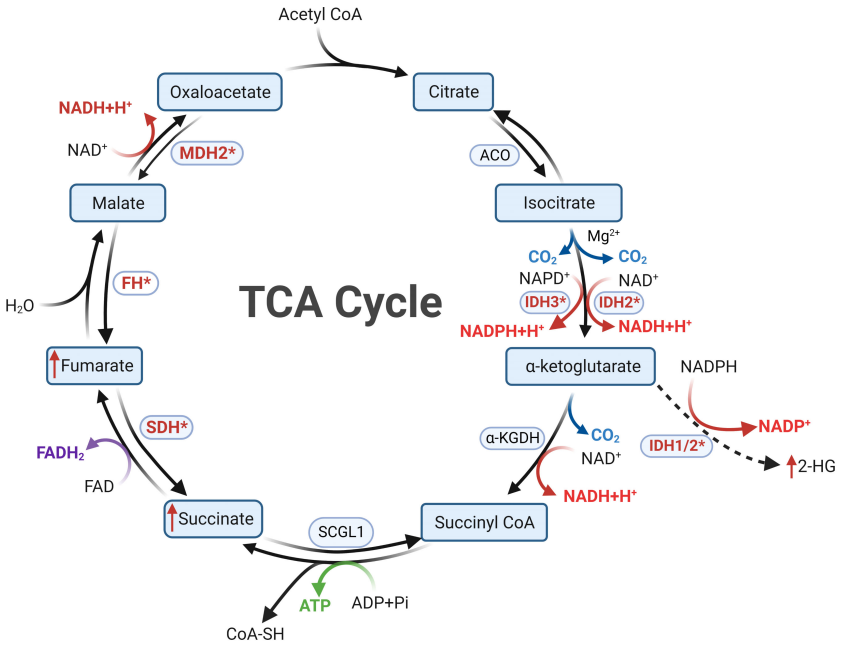


FIGURE 2
Metabolic reprogramming following mutations in tricarboxylic acid cycle enzymes is a key feature of Cluster 1a. In cells with normal mitochondrial function, the tricarboxylic acid cycle proceeds in a clockwise order. Mutations in SDHx and FH result in diminished substrate metabolism, leading to the accumulation of succinate and fumarate, respectively. Mutations in IDH confer the ability to convert αKG into 2-HG, resulting in 2-HG accumulation. Succinate, fumarate, and 2-HG all possess the capability to inhibit PHDs, thereby inducing a pseudohypoxic state. The oncogenic mechanisms following MDH mutations in PPGLs remain currently unclear.

progression of PPGLs. Subsequent discourse delves into the myriad mutations within these four enzyme categories, expounding on their repercussions on intermediary metabolism.

## SDHx and succinate

Within the context of PPGLs, SDHx-related genetic mutations stand out as the most prevalent, accounting for approximately 15% (59). SDHx comprises four core subunits (SDHA, SDHB, SDHC, SDHD) and an assembly factor (SDHAF2) (8, 60). Among the five constituent molecules of SDHx, mutations associated with SDHD and SDHB are more commonly observed, while those affecting SDHA, SDHC, and SDHAF2 are relatively less frequent. In patients with SDHB mutations, approximately 50% experience metastatic progression, whereas patients with SDHD mutations typically manifest with multiple neck paragangliomas (8, 61–63).

SDHx plays a dual role by participating in both the TCA cycle, where it oxidizes succinate to fumarate, and serving as a constituent of mitochondrial complex II in the electron transport chain (ETC), catalyzing electron transfer to the ubiquinone pool (59). In the realm of PPGLs, SDHx serves as suppressors of tumorigenesis. When germline or somatic mutations occur, the functional integrity of succinate dehydrogenase is compromised, leading to interruptions in the TCA cycle and impairment of the electron transport chain. Following such disruption, the accumulation of succinate, a metabolic substrate of SDHx, occurs intracellularly. This accumulation is responsible for reduced metabolic product generation, leading to diminished mitochondrial energy production. Concurrently, tumor cells undergo metabolic reprogramming to satisfy the demands for crucial synthesis processes. In cells with SDHx functional defects, heightened glycolysis and enhanced citric acid cycle flux are observed, primarily to sustain aspartate requirements, crucial for protein and nucleic acid synthesis (64, 65). Additionally, the terminal product of compensatory upregulated glycolysis, lactate, has been demonstrated to stimulate tumor cell growth (66).

The accrual of succinate in cells with SDHx functional defects is deemed a primary mediator of SDH-associated tumorigenesis (67). Pathological succinate accumulation leads to its leakage from the mitochondrial matrix to the cytoplasm. As a competitor of α-ketoglutarate (αKG), succinate broadly inhibits αKG-dependent dioxygenases, including the Ten-Eleven Translocation (TET) DNA hydroxylases and Jumonji (JMJ) histone demethylases (KDMs). Consequently, a global hypermethylation characterized by the CpG island methylator phenotype (CIMP) emerges in tumor cells, inducing alterations in gene expression and facilitating tumorigenesis (60, 68). Furthermore, SDHx deficiency-induced succinate accumulation competitively inhibits the αKG -dependent PHDs family (PHD1-3) in the cytoplasm. This leads to the stabilization of HIFα under normoxic conditions, thereby contributing to the activation of the pseudohypoxia pathway (25, 69, 70). Notably, succinate serves not only as a substrate for mitochondrial SDHx but also as a product of cytoplasmic PHDs (33, 69, 71–74). Consequently, the accumulation of succinate, through negative feedback regulation, inhibits the activity of

PHDs, resulting in further stabilization and activation of HIF complexes under normoxic conditions. Research by Celada et al. suggests that in SDHx mutation-driven PPGLs, diminished expression of PD-L1 and lower infiltration of cytotoxic T lymphocytes (CTLs) contribute to a 'cold' immunophenotype significantly associated with SDHx mutations (25). This hints at the potential of SDHx mutations to foster an immune-suppressive tumor microenvironment.

Furthermore, extracellular succinate secretion by tumor cells with SDH defects yields functional consequences (75). Extracellular succinate, upon binding to succinate receptor-1 (SUCNR-1), activates several oncogenic signaling molecules, such as ERK1/2, Akt, and AMPK, thereby enhancing tumor cell invasion and metastasis (75–77). Notably, Wu et al. found that the accumulated succinate in SDH-deficient tumor cells not only upregulates HIF-1A expression via the activation of the intracellular PI3K/Akt signaling pathway but also contributes to tumor invasion by activating macrophage surface SUCNR-1, subsequently inducing M1 polarization and promoting a malignant tumor phenotype (75, 78). Beyond immune cell interactions, secreted succinate from tumor cells binds to endothelial cell SUCNR-1, activating downstream STAT3-ERK1/2 in a HIF-independent manner and subsequently upregulating VEGF, thereby fostering angiogenesis.

## FH and fumarate

FH utilizes fumarate as a metabolic substrate, catalyzing its reversible hydration into malate (79). Mutations in FH result in reduced or loss of enzymatic activity, leading to the accumulation of high levels of fumarate (at millimolar levels). This accumulation profoundly alters mitochondrial function and cellular metabolism. Upon mitochondrial dysfunction due to FH mutations, cells undergo metabolic reprogramming, transitioning from mitochondrial oxidative respiration to cytoplasmic glycolysis. This metabolic shift also leads to a further reduction in carbon sources entering the mitochondria, which poses a risk of decreased membrane potential, potentially resulting in increased ROS and cell death. In this scenario, glutamine becomes an alternative carbon source to sustain the compromised TCA cycle, generating NADH for subsequent OXPHOS and ATP production to maintain mitochondrial membrane potential (80). To prevent the accumulation of other metabolic intermediates within this compensatory pathway, a portion of the glutamine-derived product is utilized for heme biosynthesis and degradation pathways, crucial for maintaining mitochondrial quality control and cell viability in FH-deficient cells (80, 81).

In addition to the metabolic reprogramming caused by FH deficiency and fumarate accumulation, these changes can also activate pro-oncogenic signaling pathways in FH-deficient cells. Fumarate can stabilize the majority of proteins through succination, a modification in which fumarate reacts with exposed cysteine residues on protein surfaces to form stable thiols. This leads to functional inactivation of proteins within the dynamic intracellular environment of tumor cells (82, 83). In a cellular environment characterized by elevated intracellular fumarate levels, succination of various oncoproteins promotes cell survival and proliferation. For example, fumarate succination of KEAP1 inactivates its ubiquitin ligase function, resulting in the stabilization and activation of its downstream target NRF2. As a transcription factor, NRF2 further upregulates the transcription of heme oxygenase 1 (HMOX1), a process crucial for maintaining heme metabolism. Additionally, iron-responsive element-binding protein 2 (IRP2) is a critical regulator of cellular iron metabolism, maintaining intracellular iron levels by inhibiting ferritin translation. Succination of IRP2 reduces its translational regulatory capacity on ferritin, leading to increased ferritin levels and decreased iron ions, disrupting intracellular iron homeostasis (84, 85). Furthermore, ferritin upregulates the expression of forkhead box protein M1 (FOXM1), promoting tumor cells to undergo mitosis (85).

Similar to succinate, fumarate also competitively inhibits PHDs, leading to increased stability of HIFs and inducing a pseudohypoxic state in tumorigenesis (86, 87). Thus, even in the context of mitochondrial defects in the energy metabolism chain, tumor cells maintain their malignant potential. Worth noting is that in FH-deficient tumor cells, activation of downstream pathways by HIFs results in significant upregulation of GLUT1, facilitating glucose uptake (86). Conversely, the expressions of pyruvate dehydrogenase kinase and lactate dehydrogenase are suppressed (88, 89). These changes in HIF-mediated metabolic genes lead to inhibition of mitochondrial oxidative metabolism, redirecting cells toward glycolysis and lactate synthesis, which hold essential significance in maintaining mitochondrial homeostasis.

## IDH and 2-HG

There are two forms of IDH in cells: IDH1/2 and IDH3, with IDH1/2 being NADP-dependent and IDH3 being NAD-dependent. While IDH1 and IDH2 share similarities in structure and function, they differ in subcellular localization. IDH1 is located in the cytoplasm and peroxisomes, whereas IDH2 is localized in the mitochondria. The function of IDH1/2 is to catalyze the oxidative decarboxylation of isocitrate to form αKG, simultaneously reducing NAD(P) to NAD(P)H (90). Unlike IDH1/2, IDH3 is found in the mitochondria and functions in the respiratory chain by catalyzing the forward decarboxylation of isocitrate to produce αKG (91). In 2010, Gaal and colleagues first identified a solitary IDH1 mutation in a case of sporadic carotid paraganglioma among 365 PPGLs specimens (92). Unfortunately, in another study by Yao and colleagues involving 104 PPGLs samples, no IDH1 mutations were detected (93). This suggests that pathogenic IDH mutations in PPGL are rare. Currently, there is a lack of authoritative research on the mechanisms by which IDH mutations contribute to PPGLs pathogenesis and progression, although the oncogenic mechanisms of IDH mutations have been extensively studied in diseases like gliomas and leukemias.

IDH1/2 mutations are considered gain-of-function oncogenic mutations. A single amino acid residue mutation in the IDH catalytic subunit prevents the conversion of isocitrate to α-

ketoglutarate, while gaining new enzymatic activity to generate D-2HG from αKG (94–96). This leads to a significant accumulation of this oncogenic metabolite in cells. Simultaneously, D-2HG disrupts the balance of αKG-assisted dioxygenases, including histone lysine demethylases, TET DNA hydroxylases, and PHDs. For example, inhibition of histone lysine demethylase activity results in increased methylation levels of histone lysine residues in chromatin (91, 97, 98). Furthermore, D-2HG inhibits PHDs, thereby preventing the ubiquitination and degradation of HIFs, leading to their stabilization and accumulation within cells (99, 100). Consequently, this elevation in HIFs target gene transcription promotes the formation of a pro-tumorigenic immune microenvironment. Under physiological metabolic conditions, NADPH is a reduction product of IDH. After IDH mutation, reduced NADPH generation impairs the maintenance of the reduced glutathione (GSH) pool, causing a decrease in the ratio of GSH to GSSG and disrupting intracellular antioxidant system balance, resulting in increased ROS (98). However, in the context of elevated intracellular ROS due to IDH1 loss-of-function, HIF2α stabilization can be induced in a ROS-dependent manner (101).

On the other hand, IDH mutation alters its original catalytic pathway, resulting in reduced metabolic flux of αKG and NADPH in the cell, profoundly affecting cellular metabolic status (91). Interestingly, in contrast to the outcome of HIF signaling pathway activation observed after IDH mutation, studies suggest that tumor cells may release D-2HG into the tumor microenvironment, triggering instability of HIF-1α in immune cells (regulatory T cells and Th17 cells) of the immune microenvironment (102). This subsequently modulates the energy metabolism and anti-tumor immune function of immune cells, although the precise mechanisms remain unclear. In a study focusing on enantiomer-specific mechanisms, it was found that IDH1/2 mutant variants can convert 2-oxoglutarate (2-OG) to (R)-2HG rather than (S)-2HG. (R)-2HG can activate PHD activity, thereby reducing the stability and levels of HIFs (103). Overall, this complex interplay contributes to malignant transformation of normal cells and enables tumor cells to survive energy reprogramming (97, 98, 104, 105).

## MDH2

Malate dehydrogenase 2 (encoded by the MDH2 gene) is downstream of fumarase and functions to oxidize malate into oxaloacetate. This enzyme is also involved in the malate-aspartate shuttle, which is essential for cellular respiration. In recent years, MDH2 has been considered a potential susceptibility gene for PPGLs (106). Reported cases of PPGLs associated with MDH2 mutations are extremely rare, with only a few cases retrievable in databases since the initial report by Alberto et al. in 2015 (106–108). MDH2 variants have been identified in metastatic cases, with approximately 50% of cases estimated to progress to metastasis (106), suggesting a potential association between MDH2 polymorphic variations and the metastatic nature of PPGLs. However, the mechanisms underlying the relationship between MDH2 mutations and the onset and progression of PPGLs remain unclear. In a larger-scale study, germline mutations in MDH2 were found to account for about 0.6% of overall PPGLs, and the p.K314del variant's potential pathogenicity in PPGLs was identified, possibly due to its impact on amino acid stability, although the specific mechanism is not yet understood (106).

Research has indicated that MDH2 mutations can promote HIFs stability by inhibiting PHDs, thereby facilitating pseudohypoxic responses in PPGLs (109–111). Conversely, some pharmacological studies have shown that LW6, an aroxyacetaminobenzoic acid analogue, can inhibit MDH1 activity. This leads to mitochondrial respiratory impairment, reducing cellular oxygen consumption and ATP production, resulting in elevated intracellular oxygen levels and triggering oxygen-dependent degradation of HIFs (112, 113).

## Conclusion and future perspectives

In summary, the intricate and complex interplay between metabolic enzyme mutations within the TCA cycle and the pseudohypoxic signaling has illuminated the potential mechanisms underlying the pathogenesis of PPGLs. The identification of key genetic mutations and their impact on critical metabolic intermediates such as succinate, fumarate, and 2-hydroxyglutarate underscores the significance of pseudo-hypoxia in promoting tumor initiation and progression. Under normoxic conditions, the activation of HIFs and their downstream effector pathways highlights the adaptive advantage of tumor cells within adverse microenvironments. Moreover, these mutations' influence on immune cell communication patterns and the establishment of an immune-suppressive tumor microenvironment further underscores the intricacy of PPGLs development. Insights gained from understanding alterations in PPGLs metabolism serve as the foundation for developing precise and effective therapeutic strategies. Additionally, the broader implications of these findings extend to the realm of cellular metabolism and its pivotal role in tumorigenesis.

Looking ahead, delving deeper into the intricate network of metabolic reprogramming and pseudo-hypoxic signaling in PPGLs holds great promise. Elucidating the detailed molecular mechanisms by which metabolic enzyme mutations drive HIFs activation and pseudohypoxia is paramount for designing targeted and efficacious therapeutic interventions. Furthermore, investigating the crosstalk between pseudo-hypoxic signaling and other molecular clusters such as the WNT and kinase pathways may reveal further complexities and potential therapeutic targets. The advancements in techniques such as high-throughput sequencing and metabolomics analysis offer exciting opportunities to uncover the genetic landscape and metabolic adaptations driving PPGLs development. Integrating these comprehensive datasets with functional studies will contribute to a profound understanding of the disease and aid in the discovery of novel biomarkers for early diagnosis and prognosis.

To sum up, delving into the role of TCA cycle metabolic enzyme mutations and pseudohypoxic signaling in PPGLs not only enhances our comprehension of these rare neuroendocrine tumors but also provides broader insights into cancer biology and the field of metabolism. These insights ignite the potential for

innovative therapeutic approaches and diagnostic methods, with the promise of significant clinical impact in the management of PPGLs and beyond.

## Author contributions

YXW: Writing – original draft, Writing – review & editing. BL: Conceptualization, Validation, Writing – review & editing. FL: Conceptualization, Validation, Writing – review & editing. YZ: Writing – review & editing. XG: Writing – review & editing. YSW: Funding acquisition, Supervision, Writing – review & editing. HZ: Funding acquisition, Supervision, Writing – review & editing.

## Funding

The authors declare financial support was received for the research, authorship, and/or publication of this article. This work was supported by the National Natural Science Foundation of China (No. 82270785).

## Acknowledgments

We thank reviewers for valuable suggestions.

## Conflict of interest

The authors declare that the research was conducted in the absence of any commercial or financial relationships that could be construed as a potential conflict of interest.

## Publisher's note

All claims expressed in this article are solely those of the authors and do not necessarily represent those of their affiliated organizations, or those of the publisher, the editors and the reviewers. Any product that may be evaluated in this article, or claim that may be made by its manufacturer, is not guaranteed or endorsed by the publisher.

## References

1. Al Subhi AR, Boyle V, Elston MS. Systematic review: incidence of pheochromocytoma and paraganglioma over 70 years. *J Endocrine Society* (2022) 6 (9):bvac105. doi: 10.1210/jendso/bvac105

2. Martinelli S, Amore F, Canu L, Maggi M, Rapizzi E. Tumour microenvironment in pheochromocytoma and paraganglioma. *Front Endocrinol* (2023) 14:1137456. doi: 10.3389/fendo.2023.1137456

3. Yamazaki Y, Gao X, Pecori A, Nakamura Y, Tezuka Y, Omata K, et al. Recent advances in histopathological and molecular diagnosis in pheochromocytoma and paraganglioma: challenges for predicting metastasis in individual patients. *Front Endocrinol* (2020) 11:587769. doi: 10.3389/fendo.2020.587769

4. Ebbehoj A, Stochholm K, Jacobsen SF, Trolle C, Jepsen P, Robaczyk MG, et al. Incidence and clinical presentation of pheochromocytoma and sympathetic paraganglioma: a population-based study. *J Clin Endocrinol Metab* (2021) 106(5): e2251–e61. doi: 10.1210/clinem/dgaa965

5. Jimenez C, Xu G, Varghese J, Graham PH, Campbell MT, Lu Y. New directions in treatment of metastatic or advanced pheochromocytomas and sympathetic paragangliomas: an american, contemporary, pragmatic approach. *Curr Oncol Rep* (2022) 24(1):89–98. doi: 10.1007/s11912-022-01197-0

6. Mete O, Asa SL, Gill AJ, Kimura N, de Krijger RR, Tischler A. Overview of the 2022 WHO classification of paragangliomas and pheochromocytomas. *Endocrine Pathol* (2022) 33(1):90–114. doi: 10.1007/s12022-022-09704-6

7. Tanabe A, Naruse M. Recent advances in the management of pheochromocytoma and paraganglioma. *Hypertension Res Off J Japanese Soc Hypertension* (2020) 43 (11):1141–51. doi: 10.1038/s41440-020-0531-0

8. Buffet A, Burnichon N, Favier J, Gimenez-Roqueplo AP. An overview of 20 years of genetic studies in pheochromocytoma and paraganglioma. *Best Pract Res Clin Endocrinol Metab* (2020) 34(2):101416. doi: 10.1016/j.beem.2020.101416

9. Wang K, Crona J, Beuschlein F, Grossman AB, Pacak K, Nölting S. Targeted therapies in pheochromocytoma and paraganglioma. *J Clin Endocrinol Metab* (2022) 107(11):2963–72. doi: 10.1210/clinem/dgac471

10. Kantorovich V, King KS, Pacak K. SDH-related pheochromocytoma and paraganglioma. *Best Pract Res Clin Endocrinol Metab* (2010) 24(3):415–24. doi: 10.1016/j.beem.2010.04.001

11. Jochmanová I, Yang C, Zhuang Z, Pacak K. Hypoxia-inducible factor signaling in pheochromocytoma: turning the rudder in the right direction. *J Natl Cancer Institute* (2013) 105(17):1270–83. doi: 10.1093/jnci/djt201

12. Alrezk R, Suarez A, Tena I, Pacak K. Update of pheochromocytoma syndromes: genetics, biochemical evaluation, and imaging. *Front Endocrinol* (2018) 9:515. doi: 10.3389/fendo.2018.00515

13. Eid M, Foukal J, Sochorová D, Tuček Š, Starý K, Kala Z, et al. Management of pheochromocytomas and paragangliomas: Review of current diagnosis and treatment options. *Cancer Med* (2023) 12(13):13942–57. doi: 10.1002/cam4.6010

14. Nölting S, Bechmann N, Taieb D, Beuschlein F, Fassnacht M, Kroiss M, et al. Personalized management of pheochromocytoma and paraganglioma. *Endocrine Rev* (2022) 43(2):199–239. doi: 10.1210/endrev/bnab019

15. Lenders JWM, Kerstens MN, Amar L, Prejbisz A, Robledo M, Taieb D, et al. Genetics, diagnosis, management and future directions of research of phaeochromocytoma and paraganglioma: a position statement and consensus of the Working Group on Endocrine Hypertension of the European Society of Hypertension. *J Hypertension* (2020) 38(8):1443–56. doi: 10.1097/HJH.0000000000002438

16. Mazzaglia PJ. Hereditary pheochromocytoma and paraganglioma. *J Surg Oncol* (2012) 106(5):580–5. doi: 10.1002/jso.23157

17. Lenders JW, Duh QY, Eisenhofer G, Gimenez-Roqueplo AP, Grebe SK, Murad MH, et al. Pheochromocytoma and paraganglioma: an endocrine society clinical practice guideline. *J Clin Endocrinol Metab* (2014) 99(6):1915–42. doi: 10.1210/jc.2014-1498

18. Favier J, Amar L, Gimenez-Roqueplo AP. Paraganglioma and phaeochromocytoma: from genetics to personalized medicine. *Nat Rev Endocrinol* (2015) 11(2):101–11. doi: 10.1038/nrendo.2014.188

19. Muth A, Crona J, Gimm O, Elmgren A, Filipsson K, Stenmark Askmalm M, et al. Genetic testing and surveillance guidelines in hereditary pheochromocytoma and paraganglioma. *J Internal Med* (2019) 285(2):187–204. doi: 10.1111/joim.12869

20. Erlic Z, Rybicki L, Peczkowska M, Golcher H, Kann PH, Brauckhoff M, et al. Clinical predictors and algorithm for the genetic diagnosis of pheochromocytoma patients. *Clin Cancer Res* (2009) 15(20):6378–85. doi: 10.1158/1078-0432.CCR-09-1237

21. Jha A, de Luna K, Balili CA, Millo C, Paraiso CA, Ling A, et al. Clinical, diagnostic, and treatment characteristics of SDHA-related metastatic pheochromocytoma and paraganglioma. *Front Oncol* (2019) 9:53. doi: 10.3389/fonc.2019.00053

22. Else T, Marvin ML, Everett JN, Gruber SB, Arts HA, Stoffel EM, et al. The clinical phenotype of SDHC-associated hereditary paraganglioma syndrome (PGL3). *J Clin Endocrinol Metab* (2014) 99(8):E1482–6. doi: 10.1210/jc.2013-3853

23. Hescot S, Curras-Freixes M, Deutschbein T, van Berkel A, Vezzosi D, Amar L, et al. Prognosis of Malignant pheochromocytoma and paraganglioma (MAPP-prono study): a european network for the study of adrenal tumors retrospective study. *J Clin Endocrinol Metab* (2019) 104(6):2367–74. doi: 10.1210/jc.2018-01968

24. Taïeb D, Kaliski A, Boedeker CC, Martucci V, Fojo T, Adler JR Jr., et al. Current approaches and recent developments in the management of head and neck paragangliomas. *Endocrine Rev* (2014) 35(5):795–819. doi: 10.1210/er.2014-1026

25. Celada L, Cubiella T, San-Juan-Guardado J, Gutiérrez G, Beiguela B, Rodriguez R, et al. Pseudohypoxia in paraganglioma and pheochromocytoma is associated with an immunosuppressive phenotype. *J Pathol* (2023) 259(1):103–14. doi: 10.1002/path.6026

26. Bratslavsky G, Sudarshan S, Neckers L, Linehan WM. Pseudohypoxic pathways in renal cell carcinoma. *Clin Cancer Res* (2007) 13(16):4667–71. doi: 10.1158/1078-0432.CCR-06-2510

27. Talty R, Olino K. Metabolism of innate immune cells in cancer. *Cancers* (2021) 13(4). doi: 10.3390/cancers13040904

28. Mohlin S, Wigerup C, Jögi A, Påhlman S. Hypoxia, pseudohypoxia and cellular differentiation. *Exp Cell Res* (2017) 356(2):192–6. doi: 10.1016/j.yexcr.2017.03.007

29. Brereton CJ, Yao L, Davies ER, Zhou Y, Vukmirovic M, Bell JA, et al. Pseudohypoxic HIF pathway activation dysregulates collagen structure-function in human lung fibrosis. *eLife* (2022) 11. doi: 10.7554/eLife.69348

30. Menendez JA, Alarcón T, Joven J. Gerometabolites: the pseudohypoxic aging side of cancer oncometabolites. *Cell Cycle (Georgetown Tex)* (2014) 13(5):699–709. doi: 10.4161/cc.28079

31. Jochmanova I, Pacak K. Genomic landscape of pheochromocytoma and paraganglioma. *Trends Cancer* (2018) 4(1):6–9. doi: 10.1016/j.trecan.2017.11.001

32. Redlich A, Pamporaki C, Lessel L, Frühwald MC, Vorwerk P, Kuhlen M. Pseudohypoxic pheochromocytomas and paragangliomas dominate in children. *Pediatr Blood Cancer* (2021) 68(7):e28981. doi: 10.1002/pbc.28981

33. Jhawar S, Arakawa Y, Kumar S, Varghese D, Kim YS, Roper N, et al. New insights on the genetics of pheochromocytoma and paraganglioma and its clinical implications. *Cancers* (2022) 14(3). doi: 10.3390/cancers14030594

34. Ilanchezhian M, Jha A, Pacak K, Del Rivero J. Emerging treatments for advanced/metastatic pheochromocytoma and paraganglioma. *Curr Treat Options Oncol* (2020) 21(11):85. doi: 10.1007/s11864-020-00787-z

35. Pouysségur J, Dayan F, Mazure NM. Hypoxia signalling in cancer and approaches to enforce tumour regression. *Nature* (2006) 441(7092):437–43. doi: 10.1038/nature04871

36. Lonser RR, Glenn GM, Walther M, Chew EY, Libutti SK, Linehan WM, et al. von hippel-lindau disease. *Lancet (London England)* (2003) 361(9374):2059–67. doi: 10.1016/S0140-6736(03)13643-4

37. Kaelin WG Jr., Ratcliffe PJ. Oxygen sensing by metazoans: the central role of the HIF hydroxylase pathway. *Mol Cell* (2008) 30(4):393–402. doi: 10.1016/j.molcel.2008.04.009

38. Shen C, Kaelin WG Jr. The VHL/HIF axis in clear cell renal carcinoma. *Semin Cancer Biol* (2013) 23(1):18–25. doi: 10.1016/j.semcancer.2012.06.001

39. Jang M, Kim SS, Lee J. Cancer cell metabolism: implications for therapeutic targets. *Exp Mol Med* (2013) 45(10):e45. doi: 10.1038/emm.2013.85

40. Watts D, Jaykar MT, Bechmann N, Wielockx B. Hypoxia signaling pathway: a central mediator in endocrine tumors. *Front Endocrinol* (2022) 13:1103075. doi: 10.3389/fendo.2022.1103075

41. Kaelin WG Jr. Von Hippel-Lindau disease: insights into oxygen sensing, protein degradation, and cancer. *J Clin Invest* (2022) 132(18). doi: 10.1172/JCI162480

42. Burnichon N, Vescovo L, Amar L, Libé R, de Reynies A, Venisse A, et al. Integrative genomic analysis reveals somatic mutations in pheochromocytoma and paraganglioma. *Hum Mol Genet* (2011) 20(20):3974–85. doi: 10.1093/hmg/ddr324

43. Peng S, Zhang J, Tan X, Huang Y, Xu J, Silk N, et al. The VHL/HIF axis in the development and treatment of pheochromocytoma/paraganglioma. *Front Endocrinol* (2020) 11:586857. doi: 10.3389/fendo.2020.586857

44. Ong KR, Woodward ER, Killick P, Lim C, Macdonald F, Maher ER. Genotype-phenotype correlations in von Hippel-Lindau disease. *Hum Mutation* (2007) 28 (2):143–9. doi: 10.1002/humu.20385

45. Liu SJ, Wang JY, Peng SH, Li T, Ning XH, Hong BA, et al. Genotype and phenotype correlation in von Hippel-Lindau disease based on alteration of the HIF-α binding site in VHL protein. *Genet Med* (2018) 20(10):1266–73. doi: 10.1038/gim.2017.261

46. Andreasson A, Kiss NB, Caramuta S, Sulaiman L, Svahn F, Bäckdahl M, et al. The VHL gene is epigenetically inactivated in pheochromocytomas and abdominal paragangliomas. *Epigenetics* (2013) 8(12):1347–54. doi: 10.4161/epi.26686

47. Lorenzo FR, Yang C, Ng Tang Fui M, Vankayalapati H, Zhuang Z, Huynh T, et al. A novel EPAS1/HIF2A germline mutation in a congenital polycythemia with paraganglioma. *J Mol Med (Berlin Germany)* (2013) 91(4):507–12. doi: 10.1007/s00109-012-0967-z

48. Ladroue C, Carcenac R, Leporrier M, Gad S, Le Hello C, Galateau-Salle F, et al. PHD2 mutation and congenital erythrocytosis with paraganglioma. *New Engl J Med* (2008) 359(25):2685–92. doi: 10.1056/NEJMoa0806277

49. Richter S, Peitzsch M, Rapizzi E, Lenders JW, Qin N, de Cubas AA, et al. Krebs cycle metabolite profiling for identification and stratification of pheochromocytomas/paragangliomas due to succinate dehydrogenase deficiency. *J Clin Endocrinol Metab* (2014) 99(10):3903–11. doi: 10.1210/jc.2014-2151

50. Ma X, Li M, Tong A, Wang F, Cui Y, Zhang X, et al. Genetic and clinical profiles of pheochromocytoma and paraganglioma: A single center study. *Front Endocrinol* (2020) 11:574662. doi: 10.3389/fendo.2020.574662

51. Richter S, Garrett TJ, Bechmann N, Clifton-Bligh RJ, Ghayee HK. Metabolomics in paraganglioma: applications and perspectives from genetics to therapy. *Endocrine-related Cancer* (2023) 30(6). doi: 10.1530/ERC-22-0376

52. Cascón A, Remacha L, Calsina B, Robledo M. Pheochromocytomas and paragangliomas: bypassing cellular respiration. *Cancers* (2019) 11(5). doi: 10.3390/cancers11050683

53. Eniafe J, Jiang S. The functional roles of TCA cycle metabolites in cancer. *Oncogene* (2021) 40(19):3351–63. doi: 10.1038/s41388-020-01639-8

54. Owen OE, Kalhan SC, Hanson RW. The key role of anaplerosis and cataplerosis for citric acid cycle function. *J Biol Chem* (2002) 277(34):30409–12. doi: 10.1074/jbc.R200006200

55. Haddad A, Mohiuddin SS. *Biochemistry, Citric Acid Cycle. StatPearls. Treasure Island (FL) ineligible companies. Disclosure: Shamim Mohiuddin declares no relevant financial relationships with ineligible companies*. StatPearls Publishing Copyright © 2023, StatPearls Publishing LLC (2023).

56. Mannelli M, Rapizzi E, Fucci R, Canu L, Ercolino T, Luconi M, et al. 15 YEARS OF PARAGANGLIOMA: metabolism and pheochromocytoma/paraganglioma. *Endocrine-related Cancer* (2015) 22(4):T83–90. doi: 10.1530/ERC-15-0215

57. Cascón A, Calsina B, Monteagudo M, Mellid S, Díaz-Talavera A, Currás-Freixes M, et al. Genetic bases of pheochromocytoma and paraganglioma. *J Mol Endocrinol* (2023) 70(3). doi: 10.1530/JME-22-0167

58. Hadrava Vanova K, Pang Y, Krobova L, Kraus M, Nahacka Z, Boukalova S, et al. Germline SUCLG2 variants in patients with pheochromocytoma and paraganglioma. *J Natl Cancer Institute* (2022) 114(1):130–8. doi: 10.1093/jnci/djab158

59. Gill AJ. Succinate dehydrogenase (SDH)-deficient neoplasia. *Histopathology* (2018) 72(1):106–16. doi: 10.1111/his.13277

60. Moog S, Lussey-Lepoutre C, Favier J. Epigenetic and metabolic reprogramming of SDH-deficient paragangliomas. *Endocrine-related Cancer* (2020) 27(12):R451–r63. doi: 10.1530/ERC-20-0346

61. Benn DE, Richardson AL, Marsh DJ, Robinson BG. Genetic testing in pheochromocytoma- and paraganglioma-associated syndromes. *Ann New York Acad Sci* (2006) 1073:104–11. doi: 10.1196/annals.1353.011

62. Amar L, Baudin E, Burnichon N, Peyrard S, Silvera S, Bertherat J, et al. Succinate dehydrogenase B gene mutations predict survival in patients with Malignant pheochromocytomas or paragangliomas. *J Clin Endocrinol Metab* (2007) 92 (10):3822–8. doi: 10.1210/jc.2007-0709

63. Taïeb D, Wanna GB, Ahmad M, Lussey-Lepoutre C, Perrier ND, Nölting S, et al. Clinical consensus guideline on the management of phaeochromocytoma and paraganglioma in patients harbouring germline SDHD pathogenic variants. *Lancet Diabetes Endocrinol* (2023) 11(5):345–61. doi: 10.1016/S2213-8587(23)00038-4

64. Cardaci S, Zheng L, MacKay G, van den Broek NJ, MacKenzie ED, Nixon C, et al. Pyruvate carboxylation enables growth of SDH-deficient cells by supporting aspartate biosynthesis. *Nat Cell Biol* (2015) 17(10):1317–26. doi: 10.1038/ncb3233

65. Lussey-Lepoutre C, Hollinshead KE, Ludwig C, Menara M, Morin A, Castro-Vega LJ, et al. Loss of succinate dehydrogenase activity results in dependency on pyruvate carboxylation for cellular anabolism. *Nat Commun* (2015) 6:8784. doi: 10.1038/ncomms9784

66. Faubert B, Li KY, Cai L, Hensley CT, Kim J, Zacharias LG, et al. Lactate metabolism in human lung tumors. *Cell* (2017) 171(2):358–71.e9. doi: 10.1016/j.cell.2017.09.019

67. Pollard PJ, Brière JJ, Alam NA, Barwell J, Barclay E, Wortham NC, et al. Accumulation of Krebs cycle intermediates and over-expression of HIF1alpha in tumours which result from germline FH and SDH mutations. *Hum Mol Genet* (2005) 14(15):2231–9. doi: 10.1093/hmg/ddi227

68. Liu Y, Pang Y, Zhu B, Uher O, Caisova V, Huynh TT, et al. Therapeutic targeting of SDHB-mutated pheochromocytoma/paraganglioma with pharmacologic ascorbic acid. *Clin Cancer Res* (2020) 26(14):3868–80. doi: 10.1158/1078-0432.CCR-19-2335

69. King A, Selak MA, Gottlieb E. Succinate dehydrogenase and fumarate hydratase: linking mitochondrial dysfunction and cancer. *Oncogene* (2006) 25(34):4675–82. doi: 10.1038/sj.onc.1209594

70. Kuo CC, Wu JY, Wu KK. Cancer-derived extracellular succinate: a driver of cancer metastasis. *J Biomed Science* (2022) 29(1):93. doi: 10.1186/s12929-022-00878-z

71. Selak MA, Armour SM, MacKenzie ED, Boulahbel H, Watson DG, Mansfield KD, et al. Succinate links TCA cycle dysfunction to oncogenesis by inhibiting HIF-alpha prolyl hydroxylase. *Cancer Cell* (2005) 7(1):77–85. doi: 10.1016/j.ccr.2004.11.022

72. Singleton DC, Macann A, Wilson WR. Therapeutic targeting of the hypoxic tumour microenvironment. *Nat Rev Clin Oncol* (2021) 18(12):751–72. doi: 10.1038/s41571-021-00539-4

73. Chen X, Sunkel B, Wang M, Kang S, Wang T, Gnanaprakasam JNR, et al. Succinate dehydrogenase/complex II is critical for metabolic and epigenetic regulation of T cell proliferation and inflammation. *Sci Immunol* (2022) 7(70):eabm8161. doi: 10.1126/sciimmunol.abm8161

74. Germanova E, Khmil N, Pavlik L, Mikheeva I, Mironova G, Lukyanova L. The role of mitochondrial enzymes, succinate-coupled signaling pathways and mitochondrial ultrastructure in the formation of urgent adaptation to acute hypoxia in the myocardium. *Int J Mol Sci* (2022) 23(22). doi: 10.3390/ijms232214248

75. Wu JY, Huang TW, Hsieh YT, Wang YF, Yen CC, Lee GL, et al. Cancer-derived succinate promotes macrophage polarization and cancer metastasis *via* succinate receptor. *Mol Cell* (2020) 77(2):213–27.e5. doi: 10.1016/j.molcel.2019.10.023

76. Matlac DM, Hadrava Vanova K, Bechmann N, Richter S, Folberth J, Ghayee HK, et al. Succinate mediates tumorigenic effects *via* succinate receptor 1: potential for new

targeted treatment strategies in succinate dehydrogenase deficient paragangliomas. *Front Endocrinol* (2021) 12:589451. doi: 10.3389/fendo.2021.589451

77. de Castro Fonseca M, Aguiar CJ, da Rocha Franco JA, Gingold RN, Leite MF. GPR91: expanding the frontiers of Krebs cycle intermediates. *Cell Communication Signaling CCS* (2016) 14:3. doi: 10.1186/s12964-016-0126-1

78. Trauelsen M, Hiron TK, Lin D, Petersen JE, Breton B, Husted AS, et al. Extracellular succinate hyperpolarizes M2 macrophages through SUCNR1/GPR91-mediated Gq signaling. *Cell Rep* (2021) 35(11):109246. doi: 10.1016/j.celrep.2021.109246

79. Frezza C. Mitochondrial metabolites: undercover signalling molecules. *Interface Focus* (2017) 7(2):20160100. doi: 10.1098/rsfs.2016.0100

80. Frezza C, Zheng L, Folger O, Rajagopalan KN, MacKenzie ED, Jerby L, et al. Haem oxygenase is synthetically lethal with the tumour suppressor fumarate hydratase. *Nature* (2011) 477(7363):225–8. doi: 10.1038/nature10363

81. Zorova LD, Popkov VA, Plotnikov EY, Silachev DN, Pevzner IB, Jankauskas SS, et al. Mitochondrial membrane potential. *Analytical Biochem* (2018) 552:50–9. doi: 10.1016/j.ab.2017.07.009

82. Bardella C, El-Bahrawy M, Frizzell N, Adam J, Ternette N, Hatipoglu E, et al. Aberrant succination of proteins in fumarate hydratase-deficient mice and HLRCC patients is a robust biomarker of mutation status. *J Pathol* (2011) 225(1):4–11. doi: 10.1002/path.2932

83. Alderson NL, Wang Y, Blatnik M, Frizzell N, Walla MD, Lyons TJ, et al. S-(2-Succinyl)cysteine: a novel chemical modification of tissue proteins by a Krebs cycle intermediate. *Arch Biochem Biophysics* (2006) 450(1):1–8. doi: 10.1016/j.abb.2006.03.005

84. Anderson CP, Shen M, Eisenstein RS, Leibold EA. Mammalian iron metabolism and its control by iron regulatory proteins. *Biochim Biophys Acta* (2012) 1823(9):1468–83. doi: 10.1016/j.bbamcr.2012.05.010

85. Kerins MJ, Vashisht AA, Liang BX, Duckworth SJ, Praslicka BJ, Wohlschlegel JA, et al. Fumarate mediates a chronic proliferative signal in fumarate hydratase-inactivated cancer cells by increasing transcription and translation of ferritin genes. *Mol Cell Biol* (2017) 37(11). doi: 10.1128/MCB.00079-17

86. Isaacs JS, Jung YJ, Mole DR, Lee S, Torres-Cabala C, Chung YL, et al. HIF overexpression correlates with biallelic loss of fumarate hydratase in renal cancer: novel role of fumarate in regulation of HIF stability. *Cancer Cell* (2005) 8(2):143–53. doi: 10.1016/j.ccr.2005.06.017

87. Frezza C, Pollard PJ, Gottlieb E. Inborn and acquired metabolic defects in cancer. *J Mol Med (Berlin Germany)* (2011) 89(3):213–20. doi: 10.1007/s00109-011-0728-4

88. Kim JW, Tchernyshyov I, Semenza GL, Dang CV. HIF-1-mediated expression of pyruvate dehydrogenase kinase: a metabolic switch required for cellular adaptation to hypoxia. *Cell Metab* (2006) 3(3):177–85. doi: 10.1016/j.cmet.2006.02.002

89. Xie H, Valera VA, Merino MJ, Amato AM, Signoretti S, Linehan WM, et al. LDH-A inhibition, a therapeutic strategy for treatment of hereditary leiomyomatosis and renal cell cancer. *Mol Cancer Ther* (2009) 8(3):626–35. doi: 10.1158/1535-7163.MCT-08-1049

90. Pillai S, Gopalan V, Smith RA, Lam AK. Updates on the genetics and the clinical impacts on phaeochromocytoma and paraganglioma in the new era. *Crit Rev Oncol/Hematol* (2016) 100:190–208. doi: 10.1016/j.critrevonc.2016.01.022

91. Waitkus MS, Diplas BH, Yan H. Isocitrate dehydrogenase mutations in gliomas. *Neuro-Oncology* (2016) 18(1):16–26. doi: 10.1093/neuonc/nov136

92. Gaal J, Burnichon N, Korpershoek E, Roncelin I, Bertherat J, Plouin PF, et al. Isocitrate dehydrogenase mutations are rare in pheochromocytomas and paragangliomas. *J Clin Endocrinol Metab* (2010) 95(3):1274–8. doi: 10.1210/jc.2009-2170

93. Yao L, Schiavi F, Cascon A, Qin Y, Inglada-Pérez L, King EE, et al. Spectrum and prevalence of FP/TMEM127 gene mutations in pheochromocytomas and paragangliomas. *Jama* (2010) 304(23):2611–9. doi: 10.1001/jama.2010.1830

94. Notarangelo G, Spinelli JB, Perez EM, Baker GJ, Kurmi K, Elia I, et al. Oncometabolite d-2HG alters T cell metabolism to impair CD8(+) T cell function. *Sci (New York NY)* (2022) 377(6614):1519–29. doi: 10.1126/science.abj5104

95. Ward PS, Patel J, Wise DR, Abdel-Wahab O, Bennett BD, Coller HA, et al. The common feature of leukemia-associated IDH1 and IDH2 mutations is a neomorphic enzyme activity converting α-ketoglutarate to 2-hydroxyglutarate. *Cancer Cell* (2010) 17(3):225–34. doi: 10.1016/j.ccr.2010.01.020

96. Dang L, White DW, Gross S, Bennett BD, Bittinger MA, Driggers EM, et al. Cancer-associated IDH1 mutations produce 2-hydroxyglutarate. *Nature* (2009) 462(7274):739–44. doi: 10.1038/nature08617

97. Zhao S, Lin Y, Xu W, Jiang W, Zha Z, Wang P, et al. Glioma-derived mutations in IDH1 dominantly inhibit IDH1 catalytic activity and induce HIF-1alpha. *Sci (New York NY)* (2009) 324(5924):261–5. doi: 10.1126/science.1170944

98. Laurenti G, Tennant DA. Isocitrate dehydrogenase (IDH), succinate dehydrogenase (SDH), fumarate hydratase (FH): three players for one phenotype in cancer? *Biochem Soc Trans* (2016) 44(4):1111–6. doi: 10.1042/BST20160099

99. Keith B, Johnson RS, Simon MC. HIF1α and HIF2α: sibling rivalry in hypoxic tumour growth and progression. *Nat Rev Cancer* (2011) 12(1):9–22. doi: 10.1042/BST20160099

100. Huang J, Yu J, Tu L, Huang N, Li H, Luo Y. Isocitrate dehydrogenase mutations in glioma: from basic discovery to therapeutics development. *Front Oncol* (2019) 9:506. doi: 10.3389/fonc.2019.00506

101. Wang Y, Agarwal E, Bertolini I, Ghosh JC, Seo JH, Altieri DC. IDH2 reprograms mitochondrial dynamics in cancer through a HIF-1α-regulated pseudohypoxic state. *FASEB J* (2019) 33(12):13398–411. doi: 10.1096/fj.201901366R

102. Böttcher M, Renner K, Berger R, Mentz K, Thomas S, Cardenas-Conejo ZE, et al. D-2-hydroxyglutarate interferes with HIF-1α stability skewing T-cell metabolism towards oxidative phosphorylation and impairing Th17 polarization. *Oncoimmunology* (2018) 7(7):e1445454. doi: 10.1096/fj.201901366R

103. Koivunen P, Lee S, Duncan CG, Lopez G, Lu G, Ramkissoon S, et al. Transformation by the (R)-enantiomer of 2-hydroxyglutarate linked to EGLN activation. *Nature* (2012) 483(7390):484–8. doi: 10.1038/nature10898

104. Velasco-Hernandez T, Hyrenius-Wittsten A, Rehn M, Bryder D, Cammenga J. HIF-1α can act as a tumor suppressor gene in murine acute myeloid leukemia. *Blood* (2014) 124(24):3597–607. doi: 10.1182/blood-2014-04-567065

105. Semukunzi H, Roy D, Li H, Khan GJ, Lyu X, Yuan S, et al. IDH mutations associated impact on related cancer epidemiology and subsequent effect toward HIF-1α. *Biomed Pharmacother* (2017) 89:805–11. doi: 10.1016/j.biopha.2017.02.083

106. Calsina B, Currás-Freixes M, Buffet A, Pons T, Contreras L, Letón R, et al. Role of MDH2 pathogenic variant in pheochromocytoma and paraganglioma patients. *Genet Med* (2018) 20(12):1652–62. doi: 10.1038/s41436-018-0068-7

107. Cascón A, Comino-Méndez I, Currás-Freixes M, de Cubas AA, Contreras L, Richter S, et al. Whole-exome sequencing identifies MDH2 as a new familial paraganglioma gene. *J Natl Cancer Institute* (2015) 107(5). doi: 10.1093/jnci/djv053

108. Mellid S, Gil E, Letón R, Caleiras E, Honrado E, Richter S, et al. Co-occurrence of mutations in NF1 and other susceptibility genes in pheochromocytoma and paraganglioma. *Front Endocrinol* (2022) 13:1070074. doi: 10.3389/fendo.2022.1070074

109. Jochmanová I, Zhuang Z, Pacak K. Pheochromocytoma: gasping for air. *Hormones Cancer* (2015) 6(5-6):191–205. doi: 10.1007/s12672-015-0231-4

110. Mercado-Asis LB, Wolf KI, Jochmanova I, Taïeb D. Pheochromocytoma: a genetic and diagnostic update. *Endocrine Pract* (2018) 24(1):78–90. doi: 10.4158/EP-2017-0057

111. Toledo RA, Jimenez C, Armaiz-Pena G, Arenillas C, Capdevila J, Dahia PLM. Hypoxia-inducible factor 2 alpha (HIF2α) inhibitors: targeting genetically driven tumor hypoxia. *Endocrine Rev* (2023) 44(2):312–22. doi: 10.1210/endrev/bnac025

112. Naik R, Won M, Ban HS, Bhattarai D, Xu X, Eo Y, et al. Synthesis and structure-activity relationship study of chemical probes as hypoxia induced factor-1α/malate dehydrogenase 2 inhibitors. *J Medicinal Chem* (2014) 57(22):9522–38. doi: 10.1021/jm501241g

113. Ban HS, Xu X, Jang K, Kim I, Kim BK, Lee K, et al. A novel malate dehydrogenase 2 inhibitor suppresses hypoxia-inducible factor-1 by regulating mitochondrial respiration. *PloS One* (2016) 11(9):e0162568. doi: 10.1371/journal.pone.0162568

frontiers | Frontiers in Endocrinology

TYPE Original Research
PUBLISHED 11 October 2023
DOI 10.3389/fendo.2023.1275813

Check for updates

OPEN ACCESS

EDITED BY
Ichiro Abe,
Fukuoka University Chikushi Hospital, Japan

REVIEWED BY
Monica Livia Gheorghiu,
Carol Davila University of Medicine and Pharmacy, Romania
Kimitaka Shibue,
Kitano Hospital, Japan

*CORRESPONDENCE
Frank I. Lin
frank.lin2@nih.gov

†These authors have contributed equally to this work and share senior authorship

RECEIVED 10 August 2023
ACCEPTED 28 September 2023
PUBLISHED 11 October 2023

CITATION
Gubbi S, Al-Jundi M, Auh S, Jha A, Zou J, Shamis I, Meuter L, Knue M, Turkbey B, Lindenberg L, Mena E, Carrasquillo JA, Teng Y, Pacak K, Klubo-Gwiezdzinska J, Del Rivero J and Lin FI (2023) Early short-term effects on catecholamine levels and pituitary function in patients with pheochromocytoma or paraganglioma treated with [$^{177}$Lu]Lu-DOTA-TATE therapy. *Front. Endocrinol.* 14:1275813. doi: 10.3389/fendo.2023.1275813

COPYRIGHT
© 2023 Gubbi, Al-Jundi, Auh, Jha, Zou, Shamis, Meuter, Knue, Turkbey, Lindenberg, Mena, Carrasquillo, Teng, Pacak, Klubo-Gwiezdzinska, Del Rivero and Lin. This is an open-access article distributed under the terms of the Creative Commons Attribution License (CC BY). The use, distribution or reproduction in other forums is permitted, provided the original author(s) and the copyright owner(s) are credited and that the original publication in this journal is cited, in accordance with accepted academic practice. No use, distribution or reproduction is permitted which does not comply with these terms.

# Early short-term effects on catecholamine levels and pituitary function in patients with pheochromocytoma or paraganglioma treated with [$^{177}$Lu]Lu-DOTA-TATE therapy

Sriram Gubbi[1], Mohammad Al-Jundi[2], Sungyoung Auh[1], Abhishek Jha[2], Joy Zou[3], Inna Shamis[3], Leah Meuter[2], Marianne Knue[2], Baris Turkbey[3], Liza Lindenberg[3], Esther Mena[3], Jorge A. Carrasquillo[3,4], Yating Teng[5], Karel Pacak[2], Joanna Klubo-Gwiezdzinska[1], Jaydira Del Rivero[6†] and Frank I. Lin[3*†]

[1]Metabolic Diseases Branch, National Institute of Diabetes and Digestive and Kidney Diseases, Bethesda, MD, United States, [2]Department of Endocrinology, Eunice Kennedy Shriver National Institute of Child and Human Development, Bethesda, MD, United States, [3]Molecular Imaging Branch, National Cancer Institute, Bethesda, MD, United States, [4]Department of Radiology, Memorial Sloan Kettering Cancer Center, New York, NY, United States, [5]Center for Health Professions Education, Uniformed Services University of the Health Sciences, Bethesda, MD, United States, [6]Developmental Therapeutics Branch, National Cancer Institute, Bethesda, MD, United States

**Purpose:** While there are reports of treatment-related endocrine disruptions and catecholamine surges in pheochromocytoma/paraganglioma (PPGL) patients treated with [$^{177}$Lu]Lu-DOTA-TATE therapy, the spectrum of these abnormalities in the immediate post-treatment period (within 48 hours) has not been previously evaluated and is likely underestimated.

**Methods:** The study population included patients (≥18 years) enrolled in a phase 2 trial for treatment of somatostatin receptor (SSTR)-2+ inoperable/metastatic pheochromocytoma/paraganglioma with [$^{177}$Lu]Lu-DOTA-TATE (7.4 GBq per cycle for 1 – 4 cycles). Hormonal measurements [adrenocorticotropic hormone (ACTH), cortisol, thyroid stimulating hormone (TSH), free thyroxine (FT4), follicle stimulating hormone (FSH), luteinizing hormone (LH), testosterone, estradiol, growth hormone, prolactin], catecholamines, and metanephrines were obtained on days-1, 2, 3, 30, and 60 per cycle as per trial protocol, and were retrospectively analyzed.

**Results:** Among the 27 patients (age: 54 ± 12.7 years, 48.1% females) who underwent hormonal evaluation, hypoprolactinemia (14.1%), elevated FSH (13.1%), and elevated LH (12.5%) were the most frequent hormonal abnormalities across all 4 cycles combined. On longitudinal follow-up, significant reductions were noted in i. ACTH without corresponding changes in cortisol, ii. TSH, and FT4, and iii. prolactin at or before day-30 of [$^{177}$Lu]Lu-DOTA-TATE. No significant changes were observed in the gonadotropic axis and GH

levels. Levels of all hormones on day-60 were not significantly different from day-1 values, suggesting the transient nature of these changes. However, two patients developed clinical, persistent endocrinopathies (primary hypothyroidism: n=1 male; early menopause: n=1 female). Compared to day-1, a significant % increase in norepinephrine, dopamine, and normetanephrine levels were noted at 24 hours following [$^{177}$Lu]Lu-DOTA-TATE dose and peaked within 48 hours.

**Conclusions:** [$^{177}$Lu]Lu-DOTA-TATE therapy is associated with alterations in endocrine function likely from radiation exposure to SSTR2+ endocrine tissues. However, these changes may sometimes manifest as clinically significant endocrinopathies. It is therefore important to periodically assess endocrine function during [$^{177}$Lu]Lu-DOTA-TATE therapy, especially among symptomatic patients.

**Clinical trial registration:** https://clinicaltrials.gov/ct2/show/NCT03206060?term=NCT03206060&draw=2&rank=1, identifier NCT03206060.

KEYWORDS

DOTATATE, PRRT, [177 Lu], [68 Ga], targeted radiotherapy, pituitary, catecholamines, pheochromocytoma and paraganglioma

## Introduction

[$^{177}$Lu]Lutetium-DOTA-DPhe1, Tyr3-octreotate ([$^{177}$Lu]Lu-DOTA-TATE), is an analog of somatostatin with high affinity to somatostatin receptor type 2 (SSTR2) (1), which is overexpressed in various neuroendocrine tumors (NETs), including pheochromocytomas/paragangliomas. Radiolabeled somatostatin analogs have been used successfully in peptide receptor radionuclide therapy (PRRT) and are recommended treatments in societal guidelines for metastatic NETs (2) and for inoperable pheochromocytomas and paragangliomas (PPGL) (3).

As identified in the phase 3 NETTER-1 study, [$^{177}$Lu]Lu-DOTA-TATE is associated with several adverse effects that result primarily from unintended radiation exposure to non-tumor sites (4), and it is known that several endocrine glands (thyroid, pituitary, adrenals, and gonads) express SSTRs (especially SSTR2) on their surfaces (5, 6). In fact, prior dosimetry analyses have demonstrated delivery of significant radiation doses to various endocrine glands after a 7.4 GBq infusion (7). While the clinical effects of PRRT on the endocrine system have been described previously (8, 9), none have investigated the effects of PRRT on the endocrine system in the immediate (<48 hours) time period post administration. This is an important time frame to investigate because patients can exhibit clinical signs of endocrinopathies such as neurohormonal crisis and catecholamine crisis during this early post-administration period, with the package insert for [$^{177}$Lu]Lu-DOTA-TATE indicating that the risk of neurohormonal crisis is in fact the highest during this period (10). In this study, we present the results from a subset of patients enrolled in a prospective trial where the endocrine function and catecholamines levels of PPGL patients treated with [$^{177}$Lu]Lu-DOTA-TATE were evaluated in the immediate post-administration setting at 24h, 48h, and 30 days after each administration of the agent, with the goal of demonstrating that endocrine disruptions can occur very early, perhaps immediately, after the administration of PRRT.

## Materials and methods

This study was a retrospective analysis of prospectively collected data from the trial. Serial blood samples at baseline then at approximately 24h, 48h, and 30 days after each [$^{177}$Lu]Lu-DOTA-TATE administration were obtained from patients aged ≥18 years who were enrolled in the phase 2 [$^{177}$Lu]Lu-DOTA-TATE trial for metastatic/inoperable PPGL (NCT03206060) at the National Institutes of Health (NIH) from October 2017 to March 2020. Hormonal, catecholamine, and metanephrine testing protocols were predetermined by the clinical trial and were performed on day 1 (pre-[$^{177}$Lu]Lu-DOTA-TATE infusion; d1), day 2 (day 1 post-[$^{177}$Lu]Lu-DOTA-TATE infusion; d2), day 3 (day 2 post-[$^{177}$Lu]Lu-DOTA-TATE infusion; d3), day 30 (day 29 post-[$^{177}$Lu]Lu-DOTA-TATE infusion; d30), and day 60 (day 59 post-[$^{177}$Lu]Lu-DOTA-TATE infusion, which is also the day 1 of the next cycle; d60). Pituitary and target organ hormones collected included ACTH, cortisol, thyroid stimulating hormone (TSH), free thyroxine (FT4), gonadotrophs (FSH, LH), testosterone, estradiol, growth hormone (GH), and prolactin, which were measured using immunoassays. Catecholamines and metanephrines were measured using high-performance liquid chromatography. All assays were performed at our institution, except for uninterpretable metanephrine values

due to potential interfering substances, which were measured at the Mayo Clinic laboratories using liquid chromatography/mass spectrometry. To ensure accuracy and reproducibility particularly of serum catecholamine levels, all blood samples were drawn at rest and followed a strict protocol where patients laid recumbent for 30 minutes prior and had samples taken from an indwelling venous catheter.

Eligibility criteria for the trial included histologically proven PPGL and documented SSTR+ tumors on a [$^{68}$Ga]Ga-DOTA-TATE positron emission tomography/computed tomography (PET/CT) scan within 12 weeks of treatment. Patients with baseline persistent endocrine abnormalities such as hypogonadism, hypothyroidism, or adrenal insufficiency were excluded from this analysis. [$^{177}$Lu]Lu-DOTA-TATE was administered intravenously every 8 weeks at 7.4 GBq (200 mCi) up to a total of 4 administrations. Concomitant administration of 2.5% Lys/Arg amino acid solution was used for renal protection. The exclusion criteria included the following: 1. Baseline persistent endocrine abnormalities from a clear underlying cause, 2. Gonadotropins in premenopausal women, 3. Unexplained baseline endocrine abnormalities that persisted throughout the course of treatment, and 4. Catecholamine and metanephrine data from patients harboring 'non-secretory' PPGL. Further details regarding the exclusion criteria are described in the Supplementary Information (Section A).

Baseline parameters consisting of age, sex, body mass index (BMI), blood pressure (BP) comprising systolic blood pressure (SBP), diastolic blood pressure (DBP), and heart rate (HR), were measured prior to the first [$^{177}$Lu]Lu-DOTA-TATE dose, and then at varying intervals during each cycle: once daily to 2–4 hours/day depending on patient's clinical stability. Per trial protocol, blood samples were collected from patients on 1, 4, 8, 12, 16, 20, 24, 28, and 32 (+/- 2) weeks of treatment through an indwelling intravenous cannula in a supine, resting state. The timings of the plasma collection were predetermined by the trial protocol at 24-hour intervals post-[$^{177}$Lu]Lu-DOTA-TATE infusion. However, most of these samples were collected between 05:30 AM and 11:30 AM. We also looked into the clinical records of these patients to identify whether any of the patients had undergone an ACTH stimulation test. The study was approved by the institutional review board at the NIH Clinical Center and all patients provided informed consent.

## Statistical analysis

Continuous data were represented as mean ± standard deviation (SD) for normally distributed parameters and as median and interquartile range for skewed data. The longitudinal graphical data were represented as mean ± standard error of mean (SEM). Categorical data were represented as proportions. Longitudinal analysis was performed using linear mixed-effects model analysis. Catecholamine/metanephrine levels were analyzed using two-way repeated measures ANOVA. All longitudinal data were clustered into 5 groups: 'Day 1' (D1), 'Day 2' (D2), 'Day 3' (D3), 'Day 30' (D30), and 'Day 60' (D60). For example, 'D1' comprised d1 values of all cycles (cycle 1 d1, cycle 2 d1, cycle 3 d1, and cycle 4 d1). The 'D60' values comprised the d1 values of the subsequent cycles: for example, cycle 2 d1 was not only d1 of the second cycle under 'D1' data but was also d60 of the first cycle in the 'D60' data. The hormonal measurements were labelled as either 'high' or 'low' based on the value being above or below the reference range, respectively for the given hormone. Further details on statistics are provided in the Supplementary Information (Section B). All analyses were two-tailed, and the p-value was set to 0.05. Statistical analyses were performed using GraphPad Prism 8 Version 8·3·1 and SAS Version 9.4.

# Results

## Baseline characteristics

Twenty-seven consecutive patients [age: 54 ± 12.7 years, 13 females, BMI: 24.9 (22.7 – 30.9) Kg/m$^2$] were enrolled (Table 1). At completion of the longitudinal follow-up, 21 (77.8%), 16 (59.3%), and 13 (48.1%) patients had completed the second, third, and fourth doses of [$^{177}$Lu]Lu-DOTA-TATE, respectively. The average pituitary and target gland hormones levels were within the normal reference range. The median baseline levels of plasma normetanephrine and norepinephrine were 5.25x (588 pg/mL; 18 – 112 pg/mL) and 1.04x (826 pg/mL; 84 – 794 pg/mL) the upper limit of normal, respectively. The median baseline epinephrine and metanephrine levels were normal.

## Hormonal variations in the immediate post-treatment period

Regarding prevalence of biochemical abnormalities per patient, estradiol (60%; 3/5 patients – all pre-menopausal women) and prolactin (50%; 10/20 patients) abnormalities were most frequent, followed by testosterone (27.3%; 3/11 patients), ACTH (24%; 6/25 patients), and TSH (20.8%; 6/24 patients) (Table 2). Across all measurements, prolactin abnormalities were most frequent (25.4%), with hypoprolactinemia constituting 14.1%, and hyperprolactinemia constituting 11.3%, followed by high FSH (13.1%), high LH (12.5%), and high ACTH (9.8%) (Table 3). The descriptions of specific findings from Table 3 based on individual pituitary-target gland axis is provided in Supplementary Information (Section C). The frequency of all the biochemical endocrine abnormalities on each day of measurement of every cycle is listed in Supplementary Information (Section D). Longitudinal follow-up revealed a reduction in the average levels of several hormones immediately following [$^{177}$Lu]Lu-DOTA-TATE dosing, especially on D2 and D3, with gradual return to pre-[$^{177}$Lu]Lu-DOTA-TATE baseline values at D60 (Figure 1). In the pituitary-adrenal axis, compared to D1, the ACTH levels on D2 (D1 = 36.8 ± 34.1 pg/mL vs. D2 = 23.1 ± 21 pg/mL; p<0.0001), D3 (D1 = 36.8 ± 34.1 pg/mL vs. D3 = 24.3 ± 19.4 pg/mL; p<0.0001), and D30 (D1 = 36.8 ± 34.1 pg/mL vs. D30 = 27.7 ± 19.1 pg/mL; p=0.01) were significantly lower, while there were no

10.3389/fendo.2023.1275813

TABLE 1 Baseline characteristics of the study population.

| Baseline characteristics (n=27) | Values |
|---|---|
| 1. Age (years) | 54 ± 12.7 |
| 2. Sex: male (%)/female (%) | 14 (51.9%) / 13 (48.1%) |
| 3. Body mass index (Kg/m$^2$) | 24.9 (22.7 – 30.9) |
| 4. Cycles of treatment received: number of patients (%)<br>○Cycle-1<br>○ Cycle-2<br>○ Cycle-3<br>○ Cycle-4 | 27 (100%)<br>21 (77.8%)<br>16 (59.3%)<br>13 (48.1%) |
| 5. Adrenocorticotropic hormone (5 – 46 pg/mL; n=25) | 24.8 (17.2 – 49.6) |
| 6. Cortisol (5 – 25 mcg/dL; n=25) | 11.1 (7.8 – 16) |
| 7. Thyroid stimulating hormone (0.27 – 4.2 microIU/mL; n=24) | 2.2 ± 1.12 |
| 8. Free thyroxine (0.9 – 1.7 ng/dL; n=24) | 1.15 ± 0.19 |
| 9. Follicle stimulating hormone (FSH; male; 1 – 11 U/L; n=9) | 6.29 ± 3.4 |
| 10. Luteinizing hormone (LH; male; 1 – 8 U/L; n=10) | 4.67 ± 1.94 |
| 11. FSH (postmenopausal female; 22 – 153 U/L; n=7) | 70 (51.4 – 83.6) |
| 12. LH (postmenopausal female; 11 – 40 U/L; n=7) | 28.8 (25.1 – 40.2) |
| 13. Testosterone (male; 181-758 ng/dL; n=11) | 332.3 ± 120.1 |
| 14. Estradiol (premenopausal female; 15 – 350 pg/mL; n=5) | 96.1 (33.8 – 214.3) |
| 15. Growth hormone (0 – 3 ng/mL; n=26) | 0.16 (0.07 – 0.41) |
| 16. Prolactin (4 – 15.2 ng/mL; n=20) | 7.65 (2.25 – 13.25) |
| 17. Epinephrine (0 – 57 pg/mL; n=27) | 19 (17 – 23) |
| 18. Norepinephrine (84 – 794 pg/mL; n=27) | 826 (221 – 4520) |
| 19. Metanephrine (12 – 61 pg/mL; n=27) | 45 (26 – 70) |
| 20. Normetanephrine (18 – 112 pg/mL; n=27) | 588 (91 – 2285) |
| 21. Dopamine (0 – 25 pg/mL; n=27) | 25 (25 – 174) |

Data are represented as mean ± standard deviation or as median (interquartile range).

such corresponding changes in the cortisol levels (Figure 1A). In the pituitary-thyroid axis, the TSH on D2 (D1 = 2.2 ± 1.4 microIU/L vs. D2 = 1.4 ± 0.9 microIU/L; p<0.0001), and D3 (D1 = 2.2 ± 1.4 microIU/L vs. D3 = 1.7 ± 1.3 microIU/L; p=0.001) was significantly lower compared to its D1 value, while the FT4 on D2 (D1 = 1.1 ± 0.2 ng/dL vs. D2 = 1 ± 0.2 ng/dL; p=0.002) was significantly lower than the D1 value (Figure 1B). There were no significant changes noted on D2, D3, and D30 compared to D1 in the somatotropic axis (GH) (Figure 1C), or in the pituitary-gonadal axis (FSH, LH, testosterone, and estradiol) (Figure 1D). Compared to D1, significantly lower levels of prolactin were noted on D2 (D1 = 10.2 ± 6.9 ng/mL vs. D2 = 7.2 ± 5.7 ng/mL; p<0.0001), D3 (D1 = 10.2 ± 6.9 ng/mL vs. D3 = 7.3 ± 5.4 ng/mL; p=0.0001), and D30 (D1 = 10.2 ± 6.9 ng/mL vs. D30 = 7.7 ± 5.7 ng/mL; p=0.004) (Figure 1E). Five (18.5%) patients had undergone a 250mcg ACTH stimulation test for either a cortisol of <5 mcg/dL or for a cortisol of <10 mcg/dL as clinically indicated, and all the patients demonstrated robust increase in cortisol levels and adrenal insufficiency was ruled out.

TABLE 2 Prevalence of biochemical endocrine abnormalities in the study cohort over four cycles.

| Hormone | Number of patients with abnormal results / total number of patients |
|---|---|
| 1. Adrenocorticotropic hormone | 6/25 (24%) |
| 2. Cortisol | 5/25 (20%) |
| 3. Thyroid stimulating hormone | 5/24 (20.8%) |
| 4. Free thyroxine | 4/24 (16.7%) |
| 5. Follicle stimulating hormone (males and postmenopausal females) | 3/16 (18.8%) |
| 6. Luteinizing hormone (males and postmenopausal females) | 4/17 (23.5%) |
| 7. Testosterone (males) | 3/11 (27.3%) |
| 8. Estradiol (premenopausal females) | 3/5 (60%) |
| 9. Growth hormone | 4/26 (15.4%) |
| 10. Prolactin | 10/20 (50%) |

Most biochemical abnormalities were transient and clinically inconsequential. However, clinically symptomatic, and persistent endocrinopathies developed in two patients (Figure 2). A 29-year-old male (Patient A) was diagnosed with asymptomatic primary hyperthyroidism due to Hashimoto's thyroiditis prior to [$^{177}$Lu]Lu-DOTA-TATE therapy (Figure 2A). One month after the first dose of [$^{177}$Lu]Lu-DOTA-TATE, the patient developed marked, symptomatic primary hypothyroidism requiring levothyroxine therapy. The pre-treatment [$^{68}$Ga]Ga-DOTA-TATE PET/CT revealed diffuse thyroid uptake with a maximum standardized uptake ($SUV_{max}$) of 14.3, and a diffuse thyroidal uptake of [$^{177}$Lu]Lu-DOTA-TATE was also noted on the 24-hour post-treatment whole body single-photon emission computed tomography (SPECT) scan, with more details described elsewhere (11). A 43-year-old premenopausal woman (Patient B) with normal gonadal function prior to [$^{177}$Lu]Lu-DOTA-TATE therapy developed hot flashes and cessation of menses close to the fourth dose of [$^{177}$Lu]Lu-DOTA-TATE therapy (Figure 2B). Towards the end of the fourth cycle, there were elevations in gonadotrophins to menopausal ranges [FSH: 42.3 (menopausal reference range: 22 – 153 U/L); LH: 36.2 (menopausal reference range: 11 – 40 U/L)], with undetectable estradiol levels (<5 pg/mL; normal menopausal value: <10 pg/mL) suggestive of early menopause (onset of menopause at age <45 years) due to hypergonadotropic hypogonadism. The undetectable estradiol was preceded by a marked increase in estradiol levels (up to 470 pg/mL) followed by a gradual decline to undetectable levels, a phenomenon often observed during perimenopause (12).

10.3389/fendo.2023.1275813

TABLE 3 Proportion of biochemical endocrine abnormalities among all measurements over four cycles.

| Hormone | High | Low |
|---|---|---|
| 1. Adrenocorticotropic hormone | 26/263 (9.8%) | 3/263 (1.1%) |
| 2. Cortisol | 2/264 (0.8%) | 11/264 (4.2%) |
| 3. Thyroid stimulating hormone | 17/225 (7.6%) | 16/225 (7.1%) |
| 4. Free thyroxine | 0/230 (0%) | 8/230 (3.5%) |
| 5. Follicle stimulating hormone (males and postmenopausal females) | 20/153 (13.1%) | 0/153 (0%) |
| 6. Luteinizing hormone (males and postmenopausal females) | 21/168 (12.5%) | 0/170 (0%) |
| 7. Testosterone (males) | 1/122 (0.8%) | 10/122 (8.2%) |
| 8. Estradiol (premenopausal females) | 3/58 (5.6%) | 2/58 (3.4%) |
| 9. Growth hormone | 20/274 (7.3%) | 0/274 (0%) |
| 10. Prolactin | 24/213 (11.3%) | 30/213 (14.1%) |

## Functional imaging characteristics in patients with clinical endocrinopathies

A comparison of the $SUV_{max}$ values of the primary endocrine organs of involvement was performed between patient A and patients who never developed biochemical abnormalities in these respective hormonal axes ('controls') on the pre-treatment [$^{68}$Ga]Ga-DOTA-TATE PET/CT scan. Due to poor visualization of ovaries on the functional imaging, patient B was excluded from this analysis. The $SUV_{max}$ of the thyroid in patient A was higher than the mean thyroid $SUV_{max}$ among controls, while the $SUV_{max}$ of the pituitary was lower compared to controls (Supplementary Information; Section E). Diffuse thyroid uptake was evident on the pre-treatment diagnostic [$^{68}$Ga]Ga-DOTA-TATE scan and on the post-treatment single-photon emission CT (SPECT) scan, as previously described (11).

## Catecholamine, metanephrine, blood pressure, and heart rate variations

Compared to D1, significant mean % increase was noted with plasma levels of norepinephrine (53.3% on D2; p=0.0004, and 51.5% on D3; p=0.0006), dopamine (48% on D2; p=0.002, and 44.4% on D3; p=0.004), and normetanephrine (43.9% on D2; p=0.02) (Figures 3A, B). The mean % change on D3 for plasma metanephrine tended towards a significant change (41.4%, p=0.06). The % changes for plasma epinephrine and chromogranin A were not significant (Figures 3A, C). We also noted an increase in the absolute values in catecholamines and metanephrines, particularly of plasma norepinephrine, normetanephrine, and dopamine at 24- and 48-hours post [$^{177}$Lu]Lu-DOTA-TATE infusion, and the levels returned to baseline by D30 (Figure 3D).

Compared to D1, the SBP was significantly lower on D2 (122.6 ± 23.5 mmHg vs. 118.1 ± 20.7 mmHg; p<0.0001), but significantly higher on D3 (122.6 ± 23.5 mmHg vs. 123.4 ± 22.7 mmHg; p=0.001), while the DBP was significantly lower on D2 (66.2 ± 11.6 mmHg vs. 63.6 ± 11.7 mmHg; p<0.0001) and D3 (66.2 ± 11.6 mmHg vs. 65.1 ± 12.3 mmHg; p=0.003), and the HR was significantly higher on D30 (74.8 ± 12.9/min vs. 80.7 ± 15.2/min; p<0.0001) (Figures 4A-C).

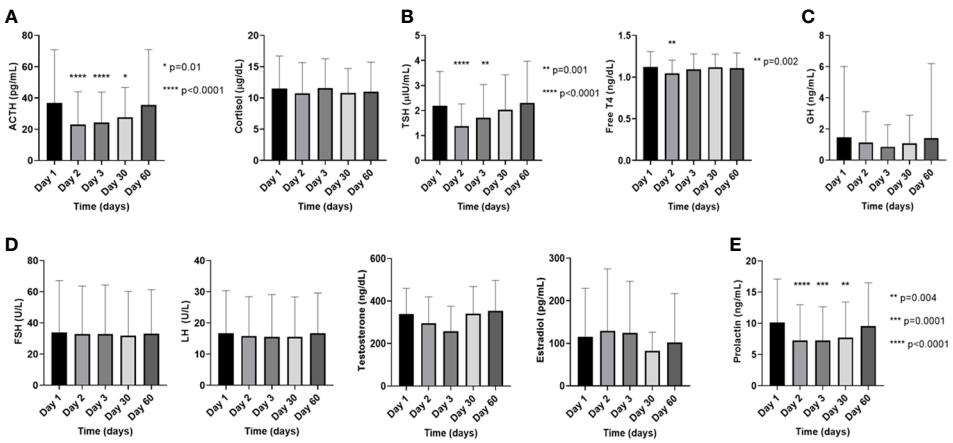


FIGURE 1
Changes in the pituitary and target endocrine gland hormone levels in the plasma on the day of [177Lu]Lu-DOTA-TATE therapy prior to the infusion (day 1) and during the immediate post-treatment period (day 2 – day 60) in **(A)**. the pituitary-adrenal axis, **(B)**. the pituitary-thyroid axis, **(C)**. the somatotropic axis, **(D)**. the pituitary-gonadal axis, and **(E)**. prolactin. The data on testosterone is exclusively from males and the data on estradiol is exclusively from premenopausal females, while the FSH and LH are combined data from males and postmenopausal females. Each 'day' comprises data from all four cycles. Data are represented as mean ± SD.

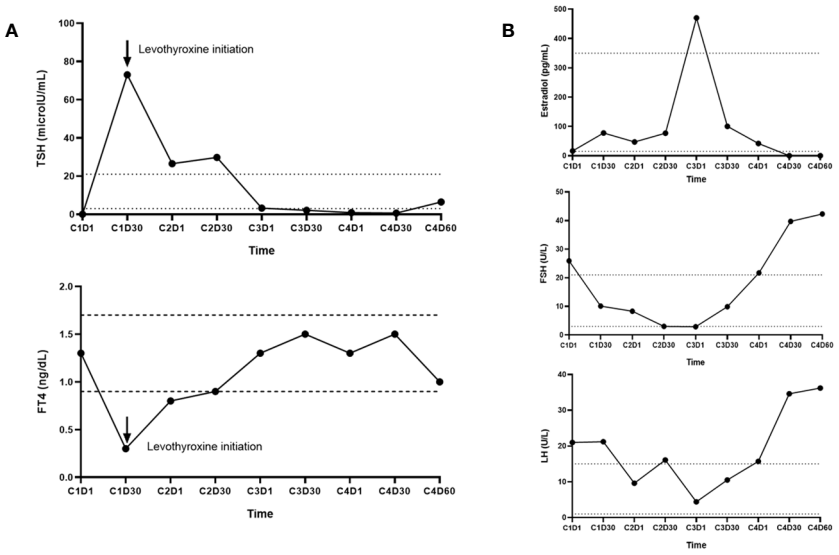


FIGURE 2
**(A)** Immunoassay measurements of thyroid stimulating hormone (TSH) and free thyroxine (FT4) levels in Patient A who was initially diagnosed with primary thyrotoxicosis prior to [177Lu]Lu-DOTA-TATE therapy initiation and later developed symptomatic primary hypothyroidism 30 days after the first dose of [177Lu]Lu-DOTA-TATE. **(B)** Immunoassay measurements of estradiol, follicle stimulating hormone (FSH), and luteinizing hormone (LH) levels in Patient B who developed secondary amenorrhea and hot flashes close to the 4th cycle dose of [177Lu]Lu-DOTA-TATE. Towards the end of cycle 4, there were elevations in gonadotrophins to menopausal ranges [FSH: 42.3 (menopausal range: 22–153 U/L); LH: 36.2 (menopausal range: 11–40 U/L)], with undetectable estradiol levels (<5 pg/mL; normal menopausal value: <10 pg/mL) suggestive of early menopause (onset of menopause at age <45 years). Estradiol levels demonstrated an initial marked increase (up to 470 pg/mL) followed by a gradual decline to undetectable levels, a phenomenon often observed during perimenopause.

## Discussion

In this study, we demonstrate that [$^{177}$Lu]Lu-DOTA-TATE treatment is associated with endocrine function fluctuations and catecholamine level surges that are detectable and statistically significant as early as 24 hours and peaking by 48 hours after administration. We also provide prospective evidence that these abnormalities mostly return to pre-treatment levels towards the end of the treatment cycle. These changes are important for the clinician to recognize for safely managing catecholamine surges post [$^{177}$Lu]Lu-DOTA-TATE treatment but also to expect the transient nature of observed pituitary dysfunction.

The longitudinal data in our study revealed a tendency for the average pituitary hormonal levels to decrease on the days immediately following [$^{177}$Lu]Lu-DOTA-TATE infusion, and then return towards baseline by the end of the cycle. These observations suggest that hormonal changes were mostly transient and likely clinically inconsequential. However, clinically evident endocrinopathy developed in 2/27 (7.4%) patients who either had an underlying pre-existing endocrinopathy of target gland (Patient A) or were at risk for developing endocrinopathy (Patient B). SSTRs have been identified in both human thyroid and ovarian tissues (13). Early studies on somatostatin analogs have demonstrated transient suppressive effects on various pituitary hormones a few hours post-administration. Octreotide doses of 50 – 100 mcg have been shown to reduce average GH levels within a few hours in both healthy adults and acromegaly patients (14, 15), as well as reduction in TSH within 6 – 10 hours among patients with TSH-secreting pituitary adenomas (16, 17). A single dose of [$^{177}$Lu]Lu-DOTA-TATE contains about 200mcg (10mcg/mL) of the somatostatin analog component (DOTA-TATE) (18). Although the pharmacokinetic properties of DOTA-TATE have been evaluated (19, 20), it is not clear whether the hormonal secretion-inhibitory properties of the octreotate component of DOTA-TATE are comparable to that of octreotide at similar doses. If this were to be the case, then one could expect similar inhibitory effects on endocrine function, as observed in our study. However, such deductions should be made with caution. Inhibitory effects of octreotide are less obvious on ACTH, cortisol, and FSH secretion (21), yet, we identified 'low' values in these hormones, thus suggesting probable mechanisms, independent of the somatostatin analog component of [$^{177}$Lu]Lu-DOTA-TATE, contributing to these effects. The frequently observed pituitary hormonal abnormalities in our study could therefore be due to the effect of [$^{177}$Lu]Lu-DOTA-TATE on the pituitary gland, leading to transient decreases of ACTH, TSH, PRL, while a potential effect of [$^{177}$Lu]Lu-DOTA-TATE on the gonads may have led to a degree of gonadal insufficiency, manifested as increases in FSH and LH, associated with low testosterone in males or to induction of menopause in women (as observed in Patient B) (8, 13).

Hyperprolactinemia/hypoprolactinemia were the most frequently observed abnormalities in our study. Immunohistochemical analysis has demonstrated high-SSTR2 expression in the human lactotrophs, which might explain our observation (22). Similar disruptive effects of [$^{177}$Lu]Lu-DOTA-TATE on other endocrine glands may have contributed towards clinically significant abnormalities in patients-A and B in our study. In a study utilizing [$^{177}$Lu]Lu-DOTA-TATE therapy for gastroenteropancreatic NETs, transient reduction in

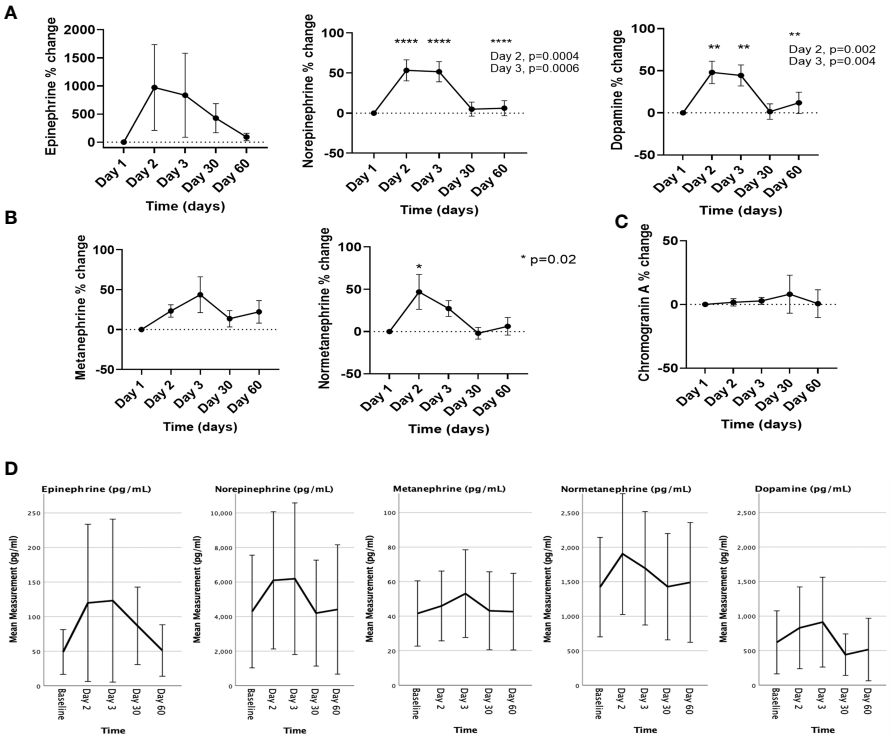


FIGURE 3
The % changes in the levels of **(A)** catecholamines, **(B)** metanephrines, and **(C)** chromogranin A, and **(D)** the changes in the absolute values of catecholamines and metanephrines on the day of [$^{177}$Lu]Lu-DOTA-TATE therapy prior to the infusion (day 1) and during the immediate post-treatment period (day 2 – day 60). Each 'day' comprises data from all four cycles. Data are represented as mean ± SEM.

testosterone and inhibin-B levels, with FSH elevations were identified in men in the first 24 months of therapy, suggesting a potential radiation-induced effect on Sertoli cells (23). Four cycles of 7.4 GBq dose of [$^{177}$Lu]Lu-DOTA-TATE therapy delivers small radiation doses to the adrenals (1.1 Gy), ovaries (0.9 Gy), testes (0.8 Gy), and thyroid (0.8 Gy). These doses are modest, and data from external beam radiation to the pituitary have demonstrated low incidence of hormonal abnormalities with doses <20 Gy, with GH secretion being more susceptible to radiation (<30 Gy), and TSH/ACTH axes being more resistant (up to 50 Gy) (24, 25).

Evidence on [$^{177}$Lu]Lu-DOTA-TATE -associated endocrine disruption has been reported in other studies. Teunissen et al. evaluated endocrine function from baseline up to 24-months follow-up among patients receiving [$^{177}$Lu]Lu-DOTA-TATE (9). At 24 months, the mean total testosterone level in men decreased by 30%, and in postmenopausal women, the mean baseline FSH and LH levels reduced by 16% and 21% respectively from baseline. The mean baseline FT4 levels reduced by 12% at 24 months, with two patients eventually developing primary hypothyroidism. In a phase 2 [$^{177}$Lu]Lu-DOTA-TATE trial on patients with NETs, baseline and yearly pituitary function assessment was performed (8). Plasma IGF-1 decreased by 30% at 48 months, while ACTH increased by 58% during the first year and normalized later. Plasma FSH and LH in males also demonstrated a significant increase within 12 months of [$^{177}$Lu]Lu-DOTA-TATE, followed by normalization of levels, and then followed by an increase in levels after 48 months. In

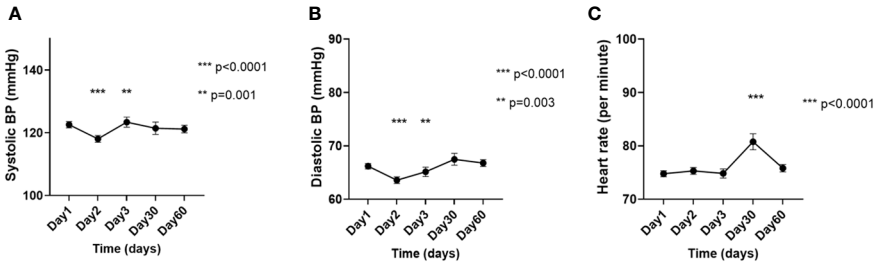


FIGURE 4
Changes in the **(A)** systolic blood pressure, **(B)** diastolic blood pressure, and **(C)** heart rate on the day of [$^{177}$Lu]Lu-DOTA-TATE therapy, prior to the infusion (day 1) and during the immediate post-treatment period (day 2 – day 60). Each 'day' comprises data from all four cycles. Data are represented as mean ± SEM.

10.3389/fendo.2023.1275813

another study, [$^{177}$Lu]Lu-DOTA-TATE therapy in previously normocalcemic patients with NETs (n=47) resulted in significant reductions in serum calcium levels and a significant increase in serum parathyroid hormone (PTH) levels manifesting as secondary hyperparathyroidism when followed up to 6 months after therapy, and 11% of the patients required calcium supplementation (26).

We identified a 2.7-fold higher thyroid uptake on the pre-treatment [$^{68}$Ga]Ga-DOTA-TATE PET/CT scan in Patient A, as compared to the mean uptake among individuals with normal pituitary-thyroid axis in our cohort. Prior studies have shown the thyroid $SUV_{max}$ to be about 4.6 on [$^{68}$Ga]Ga-DOTA-TATE PET/CT scans (27), and in comparison, the uptake ($SUV_{max}$=14.3) in Patient A was 3 times this value. This suggests that there may have been a higher density of SSTRs on the thyroid in Patient A, which may have led to higher uptake of [$^{177}$Lu]Lu-DOTA-TATE, potentially leading to rapid worsening of thyroid function. In fact, thyroid dysfunction (subclinical hypothyroidism) has also been recently reported following the use of α emitter-based PRRT, [$^{225}$Ac]Actinium-DOTA-TATE (28). Our findings warrant careful interpretation as these are findings from a single 'case' subject. Dosimetry allows for calculation of thyroid radiation exposure, but dosimetry was not included in our trial's protocol. A similar mechanism may have contributed to early menopause in Patient B although we could not measure the $SUV_{max}$ in this patient. Further studies evaluating the association between such uptake patterns in other endocrine glands and clinical endocrinopathies are necessary.

We identified significant elevations in catecholamine and metanephrine levels in the initial 30 days following [$^{177}$Lu]Lu-DOTA-TATE dose, findings not previously reported per our knowledge. These elevations started within 24 hours post-administration and had peaked by 48 hours. Direct cytotoxicity from $^{177}$Lu radionuclide on chromaffin cells of PPGL leading to the spillage of catecholamines and metanephrines could be the most likely mechanism. Moreover, among the patients with secretory PPGL in our cohort, five patients with profoundly high levels of plasma catecholamines were treated with metyrosine, a catecholamine synthesis inhibitor (29), during [$^{177}$Lu]Lu-DOTA-TATE therapy. Even in these patients, catecholamine/metanephrine levels increased following [$^{177}$Lu]Lu-DOTA-TATE infusion, suggesting the increase in plasma catecholamines/metanephrines to be likely due to spillage of preformed molecules from the PPGL. As PPGLs can be SSTR2+ (30), the octreotate component of [$^{177}$Lu]Lu-DOTA-TATE may potentially affect catecholamine production. However, somatostatin analogs decrease catecholamine synthesis from PPGL chromaffin cells (31). Therefore, the somatostatin-mediated effects do not explain the post-treatment increase in catecholamine/metanephrine levels that most likely occurs due to radiation-related tumor disruption. Furthermore, [$^{177}$Lu]Lu-DOTA-TATE-mediated alterations in the dynamics of cytosolic-vesicular catecholamine uptake/reuptake/metabolism, and interactions with adrenal-medullary peptides modulating catecholamine secretion are possible (32), but require further investigation. Another minor contribution to these findings could be from the renoprotective amino acid infusion containing phenylalanine/tyrosine which some of our patients received prior to [$^{177}$Lu]Lu-DOTA-TATE infusion. As phenylalanine/tyrosine are precursors for catecholamine synthesis, they may increase catecholamines in patients with secretory forms of PPGL (33). However, several patients in our study received exclusively lysine/arginine containing amino acid infusions, instead of phenylalanine/tyrosine containing infusions. The BP and HR variability and their correlation with catecholamine/metanephrine changes are challenging to interpret in our study due to patients receiving multiple forms of anti-hypertensive therapy prophylactically or following [$^{177}$Lu]Lu-DOTA-TATE infusion, or due to effects of amino acid infusion on vascular tone. However, hypertension associated with [$^{177}$Lu]Lu-DOTA-TATE have been reported in the literature (34).

Our study has several strengths. Hormonal assays were performed in the same laboratory, thus minimizing inter-institute assay variations. Blood samples were collected through an indwelling intravenous catheter which reduced potential needle trauma-related fluctuations in ACTH and prolactin. Concerns for interference by the non-radiolabeled ('cold') somatostatin analogs with [$^{177}$Lu]Lu-DOTA-TATE therapy were unlikely as the trial protocol necessitated the criteria of no initiation/alteration of somatostatin analog therapy within 3 months of enrollment for long-acting octreotide/lanreotide therapies and withholding of short-acting octreotide for 24 hours prior to [$^{177}$Lu]Lu-DOTA-TATE infusion.

However, our study does have limitations. All 4 cycles of [$^{177}$Lu]Lu-DOTA-TATE therapy were completed in 13/27 patients, and data till the end of the 4$^{th}$ cycle was available in 11/27 patients. The list of hormones to be measured were predetermined in the clinical trial protocol, and the data was only available for retrospective analysis. Therefore, effects of [$^{177}$Lu]Lu-DOTA-TATE therapy on several hormones of interest, such as IGF-1, inhibins-A and -B, anti-Müllerian hormone, pancreatic islet hormone function (insulin, hemoglobin A1c), and PTH, could not be assessed. Similarly, per trial protocol, the timings of plasma collection were pre-set at 24-hour intervals post-[$^{177}$Lu]Lu-DOTA-TATE infusion, and the timings of the infusion during the day varied across different cycles and patients. This could have affected the levels of certain hormones measured in our study (such as cortisol and testosterone) which demonstrate diurnal variations in plasma concentration (35, 36). However, most blood samples were obtained no later than 11:30 AM, and we utilized the wide reference range provided by our institutional immunoassays for each hormone such that those hormone levels resulted by our laboratory as 'high' or 'low' were unequivocal. We also acknowledge the limited utility of random GH measurements due to pulsatile nature of its secretion, as well as the unknown significance of random ACTH measurements in the absence of an underlying/suspected corticotrope or adrenocortical disorder. There is a likelihood for some of the 'low' hormonal values to be a result of either a transient inhibition of pituitary hormones by the somatostatin component of [$^{177}$Lu]Lu-DOTA-TATE, or from the dilutional effect from intravenous hydration with 2L normal saline prior to [$^{177}$Lu]Lu-DOTA-TATE infusion. However, this does not explain the several elevated hormonal values that were observed after [$^{177}$Lu]Lu-DOTA-TATE infusion, and therefore, the

somatostatin inhibitory effect or the dilutional effect are unlikely to be entirely responsible for the observed changes. Certain 'low' values in the thyrotropic and gonadotropic axis hormones could be due to euthyroid sick or eugonadal sick syndromes respectively, which cannot be ruled out in this study population. While all assays were performed at our institution, a few uninterpretable metanephrine values due to potential interfering substances, which were measured at the Mayo Clinic laboratories using liquid chromatography/mass spectrometry. Hormonal evaluation was performed using immunoassays which are highly susceptible to interfering substances and can show wide inter- and intra-assay variations. While the clinically significant endocrinopathies noted in patients A and B persisted till the time of last follow-up in these patients, whether these changes are permanent or whether these were mere coincidental findings remains to be determined.

In conclusion, [$^{177}$Lu]Lu-DOTA-TATE therapy is associated with variations in biochemical endocrine function and with significant changes in plasma catecholamine and metanephrine levels in the immediate post-treatment period. While most hormonal abnormalities are transient and clinically silent, some abnormalities can become profound, clinically significant, and potentially persistent, especially among patients with pre-existing endocrinopathy or those who are at risk for developing an endocrinopathy. Moreover, these observable changes serve as a reminder for potentially more persistent pituitary damage and severe catecholamine surges that may be seen by more powerful agents such as alpha-particle PRRT. Current practice lacks emphasis on evaluating the off-tumor radiation effects in the immediate post-treatment period of [$^{177}$Lu]Lu-DOTA-TATE infusion or other PRRTs. Our data demonstrates that such effects indeed occur post [$^{177}$Lu]Lu-DOTA-TATE infusion. Therefore, early, and serial endocrine function testing should be considered among patients undergoing [$^{177}$Lu]Lu-DOTA-TATE therapy.

## Data availability statement

The original contributions presented in the study are included in the article/Supplementary Material. Further inquiries can be directed to the corresponding author.

## Ethics statement

The studies involving humans were approved by National Institutes of Health Clinical Center. The studies were conducted in accordance with the local legislation and institutional requirements. The participants provided their written informed consent to participate in this study.

## Author contributions

SG: Data curation, Formal Analysis, Software, Writing – original draft, Writing – review & editing. MA-J: Formal Analysis, Writing – review & editing. SA: Data curation, Formal Analysis, Software, Writing – review & editing. AJ: Writing – review & editing. JZ: Writing – review & editing. IS: Writing – review & editing. LM: Writing – review & editing. MK: Writing – review & editing. BT: Writing – review & editing. LL: Writing – review & editing. EM: Writing – review & editing. JC: Data curation, Methodology, Supervision, Validation, Writing – review & editing. YT: Formal Analysis, Writing – review & editing. KP: Supervision, Writing – review & editing. JK-G: Supervision, Validation, Writing – review & editing. JD: Supervision, Validation, Writing – review & editing, Methodology. FL: Conceptualization, Funding acquisition, Investigation, Methodology, Resources, Supervision, Validation, Writing – review & editing.

## Funding

The authors declare financial support was received for the research, authorship, and/or publication of this article. This work was supported by the National Institutes of Health Intramural Programs (1ZIABC011789 and Z1A HD008735).

## Acknowledgments

We thank the physicians and nurses who provided care to the clinical trial patients at the NIH Clinical Center.

## Conflict of interest

The authors declare that the research was conducted in the absence of any commercial or financial relationships that could be construed as a potential conflict of interest.

The author(s) declared that they were an editorial board member of Frontiers at the time of submission. This had no impact on the peer review process and the final decision.

## Publisher's note

All claims expressed in this article are solely those of the authors and do not necessarily represent those of their affiliated organizations, or those of the publisher, the editors and the reviewers. Any product that may be evaluated in this article, or claim that may be made by its manufacturer, is not guaranteed or endorsed by the publisher.

## Supplementary material

The Supplementary Material for this article can be found online at: https://www.frontiersin.org/articles/10.3389/fendo.2023.1275813/full#supplementary-material

# References


1. Reubi J, Waser B, Schaer J-C, Laissue JA. Somatostatin receptor sst1–sst5 expression in normal and neoplastic human tissues using receptor autoradiography with subtype-selective ligands. *Eur J Nucl Med* (2001) 28(7):836–46. doi: 10.1007/s002590100541

2. Shah MH, Goldner WS, Halfdanarson TR, Bergsland E, Berlin JD, Halperin D, et al. NCCN guidelines insights: neuroendocrine and adrenal tumors, version 2. *2018. J Natl Compr Canc Netw* (2018) 16(6):693–702. doi: 10.6004/jnccn.2018.0056

3. Fishbein L, Del Rivero J, Else T, Howe JR, Asa SL, Cohen DL, et al. The north american neuroendocrine tumor society consensus guidelines for surveillance and management of metastatic and/or unresectable pheochromocytoma and paraganglioma. *Pancreas* (2021) 50(4):469–93. doi: 10.1097/MPA.0000000000001792

4. Strosberg J, El-Haddad G, Wolin E, Hendifar A, Yao J, Chasen B, et al. Phase 3 trial of 177Lu-Dotatate for midgut neuroendocrine tumors. *New Engl J Med* (2017) 376 (2):125–35. doi: 10.1056/NEJMoa1607427

5. Nockel P, Millo C, Keutgen X, Klubo-Gwiezdzinska J, Shell J, Patel D, et al. The rate and clinical significance of incidental thyroid uptake as detected by Gallium-68 DOTATATE positron emission tomography/computed tomography. *Thyroid* (2016) 26(6):831–5. doi: 10.1089/thy.2016.0174

6. Batchala PP, Dyer A, Mukherjee S, Rehm PK. Lateral ectopic thyroid mimics carotid body tumor on Indium-111 pentetreotide scintigraphy. *Clin imaging* (2019) 58:46–9. doi: 10.1016/j.clinimag.2019.05.012

7. Gupta SK, Singla S, Thakral P, Bal CS. Dosimetric analyses of kidneys, liver, spleen, pituitary gland, and neuroendocrine tumors of patients treated with 177Lu-DOTATATE. *Clin Nucl Med* (2013) 38(3):188–94. doi: 10.1097/RLU.0b013e3182814ac1

8. Sundlöv A, Sjögreen-Gleisner K, Tennvall J, Dahl L, Svensson J, Åkesson A, et al. Pituitary function after high-dose 177Lu-DOTATATE therapy and long-term follow-up. *Neuroendocrinology* (2021) 111(4):344–53. doi: 10.1159/000507761

9. Teunissen JJ, Krenning EP, de Jong FH, de Rijke YB, Feelders RA, van Aken MO, et al. Effects of therapy with [177 Lu-DOTA 0, Tyr 3] octreotate on endocrine function. *Eur J Nucl Med Mol imaging* (2009) 36(11):1758. doi: 10.1007/s00259-009-1151-8

10. *LUTATHERA® Full Prescribing Information* (2021). Available at: https://www.novartis.us/sites/www.novartis.us/files/lutathera.pdf.

11. Gubbi S, Al-Jundi M, Del Rivero J, Jha A, Knue M, Zou J, et al. Case report: primary hypothyroidism associated with lutetium 177-DOTATATE therapy for metastatic paraganglioma. *Front Endocrinol* (2020) 11. doi: 10.3389/fendo.2020.587065

12. Santoro N, Brown JR, Adel T, Skurnick JH. Characterization of reproductive hormonal dynamics in the perimenopause. *J Clin Endocrinol Metab* (1996) 81(4):1495–501. doi: 10.1210/jcem.81.4.8636357

13. Boy C, Heusner TA, Poeppel TD, Redmann-Bischofs A, Unger N, Jentzen W, et al. 68Ga-DOTATOC PET/CT and somatostatin receptor (sst1-sst5) expression in normal human tissue: correlation of sst2 mRNA and SUVmax. *Eur J Nucl Med Mol Imaging* (2011) 38(7):1224–36. doi: 10.1007/s00259-011-1760-x

14. Gilbert JA, Miell JP, Chambers SM, McGregor AM, Aylwin SJ. The nadir growth hormone after an octreotide test dose predicts the long-term efficacy of somatostatin analogue therapy in acromegaly. *Clin Endocrinol (Oxf).* (2005) 62(6):742–7. doi: 10.1111/j.1365-2265.2005.02278.x

15. Mulligan T, Jaen-Vinuales A, Godschalk M, Iranmanesh A, Veldhuis JD. Synthetic somatostatin analog (octreotide) suppresses daytime growth hormone secretion equivalently in young and older men: preserved pituitary responsiveness to somatostatin's inhibition in aging. *J Am Geriatr Soc* (1999) 47(12):1422–4. doi: 10.1111/j.1532-5415.1999.tb01560.x

16. Losa M, Magnani P, Mortini P, Persani L, Acerno S, Giugni E, et al. Indium-111 pentetreotide single-photon emission tomography in patients with TSH-secreting pituitary adenomas: correlation with the effect of a single administration of octreotide on serum TSH levels. *Eur J Nucl Med* (1997) 24(7):728–31. doi: 10.1007/BF00879659

17. Chayen SD, Gross D, Makhoul O, Glaser B. TSH producing pituitary tumor. *Hormone Metab Res* (1992) 24(01):34–8. doi: 10.1055/s-2007-1003247

18. *LUTATHERA® Summary of Product Characteristics* (2018). Available at: http://www.ema.europa.eu.

19. Shastry M, Kayani I, Wild D, Caplin M, Visvikis D, Gacinovic S, et al. Distribution pattern of 68Ga-DOTATATE in disease-free patients. *Nucl Med Commun* (2010) 31(12):1025–32. doi: 10.1097/MNM.0b013e32833f635e

20. Siebinga H, de Wit-van der Veen BJ, Beijnen JH, Stokkel MPM, Dorlo TPC, Huitema ADR, et al. A physiologically based pharmacokinetic (PBPK) model to describe organ distribution of (68)Ga-DOTATATE in patients without neuroendocrine tumors. *EJNMMI Res* (2021) 11(1):73. doi: 10.1186/s13550-021-00821-7

21. Lightman S, Fox P, Dunne M. The effect of SMS 201-995, a long-acting somatostatin analogue, on anterior pituitary function in healthy male volunteers. *Scandinavian J Gastroenterol* (1986) 21(sup119):84–95. doi: 10.3109/00365528609087435

22. Thodou E, Kontogeorgos G, Theodossiou D, Pateraki M. Mapping of somatostatin receptor types in GH or/and PRL producing pituitary adenomas. *J Clin Pathol* (2006) 59(3):274–9. doi: 10.1136/jcp.2005.026914

23. Kwekkeboom DJ, de Herder WW, Kam BL, van Eijck CH, van Essen M, Kooij PP, et al. Treatment with the radiolabeled somatostatin analog [177 Lu-DOTA 0,Tyr3] octreotate: toxicity, efficacy, and survival. *J Clin Oncol* (2008) 26(13):2124–30. doi: 10.1200/JCO.2007.15.2553

24. Vatner RE, Niemierko A, Misra M, Weyman EA, Goebel CP, Ebb DH, et al. Endocrine deficiency as a function of radiation dose to the hypothalamus and pituitary in pediatric and young adult patients with brain tumors. *J Clin Oncol* (2018) 36 (28):2854–62. doi: 10.1200/JCO.2018.78.1492

25. Darzy KH, Shalet SM. Hypopituitarism following radiotherapy. *Pituitary* (2009) 12(1):40–50. doi: 10.1007/s11102-008-0088-4

26. van Vliet EI, de Herder WW, de Rijke YB, Zillikens MC, Kam BL, Teunissen JJ, et al. Hypocalcaemia after treatment with [177Lu-DOTA 0,Tyr3]octreotate. *Eur J Nucl Med Mol Imaging* (2013) 40(12):1843–52. doi: 10.1007/s00259-013-2503-y

27. Kunikowska J, Matyskiel R, Zemczak A, Strzelczyk J, Pawlak D, Królicki L, et al. How often do we see incidental 68Ga-DOTATATE thyroid uptake in PET/CT in patients with neuroendocrine tumours? *Endokrynol Pol* (2015) 66(3):231–6. doi: 10.5603/EP.2015.0030

28. Kavanal AJ, Satapathy S, Sood A, Khosla D, Mittal BR. Subclinical hypothyroidism after 225Ac-DOTATATE therapy in a case of metastatic neuroendocrine tumor: unknown adverse effect of PRRT. *Clin Nucl Med* (2022) 47 (2):e184–e6. doi: 10.1097/RLU.0000000000003893

29. Jones NF, Walker G, Ruthven CR, Sandler M. Alpha-methyl-p-tyrosine in the management of phaeochromocytoma. *Lancet* (1968) 2(7578):1105–9. doi: 10.1016/S0140-6736(68)91579-1

30. Elston MS, Meyer-Rochow GY, Conaglen HM, Clarkson A, Clifton-Bligh RJ, Conaglen JV, et al. Increased SSTR2A and SSTR3 expression in succinate dehydrogenase-deficient pheochromocytomas and paragangliomas. *Hum Pathol* (2015) 46(3):390–6. doi: 10.1016/j.humpath.2014.11.012

31. Pasquali D, Rossi V, Conzo G, Pannone G, Bufo P, De Bellis A, et al. Effects of somatostatin analog SOM230 on cell proliferation, apoptosis, and catecholamine levels in cultured pheochromocytoma cells. *J Mol endocrinol* (2008) 40(6):263–71. doi: 10.1677/JME-08-0012

32. Berends AMA, Eisenhofer G, Fishbein L, Horst-Schrivers A, Kema IP, Links TP, et al. Intricacies of the molecular machinery of catecholamine biosynthesis and secretion by chromaffin cells of the normal adrenal medulla and in pheochromocytoma and paraganglioma. *Cancers (Basel)* (2019) 11(8):1121. doi: 10.3390/cancers11081121

33. Lin F, Carrasquillo J, Jha A, Gonzales M, del Rivero J, Forest A, et al. Effects of amino acid co-infusion on increased catecholamine symptoms in metastatic pheochromocytoma patients treated with 177Lu-DOTATATE. *J Nucl Med* (2019) 60 (supplement 1):76.

34. Makis W, McCann K, McEwan AJ. The challenges of treating paraganglioma patients with (177)Lu-DOTATATE PRRT: catecholamine crises, tumor lysis syndrome and the need for modification of treatment protocols. *Nucl Med Mol Imaging* (2015) 49 (3):223–30. doi: 10.1007/s13139-015-0332-6

35. Bhasin S, Brito JP, Cunningham GR, Hayes FJ, Hodis HN, Matsumoto AM, et al. Testosterone therapy in men with hypogonadism: an endocrine society clinical practice guideline. *J Clin Endocrinol Metab* (2018) 103(5):1715–44. doi: 10.1210/jc.2018-00229

36. Bornstein SR, Allolio B, Arlt W, Barthel A, Don-Wauchope A, Hammer GD, et al. Diagnosis and treatment of primary adrenal insufficiency: an endocrine society clinical practice guideline. *J Clin Endocrinol Metab* (2016) 101(2):364–89. doi: 10.1210/jc.2015-1710

frontiers | Frontiers in Oncology

TYPE Case Report
PUBLISHED 21 May 2024
DOI 10.3389/fonc.2024.1394552

Check for updates

OPEN ACCESS

EDITED BY
Ichiro Abe,
Fukuoka University Chikushi Hospital, Japan

REVIEWED BY
Piotr Glinicki,
Centre of Postgraduate Medical Education, Poland
Yuichi Yoshida,
Oita University, Japan
Yoshikiyo Ono,
Tohoku University Hospital, Japan

*CORRESPONDENCE
Rui Liu
liur@jlu.edu.cn

RECEIVED 01 March 2024
ACCEPTED 06 May 2024
PUBLISHED 21 May 2024

CITATION
Li C, Han L, Song Y and Liu R (2024) Case report: A rare DLST mutation in patient with metastatic pheochromocytoma: clinical implications and management challenges. *Front. Oncol.* 14:1394552.
doi: 10.3389/fonc.2024.1394552

COPYRIGHT
© 2024 Li, Han, Song and Liu. This is an open-access article distributed under the terms of the Creative Commons Attribution License (CC BY). The use, distribution or reproduction in other forums is permitted, provided the original author(s) and the copyright owner(s) are credited and that the original publication in this journal is cited, in accordance with accepted academic practice. No use, distribution or reproduction is permitted which does not comply with these terms.

# Case report: A rare DLST mutation in patient with metastatic pheochromocytoma: clinical implications and management challenges

Chang Li[1], Liang Han[2], Yuming Song[1] and Rui Liu[1]*

[1]Department of VIP Unit, China-Japan Union Hospital of Jilin University, Changchun, Jilin, China, [2]Department of Pathology, China-Japan Union Hospital of Jilin University, Changchun, Jilin, China

**Background:** Pheochromocytoma is one of the most hereditary human tumors with at least 20 susceptible genes undergoing germline and somatic mutations, and other mutations less than 1% -2%. In recent years, other rare mutations have gradually been discovered to be possibly related to the pathogenesis and metastasis of pheochromocytoma. Most patients with pheochromocytoma experience common symptoms like headaches, palpitations, and sweating, while some may have less common symptoms. The diversity of symptoms, genetic mutations, and limited treatment options make management challenging.

**Case presentation:** A 53-year-old woman was hospitalized after experiencing episodic epigastric pain for one month. A mass was found in her right adrenal gland and she underwent robot-assisted laparoscopic surgery, revealing a pheochromocytoma. At the 16-month follow-up, multiple metastatic lesions consistent with metastatic pheochromocytoma were found. A germline mutation in the dihydrolipoamide succinyltransferase (DLST) gene (c.330 + 14A>G) was detected, and despite trying chemotherapy and adjuvant therapy, the patient had a limited response with an overall survival of 27 months.

**Conclusions:** DLST mutation is one of the rare pheochromocytoma-related mutated genes, and genetic sequencing is crucial for effective clinical management.

KEYWORDS

**pheochromocytoma, neoplasm metastasis, exome sequencing, dihydrolipoamide succinyltransferase, case report**

# 1 Introduction

Pheochromocytoma (PCC) and paraganglioma (PGL) are collectively known as PPGL (1). Clinical manifestations of hypertension are present in over 90% of patients, while symptoms such as headache, palpitations, and sweating are reported in more than 50% of cases. PPGL has been categorized into metastatic and non-metastatic forms (1). 10% of PCC and 15–35% of PGL are malignant but metastatic diseases are rare (2, 3). PPGL is recognized as one of the most heritable tumors among all human malignancies, with genetic factors accounting for approximately 40% (4). The activation of susceptibility genes in key pathways, including pseudohypoxia, kinase, and Wnt signaling, are identified (5–8). Tumors classified within Cluster 1 typically exhibit a noradrenergic biochemical phenotype and are associated with a heightened risk of sustained hypertension. Gene sequencing, metaphranes, and abdominal imaging are useful for diagnosing PCC (9). Surgery is the preferred treatment, but systemic options are available for inoperable cases with limited effectiveness. Patients with mutation should receive personalized lifelong monitoring (10).

A case study of a female with PCC metastasis occurring 16 months post-surgery was presented, characterized by atypical clinical manifestations. Whole-exome sequencing revealed DLST gene mutations, suggesting a potential association with PCC development. A comprehensive review of literature was conducted to discuss the clinical management.

# 2 Case presentation

## 2.1 Medical history and preoperative examination

A 53-year-old female without prior medical history presented with episodic upper abdominal pain in June 2021.The patient exhibited no symptoms of paroxysmal or persistent hypertension, headache, palpitations, sweating, vision loss, body weight loss or other related manifestations. No retinal hemangioma was detected. In July 2021, the patient exhibited normal respiration, heart rate (80 beats/min), and blood pressure (130/80mmHg), with no abnormal findings noted during cardiopulmonary and abdominal examinations. Adrenal enhancement computed tomography (CT) revealed a space occupying lesion in the right adrenal region (about 4.2×5.9cm in size) (Figures 1A, B) and normal lung CT. 18F-fuorodeoxyglucose positron emission tomography (PET)/CT revealed a mass in the right adrenal region with unevenly increased glucose metabolism (maximum cross-sectional area of 5.68×4.81 cm). Auxiliary examinations of the central nervous system, heart, kidney, and pancreas revealed no abnormalities. Metanephrine (MN) and neuron specific enolase (NSE) showed no abnormalities. Blood normetanephrine (NMN) was about three times than the normal upper limit (Supplementary Table 1). CgA concentration in blood and fractionated metanephrines in 24 hour urine weren't conducted. The patient's blood routine, liver and kidney function, blood glucose levels, urinary occult blood, and other biochemical indicators showed no significant abnormalities. Normal ACTH rhythm, cortisol rhythm, and renin activity were observed (Supplementary Table 4). Aldosterone levels in the supine position were measured at 219.4pg/ml (reference range 10.0–160.0pg/ml), while orthostatic aldosterone levels were recorded at 415.5pg/ml (reference range 40–310pg/ml).

## 2.2 Surgical treatment and postoperative pathology

To mitigate the risk of cardiovascular complications, the patient was administered oral doxazosin in July 2021, followed by oral bisoprolol prior to surgery. The planned procedures include laparoscopic retroperitoneal lesion resection, right adrenal mass resection, and abdominal adhesiolysis. Intraoperatively, the presence of greater omentum tissue at the inferior margin of the liver and intestinal adhesions was noted. Following dissociation, a mass measuring approximately 5.0 x 5.0 cm, exhibiting moderate activity and in close proximity to the right adrenal gland, was identified. No discernible abnormalities were detected in the liver,

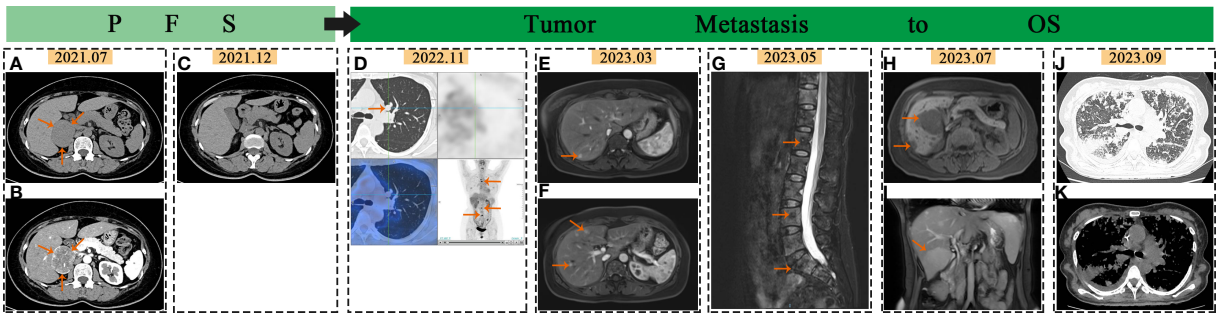


FIGURE 1
Imaging changes in PCC: In July 2021, the arrows pointed to the adrenal mass on abdominal and enhanced CT scans **(A, B)**. In December 2021, no abnormalities were seen in abdominal CT scans **(C)**. In November 2022, the arrows pointed to lung and bone metastasis on PET-CT **(D)**. In March 2023, the arrows indicated liver metastases on liver MR images **(E, F)**. In May 2023, the arrows pointed to spine metastases on MR images **(G)**. In July 2023, the arrows indicated liver metastases on liver MR images **(H, I)**. In September 2023, CT scan showed extensive lung metastases with inflammation **(J, K)**.

stomach, colon, or small intestine. Based on preoperative evaluations and intraoperative observations, the surgical approach was maintained without alterations. The surrounding tissue of the tumor was found to be fully free, allowing for the complete removal of the tumor. Postoperative pathology revealed a retroperitoneal adrenal tumor measuring 5.7 x 4.5 x 4cm and weighing 75g, with incomplete capsular involvement. Histological examination revealed the presence of small nests of chief cells accompanied by small and interspersed blood vessels. Immunohistochemical (IHC) staining indicated positivity for chromogranin A (CgA), synaptophysin (SyN), Ki-67 (5%+), succinate dehydrogenase B (SDHB), NSE, and sustentacular cells (individual cells+) (Figures 2A–D). The patient presented with atypical symptoms and signs of PCC. Based on qualitative diagnostic criteria (elevated blood NMN levels exceeding twice the upper limit of normal) and localization diagnostic methods (adrenal CT, PETCT) conducted prior to surgery, PCC was highly suspected. GAPP score was 5. The final clinical diagnosis was PCC (T3N0M0 stageIII).

## 2.3 Metastasis and postoperative treatment

The patient remained asymptomatic during routine postoperative follow-up. The adrenal CT was normal 5 months after operation (Figure 1C). Levels of MN, NMN, and NSE were within normal limits. 16 months post-operation,18F-FDG PET/CT imaging revealed increased glucose metabolism in the bilateral lungs and subpleural region. Additionally, heightened glucose metabolism was observed in the sternum, cervical 2, thoracic 4, 5, 7, 8, lumbar 3–5 vertebral bodies, left iliac bone, and right femur (Figure 1D). Lung CT showed multiple metastases. Further imaging with Gallium-68 labeled 1,4,7,10-tetraazacyclododecane-1,4,7,10-tetraacetic acid-N-octyl-D-phenylalanine and 18F-Dihydroxyphenylalanine PET/CT demonstrated widespread bone metastases, multiple lung metastases with high expression of growth inhibitory receptors, and liver metastases in both lobes with low expression of growth inhibitory receptors. The lung and bone lesions showed positive results for CgA, SyN, SDHB, vimentin (VIM), CD56, GATA3, and somatostatin receptor 2 (SSTR 2), with Ki-67 levels at 30% in the lung and 5% in the bone, indicating metastatic PCC (Figures 2E–H). Levels of MN, NMN,catecholamine (CA) and NSE were still within normal range.

Whole Exome Sequencing Analysis Reveals: A point mutation in the DLST Gene (c.330 + 14A>G), potentially linked to PGL Type 7, and a mutation in the Cyclin D1 (CCND1) Gene (c.575–13C>T), potentially associated with Von Hippel-Lindau Syndrome (Supplementary Table 2). The patient underwent pre-treatment evaluation and preparation for systemic therapy of metastatic PCC. The evident adverse reactions of nausea and vomiting were observed in patients receiving 68Ga-dotatate PET/CT. Taking into consideration the patient's physical tolerance, the ultimate treatment regimen consisted of oral temozolomide (300mg administered once daily for 1–5 days, with a treatment course repeated every 28 days) and subcutaneous denosumab (120mg administered once every 4 weeks). Following the completion of one course of oral temozolomide, treatment was discontinued due to notable gastrointestinal symptoms. Subsequent treatment included continuation of the denosumab regimen alongside subcutaneous injections of octreotide acetate microspheres (60mg administered once every 4 weeks), interspersed with traditional Chinese medicine anti-tumor therapy. Subsequent to treatment initiation, the frequency of follow-up assessments was escalated. Blood parameter monitoring was conducted based on clinical status, with imaging evaluations scheduled approximately every two months. The imaging changes of metastatic lesions in March and May 2023 are shown in Figures 1E–G. By July 2023, the patient began experiencing significant dyspnea and intermittent hemoptysis, indicating rapid disease progression (Figures 1H, I).

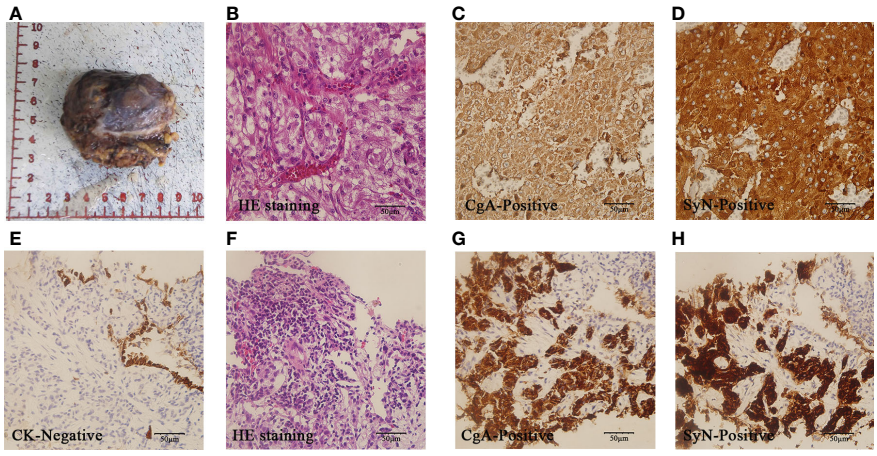


FIGURE 2
Pathology of PCC after surgery and metastasis:A-D showed pathology images of PCC after surgery. The gross specimen was a right retroperitoneal adrenal mass with incomplete capsule **(A)**. HE staining revealed small nests of chief cells with small and interspersed blood vessels(× 400) **(B)**. Tumor cells demonstrated diffuse CgA positivity (× 400) **(C)** and SyN positivity(×400) **(D)**. **(E–H)** displayed pathology images of lung metastases. Lung metastatic cells were negative for CK (× 400) **(E)**. The HE staining showed similar characteristics to the primary tumor (× 400) **(F)**. The lung metastatic cells exhibited diffuse CgA positivity (× 400) **(G)** and SyN positive (× 400) **(H)**.

The adverse bleeding reaction associated with tyrosine kinase inhibitors (TKIs) treatment poses a limitation on the utilization of these drugs by the patient. In September 2023, she was hospitalized for worsening breathing difficulties, vomiting, and anemia. Metastatic lesions in the liver and lungs had increased (Figures 1J, K), along with elevated levels of NMN, NE, and NSE (Supplementary Table 1). She was diagnosed with advanced stage IV PCC. Palliative treatment was provided as she was in the terminal stage of the tumor. Supplementary Table 3 showed the detailed timeline, symptoms and the treatment process.

# 3 Discussion

PPGL have a poor prognosis and limited treatment options. The key to diagnosis lies in appropriate biochemical tests and molecular IHC (11). Approximately 40% of PPGL cases are associated with germline mutations, making genetic testing crucial for early detection of genetic syndromes, follow-up of high-risk patients, and guidance of treatment (12). Half of the mutated genes in PPGL are members of the tricarboxylic acid (TCA) cycle. Recent studies have identified DLST as a component of the rate-limiting enzyme of the TCA cycle, and disruption of DLST has been linked to pseudohypoxia, which contributes to the occurrence and progression of PPGL (13). However, the reported cases are limited in number, and there is lack of comprehensive clinical data. Our patient exhibited DLST point mutations, PCC characterized by atypical clinical symptoms but high malignancy, multiple site metastasis, and a suboptimal response to treatment.

## 3.1 PCC gene sequencing

There has been a growing recognition of asymptomatic cases of PPGL through familial and germline mutation testing in recent years (9). About 15–17% of patients with PPGL will develop metastasis (14). The natural course of metastatic PPGL is highly heterogeneous, with 5-year survival rates ranging from 40% to 85% (15, 16). Stage IV PPGL has a significantly shorter overall survival (OS) (median OS 8.8 years) compared to stages I-III (17). Current guidelines recommend a comprehensive approach involving simultaneous localization diagnosis, qualitative diagnosis, and genetic counseling to accurately diagnose PCC/PGL (18). PPGL is linked to mutations in 20+ genes, categorized into three groups by TCGA: pseudohypoxia (cluster 1), kinase signaling (cluster 2), and Wnt signaling (cluster 3) (5–8). These mutations cause metabolic and epigenetic imbalances, promoting tumor invasiveness and metastasis (8). Our review focuses on PPGL patients with mutations in these clusters (Table 1).

In recent years, DLST mutations, accounting for less than 1% of cases, have also been identified as contributing to PPGL. A review of cases reported in the literature on DLST mutations reveals that only

TABLE 1 Clinical features of PPGL with mutations in susceptibility genes.

| Gene | Mutation Frequency% | Gene Type | Tumor Type | Syndrome/Other Tumors | Family History % | Metastatic Risk% | References |
|---|---|---|---|---|---|---|---|
| Cluster 1 A (Krebs cycle) | | | | | | | |
| SDHD | 7–10 | AD, maternal imprinting | HNPGL>>PGL/PCC | PGL1/GIST, RCC, PA | 40–50 | 1–9 | (19) |
| SDHB | 8–10 | AD | ATPGL>>HNPGL/PCC | PGL4/GIST, RCC, PA, TT | 10–24 | 25–50 | (20) |
| SDHA | <5 | AD | PCC/PGL | PGL5/GIST, RCC, PA | <10 | Rare | (21) |
| SDHAF2 | <1 | AD, maternal imprinting | HNPGL>PCC | PGL2 | >50 | Rare | (22) |
| SDHC | 1 | AD | HNPGL>PCC/PGL | PGL3/GIST, RCC | <50 | Rare | (23) |
| FH | <5 | AD | PCC/PGL | Leiomyoma, RCC | Not obvious | >50 | (24) |
| MDH2 | <1 | AD | PCC/ATPGL | NA | Not obvious | 40 | (25) |
| IDHx | <1 | GM/SM | PGL | Brain tumor glioblastoma, AML | NA | NA | (26) |
| SLC25A11 | <1 | GM | PGL | NA | Not obvious | High? | (27) |
| GOT2 | <1 | GM | ATPGL | NA | NA | NA | (28) |
| DNMT3A | <1 | GM | PGL | AML | NA | NA | (29) |
| DLST | <1 | GM | PCC/PGL | NA | NA | Rare | (13) |

*(Continued)*

TABLE 1 Continued

| Gene | Mutation Frequency% | Gene Type | Tumor Type | Syndrome/Other Tumors | Family History % | Metastatic Risk% | References |
|---|---|---|---|---|---|---|---|
| **Cluster 1B Hypoxia signaling** | | | | | | | |
| VHL | 5–10 | AD | PCC>>PGL | VHL | 25–50 | 1–9 | (30) |
| EPAS1 | 1 | SM>GM | PCC/ATPGL | Pacak-Zhuang syndrome/Hereditary erythrocytosis, Somatostatinoma | NA | Rare | (31) |
| EGLN1/ EGLN2 | <1 | GM | PCC/ATPGL | Erythrocytosis | NA | Rare | (32) |
| **Cluster 2** | | | | | | | |
| RET | 5 | AD | PCC | MEN2 syndrome | 25–50 | <1 | (33) |
| NF1 | 3–30 | SM>GM | PCC | NF1syndrome | 10–24 | 1–9 | (34) |
| TMEM127 | <2 | AD | PCC>PGL | RCC | Rare | 15 | (35) |
| MAX | 1 | AD | PCC>PGL | Renal oncocytoma | 25–50 | Rare | (36) |
| H-RAS | 7 | GM/SM | PCC | NA | NA | NA | (37) |
| KIF1B | <1 | GM | PCC | Neuroblastoma | NA | NA | (38) |
| MEN1 | <1 | GM | PCC/HNPGL | MEN1syndrome | NA | NA | (39) |
| **Cluster 3** | | | | | | | |
| MAML3 | 7 | Fusion genes | PCC/PGL | Neuroblastoma | NA | High? | (40) |
| CSDE1 | <1 | SM | PCC/PGL | NA | NA | NA | (4) |

AD, Autosomal dominant inheritance; GM, Germline mutation; SM, Somatic mutation; HNPGL, head and neck paraganglioma; GIST, gastrointestinal stromal tumor; RCC, pheochromocytoma; PA, pituitary adenoma; ATPGL, abdominal or thoracic paraganglioma; TT, Thyroid tumor; NA, Not Available.

three authors have reported a total of 12 patients (Table 2). In 2019, Remacha et al. have described a new PPGL susceptibility gene DLST, which encodes the dihydrolipoamide S-succinyltransferase (13). The dihydrothiamide S-succinyltransferase encoded by the DLST gene is a rate limiting enzyme in the Krebs cycle of cluster 1 subgroup (43). Additionally, Alexandre et al.'s study indicated that DLST likely pathogenic variants may confer susceptibility to PPGL, with a predicted low penetrance (41). The DLST germline variant (p.gly374glu) can cause functional impairment and promote tumorigenesis by increasing α-ketoglutarate levels and activating the pseudohypoxic pathway (13). These patients exhibit sporadic occurrences, with NM abnormalities being more prevalent, and are

TABLE 2 Clinical data of DLST mutations in PPGL patients.

| Year | Gender | Age | Tumor Type | Other tumors | Metastasis | Biochemical phenotype | cDNA variants | Protein changes | Prediction | LOH |
|---|---|---|---|---|---|---|---|---|---|---|
| Remacha et al., 2019 (13) | male | 45 | PCC | — | yes | NM | c.692G>A | p.Arg231Gln | deleterious | no |
| Remacha et al., 2019 | female | 63 | HNPGL | — | no | NS | c.910G>A | p.Asp304Asn | neutral | NA |
| Remacha et al., 2019 | female | 27 | ATPGL | UEC | no | NM | c.1121G>A | p.Gly374Glu | deleterious | yes |
| Remacha et al., 2019 | male | 38 | ATPGL | — | no | NM | c.1121G>A | p.Gly374Glu | deleterious | yes |
| Remacha et al., 2019 | female | 24 | ATPGL and PCC | — | no | NM | c.1121G>A | p.Gly374Glu | deleterious | yes |
| Remacha et al., 2019 | male | 29 | ATPGL | — | no | NM | c.1121G>A | p.Gly374Glu | deleterious | NA |

*(Continued)*

TABLE 2 Continued

| Year | Gender | Age | Tumor Type | Other tumors | Metastasis | Biochemical phenotype | cDNA variants | Protein changes | Prediction | LOH |
|---|---|---|---|---|---|---|---|---|---|---|
| Remacha et al., 2019 | male | 29 | ATPGL | — | no | NM | c.1265A>G | p.Tyr422Cys | deleterious | NA |
| Remacha et al., 2019 | male | 54 | PCC | PA | no | NM | c.1060–3T>A | — | — | no |
| Buffet et al., 2021 (41) | male | 23 | ATPGL | — | no | CA | c.1151C>T | p.Pro384Leu | probably damaging | yes |
| Buffet et al., 2021[a] | male | 71 | PCC and ATPGL | — | no | NM | c.1121G>A | p.Gly374Glu | deleterious | no |
| Mellid et al., 2023[b] (42) | male | 56 | bilateral PCC | MTC, NF1syndrome | no | NM | NA | p.Gly374Glu | deleterious | no |
| Mellid et al., 2023[c] | female | 55 | PCC | — | no | M>NM | NA | p.Gly374Glu | deleterious | no |

LOH, Loss of heterozygosity; PCC, pheochromocytoma; PGL, paraganglioma; HNPGL, head and neck paraganglioma; ATPGL, abdominal or thoracic paraganglioma; NM, normetanephrine; NS, non-secretory; CA, catecholamine; M, metanephrine; NA, not available; UPD, uniparental disomy; PA, pituitary adenoma; MTC, medullary thyroid carcinoma; NF1,neurofibromatosis type 1;a,with DLST somatic mutation; b, with NF1 germline mutation; c, with NF1 somatic mutation.
"-" means no.

more likely to develop chest and abdominal PPGL (41). Our case identified a mutation near the splice site of the DLST gene, which may lead to abnormal protein synthesis. The patient did not show typical symptoms of PCC, but NM levels were elevated before surgery and during metastasis, consistent with PCC caused by DLST mutation. There was no evidence of CCND1 gene mutations in the pathogenesis of PCC. The absence of consistent clinical manifestations and test results throughout the disease process of von Hippel Lindau syndrome due to CCND1 gene mutations suggests that the correlation between this specific mutation and the onset of pheochromocytoma was not present in this case (43). The patient's lack of VHL gene mutations and absence of literature on VHL and DLST dual mutations were noted. Unfortunately, further genetic sequencing and epigenetic analysis of the patient's family were unsuccessful.

## 3.2 Symptoms, test results, and treatment for PCC

The primary symptom of PPGL is persistent or paroxysmal hypertension with target tissue damage (44). Clinical symptoms can vary from no symptoms to life-threatening events, even with normal blood pressure (45). Our patient initially had mild abdominal pain. Preoperative levels of NMN were found to be significantly elevated, while other blood test results did not show any significant abnormalities. The synthesis, secretion and release of CA are not completely dependent on the adrenal medulla, which may also be the reason why our patient had no typical symptoms despite the increase of NMN (11). Adrenal CT and PETCT imaging supported the diagnosis of PCC without evidence of lesions in other areas. The Endocrine Hypertension Working Group of the European Society for Hypertension recommends minimally invasive adrenalectomy as the preferred surgical approach for PCC, as it can minimize blood loss and shorten postoperative hospitalization (18). While guidelines suggest considering a cesarean section for PCC tumors larger than 5cm,as for our patient the PCC measures approximately 5cm in diameter. The surgical team observed only hepatic omentum tissue and some intestinal adhesions during the procedure, with no apparent abnormalities in the neighboring organs of the tumor. Consequently, they opted for laparoscopic right adrenal mass resection surgery. Surgical intervention has been shown to enhance overall survival (OS) (46). European guidelines suggest postoperative monitoring through blood tests, such as measurement of MN and NMN at 2–6 weeks post-surgery and annually thereafter, as well as imaging studies (CT/MRI) at 3 months, 6 months, and biennially thereafter (18). Another study proposes that patients with SDHA/B PPGL who are at a high risk of metastasis should consider undergoing biochemical tests every 6 to 12 months and imaging every 1 to 2 years (10). Following postoperative normalization of NMN levels, no recurrence or metastasis was detected five months post-operation for our patient. However, distant metastasis (lung, liver, bone) of PCC was discovered 16 months post-surgery. Imaging studies, including lung and liver CT, PETCT, and subsequent pathological examination of lung and bone metastases, provided compelling evidence of multiple site metastasis of PCC. The potential benefit of increasing the frequency of postoperative follow-up, such as every 6 months, for these patients is worth exploring. There is no standardized treatment for metastatic PPGL, but options include surgical resection, targeted radiolabeled carriers, thermal ablation, chemotherapy, and external irradiation (9). Chemotherapy, specifically with drugs like cyclophosphamide, vincristine, and dacarbazine, is preferred for advanced PPGL, especially in rapidly progressing cases. Tumors with mutations in the gene encoding Krebs cycle enzyme may respond better to temozolomide due to reduced expression of methylguanidine DNA methyltransferase (44, 47). Temozolomide chemotherapy was chosen based on the patient's tolerance, however, due to significant side effects, treatment was discontinued after a single

course. Octreotide and denosumab were administered subcutaneously starting at 16 months post-operation. The patient experienced intermittent hemoptysis during the advanced stage of lung metastasis, and TKIs were not utilized. Radionuclide therapy was deemed unsuitable due to the evident adverse effects observed during the relevant radionuclide examination. The patient had a low tolerance to certain treatments and a lower OS rate compared to previous reports on metastatic PPGL.

## 4 Conclusions

This study presents a case of metastatic PCC with uncommon DLST point mutations, characterized by high malignancy, rapid disease progression, and limited therapeutic efficacy. These cases warrant additional attention in determining the optimal timing for genetic sequencing, enhancing the frequency of monitoring, and developing personalized treatment strategies.

## Data availability statement

The original contributions presented in the study are included in the article/Supplementary Material. Further inquiries can be directed to the corresponding author.

## Ethics statement

The studies involving humans were approved by Ethics Committee of China-Japan Union Hospital of Jilin University. The studies were conducted in accordance with the local legislation and institutional requirements. The participants provided their written informed consent to participate in this study. Written informed consent was obtained from the individual(s) for the publication of any potentially identifiable images or data included in this article.

## Author contributions

CL: Conceptualization, Data curation, Formal Analysis, Funding acquisition, Validation, Writing – original draft. LH: Data curation, Resources, Writing – original draft. YS: Conceptualization, Formal Analysis, Project administration, Visualization, Writing – review & editing. RL: Formal Analysis, Funding acquisition, Validation, Visualization, Writing – review & editing.

## Funding

The author(s) declare that financial support was received for the research, authorship, and/or publication of this article. This study was funded by Jilin Province Health Science and Technology Capability Enhancement Project (No. 2022LC119) and Jilin Province health research talents special project (No. 2023SCI32).

## Acknowledgments

We thank the patient and their families in this paper for their consent.

## Conflict of interest

The authors declare that the research was conducted in the absence of any commercial or financial relationships that could be construed as a potential conflict of interest.

## Publisher's note

All claims expressed in this article are solely those of the authors and do not necessarily represent those of their affiliated organizations, or those of the publisher, the editors and the reviewers. Any product that may be evaluated in this article, or claim that may be made by its manufacturer, is not guaranteed or endorsed by the publisher.

## Supplementary material

The Supplementary Material for this article can be found online at: https://www.frontiersin.org/articles/10.3389/fonc.2024.1394552/full#supplementary-material

## References

1. Rindi G, Klimstra DS, Abedi-Ardekani B, Asa SL, Bosman FT, Brambilla E, et al. A common classification framework for neuroendocrine neoplasms: an International Agency for Research on Cancer (IARC) and World Health Organization (WHO) expert consensus proposal. *Mod Pathol.* (2018) 31:1770–86. doi: 10.1038/s41379-018-0110-y

2. Ma XS, Li M, Tong AL, Wang F, Cui YY, Zhang XB, et al. Genetic and clinical profiles of pheochromocytoma and paraganglioma: A single center study. *Front Endocrinol.* (2020) 11:574662. doi: 10.3389/fendo.2020.574662

3. Martins R, Bugalho MJ. Paragangliomas/pheochromocytomas: clinically oriented genetic testing. *Int J Endocrinol.* (2014) 2014:794187. doi: 10.1155/2014/794187

4. Fishbein L, Leshchiner I, Walter V, Danilova L, Robertson A, Johnson A, et al. Comprehensive molecular characterization of pheochromocytoma and paraganglioma. *J Cancer Cell.* (2017) 31:181–93. doi: 10.1016/j.ccell.2017.01.001

5. Taieb D, Pacak K. New insights into the nuclear imaging phenotypes of cluster 1 pheochromocytoma and paraganglioma. *Trends Endocrinol Metab.* (2017) 28:807–17. doi: 10.1016/j.tem.2017.08.001

6. Crona J, Taieb D, Pacak K. New perspectives on pheochromocytoma and paraganglioma: toward a molecular classification. *Endocr. Rev.* (2017) 38:489–515. doi: 10.1210/er.2017–00062

7. Koopman K, Gaal J, de Krijger R. Pheochromocytomas and paragangliomas: new developments with regard to classification, genetics, and cell of origin. *J Cancers*. (2019) 11:1070. doi: 10.3390/cancers11081070

8. Jochmanova I, Pacak K. Genomic landscape of pheochromocytoma and paraganglioma. *J Trends Cancer*. (2018) 4:6–9. doi: 10.1016/j.trecan.2017.11.001

9. Neumann H, Young W, Eng C. Pheochromocytoma and paraganglioma. *N Engl J Med*. (2019) 381:552–65. doi: 10.1056/NEJMra1806651

10. Nolting S, Bechmann N, Taieb D, Beuschlein F, Fassnacht M, Kroiss M, et al. Personalized management of pheochromocytoma and paraganglioma. *Endocr. Rev.* (2022) 43:199–239. doi: 10.1210/endrev/bnab019

11. Eisenhofer G, Pamporaki C, Lenders J. Biochemical assessment of pheochromocytoma and paraganglioma. *J Endocrine Rev*. (2023) 44:862–909. doi: 10.1210/endrev/bnad011

12. Jhawar S, Arakawa Y, Kumar S, Varghese D, Kim Y, Roper N, et al. New insights on the genetics of pheochromocytoma and paraganglioma and its clinical implications. *J Cancers*. (2022) 14:594. doi: 10.3390/cancers14030594

13. Remacha L, Pirman D, Mahoney C, Coloma J, Calsina B, Currás-Freixes M, et al. Recurrent germline DLST mutations in individuals with multiple pheochromocytomas and paragangliomas. *J Am J Hum Genet*. (2019) 104:651–64. doi: 10.1016/j.ajhg.2019.02.017

14. Ayala-Ramirez M, Feng L, Johnson MM, Ejaz S, Habra MA, Rich T, et al. Clinical risk factors for Malignancy and overall survival in patients with pheochromocytomas and sympathetic paragangliomas: primary tumor size and primary tumor location as prognostic indicators. *J Clin Endocrinol Metab*. (2011) 96:717–25. doi: 10.1210/jc.2010–1946

15. Angelousi A, Peppa M, Chrisoulidou A, Alexandraki K, Berthon A, Faucz FR, et al. Malignant pheochromocytomas/paragangliomas and ectopic hormonal secretion: A case series and review of the literature. *Cancers*. (2019) 11:724. doi: 10.3390/cancers11050724

16. Bravo EL, Tagle R. Pheochromocytoma: State-of-the-art and future prospects. *Endocr. Rev.* (2003) 24:539–53. doi: 10.1210/er.2002–0013

17. Jimenez C, Ma J, Gonzalez AR, Varghese J, Zhang M, Perrier N, et al. TNM staging and overall survival in patients with pheochromocytoma and sympathetic paraganglioma. *J Clin Endocrinol Metab*. (2023) 108:1132–42. doi: 10.1210/clinem/dgac677

18. Lenders JWM, Kerstens MN, Amar L, Prejbisz A, Robledo M, Taieb D, et al. Genetics, diagnosis, management and future directions of research of phaeochromocytoma and paraganglioma: a position statement and consensus of the Working Group on Endocrine Hypertension of the European Society of Hypertension. *J Hypertens*. (2020) 38:1443–56. doi: 10.1097/hjh.0000000000002438

19. Taieb D, Wanna GB, Ahmad M, Lussey-Lepoutre C, Perrier N, Noelting S, et al. Clinical consensus guideline on the management of phaeochromocytoma and paraganglioma in patients harbouring germline SDHD pathogenic variants. *Lancet Diabetes Endocrinol*. (2023) 11:345–61. doi: 10.1016/s2213–8587(23)00038–4

20. Andrews KA, Ascher DB, Pires DEV, Barnes DR, Vialard L, Casey RT, et al. Tumour risks and genotype-phenotype correlations associated with germline variants in succinate dehydrogenase subunit genes SDHB, SDHC and SDHD. *J Med Genet*. (2018) 55:384–94. doi: 10.1136/jmedgenet-2017–105127

21. Hanson H, Durkie M, Lalloo F, Izatt L, McVeigh TP, Cook JA, et al. K recommendations for SDHA germline genetic testing and surveillance in clinical practice. *J Med Genet*. (2023) 60:107–11. doi: 10.1136/jmedgenet-2021–108355

22. Lee H, Jeong S, Yu Y, Kang J, Sun H, Rhee J-K, et al. Risk of metastatic pheochromocytoma and paraganglioma in SDHx mutation carriers: a systematic review and updated meta-analysis. *J Med Genet*. (2020) 57:217–25. doi: 10.1136/jmedgenet-2019–106324

23. Williams ST, Chatzikyriakou P, Carroll PV, McGowan BM, Velusamy A, White G, et al. SDHC phaeochromocytoma and paraganglioma: A UK-wide case series. *Clin Endocrinol (Oxf.)*. (2022) 96:499–512. doi: 10.1111/cen.14594

24. Fuchs TL, Luxford C, Clarkson A, Sheen A, Sioson L, Elston M, et al. A clinicopathologic and molecular analysis of fumarate hydratase-deficient pheochromocytoma and paraganglioma. *Am J Surg Pathol*. (2023) 47:25–36. doi: 10.1097/pas.0000000000001945

25. Calsina B, Curras-Freixes M, Buffet A, Pons T, Contreras L, Leton R, et al. Role of MDH2 pathogenic variant in pheochromocytoma and paraganglioma patients. *Genet Med*. (2018) 20:1652–62. doi: 10.1038/s41436–018-0068–7

26. Richter S, Gieldon L, Pang Y, Peitzsch M, Thanh H, Leton R, et al. Metabolome-guided genomics to identify pathogenic variants in isocitrate dehydrogenase, fumarate hydratase, and succinate dehydrogenase genes in pheochromocytoma and paraganglioma. *Genet Med*. (2019) 21:705–17. doi: 10.1038/s41436–018-0106–5

27. Buffet A, Morin A, Castro-Vega L-J, Habarou F, Lussey-Lepoutre C, Letouze E, et al. Germline mutations in the mitochondrial 2-oxoglutarate/malate carrier *SLC25A11* gene confer a predisposition to metastatic paragangliomas. *Cancer Res*. (2018) 78:1914–22. doi: 10.1158/0008–5472.Can-17–2463

28. Remacha L, Comino-Mendez I, Richter S, Contreras L, Curras-Freixes M, Pita G, et al. Targeted exome sequencing of krebs cycle genes reveals candidate cancer-predisposing mutations in pheochromocytomas and paragangliomas. *Clin Cancer Res*. (2017) 23:6315–24. doi: 10.1158/1078–0432.Ccr-16–2250

29. Remacha L, Curras-Freixes M, Torres-Ruiz R, Schiavi F, Torres-Perez R, Calsina B, et al. Gain-of-function mutations in DNMT3A in patients with paraganglioma. *Genet Med*. (2018) 20:1644–51. doi: 10.1038/s41436-018-0003-y

30. Tarade D, Ohh M. The HIF and other quandaries in VHL disease. *Oncogene*. (2018) 37:139–47. doi: 10.1038/onc.2017.338

31. Rosenblum JS, Wang H, Nazari MA, Zhuang Z, Pacak K. Pacak-Zhuang syndrome: a model providing new insights into tumor syndromes. *Endocr. Relat Cancer*. (2023) 30:e230050. doi: 10.1530/erc-23–0050

32. Eckardt L, Prange-Barczynska M, Hodson EJ, Fielding JW, Cheng X, Lima JDCC, et al. Developmental role of PHD2 in the pathogenesis of pseudohypoxic pheochromocytoma. *Endocr. Relat Cancer*. (2021) 28:757–72. doi: 10.1530/erc-21–0211

33. Castinetti F, Waguespack SG, Machens A, Uchino S, Hasse-Lazar K, Sanso G, et al. Natural history, treatment, and long-term follow up of patients with multiple endocrine neoplasia type 2B: an international, multicentre, retrospective study. *Lancet Diabetes Endocrinol*. (2019) 7:213–20. doi: 10.1016/S2213-8587(18)30336-X

34. Welander J, Soderkvist P, Gimm O. The NF1 gene: a frequent mutational target in sporadic pheochromocytomas and beyond. *Endocr. Relat Cancer*. (2013) 20:C13–C7. doi: 10.1530/erc-13–0046

35. Armaiz-Pena G, Flores SK, Cheng Z-M, Zhang X, Esquivel E, Poullard N, et al. Genotype-phenotype features of germline variants of the *TMEM127* pheochromocytoma susceptibility gene: A 10-year update. *J Clin Endocrinol Metab*. (2021) 106:E350–E64. doi: 10.1210/clinem/dgaa741

36. Bausch B, Schiavi F, Ni Y, Welander J, Patocs A, Ngeow J, et al. Clinical characterization of the pheochromocytoma and paraganglioma susceptibility genes *SDHA*, *TMEM127*, MAX, and *SDHAF2* for gene-informed prevention. *JAMA Oncol*. (2017) 3:1204–12. doi: 10.1001/jamaoncol.2017.0223

37. Oudijk L, de Krijger RR, Rapa I, Beuschlein F, de Cubas AA, Tos APD, et al. H-RAS mutations are restricted to sporadic pheochromocytomas lacking specific clinical or pathological features: data from a multi-institutional series. *J Clin Endocrinol Metab*. (2014) 99:E1376–E80. doi: 10.1210/jc.2013–3879

38. Schlisio S, Kenchappa RS, Vredeveld LCW, George RE, Stewart R, Greulich H, et al. The kinesin KIF1Bβ acts downstream from EglN3 to induce apoptosis and is a potential 1p36 tumor suppressor. *Genes Dev*. (2008) 22:884–93. doi: 10.1101/gad.1648608

39. Guerin C, Romanet P, Taieb D, Brue T, Lacroix A, Sebag F, et al. Looking beyond the thyroid: advances in the understanding of pheochromocytoma and hyperparathyroidism phenotypes in MEN2 and of non-MEN2 familial forms. *Endocr. Relat Cancer.*(2018) 25:T15–28doi: 10.1530/erc-17–0266

40. Alzofon N, Koc K, Panwell K, Pozdeyev N, Marshall CB, Albuja-Cruz M, et al. Mastermind like transcriptional coactivator 3 (MAML3) drives neuroendocrine tumor progression. *Mol Cancer Res*. (2021) 19:1476–85. doi: 10.1158/1541–7786.Mcr-20–0992

41. Buffet A, Zhang J, Rebel H, Corssmit EPM, Jansen JC, Hensen EF, et al. Germline DLST variants promote epigenetic modifications in pheochromocytoma-paraganglioma. *J Clin Endocrinol Metab*. (2021) 106:459–71. doi: 10.1210/clinem/dgaa819

42. Mellid S, Garcia F, Leandro-Garcia LJ, Diaz-Talavera A, Martinez-Montes AM, Gil E, et al. DLST mutations in pheochromocytoma and paraganglioma cause proteome hyposuccinylation and metabolic remodeling. *Cancer Commun*. (2023) 43:838–43. doi: 10.1002/cac2.12427

43. Buffet A, Burnichon N, Favier J, Gimenez-Roqueplo A-P. An overview of 20 years of genetic studies in pheochromocytoma and paraganglioma. *Best Pract Res Clin Endocrinol Metab*. (2020) 34:101416. doi: 10.1016/j.beem.2020.101416

44. Garcia-Carbonero R, Matute Teresa F, Mercader-Cidoncha E, Mitjavila-Casanovas M, Robledo M, Tena I, et al. Multidisciplinary practice guidelines for the diagnosis, genetic counseling and treatment of pheochromocytomas and paragangliomas. *J Clin Trans oncology: Off Publ Fed Spanish Oncol Societies Natl Cancer Institute Mexico*. (2021) 23:1995–2019. doi: 10.1007/s12094–021-02622–9

45. Zhao L, Zhang T, Meng X, Fan H, Zhang Z, Liu Y, et al. The clinical characteristics of patients with normotension in pheochromocytomas and paragangliomas. *J Endocrine*. (2023) 80:174–82. doi: 10.1007/s12020–022-03293–4

46. Roman-Gonzalez A, Zhou S, Ayala-Ramirez M, Shen C, Waguespack SG, Habra MA, et al. Impact of surgical resection of the primary tumor on overall survival in patients with metastatic pheochromocytoma or sympathetic paraganglioma. *Ann Surg*. (2018) 268:172–8. doi: 10.1097/sla.0000000000002195

47. Corssmit EPM, Snel M, Kapiteijn E. Malignant pheochromocytoma and paraganglioma: management options. *Curr Opin Oncol*. (2020) 32:20–6. doi: 10.1097/cco.0000000000000589

frontiers | Frontiers in Endocrinology

TYPE Review
PUBLISHED 13 December 2024
DOI 10.3389/fendo.2024.1433582

Check for updates

OPEN ACCESS

EDITED BY
Farhadul Islam,
University of Rajshahi, Bangladesh

REVIEWED BY
Sergei Tevosian,
University of Florida, United States
Camilo Jimenez,
University of Texas MD Anderson Cancer Center, United States

*CORRESPONDENCE
Juan S. Izquierdo-Condoy
juan1izquierdo11@gmail.com

RECEIVED 16 May 2024
ACCEPTED 15 November 2024
PUBLISHED 13 December 2024

CITATION
Saavedra T. JS, Nati-Castillo HA, Valderrama Cometa LA, Rivera-Martínez WA, Asprilla J, Castaño-Giraldo CM, Sánchez S. L, Heredia-Espín M, Arias-Intriago M and Izquierdo-Condoy JS (2024) Pheochromocytoma: an updated scoping review from clinical presentation to management and treatment. *Front. Endocrinol.* 15:1433582. doi: 10.3389/fendo.2024.1433582

COPYRIGHT
© 2024 Saavedra T., Nati-Castillo, Valderrama Cometa, Rivera-Martínez, Asprilla, Castaño-Giraldo, Sánchez S., Heredia-Espín, Arias-Intriago and Izquierdo-Condoy. This is an open-access article distributed under the terms of the Creative Commons Attribution License (CC BY). The use, distribution or reproduction in other forums is permitted, provided the original author(s) and the copyright owner(s) are credited and that the original publication in this journal is cited, in accordance with accepted academic practice. No use, distribution or reproduction is permitted which does not comply with these terms.

# Pheochromocytoma: an updated scoping review from clinical presentation to management and treatment

J. S. Saavedra T.[1], Humberto Alejandro Nati-Castillo[2], L. A. Valderrama Cometa[3], Wilfredo A. Rivera-Martínez[4], Josué Asprilla[5], C. M. Castaño-Giraldo[6], Leonardo Sánchez S.[7], Mishell Heredia-Espín[7], Marlon Arias-Intriago[7] and Juan S. Izquierdo-Condoy[7]*

[1]Family Medicine Department, Universidad Javeriana, Cali, Colombia, [2]Interinstitutional Group on Internal Medicine (GIMI 1), Department of Internal Medicine, Universidad Libre, Cali, Colombia, [3]Organ and Tissue Transplant Unit, Clínica Imbanaco, Cali, Colombia, [4]Facultad de Medicina, Universidad de Antioquia, Medellin, Colombia, [5]Division of Pathology, Clínica Imbanaco, Grupo Quirónsalud, Cali, Colombia, [6]Facultad de ciencias de la Salud, Universidad del Quindío, Armenia, Colombia, [7]One Health Research Group, Universidad de las Americas, Quito, Ecuador

Pheochromocytomas and paragangliomas (PPGLs) are rare neuroendocrine tumors derived from chromaffin cells, with 80–85% originating in the adrenal medulla and 15–20% from extra-adrenal chromaffin tissues (paragangliomas). Approximately 30–40% of PPGLs have a hereditary component, making them one of the most genetically predisposed tumor types. Recent advances in genetic research have classified PPGLs into three molecular clusters: pseudohypoxia-related, kinase-signaling, and *WNT*-signaling pathway variants. Specifically, the detection of *SDHB*-related tumors indicates an increased risk of metastatic disease, which may impact decisions regarding functional imaging in patients with high suspicion of metastasis and influence targeted treatment strategies. Diagnosis of PPGLs primarily relies on biochemical testing, measuring catecholamines or their metabolites in plasma or urine. However, molecular testing, functional imaging, and targeted therapies have greatly enhanced diagnostic precision and management. Personalized treatment approaches based on genetic profiling are becoming integral to the clinical management of these tumors. In South American countries like Colombia, functional imaging techniques such as positron emission tomography/computed tomography (PET/CT) with tracers like 18F-DOPA, 18F-fluorodeoxyglucose (18F-FDG), and 68Ga-DOTA-conjugated somatostatin receptor-targeting peptides (68Ga-DOTA-SST) are used to guide follow-up and treatment strategies. Radionuclide therapy with lutetium-177 DOTATATE is employed for patients showing uptake in 68Ga-DOTA-SST PET/CT scans, while access to 131-MIBG therapy remains limited due to high costs and availability. Recent clinical trials have shown promise for

10.3389/fendo.2024.1433582

systemic therapies such as sunitinib and cabozantinib, offering potential new options for patients with slow or moderate progression of PPGLs. These advancements underscore the potential of personalized and targeted therapies to improve outcomes in this challenging patient population.

KEYWORDS

**pheochromocytoma, paraganglioma, hormonal imbalance, diagnosis, management, treatment**

# 1 Introduction

Pheochromocytomas and paragangliomas (PPGLs) are closely related tumors that originate from neuroendocrine cells, arising from chromaffin cells in the adrenal medulla and neural crest progenitors located outside of adrenal gland, respectively (1). These tumors are characterized by a proliferation of chromaffin cells arranged in clustered or trabecular patterns (2, 3), Although rare, occurring in fewer than 0.1% of individuals per million (4, 5), pheochromocytomas and sympathetic paragangliomas in particular require prompt treatment to reduce associated morbidity and mortality (3, 6).

Paragangliomas (PGLs) arise in sympathetic and parasympathetic paraganglia (7–9). Those in the head and neck are predominantly parasympathetic, typically non-metastatic, and often present as palpable masses, while abdominal PGLs arise from the sympathetic neuroendocrine system and share origins with pheochromocytomas (2). Notably, carotid body tumors, a type of PGL, are highly vascularized glomus tumors located at the carotid bifurcation, where the external and internal carotid arteries diverge (10–13).

PPGL, whether located in the adrenal medulla or at extramedullary sites, secrete excessive amounts of catecholamines, adrenaline, noradrenaline, and/or dopamine. There is a subdivision based on the genotype of PPGLs in cluster 1 for variants in pseudohypoxia genes, cluster 2 for alterations in the kinase pathway and cluster 3 in WNT signaling. This classification in cases such as *SDHB*-related tumors defines the prognosis of developing metastatic disease and can modify the conduct of treatment and surveillance (14–17). Cluster 1 tumors such as *VHL* typically produce norepinephrine, whereas cluster 2, *MEN2*, or *NF1* tumors are more likely to produce epinephrine, and *SDHB*, *SDHC*, and *SDHD*-related tumors may secrete dopamine and norepinephrine (18, 19).

# 2 Epidemiology

Pheochromocytomas occur with an estimated incidence of 0.05%, primarily in adults aged 30-50 (20). They constitute around 4% of incidental adrenal masses and are implicated in approximately 0.1% of hypertension cases. Demographically, pheochromocytoma affects adults of both sexes, typically between 30 and 50 years of age, presenting, and they appear with similar frequency in both adrenal glands (2, 4, 5).

Around 20% of PPGL present metastases. 70% of pheochromocytomas are sporadic, while the remaining 30% are associated with hereditary syndromes such as multiple endocrine neoplasia type 2 (MEN II), von Hippel-Lindau disease (VHL), neurofibromatosis type 1 (NF1), and familial paraganglioma syndrome (21, 22).

Traditionally, pheochromocytomas were managed under the "10% rule," (23), which suggested that 10% occur in children, 10% are extra-adrenal, 10% are familial, 10% are bilateral in adrenal glands, and 10% are metastatic (24). However, it is currently not recommended to refer to it as "the 10 percent tumor," since approximately 25% of patients with apparently sporadic pheochromocytoma may carry pathogenic variants (18).

# 3 Clinical predictor of metastasis

All PPGLs have metastatic potential, however histological characteristics do not allow differentiating "benign" from "malignant" tumors, so the latest WHO update recommends changing these terms to metastatic, when there is evidence of distant tumor (25). The ESMO guidelines, for their part, suggest using the definition of "high risk of metastasis" when one or more of the following criteria are present: (a) tumor size greater than or equal to 5 cm; (b) any extra-adrenal PPGL; (c) known germline *SDHB* pathogenic variant; or (d) plasma 3MT > 3 times above the upper limit of normal (26). Certain tumors, particularly *SDHB*-related PGLs of the head and neck, can produce dopamine. In such cases, detecting its metabolite, methoxytyramine, in blood has shown only a modest improvement in detecting head and neck PPGL (27, 28). Although its use as a metastatic risk marker has been considered, its performance remains limited (29), and it is unavailable in most countries around the world. Management guidelines do not recommend its measurement (30, 31).

Histologically, pheochromocytomas are characterized by pleomorphic cellular nests, with large ball-shaped chromaffins

that show strong positivity for chromogranin A, synaptophysin, CD56, and focal S100 (Figure 1). There are no definitive histological criteria for malignancy; thus, the term "metastatic tumor" is preferred when chromaffin tissue invasion is confirmed beyond the site of origin into distant organs (32, 33). It is also important to assess histological criteria for aggressive biological behavior, including an insular pattern of growth, mitotic activity, and invasion of capsular blood and lymphatic vessels (34). Scores like PASS (Pheochromocytoma of the Adrenal Gland Scaled Score), Grading of Adrenal Pheochromocytoma and Paraganglioma, COOPS (Composite Pheochromocytoma/Paraganglioma Prognostic Score) and multivariate predictive models (SGAP-Score and ASES/ASS-Score) have been developed to identify PPGL patients with increased metastatic potential. However, immunohistochemistry may yield inconsistent results, lacks molecular testing which is more reliable, and scores such as PASS lack clinical validation studies supporting their application (35). These methods are not currently utilized in Colombia or Ecuador (30, 36).

On the other hand, there are more promising clinical predictors, TNM staging may be correlated with overall survival in PPGL. Jimenez et al. (37), found that a large primary tumor, an extra-adrenal location, infiltration of surrounding tissues by the primary tumor, and regional lymph node metastasis are associated with a higher risk of distant metastasis and consequently decreased overall survival, and in turn, patients with distant metastasis (stage IV) have the worst prognosis.

# 4 Hereditary and phenotypic pattern

## 4.1 Susceptibility genes

PPGL are associated with germline pathogenic variants at higher rates than any other solid tumor. Rates of germline pathogenic variants vary by tumor type: 25% in pheochromocytoma, 40% in PGL, and up to 50% in patients presenting with metastatic disease. Patients with pathogenic variants generally present with PPGL at a younger age and are more likely to have multifocal disease (18). 30% to 40% of cases occur in the context of a genetic syndrome, however, in almost half of apparently sporadic PPGLs somatic pathogenic variants are found in one of the susceptibility genes, which means that at least three quarters can be classified into a defined cluster.

The susceptibility to pheochromocytoma can be linked to germline pathogenic variants in the *RET* proto-oncogene and tumor suppressor genes such as *von Hippel-Lindau* (*VHL*), and *Neurofibromatosis type 1* (*NF1*) (2, 38, 39). Hereditary paraganglioma syndromes are caused by pathogenic variants in the succinate dehydrogenase subunit (SDHx) genes: *SDHD, SDHAF2, SDHC, SDHB, SDHA* (Paraganglioma syndromes 1-5, respectively) (40). The *VHL* gene, located on the short arm of chromosome 3 (3p25.3), has over 1,500 identified pathogenic variants in patients with VHL disease, with 20% of these being *de novo* pathogenic variants, as observed in both PGLs and pheochromocytomas (8, 23, 41). Other pathogenic variants in susceptibility genes such as *TMEM127, MAX, FH* and *MDH2* are associated with PPGL syndromes with a lower pathogenic variant frequency (42, 43).

The discovery of syndromes linked to pathogenic variants in genes has shown that the probability of metastasis may vary, being no higher than 12% in *SDHC, THEM127, NF1, VHL, RET* and *MAX*, but for *SDHD, SDHA* and *SDHB* it reaches 29, 66 and 75%, respectively (30, 42, 44–46).

## 4.2 Inheritance pattern

Pheochromocytoma is currently known to result from disorders with an autosomal dominant inheritance pattern in most cases, such as multiple endocrine neoplasia type 2 (*MEN-2*) (presenting manifestation is medullary thyroid cancer in 60%, medullary thyroid carcinoma and synchronous pheochromocytoma in 34%, and pheochromocytoma in 6%. 72% have bilateral pheochromocytoma, 82% of tumors are synchronous and are unlikely to be metastatic) and von Hippel-Lindau disease (with retinal angioma, central nervous system hemangioblastoma, renal cell carcinoma, pancreatic cysts, and epididymal cystadenoma) (24, 43, 47). The precise frequency of these syndromes in patients with pheochromocytoma is not fully known (2, 38, 39, 43). The exception are pathogenic variants in the *SDHAF2* and *SDHD* genes, in which maternal imprinting occurs with silencing of the maternal allele and therefore only pathogenic variants inherited from the father will cause the disease, they probably have the highest penetrance, greater than 50% and are usually associated with PPGL in the head, neck and chest (30, 44–46). On the other hand, the inheritance pattern for variants in the *MAX* gene is not clear; it is believed that its penetrance is high and it usually presents as bilateral pheochromocytomas and abdominal PGL (48).

## 4.3 Molecular phenotype

The genome of PPGL has been characterized, providing valuable insights into the genetic factors driving tumorigenesis and the degree of genetic instability (49, 50) (Figure 2). These tumors are generally characterized by a relatively low degree of genetic instability at both the nucleotide and chromosome levels. Although there are rare tumors that behave differently from others, most of the genes associated with the development of PPGL are categorized into three clusters based on the mechanism of tumorigenesis (49–51):

- Pseudohypoxia pathway (cluster 1), tumors that infiltrate stromal cells, which have been associated with pathogenic variants in the genes *EGLN1, EGLN2, DLST, FH, IDH3B, MDH2, SDHA, SDHAF2, SDHB, SDHC, SDHD, VHL, EPAS1, IDH1*, and *IDH2*.
- Signaling kinase pathway (cluster 2) has been associated with pathogenic variants in the *NF1, MAX, MERTK, MET, MYCN, RET*, or *TMEM127* genes.

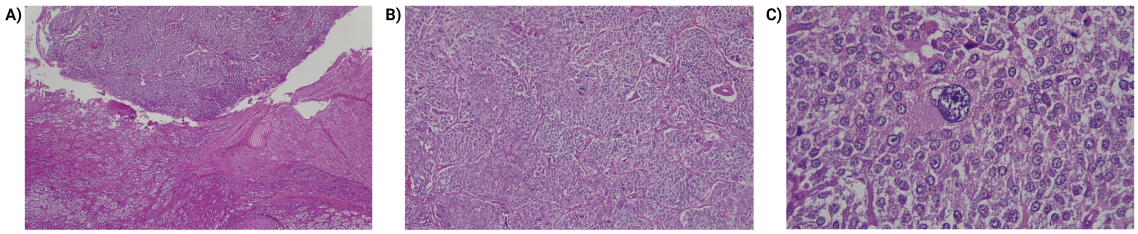


FIGURE 1
Histopathologic findings of pheochromocytoma. **(A)** Transition between the usual histology adrenal cortex (lower part of the image) and the tumor (upper part). Hematoxylin and eosin 40x. **(B)** Pheochromocytoma, cells arranged in a pattern in nests (zellballen) and trabeculae. Hematoxylin and eosin 40x. **(C)** Pheochromocytoma, lesion cells are large, polygonal, show fine, granular cytoplasm. Note the presence of pleomorphism. Hematoxylin and eosin 400x.

- In cluster 3, *MAML3* fusion gene and *CSDE1* somatic pathogenic variants affect and overactivate the Wnt/β-catenin pathway, which is responsible for the regulation of metabolism, angiogenesis, proliferation, and invasion.

Given the above pathogenic variants, one of them stands out for its potential usefulness in the prognosis of the disease. SDH (succinate dehydrogenase) is an important enzyme in energy formation pathways, taking action in the Krebs cycle and in the Electron Transfer chain within the mitochondria, where is conforming the complex ll with four functional subunits: A, B, C, and D. Inactivating germline pathogenic variants results in loss of function of SDH and, therefore, an elevation in succinate levels which diffuses back to the cytoplasm and inhibits prolyl hydroxylases, resulting in further stabilization of the Hypoxia-Inducible Factor (HIF) pathway of tumorigenesis. *SDHB* related tumors, are commonly found in the abdomen, have a high potential for recurrence, local and distant metastasis compared to *SDHD* and *SDHC* tumors, which are commonly found in the head and neck areas, each of them requiring follow-up for the possibility of relapse or extension of the disease (52, 53).

## 5 Clinical presentation

Patients with pheochromocytoma are often described as presenting with the "classic triad" of diaphoresis, headache, and palpitations, typically accompanied by hypertension (22). In a review of 200 cases, Ando et al. found that PPGL attacks are associated with multisystem involvement, 99% cardiac damage, 44% pulmonary damage, and 21.5% renal damage (54). Sustained hypertension is observed in approximately 50-55% of cases, while paroxysmal hypertension occurs in 30-45% (24, 48, 55). Additionally, hyperhidrosis occurs in 60% of cases, often accompanied by hypertensive crises (56, 57). Headache is one of the most common symptoms, and may occur in up to 40% of cases (4, 54, 58). Headache is related to the transient elevation of blood pressure. Instead of sustained hypertension, PPGL headache can occur suddenly as cluster headache, however they are usually bilateral, associated with hypertension and hyperhidrosis (Figure 3) (54, 59, 60).

PPGL is presented with sustained or episodic hypertension, sweating, palpitations, hyperglycemia, and glycosuria (5). Although

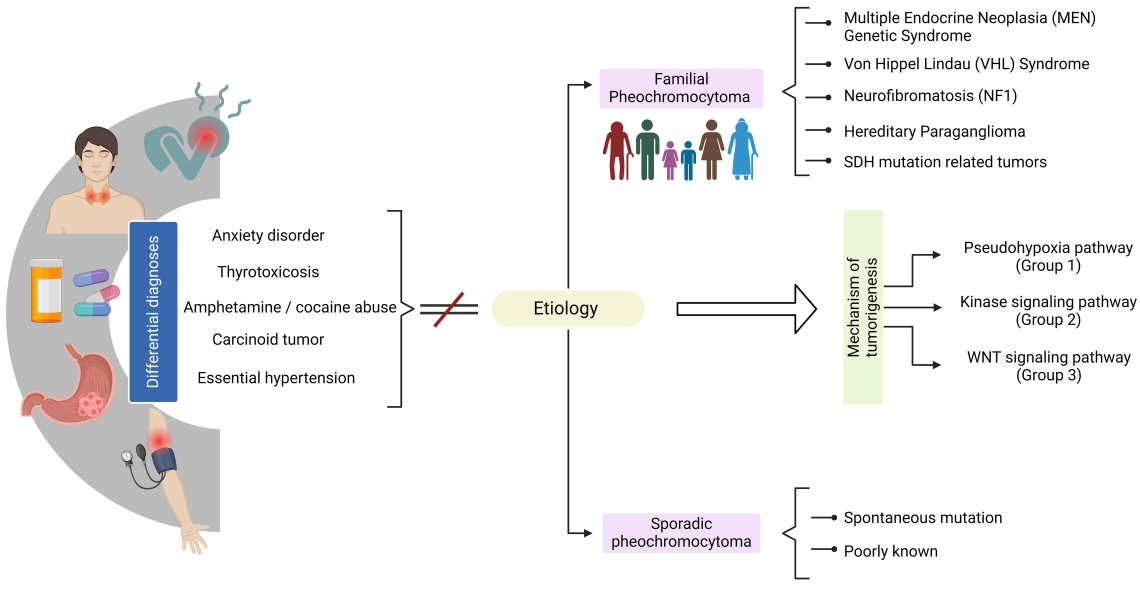


FIGURE 2
Clinical overview of pheochromocytoma diagnosis.

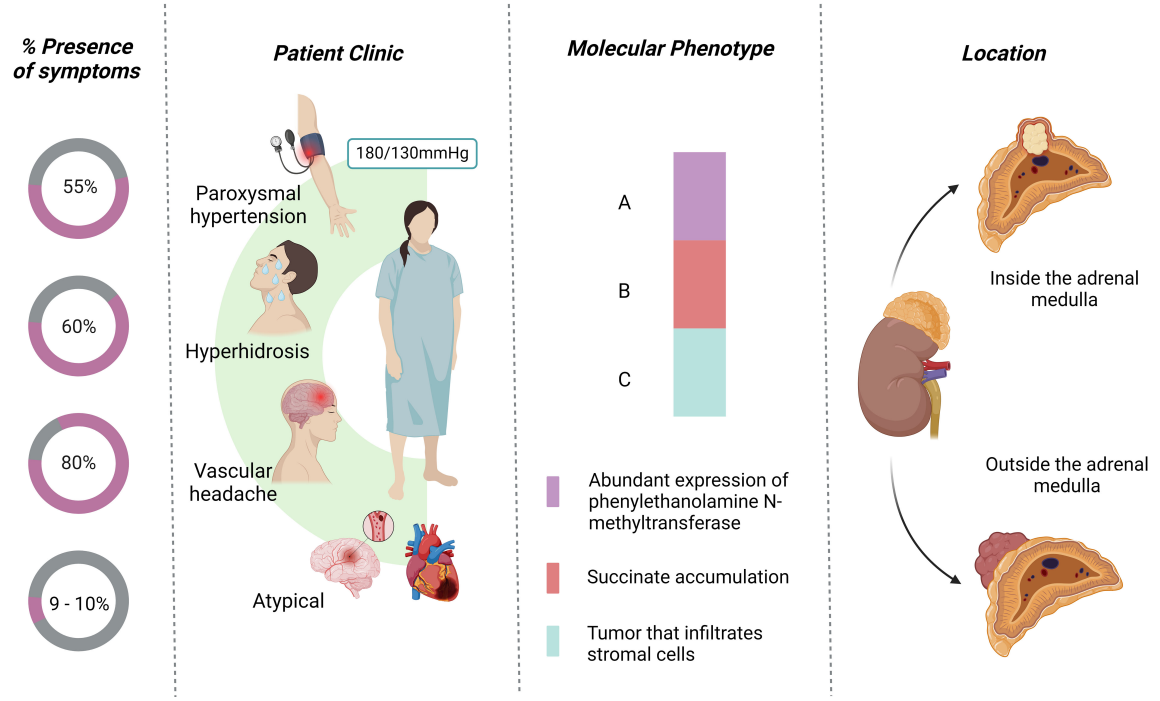


FIGURE 3
Characteristics of the presentation of pheochromocytoma.

some tumors produce dopamine, the majority secrete noradrenaline and adrenaline (5, 61). PPGLs may experience episodes of severe hypertensive crisis, with an increased likelihood of developing acute kidney injury. Over time, the vasoconstrictive effect of catecholamines released by the tumor leads to chronic kidney disease being a potential complication in PPGLs (62).

Giant pheochromocytomas, defined as those larger than 7 cm, are rare (63–65). These tumors often do not present with classic symptoms; most patients report vague discomfort, and a few may present with a palpable abdominal mass (34, 65, 66).

Table 1 summarizes the clinical translation of the conditions in patients with pheochromocytoma and sympathetic paragangliomas, and their possible complications.

Signs and symptoms alone are often nonspecific, and relying solely on them can lead to diagnostic errors. To improve diagnostic accuracy, efforts have been made to develop diagnostic scores that emphasize the most specific clinical features, such as pallor, hyperhidrosis, and palpitations (Table 2) (67).

# 6 Diagnosis

## 6.1 Laboratory tests

Diagnostic testing is crucial for confirming PPGL, although it is typically performed under specific conditions, such as the presence of known germline pathogenic variants, a history of PPGL, detection of an incidental adrenal or extra-adrenal mass suggestive of these tumors, or presentation with relevant clinical signs and symptoms (17). The 24-hour plasma metanephrine test offers the highest sensitivity (96%) and a specificity of 85% (68, 69). Studies have shown that plasma normetanephrine levels above 2.5 pmol/mL or metanephrine levels above 1.4 pmol/mL are highly indicative of pheochromocytoma, with 100% specificity. To reduce false-positive results, it is recommended that blood samples be collected with the patient in a supine position after being recumbent for at least 30 minutes (2).

The 24-hour urinary collection for catecholamines and metanephrines is another accessible test, providing a sensitivity of 87.5% and a specificity of 99.7%. Linking urinary metanephrine levels to urinary creatinine further enhances accuracy (70).

It is important to note, however, that catecholamine measurements are only informative when levels are elevated, as in a catecholaminergic crisis, which is typically not present at diagnosis. Physical activity and psychological stress can increase plasma and urinary metanephrine levels; thus, minimizing these factors before sampling is recommended. Additionally, various commonly used medications—including tricyclic antidepressants, monoamine oxidase inhibitors, atypical antipsychotics, selective adrenergic receptor blockers, stimulants, sympathomimetics, paracetamol, sulfasalazine, and amoxicillin—can interfere with test results, so these should be avoided prior to testing, if possible (71).

The clonidine suppression test helps differentiate elevated plasma norepinephrine levels due to sympathetic nerve release from those due to pheochromocytoma (70, 72). Clonidine, a centrally acting alpha-2 agonist, suppresses neuronal norepinephrine release (73, 74). However, chromaffin cells in pheochromocytomas are not regulated by clonidine and continue to release catecholamines inappropriately (73, 75). This test is thus

10.3389/fendo.2024.1433582

TABLE 1 Synthesis of clinical expression from diagnosis to complications of pheochromocytoma and sympathetic paragangliomas.

| Physiologic manifestations of catecholamines excess | |
|---|---|
| **Compromised tissue** | **Effect** |
| Heart | Tachycardia |
| | Tachyarrhythmias |
| | Increase myocardial oxygen consumption |
| | Myocarditis |
| | Cardiomyopathies |
| | Arterial hypertension |
| Blood vessels | Plasmatic volume decrease |
| Intestine | Intestinal relaxation, altered intestine motility |
| Pancreas | Carbohydrate intolerance due to Beta cells regulation changes and insulin release suppression. |
| | Hyperglycemia |
| | Glucosuria |
| Adipose tissue | Lipolysis due to free fatty acids increase |
| Apocrine glands | Diaphoresis due to stimulation |
| **Clinical presentation of pheochromocytoma** | |
| **Symptoms** | **% of presence** |
| Dizziness | 67% |
| Headache | 59% |
| Palpitations | 50% |
| Diaphoresis | 50% |
| Weight loss | 30% |
| Syncope episodes | 40% |
| Anxiety | 19% |
| **Signs** | **% of presence** |
| Sustained hypertension | 48% |
| Paroxysmic hypertension | 44% |
| Hypertension | 92% |
| Tachycardia | 15% |
| Orthostatic hypotension | 12% |
| **Pheochromocytoma complications** | |
| **Affected system** | **Clinical manifestation** |
| Cardiovascular | Arrythmia, ventricular tachycardia, Torsade de Pointes, ventricular fibrillation. |
| Respiratory | No cardiogenic pulmonary edema |
| Gastrointestinal | Ileo, constipation. |
| Renal | Renal infarction, renal artery stenosis. |
| Metabolic | Physiological Manifestations of Catecholamine Excess |

useful in evaluating false-positive results for pheochromocytoma (76), and to reliably differentiate pheochromocytomas from essential hypertension. This test has a sensitivity of 97% and a specificity of 100%. A decrease in plasma norepinephrine levels below 50% following clonidine administration is considered normal, while persistent elevations suggest pheochromocytoma (73, 74).

## 6.2 Imaging study

Once biochemical analyses suggest the presence of pheochromocytoma, imaging studies are recommended to locate the tumor. A computed tomography (CT) scan of the abdomen and pelvis is typically the initial imaging test of choice (2). CT has a sensitivity of 88%, being useful in the localization of pheochromocytomas larger than 1.3 cm in diameter with an accuracy of 90 to 95%, and represents the most common imaging method used in the diagnosis of pheochromocytomas (77). In comparison, magnetic resonance imaging, with differences in access and costs, offers better spatial resolution (65). Another imaging modality, 123I-metaiodobenzylguanidine (MIBG) scintigraphy, is especially effective for detecting adrenal and extra-adrenal pheochromocytomas (78). Magnetic resonance imaging in the diagnosis shows a differentiated appearance with a sensitivity of 100%, as well as Scintigraphy131 -MBG (sensitivity of 100%), this

TABLE 2 Scoring system to classify the probability of pheochromocytoma/paraganglioma according to symptoms and clinical signs.

| Symptoms and signs | Score per item (total score from -1 to +7)* |
|---|---|
| Pallor | + 1 point |
| Hyperhidrosis | + 1 point |
| Palpitations | + 1 point |
| Tremor | + 1 point |
| Nausea | + 1 point |
| Heart rate of 85 bpm or higher | + 1 point |
| Body mass index (BMI) < 25 kg/m2 | + 1 point |
| Obesity (BMI > 30 kg/m2) | - 1 point |
| **Odds by group** | |
| Group 1 Related Pheochromocytoma | More likely to be associated with lower scores and sustained hypertension |
| Group 2- related pheochromocytoma | More likely to be associated with higher scores |
| | Episodic presentation of symptoms, including tremor, anxiety/panic, and pallor, and older age at first diagnosis |

*Total score 3 or more indicates a 5.8-fold increased probability of pheochromocytoma/paraganglioma.

analogue is located in the adrenergic tissue, it is especially useful to locate extra-adrenal pheochromocytomas (78, 79).

In functional imaging, $^{68}$Ga-DOTA-conjugated somatostatin receptor-targeting peptide ($^{68}$Ga-DOTA-SST) positron emission tomography (PET/CT) has a detection rate of 93% (95% IC 91-95%) (80), making it the first line of functional imaging for patients without known germline pathogenic variants. However, due to the limited availability of 68Ga-DOTA-SST in Latin America, 18F-fluorodeoxyglucose (18F-FDG) PET/CT is often used as a second imaging option in these populations, with a detection rate of 74% (95% CI, 46-91%). 18F-L3,4-dihydroxiphenylalanine (18F-DOPA) PET/CT is available in Colombia and is the first choice in Hereditary pheochromocytoma cluster 2, with an 80% detection rate (95% CI, 69-88%) (17). Alternatively, a vena cava sample can be used to determine plasma catecholamines and metanephrines (81).

### 6.3 Genetic testing

Since 35-45% of PPGL patients may harbor pathogenic germline variants, genetic testing is recommended for all diagnosed cases, regardless of patient or family history (42, 44, 68). Bilateral tumors and early-onset cases are often associated with inherited syndromes such as VHL, MEN2, and NF1. At a minimum, testing should include *FH, NF1, RET, SDHB, SDHD*, and *VHL* genes. Testing for *MEN1, SDHA, SDHAF2, SDHC, TMEM127*, and *MAX* is also advised. Carrier testing should be offered to asymptomatic first-degree relatives (and to second-degree relatives in the case of *SDHD* and *SDHAF2*, which exhibit maternal imprinting) (42, 44). Following identification of a pathogenic variant, first-degree relatives should be screened (82).

### 6.4 Immunohistochemistry

Pathogenic variants in *SDHB* in PPGL patients are associated with a higher risk of tumor progression, and several studies have shown that *SDHB* pathogenic variation can be detected by the loss of *SDHB* staining in immunohistochemistry (IHC). This staining loss can serve as an independent IHC biomarker for prognosis. However, this approach is not universally applicable; under normal conditions, SDHB functions as part of the succinate dehydrogenase complex. Pathogenic variants in any gene encoding other complex subunits or auxiliary factors (such as *SDHD, SDHC, SDHA*, or *SDHAF2*) disrupt the assembly and functionality of the entire complex, resulting in an absence of *SDHB* staining on IHC (83).

## 7 Management and treatment

### 7.1 Surgical resection of the tumor

In most cases, resection of pheochromocytomas smaller than 5 cm can be effectively performed using minimally invasive laparoscopic surgery. This approach offers significant advantages, including reduced blood loss, less pain, precise dissection, shorter hospital stays, and fewer postoperative complications. The transabdominal approach provides a broader field of view and more space for maneuvering, making it suitable for bilateral tumor removal. Conversely, the retroperitoneal approach allows for unilateral resection with shorter distance to the tumor, minimizing the risk of injury to abdominal organs (2, 30, 84, 85).

Evidence suggests that patients with PPGL associated with malignancy predictors—such as primary tumor size over 5 **cm**, extra-adrenal location, or *SDHB* germline pathogenic variants—and those undergoing resection of a primary tumor with synchronous metastases may benefit more from open laparotomy with lymph node dissection (86). In cases with larger tumors or evidence of local invasion, open adrenalectomy may be preferable to ensure complete resection and minimize the risk of capsular rupture, which can lead to tumor seeding, fragmentation, peritoneal dissemination, and local recurrence due to periadrenal invasion (18, 30).

### 7.2 Preoperative stabilization

Preoperative stabilization is crucial to reducing the risk of uncontrolled hypertension, tachycardia, and volume expansion during surgery (11, 24, 59). According to the Endocrine Society, the preferred preoperative preparation involves alpha-adrenergic receptor blockers. A typical regimen includes phenoxybenzamine, starting at 10 mg orally twice daily and carefully increasing to a maximum of 1 mg/kg/day; however, its availability is limited in many countries (87). Alternatively, selective alpha-1 antagonists like doxazosin are commonly used in regions such as Latin America. They reduce the risk of postoperative hypotension but require close monitoring due to the potential for orthostatic hypotension upon initiation. Beta-blockers (e.g., propranolol, atenolol) are added 3–4 days after starting alpha-blockers to control tachycardia (87). Calcium channel blockers, such as amlodipine or nifedipine, can also be used as additional agents to manage hypertension. Increased water and salt intake is recommended 10–14 days before surgery to prevent postoperative hypotension (2, 20, 81).

During perioperative management, surgeons should minimize tumor manipulation to prevent catecholamine surges and avoid tumor spillage, especially in cystic lesions. Early control of the adrenal vein is also recommended to manage the sudden decrease in peripheral vascular resistance following tumor removal (88). Preoperative biopsies are generally not recommended (89).

### 7.3 Surveillance and restaging of patients with metastatic PPGL

For patients with secretory metastatic PPGL, biochemical monitoring of 24-hour urinary fractionated metanephrines or free plasma is recommended at least every six months, as large increases may indicate disease progression. In nonsecretory metastatic PPGL,

further measurements of plasma or 24-hour urinary metanephrines are generally unnecessary unless there is a germline pathogenic variant indicating persistent risk or if signs and symptoms of secretory disease appear (30).

Expert guidelines, such as those from NANETS, recommend surveillance imaging for metastatic PPGL with cross-sectional anatomic imaging (CT or MRI) every 3–6 months during the first year, and if disease remains stable, every 6–12 months thereafter. For liver metastases, triple-phase CT or MRI with contrast is recommended. In metastatic PPGL cases on systemic therapies, surveillance imaging with CT or MRI is suggested every 3–6 months. Functional imaging is not typically recommended for patients with primary PPGL before or after surgery; however, it can more accurately detect metastatic disease if strongly suspected (30). In such cases, PET/CT has been studied with various radiotracers, including 18F-DOPA, 18F-FDG, and 68Ga-DOTATATE. These tracers are superior to MIBG scintigraphy, which is only used when 131I-MIBG treatment is being considered. Tracer efficacy in cluster 1 PPGL depends on somatostatin receptor uptake, making 68Ga-DOTATATE highly specific and effective for detecting small tumors, and tumor glucose metabolism, which enhances the effectiveness of 18F-FDG in aggressive, undifferentiated tumors (90). For bone-only metastatic disease, both SSTR PET/CT and FDG may be useful for routine imaging surveillance (30). 18F-DOPA's effectiveness is based on tissue uptake via amino acid transporters, making it particularly suitable for non-metastatic cluster 2 tumors (90).

## 7.4 Non-surgical and novel therapies

Various local and regional therapies, including debulking surgery, cementoplasty, radiotherapy (including stereotactic and CyberKnife), radiofrequency ablation, cryotherapy, and tumor embolization, can manage symptoms associated with catecholamine production, tumor burden, or bone involvement (91–93). For patients with stable disease, low tumor burden, and oligometastatic disease, active surveillance is indicated (30, 92, 93). For resectable lesions, options include primary tumor surgery, oligometastatic disease surgery, and debulking surgery. When surgery is not feasible, and disease progression is rapid, with a high visceral tumor burden or severe symptoms, systemic chemotherapy is recommended to control disease progression and alleviate symptoms (14, 15, 92–94). Current chemotherapy regimens include cyclophosphamide, doxorubicin, dacarbazine, and vincristine, though no first-line drug has been defined. Approximately 37% of patients respond to chemotherapy, although complete responses are uncommon (95, 96). Temozolamide, an oral alternative to dacarbazine, may be an option for patients with pathogenic variants *SDHB* with methylation of the O(6)-methylguanine-DNA methyltransferase (MGMT) promoter. However, chemotherapy generally reduces tumor size and helps control blood pressure in only one-third of patients with metastatic pheochromocytoma-sympathetic paraganglioma (97, 98).

The only FDA-approved treatment for metastatic PPGL, approved in 2018, is high-specific activity iodine-131 metaiodobenzylguanidine (HSA-I-131-MIBG), targeting neuroendocrine cells with a response rate of 30–40% (35). In a multicenter phase 2 trial, 68 patients with advanced PPGL received at least one dose, with 25% (95% CI, 16%-37%) showing durable reductions in antihypertensive medication. Among evaluable patients, 92% achieved either partial response or stable disease within 12 months. Elevated serum chromogranin levels (≥1.5 times the baseline upper limit) decreased in 68% of patients (19 of 28), and median overall survival was 36.7 months (95% CI, 29.9-49.1 months). Common side effects included nausea, myelosuppression, and fatigue, with no hypertensive events (99). A real-world study by Al-Ward et al. reported a 38% objective response rate and an 83% disease control rate in 24 patients with metastatic PPGL, with complete response in two cases, 30% metanephrine normalization, and >50% improvement in 46% of cases. Blood pressure normalized in 56%, though seven patients had reversible grade 3–4 myelosuppression, and one experienced fatal pneumonitis (100). Ultratrace iobenguane 131I, a highly specific 131I-MIBG, is no longer available. In Colombia, 131I-MIBG can be imported, though its high cost—greater than tyrosine kinase inhibitors and chemotherapy—limits availability. Additionally, 50% of patients do not show 131I-MIBG uptake, further restricting its use in Latin America (101). Lutetium-177 DOTATATE/TOC has emerged as an alternative management option in patients with advanced PPGL, however its evidence so far comes from retrospective studies (102, 103). In Colombia, Lutetium-177 DOTATATE/TOC is approved for use in neuroendocrine tumors. In a phase II clinical trial conducted by Reyes et al. Lutetium was shown to be safe and effective in a population of 13 patients with inoperable and progressing advanced neuroendocrine tumors, but no patients with PPGL were included (104).

In addition, for patients with slow/moderate progression, not candidates for radionuclide therapy angiogenesis and proliferative signaling inhibitors have been tested as novel treatments, focusing on the interaction between several growth factors including vascular endothelial growth factor [VEGF], platelet-derived growth factors [PDGF] and others, with tyrosine kinase receptors (105). Sunitinib, which inhibits VEGF1, VEGF2, VEGF3, PDGF-alpha, PDGF-beta, c-kit, fms-related tyrosine kinase 3, and RET proto-oncogene receptors, has demonstrated potential in reducing angiogenesis and tumor cell growth. Small studies have shown a disease control rate of 57–83%, with median progression-free survival ranging from 4 to 13 months (106). The FIRSTMAPP study, a phase II randomized placebo-controlled trial, recently reported that Sunitinib achieved the primary endpoint of 12-month progression-free survival in 36% of patients with progressive metastatic PPGL (90% CI, 23–50%), compared to 19% in the placebo group (90% CI, 11–31%). Grade 3 or 4 adverse effects included asthenia, hypertension, and bone or back pain (107). Another drug, Cabozantinib was evaluated in the Natalie Trial, a single-arm phase II trial with 17 patients and a median follow-up of 25 months. The overall response rate was 25.0% (95% CI, 7.3–

52.4), with responses observed in 4 out of 16 patients. Grade 3 adverse events included hand-foot syndrome, hypertension, rectal fistula, QT prolongation, and asymptomatic hypomagnesemia. Additionally, two cases of asymptomatic elevations in amylase and lipase were reported (108). On the other hand, Axitinib, a VEGFR2 inhibitor, has also shown promise, particularly in metastatic pheochromocytomas where the pseudohypoxic tumor environment stimulates VEGF synthesis, promoting angiogenesis. Phase II trials of Axitinib reported a partial response in 36% of patients (105).

New therapies for metastatic PPGL under investigation include Belzutifan, a HIF-2 inhibitor used in VHL disease, currently in a phase II trial (NCT04924075) for PPGL (108). Another HIF-2 inhibitor, DFF332, is currently in a phase I/Ib trial (NCT04895748) as monotherapy and in combination with agents like everolimus, spartalizumab, and taminadenant.

Additional investigational drugs include Olaparib, a poly(ADP-ribose) polymerase (PARP) inhibitor involved in DNA repair, being tested in combination with temozolomide (NCT04394858), and Tipifarnib, a farnesyl transferase inhibitor that supports tumor cell survival (NCT04284774).

Finally, Imipridone, a promising agent targeting caseinolytic protease P (ClpP) and acting as a dopamine-like receptor antagonist, has also garnered interest. In a phase II trial, 10 patients received Imipridone at 625 mg weekly; of these, five showed partial responses, and two had stable disease. In a second cohort, where patients received two doses on consecutive days weekly, one achieved a partial response, and seven maintained stable disease (109).

## 8 Conclusions

PPLG are rare neuroendocrine tumors with relevant clinical implications, characterized predominantly by the production of catecholamines, which can manifest in a spectrum of clinical symptoms.

Pheochromocytomas have the potential to be part of inherited syndromes such as MEN-2, VHL, and NF1, which implicate a variety of other pathologies and necessitate genetic screening of affected individuals and their family members. This genetic association requires a robust approach to diagnosis and treatment, integrating advanced imaging techniques, accurate laboratory testing, and detailed genetic analysis.

Treatment strategies for pheochromocytomas involve a multidisciplinary approach, including surgical intervention as the primary therapeutic option. Preoperative preparation with alpha-blockers and beta-blockers is crucial to mitigate the risks associated with catecholamine secretion during tumor manipulation. Non-surgical approaches, including chemotherapy and novel therapies such as tyrosine kinase inhibitors, play a role in the treatment of metastatic or inoperable cases, offering symptomatic relief and possible disease control.

Although PPGL are rare, their complex clinical presentations and potential genetic basis make them a significant challenge in endocrine and oncologic practice. Early diagnosis, a thorough understanding of the genetic landscape, and a comprehensive treatment strategy are critical to improving outcomes for patients with these potentially life-threatening conditions.

## Author contributions

JT: Writing – original draft, Validation, Software, Resources, Project administration, Methodology, Investigation, Data curation, Conceptualization. HN-C: Writing – original draft, Validation, Resources, Methodology, Investigation, Data curation, Conceptualization. LC: Writing – original draft, Validation, Resources, Methodology, Investigation, Data curation, Conceptualization. WR-M: Writing – review & editing, Writing – original draft, Validation, Supervision, Resources, Methodology, Investigation, Conceptualization. JA: Writing – original draft, Validation, Software, Resources, Methodology, Investigation. CC-G: Writing – original draft, Validation, Resources, Investigation, Data curation. LS: Writing – review & editing, Writing – original draft, Validation, Resources, Methodology, Investigation. MH-E: Writing – original draft, Visualization, Software, Project administration, Methodology, Investigation. MA-I: Writing – review & editing, Writing – original draft, Visualization, Validation, Resources, Methodology, Investigation. JI-C: Writing – review & editing, Writing – original draft, Visualization, Validation, Supervision, Software, Resources, Project administration, Methodology, Investigation, Funding acquisition, Data curation.

## Funding

The author(s) declare that no financial support was received for the research, authorship, and/or publication of this article.

## Conflict of interest

The authors declare that the research was conducted in the absence of any commercial or financial relationships that could be construed as a potential conflict of interest.

## Publisher's note

All claims expressed in this article are solely those of the authors and do not necessarily represent those of their affiliated organizations, or those of the publisher, the editors and the reviewers. Any product that may be evaluated in this article, or claim that may be made by its manufacturer, is not guaranteed or endorsed by the publisher.

# References


1. Klöppel G. Tumoren des nebennierenmarks und der paraganglien. *Pathologe*. (2003) 24:280–6. doi: 10.1007/s00292-003-0635-8

2. Lenders JWM, Duh Q-Y, Eisenhofer G, Gimenez-Roqueplo A-P, Grebe SKG, Murad MH, et al. Pheochromocytoma and paraganglioma: an endocrine society clinical practice guideline. *J Clin Endocrinol Metab*. (2014) 99:1915–42. doi: 10.1210/jc.2014-1498

3. Eisenhofer G, Pamporaki C, Lenders JWM. Biochemical assessment of pheochromocytoma and paraganglioma. *Endocr Rev*. (2023) 44:862–909. doi: 10.1210/endrev/bnad011

4. Aygun N, Uludag M. Pheochromocytoma and paraganglioma: from epidemiology to clinical findings. *Sisli Etfal Hastan Tip Bul*. (2020) 54:159–68. doi: 10.14744/SEMB.2020.18794

5. Mete O, Asa SL, Gill AJ, Kimura N, de Krijger RR, Tischler A. Overview of the 2022 WHO classification of paragangliomas and pheochromocytomas. *Endocr Pathol*. (2022) 33:90–114. doi: 10.1007/s12022-022-09704-6

6. Tischler AS, Pacak K, Eisenhofer G. The adrenal medulla and extra-adrenal paraganglia: then and now. *Endocr Pathol*. (2014) 25:49–58. doi: 10.1007/s12022-013-9286-3

7. Glenn F, Gray GF. Functional tumors of the organ of Zuckerkandl. *Ann Surg*. (1976) 183:578–85. doi: 10.1097/00000658-197605000-00015

8. Ilias I, Pacak K. Diagnosis and management of tumors of the adrenal medulla. *Horm Metab Res*. (2005) 37:717–21. doi: 10.1055/s-2005-921091

9. Neumann HP, Pawlu C, Peczkowska M, Bausch B, McWhinney SR, Muresan M, et al. Distinct clinical features of paraganglioma syndromes associated with SDHB and SDHD gene mutations. *JAMA*. (2004) 292:943–51. doi: 10.1001/jama.292.8.943

10. Kihara C, Patel S, Moss R. A rapidly progressing carotid body tumor: A case report. *Cureus*. (2023) 15:e43654. doi: 10.7759/cureus.43654

11. Santarpia L, Habra MA, Jiménez C. Malignant pheochromocytomas and paragangliomas: molecular signaling pathways and emerging therapies. *Horm Metab Res*. (2009) 41:680–6. doi: 10.1055/s-0029-1214381

12. Jadhav SS, Dhok AP, Mitra KR. Carotid body paraganglioma: a case report. *Pan Afr Med J*. (2023) 44:182. doi: 10.11604/pamj.2023.44.182.38636

13. Karatas E, Sirikci A, Baglam T, Mumbuc S, Durucu C, Tutar E, et al. Synchronous bilateral carotid body tumor and vagal paraganglioma: A case report and review of literature. *Auris Nasus Larynx*. (2008) 35:171–5. doi: 10.1016/j.anl.2007.05.007

14. Bracigliano A, Marretta AL, Guerrera LP, Simioli R, Clemente O, Granata V, et al. The management of phaeochromocytomas and paragangliomas in the era of precision medicine: where are we now? Evidence-based systemic treatment options and future cluster oriented perspectives. *Pharmaceuticals*. (2024) 17:354. doi: 10.3390/ph17030354

15. Sharma S, Fishbein L. Diagnosis and management of pheochromocytomas and paragangliomas: A guide for the clinician. *Endocr Pract*. (2023) 29:999–1006. doi: 10.1016/j.eprac.2023.07.027

16. Lima JV, Kater CE. The Pheochromocytoma/Paraganglioma syndrome: an overview on mechanisms, diagnosis and management. *Int Braz J Urol*. (2023) 49:307–19. doi: 10.1590/S1677-5538.IBJU.2023.0038

17. Nölting S, Bechmann N, Taieb D, Beuschlein F, Fassnacht M, Kroiss M, et al. Personalized management of pheochromocytoma and paraganglioma. *Endocr Rev*. (2022) 43:199–239. doi: 10.1210/endrev/bnab019

18. Passman JE, Wachtel H. Management of pheochromocytomas and paragangliomas. *Surg Clin North Am*. (2024) 104:863–81. doi: 10.1016/j.suc.2024.02.014

19. Neumann HPH, Young WF, Eng C. Pheochromocytoma and paraganglioma. *N Engl J Med*. (2019) 381:552–65. doi: 10.1056/NEJMra1806651

20. Strosberg JR. Update on the management of unusual neuroendocrine tumors: pheochromocytoma and paraganglioma, medullary thyroid cancer and adrenocortical carcinoma. *Semin Oncol*. (2013) 40:120–33. doi: 10.1053/j.seminoncol.2012.11.009

21. Almeida MQ, Bezerra-Neto JE, Mendonça BB, Latronico AC, Fragoso MCBV. Primary Malignant tumors of the adrenal glands. *Clinics (Sao Paulo)*. (2018) 73:e756s. doi: 10.6061/clinics/2018/e756s

22. Lorenzo S, Luis J. Diagnóstico y tratamiento de los feocromocitomas y paragangliomas. *Rev Finlay*. (2021) 11:307–15.

23. Gimenez-Roqueplo A-P, Burnichon N, Amar L, Favier J, Jeunemaitre X, Plouin P-F. Recent advances in the genetics of phaeochromocytoma and functional paraganglioma. *Clin Exp Pharmacol Physiol*. (2008) 35:376–9. doi: 10.1111/j.1440-1681.2008.04881.x

24. Korpershoek E, Petri B-J, Van Nederveen FH, Dinjens WNM, Verhofstad AA, De Herder WW, et al. Candidate gene mutation analysis in bilateral adrenal pheochromocytoma and sympathetic paraganglioma. *Endocr Relat Cancer*. (2007) 14:453–62. doi: 10.1677/ERC-06-0044

25. Lopes MBS. The 2017 World Health Organization classification of tumors of the pituitary gland: a summary. *Acta Neuropathol*. (2017) 134:521–35. doi: 10.1007/s00401-017-1769-8

26. Fassnacht M, Assie G, Baudin E, Eisenhofer G, de la Fouchardiere C, Haak HR, et al. Adrenocortical carcinomas and Malignant phaeochromocytomas: ESMO-EURACAN Clinical Practice Guidelines for diagnosis, treatment and follow-up. *Ann Oncol*. (2020) 31:1476–90. doi: 10.1016/j.annonc.2020.08.2099

27. Mustafa K, Zadeh S, Culver SA. Dopamine-secreting carotid body paraganglioma in a patient with SDHB mutation. *AACE Clin Case Rep*. (2024) 10:109–12. doi: 10.1016/j.aace.2024.03.003

28. Rao D, Peitzsch M, Prejbisz A, Hanus K, Fassnacht M, Beuschlein F, et al. Plasma methoxytyramine: clinical utility with metanephrines for diagnosis of pheochromocytoma and paraganglioma. *Eur J Endocrinol*. (2017) 177:103–13. doi: 10.1530/EJE-17-0077

29. Pamporaki C, Berends AMA, Filippatos A, Prodanov T, Meuter L, Prejbisz A, et al. Prediction of metastatic pheochromocytoma and paraganglioma: a machine learning modelling study using data from a cross-sectional cohort. *Lancet Digit Health*. (2023) 5:e551–9. doi: 10.1016/S2589-7500(23)00094-8

30. Fishbein L, Del Rivero J, Else T, Howe JR, Asa SL, Cohen DL, et al. The north american neuroendocrine tumor society consensus guidelines for surveillance and management of metastatic and/or unresectable pheochromocytoma and paraganglioma. *Pancreas*. (2021) 50:469–93. doi: 10.1097/MPA.0000000000001792

31. Mihai R, De Crea C, Guerin C, Torresan F, Agcaoglu O, Simescu R, et al. Surgery for advanced adrenal Malignant disease: recommendations based on European Society of Endocrine Surgeons consensus meeting. *Br J Surg*. (2024) 111:znad266. doi: 10.1093/bjs/znad266

32. Roman-Gonzalez A, Jimenez C. Malignant pheochromocytoma-paraganglioma: pathogenesis, TNM staging, and current clinical trials. *Curr Opin Endocrinol Diabetes Obes*. (2017) 24:174–83. doi: 10.1097/MED.0000000000000330

33. Jandou I, Moataz A, Dakir M, Debbagh A, Aboutaieb R. Malignant pheochromocytoma: A diagnostic and therapeutic dilemma. *Int J Surg Case Rep*. (2021) 83:106009. doi: 10.1016/j.ijscr.2021.106009

34. Sangoi AR, McKenney JK. A tissue microarray-based comparative analysis of novel and traditional immunohistochemical markers in the distinction between adrenal cortical lesions and pheochromocytoma. *Am J Surg Pathol*. (2010) 34:423–32. doi: 10.1097/PAS.0b013e3181cfb506

35. Jimenez C, Erwin W, Chasen B. Targeted radionuclide therapy for patients with metastatic pheochromocytoma and paraganglioma: from low-specific-activity to high-specific-activity iodine-131 metaiodobenzylguanidine. *Cancers (Basel)*. (2019) 11:1018. doi: 10.3390/cancers11071018

36. Lam AK. Update on adrenal tumours in 2017 world health organization (WHO) of endocrine tumours. *Endocr Pathol*. (2017) 28:213–27. doi: 10.1007/s12022-017-9484-5

37. Jimenez C, Ma J, Roman Gonzalez A, Varghese J, Zhang M, Perrier N, et al. TNM staging and overall survival in patients with pheochromocytoma and sympathetic paraganglioma. *J Clin Endocrinol Metab*. (2023) 108:1132–42. doi: 10.1210/clinem/dgac677

38. Shine B. Gene targeting through O-methylated catecholamine metabolite patterns. *Clin Chem*. (2011) 57:361–2. doi: 10.1373/clinchem.2010.159178

39. Astuti D, Latif F, Dallol A, Dahia PLM, Douglas F, George E, et al. Gene mutations in the succinate dehydrogenase subunit SDHB cause susceptibility to familial pheochromocytoma and to familial paraganglioma. *Am J Hum Genet*. (2001) 69:49–54. doi: 10.1086/321282

40. Mercado-Asis LB, Wolf KI, Jochmanova I, Taïeb D. Pheochromocytoma: A genetic and diagnostic update. *Endocrine Pract*. (2018) 24:78–90. doi: 10.4158/EP-2017-0057

41. Reda SA, Japp EA, Galati S-J, Krakoff LR, Levine AC. Pheochromocytoma. In: Davies TF, editor. *A Case-Based Guide to Clinical Endocrinology*. Springer International Publishing, Cham (2022). p. 167–82. doi: 10.1007/978-3-030-84367-0_19

42. Muth A, Crona J, Gimm O, Elmgren A, Filipsson K, Stenmark Askmalm M, et al. Genetic testing and surveillance guidelines in hereditary pheochromocytoma and paraganglioma. *J Intern Med*. (2019) 285:187–204. doi: 10.1111/joim.12869

43. Bruel A-L, Vitobello A, Thiffault I, Manwaring L, Willing M, Agrawal PB, et al. ITSN1: a novel candidate gene involved in autosomal dominant neurodevelopmental disorder spectrum. *Eur J Hum Genet*. (2022) 30:111–6. doi: 10.1038/s41431-021-00985-9

44. Giacché M, Tacchetti MC, Castellano M. Genetics and Molecular Biology of Pheochromocytoma and Paraganglioma. In: Tiberio GAM, editor. *Primary Adrenal Malignancies*. Springer Nature Switzerland, Cham (2024). p. 23–30. doi: 10.1007/978-3-031-62301-1_4

45. Lian B, Lu J, Fang X, Zhang Y, Wang W, He Y, et al. Genotype and clinical phenotype characteristics of MAX germline mutation–associated pheochromocytoma/paraganglioma syndrome. *Front Endocrinol (Lausanne)*. (2024) 15:1442691. doi: 10.3389/fendo.2024.1442691

46. Szabo Yamashita T, Tame-Elorduy A, Skefos CM, Varghese JM, Habra MA, Fisher SB, et al. SDHB-associated pheochromocytomas: what is their clinical behavior? *Ann Surg Oncol*. (2024) 31:9007–13. doi: 10.1245/s10434-024-16120-z

47. Thosani S, Ayala-Ramirez M, Palmer L, Hu MI, Rich T, Gagel RF, et al. The characterization of pheochromocytoma and its impact on overall survival in multiple endocrine neoplasia type 2. *J Clin Endocrinol Metab*. (2013) 98:E1813–9. doi: 10.1210/jc.2013-1653

48. Meyer-Rochow GY, Smith JM, Richardson A-L, Marsh DJ, Sidhu SB, Robinson BG, et al. Denaturing high performance liquid chromatography detection of SDHB, SDHD, and VHL germline mutations in pheochromocytoma. *J Surg Res*. (2009) 157:55–62. doi: 10.1016/j.jss.2008.07.043

49. Björklund P, Pacak K, Crona J. Precision medicine in pheochromocytoma and paraganglioma: current and future concepts. *J Intern Med*. (2016) 280:559–73. doi: 10.1111/joim.12507

50. Sarkadi B, Saskoi E, Butz H, Patocs A. Genetics of pheochromocytomas and paragangliomas determine the therapeutical approach. *Int J Mol Sci*. (2022) 23:1450. doi: 10.3390/ijms23031450

51. Eid M, Foukal J, Sochorová D, Tuček Š, Starý K, Kala Z, et al. Management of pheochromocytomas and paragangliomas: Review of current diagnosis and treatment options. *Cancer Med*. (2023) 12:13942–57. doi: 10.1002/cam4.6010

52. Assadipour Y, Sadowski SM, Alimchandani M, Quezado M, Steinberg SM, Nilubol N, et al. SDHB mutation status and tumor size but not tumor grade are important predictors of clinical outcome in pheochromocytoma and abdominal paraganglioma. *Surgery*. (2017) 161:230–9. doi: 10.1016/j.surg.2016.05.050

53. Kantorovich V, King KS, Pacak K. SDH-related pheochromocytoma and paraganglioma. *Best Pract Res Clin Endocrinol Metab*. (2010) 24:415–24. doi: 10.1016/j.beem.2010.04.001

54. Ando Y, Ono Y, Sano A, Fujita N, Ono S, Tanaka Y. Clinical characteristics and outcomes of pheochromocytoma crisis: a literature review of 200 cases. *J Endocrinol Invest*. (2022) 45:2313–28. doi: 10.1007/s40618-022-01868-6

55. Klein RD, Jin L, Rumilla K, Young WF, Lloyd RV. Germline SDHB mutations are common in patients with apparently sporadic sympathetic paragangliomas. *Diagn Mol Pathol*. (2008) 17:94–100. doi: 10.1097/PDM.0b013e318150d67c

56. Stein PP. A simplified diagnostic approach to pheochromocytoma. *A Rev literature Rep One institution's experience*. (1991) 70:46–66. doi: 10.1097/00005792-199101000-00004

57. Greenleaf CE, Griffin LA, Shake JG, Orr WS. Hypertensive crisis secondary to pheochromocytoma. *Proc (Bayl Univ Med Cent)*. (2017) 30:314–5. doi: 10.1080/08998280.2017.11929629

58. Mannelli M. Diagnostic problems in pheochromocytoma. *J Endocrinol Invest*. (1989) 12:739–57. doi: 10.1007/BF03350050

59. Lance JW, Hinterberger H. Symptoms of pheochromocytoma, with particular reference to headache, correlated with catecholamine production. *Arch Neurol*. (1976) 33:281–8. doi: 10.1001/archneur.1976.00500040065011

60. Cortelli P, Grimaldi D, Guaraldi P, Pierangeli G. Headache and hypertension. *Neurol Sci*. (2004) 25 Suppl 3:S132–134. doi: 10.1007/s10072-004-0271-y

61. Singer M, Deutschman CS, Seymour CW, Shankar-Hari M, Annane D, Bauer M, et al. The third international consensus definitions for sepsis and septic shock (Sepsis-3). *JAMA*. (2016) 315:801–10. doi: 10.1001/jama.2016.0287

62. Roth MA, Leyba K, Garg I, Madrid WH, Quazi MA, Sohail AH, et al. Mortality and in-patient outcomes in pheochromocytoma patients with hypertensive emergency in the United States: A propensity score matched analysis. *Curr Probl Cardiol*. (2024) 49:102578. doi: 10.1016/j.cpcardiol.2024.102578

63. Rupala K, Mittal V, Gupta R, Yadav R. Atypical presentation of pheochromocytoma: Central nervous system pseudovasculitis. *Indian J Urol*. (2017) 33:82–4. doi: 10.4103/0970-1591.195760

64. Li C, Chen Y, Wang W, Teng L. A case of clinically silent giant right pheochromocytoma and review of literature. *Can Urol Assoc J*. (2012) 6:E267–9. doi: 10.5489/cuaj.11195

65. Sarveswaran V, Kumar S, Kumar A, Vamseedharan M. A giant cystic pheochromocytoma mimicking liver abscess an unusual presentation – a case report. *Clin Case Rep*. (2015) 3:64–8. doi: 10.1002/ccr3.149

66. Staren ED, Prinz RA. Selection of patients with adrenal incidentalomas for operation. *Surg Clinics North America*. (1995) 75:499–509. doi: 10.1016/S0039-6109(16)46636-3

67. Geroula A, Deutschbein T, Langton K, Masjkur J, Pamporaki C, Peitzsch M, et al. Pheochromocytoma and paraganglioma: clinical feature-based disease probability in relation to catecholamine biochemistry and reason for disease suspicion. *Eur J Endocrinol*. (2019) 181:409–20. doi: 10.1530/EJE-19-0159

68. Neumann HP, Young WF, Krauss T, Bayley J-P, Schiavi F, Opocher G, et al. 65 YEARS OF THE DOUBLE HELIX: Genetics informs precision practice in the diagnosis and management of pheochromocytoma. *Endocr Relat Cancer*. (2018) 25:T201–19. doi: 10.1530/ERC-18-0085

69. de Jong WHA, Eisenhofer G, Post WJ, Muskiet FAJ, de Vries EGE, Kema IP. Dietary influences on plasma and urinary metanephrines: implications for diagnosis of catecholamine-producing tumors. *J Clin Endocrinol Metab*. (2009) 94:2841–9. doi: 10.1210/jc.2009-0303

70. Kim HJ, Lee JI, Cho YY, Lee SY, Kim JH, Jung BC, et al. Diagnostic accuracy of plasma free metanephrines in a seated position compared with 24-hour urinary metanephrines in the investigation of pheochromocytoma. *Endocr J*. (2015) 62:243–50. doi: 10.1507/endocrj.EJ14-0384

71. Boot CS. A laboratory medicine perspective on the investigation of phaeochromocytoma and paraganglioma. *Diagnostics (Basel)*. (2023) 13:2940. doi: 10.3390/diagnostics13182940

72. Wan W, Nguyen B, Graybill S, Kim J. Clonidine suppression testing for pheochromocytoma in neurofibromatosis type 1. *BMJ Case Rep*. (2019) 12:e228263. doi: 10.1136/bcr-2018-228263

73. Tsiomidou S, Pamporaki C, Geroula A, Van Baal L, Weber F, Dralle H, et al. Clonidine suppression test for a reliable diagnosis of pheochromocytoma: When to use. *Clin Endocrinol (Oxf)*. (2022) 97:541–50. doi: 10.1111/cen.14724

74. Anderson GH, Blakeman N, Streeten DH. The effect of age on prevalence of secondary forms of hypertension in 4429 consecutively referred patients. *J Hypertens*. (1994) 12:609–15. doi: 10.1097/00004872-199405000-00015

75. Wakabayashi T. Mechanism of the calcium-regulation of muscle contraction — In pursuit of its structural basis. *Proc Jpn Acad Ser B Phys Biol Sci*. (2015) 91:321–50. doi: 10.2183/pjab.91.321

76. Shen S-J, Cheng H-M, Chiu AW, Chou C-W, Chen J-Y. Perioperative hypertensive crisis in clinically silent pheochromocytomas: report of four cases. *Chang Gung Med J*. (2005) 28:44–50.

77. Čtvrtlík F, Koranda P, Schovánek J, Škarda J, Hartmann I, Tüdös Z. Current diagnostic imaging of pheochromocytomas and implications for therapeutic strategy. *Exp Ther Med*. (2018) 15:3151–60. doi: 10.3892/etm.2018.5871

78. Berglund AS, Hulthén UL, Manhem P, Thorsson O, Wollmer P, Törnquist C. Metaiodobenzylguanidine (MIBG) scintigraphy and computed tomography (CT) in clinical practice. Primary and secondary evaluation for localization of phaeochromocytomas. *J Intern Med*. (2001) 249:247–51. doi: 10.1046/j.1365-2796.2001.00792.x

79. Bhatia KSS, Ismail MM, Sahdev A, Rockall AG, Hogarth K, Canizales A, et al. 123I-metaiodobenzylguanidine (MIBG) scintigraphy for the detection of adrenal and extra-adrenal phaeochromocytomas: CT and MRI correlation. *Clin Endocrinol (Oxf)*. (2008) 69:181–8. doi: 10.1111/j.1365-2265.2008.03256.x

80. Han S, Suh CH, Woo S, Kim YJ, Lee JJ. Performance of 68Ga-DOTA-conjugated somatostatin receptor-targeting peptide PET in detection of pheochromocytoma and paraganglioma: A systematic review and metaanalysis. *J Nucl Med*. (2019) 60:369–76. doi: 10.2967/jnumed.118.211706

81. Pacak K, Eisenhofer G, Carrasquillo JA, Chen CC, Li ST, Goldstein DS. 6-[18F] fluorodopamine positron emission tomographic (PET) scanning for diagnostic localization of pheochromocytoma. *Hypertension*. (2001) 38:6–8. doi: 10.1161/01.hyp.38.1.6

82. Neumann HPH, Hoegerle S, Manz T, Brenner K, Iliopoulos O. How many pathways to pheochromocytoma? *Semin Nephrol*. (2002) 22:89–99. doi: 10.1053/snep.2002.30207

83. Su T, Yang Y, Jiang L, Xie J, Zhong X, Wu L, et al. SDHB immunohistochemistry for prognosis of pheochromocytoma and paraganglioma: A retrospective and prospective analysis. *Front Endocrinol (Lausanne)*. (2023) 14:1121397. doi: 10.3389/fendo.2023.1121397

84. Dogrul AB, Cennet O, Dincer AH. Minimally invasive techniques in benign and Malignant adrenal tumors. *World J Clin cases*. (2022) 10:12812–21. doi: 10.12998/wjcc.v10.i35.12812

85. Wang X, Zhao Y, Liao Z, Zhang Y. Surgical strategies of complicated pheochromocytomas/paragangliomas and literature review. *Front Endocrinol (Lausanne)*. (2023) 14:1129622. doi: 10.3389/fendo.2023.1129622

86. Roman-Gonzalez A, Zhou S, Ayala-Ramirez M, Shen C, Waguespack SG, Habra MA, et al. Impact of surgical resection of the primary tumor on overall survival in patients with metastatic pheochromocytoma or sympathetic paraganglioma. *Ann Surg*. (2018) 268:172–8. doi: 10.1097/SLA.0000000000002195

87. Román-González A, Padilla-Zambrano H, Jimenez LFV. Perioperative management of pheocromocytoma/paraganglioma: a comprehensive review. *Colombian J Anesthesiology*. (2021) 49:1–12. doi: 10.5554/22562087.e958

88. Munakomi S, Rajbanshi S, Adhikary PS. Case Report: A giant but silent adrenal pheochromocytoma – a rare entity. *F1000Res*. (2016) 5:290. doi: 10.12688/f1000research.8168.1

89. Plouin PF, Amar L, Dekkers OM, Fassnacht M, Gimenez-Roqueplo AP, Lenders JWM, et al. European Society of Endocrinology Clinical Practice Guideline for long-term follow-up of patients operated on for a phaeochromocytoma or a paraganglioma. *Eur J Endocrinol*. (2016) 174:G1–G10. doi: 10.1530/EJE-16-0033

90. Marcus C, Subramaniam RM. Paragangliomas and pheochromocytomas: positron emission tomography/computed tomography diagnosis and therapy. *PET Clin*. (2023) 18:233–42. doi: 10.1016/j.cpet.2022.11.006

91. Breen W, Bancos I, Young WF, Bible KC, Laack NN, Foote RL, et al. External beam radiation therapy for advanced/unresectable Malignant paraganglioma and pheochromocytoma. *Adv Radiat Oncol*. (2018) 3:25–9. doi: 10.1016/j.adro.2017.11.002

92. Garcia-Carbonero R, Matute Teresa F, Mercader-Cidoncha E, Mitjavila-Casanovas M, Robledo M, Tena I, et al. Multidisciplinary practice guidelines for the diagnosis, genetic counseling and treatment of pheochromocytomas and paragangliomas. *Clin Transl Oncol*. (2021) 23:1995–2019. doi: 10.1007/s12094-021-02622-9

93. Wang K, Crona J, Beuschlein F, Grossman AB, Pacak K, Nölting S. Targeted therapies in pheochromocytoma and paraganglioma. *J Clin Endocrinol Metab*. (2022) 107:2963–72. doi: 10.1210/clinem/dgac471

94. Jimenez C, Xu G, Varghese J, Graham PH, Campbell MT, Lu Y. New directions in treatment of metastatic or advanced pheochromocytomas and sympathetic paragangliomas: an american, contemporary, pragmatic approach. *Curr Oncol Rep*. (2022) 24:89–98. doi: 10.1007/s11912-022-01197-0

95. Huang H, Abraham J, Hung E, Averbuch S, Merino M, Steinberg SM, et al. Treatment of Malignant pheochromocytoma/paraganglioma with cyclophosphamide, vincristine, and dacarbazine: recommendation from a 22-year follow-up of 18 patients. *Cancer*. (2008) 113:2020–8. doi: 10.1002/cncr.23812

96. Niemeijer ND, Alblas G, van Hulsteijn LT, Dekkers OM, Corssmit EPM. Chemotherapy with cyclophosphamide, vincristine and dacarbazine for Malignant paraganglioma and pheochromocytoma: systematic review and meta-analysis. *Clin Endocrinol (Oxf)*. (2014) 81:642–51. doi: 10.1111/cen.12542

97. Hadoux J, Favier J, Scoazec J-Y, Leboulleux S, Al Ghuzlan A, Caramella C, et al. SDHB mutations are associated with response to temozolomide in patients with metastatic pheochromocytoma or paraganglioma. *Int J Cancer*. (2014) 135:2711–20. doi: 10.1002/ijc.28913

98. Ayala-Ramirez M, Feng L, Habra MA, Rich T, Dickson PV, Perrier N, et al. Clinical benefits of systemic chemotherapy for patients with metastatic pheochromocytomas or sympathetic extra-adrenal paragangliomas: insights from the largest single-institutional experience. *Cancer*. (2012) 118:2804–12. doi: 10.1002/cncr.26577

99. Pryma DA, Chin BB, Noto RB, Dillon JS, Perkins S, Solnes L, et al. Efficacy and safety of high-specific-activity 131I-MIBG therapy in patients with advanced pheochromocytoma or paraganglioma. *J Nucl medicine: Off publication Soc Nucl Med*. (2019) 60:623–30. doi: 10.2967/jnumed.118.217463

100. Al-Ward R, Brondani VB, Sawani S, Potter CL, Xu G, Waguespack SG, et al. High-specific-activity 131 I-MIBG for the treatment of advanced pheochromocytoma and paraganglioma. *Clin Nucl Med*. (2024) 49:610–20. doi: 10.1097/RLU.0000000000005184

101. Román-González A. Nuevos conceptos en feocromocitoma y paraganglioma en el 2017. *Rev Colombiana Endocrinología Diabetes Metabolismo*. (2017) 4:19–23. doi: 10.53853/encr.4.4.148

102. Tang CYL, Chua WM, Huang HL, Lam WW-C, Loh LM, Tai D, et al. Safety and efficacy of peptide receptor radionuclide therapy in patients with advanced pheochromocytoma and paraganglioma: A single-institution experience and review of the literature. *J Neuroendocrinol*. (2023) 35:e13349. doi: 10.1111/jne.13349

103. Kornerup LS, Andreassen M, Knigge U, Arveschoug AK, Poulsen PL, Kjær A, et al. Effects of peptide receptor radiotherapy in patients with advanced paraganglioma and pheochromocytoma: A nation-wide cohort study. *Cancers (Basel)*. (2024) 16:1349. doi: 10.3390/cancers16071349

104. De los Reyes A, Llamas-Olier A, Martí A, Fierro F, Rojas L, Martínez MC, et al. Eficacia de lutecio-177 DOTATATE/TOC en pacientes con tumores neuroendocrinos bien diferenciados en estado avanzado. Ensayo clínico fase II. *Rev Colombiana Cancerología*. (2021) 25:13–24. doi: 10.35509/01239015.132

105. Jimenez C. Treatment for patients with Malignant pheochromocytomas and paragangliomas: A perspective from the hallmarks of cancer. *Front Endocrinol (Lausanne)*. (2018) 9:277. doi: 10.3389/fendo.2018.00277

106. O'Kane GM, Ezzat S, Joshua AM, Bourdeau I, Leibowitz-Amit R, Olney HJ, et al. A phase 2 trial of sunitinib in patients with progressive paraganglioma or pheochromocytoma: the SNIPP trial. *Br J Cancer*. (2019) 120:1113–9. doi: 10.1038/s41416-019-0474-x

107. Baudin E, Goichot B, Berruti A, Hadoux J, Moalla S, Laboureau S, et al. Sunitinib for metastatic progressive phaeochromocytomas and paragangliomas: results from FIRSTMAPPP, an academic, multicentre, international, randomised, placebo-controlled, double-blind, phase 2 trial. *Lancet (London England)*. (2024) 403:1061–70. doi: 10.1016/S0140-6736(23)02554-0

108. Jimenez C, Habra MA, Campbell MT, Tamsen G, Cruz-Goldberg D, Long J, et al. Cabozantinib in patients with unresectable and progressive metastatic phaeochromocytoma or paraganglioma (the Natalie Trial): a single-arm, phase 2 trial. *Lancet Oncol*. (2024) 25:658–67. doi: 10.1016/S1470-2045(24)00133-5

109. Anderson PM, Trucco MM, Tarapore RS, Zahler S, Thomas S, Gortz J, et al. Phase II study of ONC201 in neuroendocrine tumors including pheochromocytoma-paraganglioma and desmoplastic small round cell tumor. *Clin Cancer Res*. (2022) 28:1773–82. doi: 10.1158/1078-0432.CCR-21-4030

frontiers | Frontiers in Endocrinology

TYPE Case Report
PUBLISHED 16 December 2024
DOI 10.3389/fendo.2024.1491873

Check for updates

OPEN ACCESS

EDITED BY
Ichiro Abe,
Fukuoka University Chikushi Hospital, Japan

REVIEWED BY
Yewei Xing,
University of Michigan, United States
Shohei Sakamoto,
National Hospital Organization Kyushu Medical Center, Japan

*CORRESPONDENCE
Bobrowicz Małgorzata
malgorzata.bobrowicz@wum.edu.pl

†These authors have contributed equally to this work

RECEIVED 05 September 2024
ACCEPTED 29 November 2024
PUBLISHED 16 December 2024

CITATION
Małgorzata B, Anna N, Anna K, Marek R, Joanna H, Adrianna G, Sadegh T, Łukasz K and Urszula A (2024) Case report: Pheochromocytoma-induced pseudo-Cushing's syndrome.
*Front. Endocrinol.* 15:1491873.
doi: 10.3389/fendo.2024.1491873

COPYRIGHT
© 2024 Małgorzata, Anna, Anna, Marek, Joanna, Adrianna, Sadegh, Łukasz and Urszula. This is an open-access article distributed under the terms of the Creative Commons Attribution License (CC BY). The use, distribution or reproduction in other forums is permitted, provided the original author(s) and the copyright owner(s) are credited and that the original publication in this journal is cited, in accordance with accepted academic practice. No use, distribution or reproduction is permitted which does not comply with these terms.

# Case report: Pheochromocytoma-induced pseudo-Cushing's syndrome

Bobrowicz Małgorzata[1*†], Nagórska Anna[1†], Karpiłowska Anna[1], Rosłon Marek[1], Hubska Joanna[1,2], Gładka Adrianna[1], Toutounchi Sadegh[3], Koperski Łukasz[4] and Ambroziak Urszula[1]

[1]Department of Internal Medicine and Endocrinology, University Clinical Centre of the Medical University of Warsaw, Warsaw, Poland, [2]Doctoral School of Medical University of Warsaw, Warsaw, Poland, [3]Department of General, Endocrine, and Vascular Surgery, Medical University of Warsaw, Warsaw, Poland, [4]Department of Pathology, Medical University of Warsaw, Warsaw, Poland

Non-neoplastic hypercortisolaemia, also known as pseudo-Cushing's syndrome (PCS), is a physiological overactivation of the hypothalamic–pituitary–adrenal axis that can be triggered by conditions such as depression, eating disorders, extreme exercise, obesity, alcoholism, poorly controlled diabetes, chronic kidney disease, and cachexia. Here, we describe an unusual case of pheochromocytoma-induced PCS. A 66-year-old woman was referred to the hospital due to pronounced weakness, loss of appetite, apathy, weight loss, newly diagnosed diabetes mellitus, and poorly controlled hypertension. The biochemical evaluation suggested ACTH-dependent hypercortisolemia with severe hypokalemia, metabolic alkalosis, and hyperglycemia. Markedly elevated levels of metanephrines, along with imaging showing a heterogeneous adrenal lesion, provided evidence for pheochromocytoma. Considering the clinical features and the results of laboratory and imaging tests, there was a suspicion of hypercortisolemia due to ectopic ACTH secretion by a pheochromocytoma. The patient underwent adrenalectomy following pre-treatment with doxazosin and metyrapone, enteral feeding, protein supplementation, and insulin administration. Post-surgery, the patient did not require further antidiabetic medication, experienced gradual weight gain, improved well-being, and did not need glucocorticoid supplementation. Histopathological examination confirmed a pheochromocytoma; however, both anti-ACTH and anti-CRH stainings were negative, leading to a diagnosis of PCS. This case highlights the distinctive presentation of PCS caused by pheochromocytoma, as demonstrated through clinical, laboratory, and histopathological findings, and emphasizes the successful resolution achieved through adrenalectomy and supportive care.

KEYWORDS

**pseudo-Cushing's syndrome, ectopic ACTH secretion, hypercortisolaemia, pheochromocytoma, cachexia**

## Introduction

Pseudo-Cushing's syndrome (PCS), also referred to as non-neoplastic hypercortisolism, results from the physiological overactivity of the hypothalamic-pituitary-adrenal (HPA) axis (1). PCS can be triggered by conditions such as depression, eating disorders, severe physical stress, obesity, insulin resistance, chronic kidney disease, and chronic alcoholism (2). Although the clinical manifestations of PCS may vary between patients, it is generally accepted that their onset is rather slow (3). Importantly, the differentiation between PCS and CS is a diagnostic challenge even for experts in the field (4).

The mechanisms contributing to overactivation of the HPA axis have been elegantly reviewed by Scaroni et al. (5). Briefly, lower levels of cortisol-deactivating enzymes 5-α-reductase and 11β-hydroxysteroid dehydrogenase type 2 have been reported in patients with neurophychiatric disorders, reduced cortisol clearance, accompanied by changes in the affinity of cortisol to corticosteroid-binding globulin, elevation of corticotropic hormone (CRH) levels with resistance to glucocorticoids in patients with eating disorders, and increased secretion of CRH and increased activity of 11-βHSD type 1 in obese and alcohol-dependent individuals. PCS related to severe malnutrition has been rarely reported (6, 7).

Distinguishing PCS from Cushing syndrome (CS), including ectopic ACTH secretion (EAS), can be difficult due to their similar clinical and biochemical presentations (8). Hence, appropriate diagnosis is crucial to implement relevant treatment. Accurate decisions reduce the mortality risk associated with hypercortisolemia and preserve patient from the risk and complications associated with unnecessary procedures.

EAS is a paraneoplastic syndrome responsible for 10-20% of all cases of CS. CRH secretion by the tumor as well as CRH and ACTH co-secretion have been reported incidentally (2). It is estimated that 70% of EAS cases arise from chest tumors, with small-cell carcinomas and bronchial carcinoids being the most frequent. The other 10% to 15% are attributed to neuroendocrine tumors of the pancreas, while other rare sources include medullary thyroid cancer, pheochromocytoma, and others (9). The molecular mechanisms leading to EAS, as well as other small molecule compounds in paraneoplastic symptoms, are not fully understood (10). To date, epigenetic mechanisms, especially POMC promoter hypomethylation, have been reported in some EAS-inducing tumors (11, 12). Additionally, tumor-specific expression of transcription factors favoring ACTH production has been suggested (13, 14).

The clinical picture of EAS is heterogeneous and depends of the original cause (15). In general, two phenotypes of EAS can be observed: one associated with overt, mostly incurable malignancies, exemplified by small-cell lung cancer (SCLC), and the other associated with occult neoplasm, represented by bronchial carcinoma. While the first group is characterized with an atypical presentation dominated by muscle wasting, malignancy-induced weight loss and electrolyte and metabolic abnormalities, hyperpigmentation and rapid onset of symptoms (3-6 months), the second group exhibits characteristics of overt CS, a more slow (>6 months) development of symptomatic disease that needs to be differentiated with Cushing disease (16).

Pheochromocytomas account for approximately 5% of EAS cases (17). Extremely rare CRH-secreting pheochromocytomas leading to ectopic CS have also been reported (18). A meta-analysis by Elliot et al. (18) revealed that the vast majority (89%) of patients with ACTH-secreting or CRH-secreting pheochromocytomas presented with the characteristic cushingoid phenotype with moderate or severe hypercortisolism. Hypokalemia in these patients was more common than in patients with pituitary-dependent CS, and the degree of hypertension was more severe than in the general population of patients with pheochromocytoma as well as in patients with EAS due to other types of tumors. The frequency of diabetes (54%) almost doubled the rate reported in the general population of pheochromocytoma patients (18). Interestingly, Terzolo et al. (19) reported a case of cyclic CS in a woman with ACTH-secreting pheochromocytoma, suggesting a complexity of possible manifestations in EAS.

While ACTH-dependent hypercortisolemia in patients with pheochromocytoma is very likely caused by EAS or a coexistence of corticotroph adenoma, the possibility of PCS also has to be taken into consideration in the differential diagnosis. Herein, we present a unique case of pheochromocytoma-induced PCS evidenced by clinical, laboratory, and histopathological findings, and underscore the successful resolution through adrenalectomy and supportive care.

## Case report

A 66-year-old woman was admitted to the county hospital due to pronounced weakness, loss of appetite, apathy, and a weight loss of 5 kg within one month, along with newly diagnosed diabetes mellitus and hypertension. The patient had a history of spells; she reported high blood pressure accompanied by heart palpitations and headaches. Due to rapid weight loss, and a suspicion of malignancy, chest and abdominal computed tomography (CT) was performed. The CT revealed a heterogeneous, well-demarcated litho-cystic lesion (32x25 mm) in the right adrenal gland with inhomogeneous contrast enhancement (Figure 1A). Hormonal results suggested ACTH-dependent hypercortisolemia with ACTH of 535 pg/ml, morning cortisol of 94 μg/dl, and evening cortisol of 85 μg/dl. Persistent hypokalemia (serum potassium of 2 mmol/l) was observed. Due to these multiple abnormalities, the patient was referred to the endocrine department for further diagnosis and treatment.

On admission to the clinic, the patient was in a severe general condition, recumbent, and cachectic (body weight of 35 kg; body mass index 15.6 kg/m$^2$). She presented with impaired consciousness and a labile mood. Blood pressure was borderline (138/80 mmHg), and tachycardia (heart rate of 120 beats per minute) was observed. Apart from slight redness of the skin of the face and neckline (plethora), no other phenotypic features of hypercortisolemia were noted. Laboratory tests confirmed ACTH-dependent hypercortisolemia with a high plasma ACTH level, high plasma

10.3389/fendo.2024.1491873

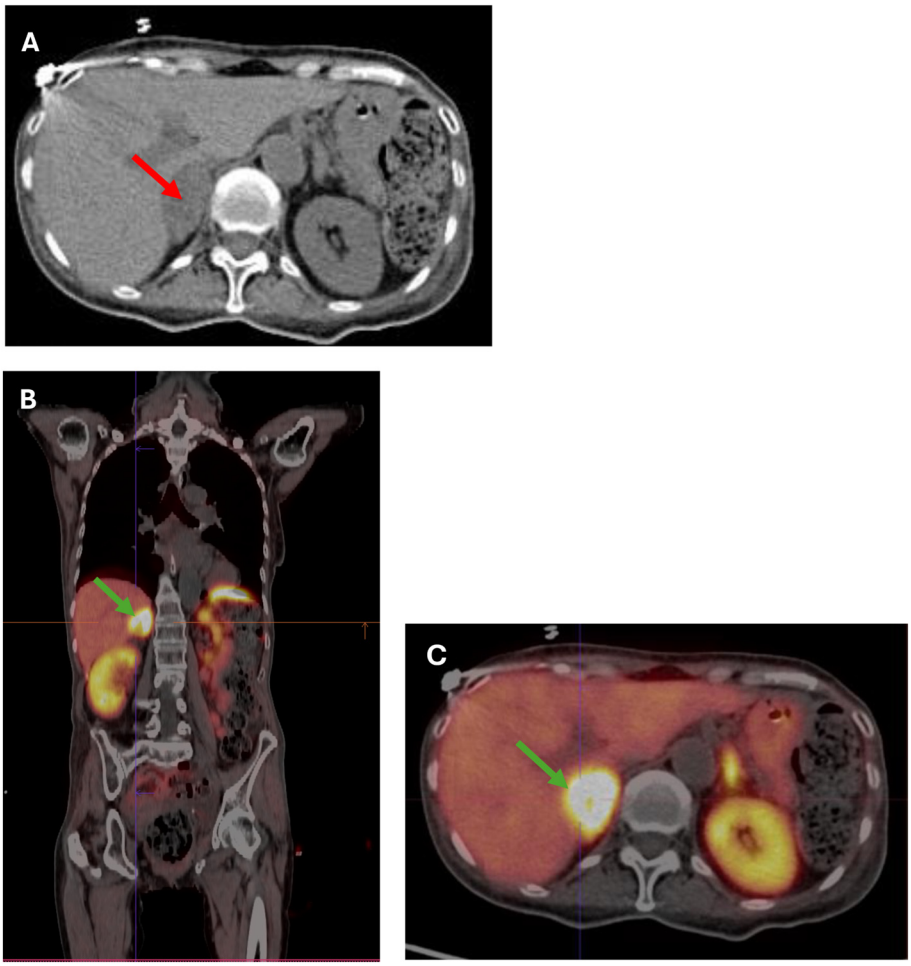


FIGURE 1
**(A)** CT scan showing a 32x35 mm heterogeneous, well-demarcated litho-cystic lesion (red arrow) in the right adrenal gland. **(B, C) (B)** Whole-body [68Ga] DOTATATE PET-CT image showing a hypodense right adrenal nodule measuring 36x22 mm (SUV max 35.4) (green arrow).
**(C)** Cross-section [68Ga]Ga-DOTA-TATE PET/CT image showing a hypodense right adrenal nodule 36x22 mm (SUV max 35.4) (green arrow).

cortisol levels with loss of diurnal rhythm, elevated 24-hour urinary free cortisol excretion, high plasma dehydroepiandrosterone sulfate (DHEA-S) and testosterone levels, and significantly elevated levels of serum metanephrines (Table 1).

TABLE 1 Hormonal workup at diagnosis.

| Parameter | Value | Reference range |
|---|---|---|
| ACTH | 476.00 | 7.20-63.30 pg/ml |
| Morning plasma cortisol | 125.00 | 4.82-19.50 ug/dl |
| Midnight plasma cortisol | 137.00 | <1.8 ug/dl |
| Urinary free cortisol | >239 | 4.30-176.00 ug/dl |
| DHEAS | 337.00 | 9.40-246.00 ug/dl |
| Testosterone | 6.19 | 0.10-1.42 ug/dl |
| Metanephrine | 1194.23 | <88.00 pg/ml |
| Normetanephrine | 965.94 | <200.00 pg/ml |
| 3-metoxythyramine | 52.27 | <17.00 pg/ml |

In the initial differential diagnosis, the coexistence of pheochromocytoma with ACTH-dependent hypercortisolemia or ectopic ACTH production by pheochromocytoma was considered. Due to the possibility of a pituitary tumor, an MRI was performed, showing no lesions in the pituitary gland. Subsequently, a [68Ga] DOTATE PET-CT scan was performed, which showed a hypodense right adrenal nodule measuring 36 x 22 mm, probably litho-fluidic with heterogeneous but high somatostatin receptor expression (SUV max 35.4) (Figures 1B, C).

Due to a strong suspicion of ACTH-producing pheochromocytoma, the patient was qualified for right adrenalectomy and prepared with increasing doses of doxazosin and a low dose of bisoprolol, potassium supplementation, parenteral hydration, protein supplementation, and intense insulin titration. The steroidogenesis inhibitor metyrapone (3x250 mg p.o. daily) was started, resulting in a rapid decrease in cortisol levels, leading to transient adrenal insufficiency requiring administration of 15 mg hydrocortisone daily (Figure 2). A rapid decrease in ACTH was observed already after first 24h of metyrapone (Figure 2) Intriguingly, a marked decrease in the

10.3389/fendo.2024.1491873

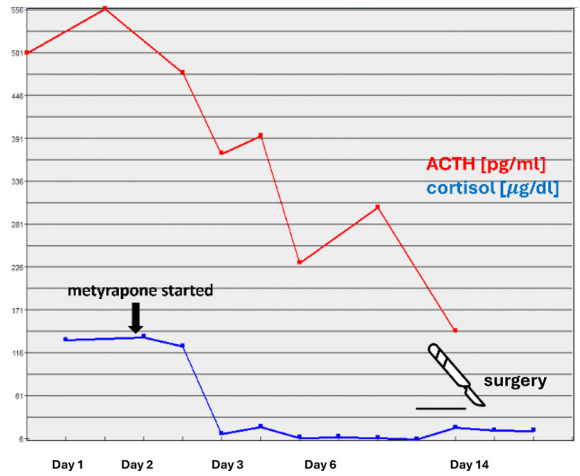


FIGURE 2
Serum levels of ACTH and cortisol following metyrapone administration.

levels of metanephrines (metanephrine to 749.35 pg/ml and normetanephrine to 593.55 pg/ml) was also observed after 12 days of metyrapone treatment.

After surgery, no clinical features nor laboratory results suggestive of adrenal insufficiency were observed (Table 2). In the 2-month period following adrenalectomy, the patient noted a gradual, slow increase in body weight (up to a BMI of 18.7 kg/m$^2$) and improvement in well-being. Diabetes resolved, and hypertension control was optimal with a single dose of bisoprolol. Normalization of the levels of metanephrines (Table 2) confirmed the complete resection of the pheochromocytoma. From the patient's perspective the patient feeled relieved after the resection of the tumor, she undergoes regular follow-up in the clinic where a constant improvement of her well-being and quality of life is observed.

The histopathological examination confirmed a diagnosis of pheochromocytoma, pT1 NX (according to AJCC, 8th ed.), PASS system - 3 points, GAPP system - 2 points (highly differentiated type). Immunohistochemistry (IHC) tests showed both negative anti-ACTH and anti-CRH stainings, thus the diagnosis of ectopic ACTH-dependent hypercortisolemia was finally rebutted (Figure 3). SDHB staining was focally positive with a weak cytoplasmic reaction (final status determination will be possible based on molecular/genetic tests). The rest of the excised adrenal did not show abnormalities, including the features of hyperplasia The patient was reluctant to perform further genetic investigations.

TABLE 2 Hormonal workup performed two months after adrenalectomy.

| Parameter | Value | Reference range |
|---|---|---|
| ACTH | 55 | 7.20-63.30 pg/ml |
| Morning plasma cortisol | 17.30 | 4.82-19.50 ug/dl |
| Midnight plasma cortisol | 5.98 | <1.8 ug/dl |
| DHEAS | 15.20 | 9.40-246.00 ug/dl |
| Testosterone | 0.11 | 0.10-1.42 ug/dl |
| Metanephrine | 18.99 | <88.00 pg/ml |
| Normetanephrine | 114.98 | <200.00 pg/ml |
| 3-metoxythyramine | <LOQ | <17.00 pg/ml |

Rapid resolution of symptoms and normalization of laboratory parameters, no apparent cushingoid features at the diagnosis, and no signs of adrenal insufficiency post-surgery, together with negative stainings for ACTH and CRH, allowed the final diagnosis of pheochromocytoma-induced PCS. Factors contributing to such intense manifestations of pheochromocytoma are yet to be identified.

## Discussion

To the best of our knowledge, no reports on PCS induced by pheochromocytoma have been published before. The presented case underscores the unique manifestation of these two coexisting conditions, evident through clinical, laboratory, and histopathological findings. It also highlights the successful resolution through adrenalectomy and supportive care.

On admission to the endocrine department, our patient presented with cachexia and no typical symptoms of CS despite significant hypercortisolemia. The reason for such a clinical picture was the chronic overproduction of catecholamines leading to a hypermetabolic state through multiple mechanisms. Hypermetabolism might be mediated directly by adrenoceptors in metabolically active organs and tissues, resulting in stimulation of lipolysis and glycogenolysis, and indirectly, through induction of inflammation, which is reflected by increased secretion of pro-inflammatory cytokines such as IL-1, IL-6, and TNF-α (20). In fact, increased resting energy expenditure (REE) measured by indirect calorimetry, accompanied by increased levels of pro-inflammatory cytokines, has been reported in a cohort of pheochromocytoma patients. Surgical treatment led to a decrease of REE to the expected calculated levels and normalization of some of the inflammation markers (20, 21). Moreover, catecholamines have been shown to activate brown adipose tissue, which was associated with decreased survival (22). Interestingly, a hypermetabolic phenotype of pheochromocytoma is more often reported in the elderly (23), and it can lead to cachexia (24), as in the described patient. In this case, we hypothesize that abundant and chronic secretion of catecholamines from the tumor led to a hypermetabolic and pro-inflammatory state that, in turn, overactivated the HPA axis (Figure 4). A rapid decrease in the level of cortisol, ACTH, and metanephrines upon initiation of metyrapone treatment suggests the existence of a glucocorticoid-dependent positive feedback loop that potentiated ACTH release and created a destructive cycle with rapid exacerbation of both hypercortisolemia and hypercatecholaminemia, with extremely elevated plasma ACTH levels. Metyrapone appeared to be clinically effective and resulted in lower levels of cortisol and catecholamines along with significantly lower levels of ACTH.

The biochemical picture of PCS may present as ACTH-dependent CS. It has been proposed that some diagnostic tests may

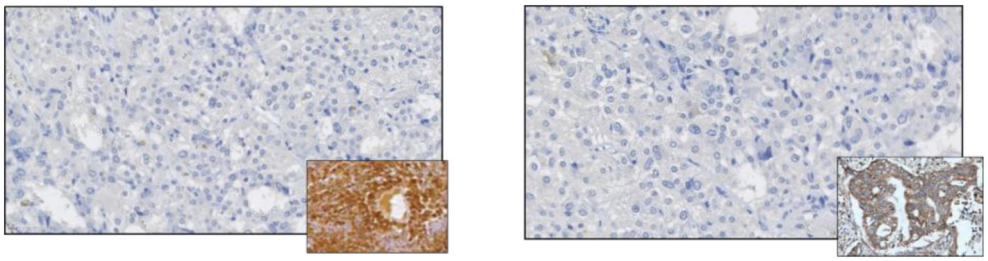

FIGURE 3
Negative immunostaining for ACTH (left panel) and negative immunostaining for CRH. Positive controls are shown in the miniatures.

facilitate distinguishing these two diagnoses (5); however, the diagnostic options are limited with no access to CRH. In the case presented here, no dynamic tests were performed due to the severity of the patient's condition. Some authors suggest that midnight cortisol serum levels above 7.5 µg/dL discriminate CS from PCS with 96% sensitivity and 100% specificity, as in PCS, an unaltered diurnal cortisol rhythm can be observed (25, 26). The disruption of the circadian rhythm of cortisol (and ACTH) is a distinguishing characteristic of CS, however, in our patient, the levels of midnight cortisol were highly elevated despite a lack of ACTH-positive cells in IHC and no other signs of CS. We did not find another case of pseudo-Cushing's in the literature in which midnight cortisol levels were as high or higher. Disruptions in this rhythm are linked to a wide variety of psychological and physical conditions, such as depression (2), cognitive impairments (27), post-traumatic stress disorder (28), chronic stress (29), burnout (30), chronic fatigue syndrome (31), and anorexia nervosa (32). Upon admission, our patient was in a severe mental state due to discomfort, anxiety, and stress related to hospitalization. It is plausible that psychological factors, combined with cachexia, contributed to the disturbances in nocturnal cortisol secretion. There are no algorithms concerning the treatment of PCS, as cortisol levels are usually normalized following the resolution of the underlying cause. So far, only a few reports address the role of steroidogenesis inhibitors in lowering cortisol and contributing to recovery (6, 33). Our case demonstrates the successful resolution of hypercortisolemia before surgery by the administration of metyrapone. The importance of therapy with steroidogenesis inhibitors lies in their ability to prevent metabolic complications and eliminate glucocorticoid-induced immunosuppression.

## Conclusions

The biochemical picture of PCS may present as ACTH dependent CS. Differentiation of PCS from other causes of hypercortisolemia poses a clinical challenge. Non-neoplastic hypercortisolemia occurs as a response to severe disorders and should always be considered in case of atypical course of hypercortisolemia. Metyrapone might be effective to block the glucocorticoid-dependent positive-feedback loop and minimalize the levels of cortisol, catecholamines, along with ACTH, thus it can reduce the perioperative risk.

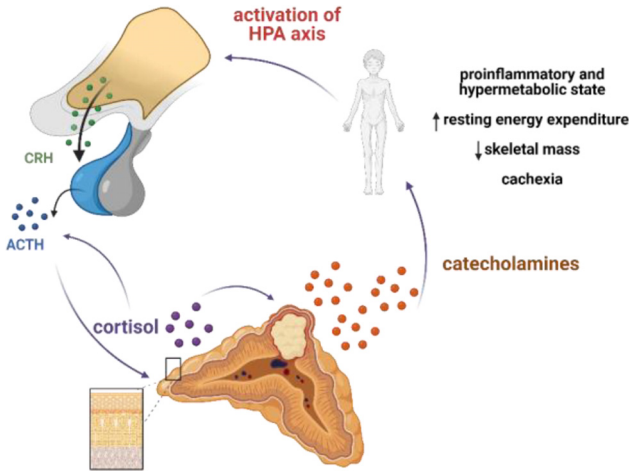


FIGURE 4
Postulated mechanism of pseudo-Cushing syndrome in our patient. Abundant and chronic secretion of catecholamines leads to hypermetabolic and proinflammatory state that in turn activates HPA axis. Cortisol may potentiate the secretion of catecholamines by increasing the expression of thyrosine hydroxylase (TH), a rate-limiting enzyme in the catecholamine synthesis pathway; and phenylethanolamine N-methyltransferase, a key enzyme in noradrenaline-to-adrenaline conversion. A glucocorticoid-dependent positive-feedback loop may potentiate ACTH release. Created with BioRender.

## Data availability statement

The original contributions presented in the study are included in the article/supplementary material. Further inquiries can be directed to the corresponding author.

## Ethics statement

Written informed consent was obtained from the individual(s) for the publication of any potentially identifiable images or data included in this article.

## Author contributions

BM: Investigation, Writing – original draft. NA: Investigation, Writing – review & editing. KA: Investigation, Writing – review & editing. RM: Conceptualization, Investigation, Writing – review & editing. HJ: Writing – review & editing. GA: Investigation, Writing – review & editing. TS: Investigation, Writing – review & editing. KL: Investigation, Writing – review & editing. AU: Conceptualization, Investigation, Methodology, Writing – review & editing.

## Funding

The author(s) declare that no financial support was received for the research, authorship, and/or publication of this article.

## Conflict of interest

The authors declare that the research was conducted in the absence of any commercial or financial relationships that could be construed as a potential conflict of interest.

## Publisher's note

All claims expressed in this article are solely those of the authors and do not necessarily represent those of their affiliated organizations, or those of the publisher, the editors and the reviewers. Any product that may be evaluated in this article, or claim that may be made by its manufacturer, is not guaranteed or endorsed by the publisher.

## References

1. Tsigos C, Chrousos GP. Hypothalamic-pituitary-adrenal axis, neuroendocrine factors and stress. *J Psychosom Res*. (2002) 53:865–71. doi: 10.1016/S0022-3999(02)00429-4

2. Newell-Price J, Trainer P, Besser M, Grossman A. The diagnosis and differential diagnosis of Cushing's syndrome and pseudo-Cushing's states. *Endocr Rev*. (1998) 19:647–72. doi: 10.1210/edrv.19.5.0346

3. Pecori Giraldi F. PseudoCushing: why a clinical challenge? *J Endocrinol Invest*. (2015) 38:1137–9. doi: 10.1007/s40618-015-0296-5

4. Pecori Giraldi F, Ambrogio AG. Pseudo-Cushing - A clinical challenge? *Front Hormone Res*. (2016) 46:1–14. doi: 10.1159/000443857

5. Scaroni C, Albiger NM, Palmieri S, Iacuaniello D, Graziadio C, Damiani L, et al. Approach to patients with pseudo-Cushing's states. *Endocr Connect*. (2019) 9:R1–13. doi: 10.1530/EC-19-0435

6. Park Y-A, Gao F, Sim I-W, Gilfillan C. Pseudo-Cushing syndrome with an atypically high cortisol burden and clinical improvement with adrenal enzyme inhibitor. *JCEM Case Rep*. (2023) 1:luad075. doi: 10.1210/jcemcr/luad075

7. Pulipati VP, Hwang J. SUN-205 pseudo-Cushing syndrome secondary to malnutrition and gluco-toxicity mimicking type 1 diabetes mellitus. *J Endocr Soc*. (2020) 4:SUN–205. doi: 10.1210/jendso/bvaa046.343

8. Chabre O. The difficulties of pseudo-Cushing's syndrome (or 'non-neoplastic hypercortisolism'). *Ann Endocrinol (Paris)*. (2018) 79:138–45. doi: 10.1016/j.ando.2018.04.017

9. Young J, Haissaguerre M, Viera-Pinto O, Chabre O, Baudin E, Tabarin A. MANAGEMENT OF ENDOCRINE DISEASE: Cushing's syndrome due to ectopic ACTH secretion: an expert operational opinion. *Eur J Endocrinol*. (2020) 182:R29–58. doi: 10.1530/EJE-19-0877

10. Dimitriadis GK, Angelousi A, Weickert MO, Randeva HS, Kaltsas G, Grossman A. Paraneoplastic endocrine syndromes. *Endocr Relat Cancer*. (2017) 24(6):R173–90. doi: 10.1530/ERC-17-0036

11. Ye L, Li X, Kong X, Wang W, Bi Y, Hu L, et al. Hypomethylation in the promoter region of POMC gene correlates with ectopic overexpression in thymic carcinoids. *J Endocrinol*. (2005) 185:337–43. doi: 10.1677/joe.1.05963

12. Newell-Price J. Proopiomelanocortin gene expression and DNA methylation: implications for Cushing's syndrome and beyond. *J Endocrinol*. (2003) 177:365–72. doi: 10.1677/joe.0.1770365

13. Uccella S, Leoni E, Kaiser S, Maragliano R, Valerio A, Libera L, et al. Heterogeneity of TPIT expression in ACTH-secreting extra-pituitary neuroendocrine tumors (NETs) supports the existence of different cellular programs in pancreatic and pulmonary NETs. *Virchows Arch*. (2023) 483:635–43. doi: 10.1007/s00428-023-03642-2

14. Araki T, Liu N, Tone Y, Cuevas-Ramos D, Heltsley R, Tone M, et al. E2F1-mediated human POMC expression in ectopic Cushing's syndrome. *Endocr Relat Cancer*. (2016) 23:857–70. doi: 10.1530/ERC-16-0206

15. Terzolo M, Reimondo G, Alì A, Bovio S, Daffara F, Paccotti P, et al. Ectopic ACTH syndrome: molecular bases and clinical heterogeneity. *Ann Oncol*. (2001) 12 Suppl:2, S83–87. doi: 10.1093/annonc/12.suppl_2.S83

16. Ragnarsson O, Juhlin CC, Torpy DJ, Falhammar H. A clinical perspective on ectopic Cushing's syndrome. *Trends Endocrinol Metab*. (2024) 35:347–60. doi: 10.1016/j.tem.2023.12.003

17. Ballav C, Naziat A, Mihai R, Karavitaki N, Ansorge O, Grossman AB. Mini-review: pheochromocytomas causing the ectopic ACTH syndrome. *Endocrine*. (2012) 42:69–73. doi: 10.1007/s12020-012-9646-7

18. Elliott PF, Berhane T, Ragnarsson O, Falhammar H. Ectopic ACTH- and/or CRH-producing pheochromocytomas. *J Clin Endocrinol Metab*. (2021) 106:598–608. doi: 10.1210/clinem/dgaa488

19. Terzolo M, Alì A, Pia A, Bollito E, Reimondo G, Paccotti P, et al. Cyclic Cushing's syndrome due to ectopic ACTH secretion by an adrenal pheochromocytoma. *J Endocrinol Invest*. (1994) 17:869–74. doi: 10.1007/BF03347794

20. Petrák O, Haluzíková D, Kaválková P, Štrauch B, Rosa J, Holaj R, et al. Changes in energy metabolism in pheochromocytoma. *J Clin Endocrinol Metab*. (2013) 98:1651–8. doi: 10.1210/jc.2012-3625

21. Bosanska L, Petrak O, Zelinka T, Mraz M, Widimsky J Jr, Haluzik M. The effect of pheochromocytoma treatment on subclinical inflammation and endocrine function of adipose tissue. *Physiol Res*. (2009) 58:319–25. doi: 10.33549/physiolres

22. Abdul Sater Z, Jha A, Hamimi A, Mandl A, Hartley IR, Gubbi S, et al. Pheochromocytoma and paraganglioma patients with poor survival often show brown adipose tissue activation. *J Clin Endocrinol Metab*. (2020) 105:1176–85. doi: 10.1210/clinem/dgz314

23. Petrák O, Haluzíková D, Klímová J, Zítek M, Holaj R, Michalský D, et al. Hypermetabolism and substrate utilization rates in pheochromocytoma and functional paraganglioma. *Biomedicines*. (2022) 10:1980. doi: 10.3390/biomedicines10081980

24. Nkodo A, Wu I, Hobgood S, Celi FS. Unexplained cachexia as a presenting symptom of pheochromocytoma in a geriatric patient. *JCEM Case Rep*. (2023) 1:luad037. doi: 10.1210/jcemcr/luad037

25. Alwani RA, Schmit Jongbloed LW, de Jong FH, van der Lely AJ, de Herder WW, Feelders RA. Differentiating between Cushing's disease and pseudo-Cushing's

syndrome: comparison of four tests. *Eur J Endocrinol*. (2014) 170:477–86. doi: 10.1530/EJE-13-0702

26. Papanicolaou DA, Yanovski JA, Cutler GB Jr., Chrousos GP. amp]]amp; Nieman, L. K. A single midnight serum cortisol measurement distinguishes Cushing's syndrome from pseudo-Cushing states1. *J Clin Endocrinol Metab*. (1998) 83:1163–7. doi: 10.1210/jcem.83.4.4681

27. Lupien SJ, McEwen BS, Gunnar MR, Heim C. Effects of stress throughout the lifespan on the brain, behaviour and cognition. *Nat Rev Neurosci*. (2009) 10:434–45. doi: 10.1038/nrn2639

28. Yehuda R, Teicher MH, Trestman RL, Levengood RA, Siever LJ. Cortisol regulation in posttraumatic stress disorder and major depression: a chronobiological analysis. *Biol Psychiatry*. (1996) 40:79–88. doi: 10.1016/0006-3223(95)00451-3

29. Ge M E, C, Es Z. If it goes up, must it come down? Chronic stress and the hypothalamic-pituitary-adrenocortical axis in humans. *psychol Bull*. (2007) 133:25–45. doi: 10.1037/0033-2909.133.1.25

30. Pruessner JC, Hellhammer DH, Kirschbaum C. Low self-esteem, induced failure and the adrenocortical stress response. *Pers Individ Dif*. (1999) 27:477–89. doi: 10.1016/S0191-8869(98)00256-6

31. Nater UM, Maloney E, Boneva RS, Gurbaxani BM, Lin JM, Jones JF, et al. Attenuated morning salivary cortisol concentrations in a population-based study of persons with chronic fatigue syndrome and well controls. *J Clin Endocrinol Metab*. (2008) 93:703–9. doi: 10.1210/jc.2007-1747

32. dos Santos E, dos Santos JE, Ribeiro RP, Rosa E, Silva AC, Moreira AC, et al. Absence of circadian salivary cortisol rhythm in women with anorexia nervosa. *J Pediatr Adolesc Gynecol*. (2007) 20:13–8. doi: 10.1016/j.jpag.2006.10.011

33. Inoue M, Okamura K, Kitaoka C, Kinoshita F, Namitome R, Nakamura U, et al. Metyrapone-responsive ectopic ACTH-secreting pheochromocytoma with a vicious cycle via a glucocorticoid-driven positive-feedback mechanism. *Endocr J*. (2018) 65:755–67. doi: 10.1507/endocrj.EJ18-0025

frontiers | Frontiers in Endocrinology

TYPE Case Report
PUBLISHED 18 December 2024
DOI 10.3389/fendo.2024.1483516

Check for updates

OPEN ACCESS

EDITED BY
Ichiro Abe,
Fukuoka University Chikushi Hospital, Japan

REVIEWED BY
Yuto Yamazaki,
Tohoku University, Japan
Tetsuro Tsumura,
Daido Hospital, Japan

*CORRESPONDENCE
Dan Cao
caodan@scu.edu.cn
Ke Cheng
183818128@qq.com

†These authors have contributed equally to this work

RECEIVED 28 October 2024
ACCEPTED 04 December 2024
PUBLISHED 18 December 2024

CITATION
Zhang C, Wei Y, Cheng K and Cao D (2024) Durable and deep response to CVD chemotherapy in SDHB-mutated metastatic paraganglioma: case report.
*Front. Endocrinol.* 15:1483516.
doi: 10.3389/fendo.2024.1483516

COPYRIGHT
© 2024 Zhang, Wei, Cheng and Cao. This is an open-access article distributed under the terms of the Creative Commons Attribution License (CC BY). The use, distribution or reproduction in other forums is permitted, provided the original author(s) and the copyright owner(s) are credited and that the original publication in this journal is cited, in accordance with accepted academic practice. No use, distribution or reproduction is permitted which does not comply with these terms.

# Durable and deep response to CVD chemotherapy in SDHB-mutated metastatic paraganglioma: case report

Chenyan Zhang†, Yuanfeng Wei†, Ke Cheng* and Dan Cao*

Division of Abdominal Tumor, Department of Medical Oncology, Cancer Center and State Key Laboratory of Biological Therapy, West China Hospital, Sichuan University, Chengdu, Sichuan, China

**Introduction:** Succinate dehydrogenase subunit B (SDHB)-mutated paragangliomas (PGLs) are rare neuroendocrine tumors characterized by increased malignancy, readily metastasizing, and poorer prognosis. Here we report a case of SDHB-mutated metastatic PGL, wherein the patient showed significant tumor shrinkage and complete symptom remission following chemotherapy. We aim to contribute additional evidence to the existing knowledge associated with SDHB-mutated PGLs.

**Case report:** A 40-year-old male patient presented with recurrent hypoglycemia and hypertension crisis. Imaging revealed a huge left retroperitoneal tumor and multiple diffuse metastases in lungs. Catecholamine was also elevated, aligning with a diagnosis of metastatic PGL. Pathology also confirmed this diagnosis. Additionally, the immunohistochemistry indicated negative expression of SDHB and gene test showed somatic SDHB mutation. Given the SDHB mutation, cyclophosphamide-vincristine-dacarbazine (CVD) chemotherapy was initiated in critical conditions. Subsequently, a significant tumor shrinkage and complete biochemical response were observed after two treatment cycles. In September 2024, CT scan revealed new pulmonary lesions. The progression-free survival (PFS) with CVD chemotherapy was 24 months.

**Conclusion:** This report reviews the distinct clinical and biochemical characteristics and treatment approaches of SDHB-mutated paragangliomas, emphasizing that the significance of incorporating both genetic testing and immunohistochemical analysis in clinical practice.

KEYWORDS

**SDHB-mutation, metastatic paraganglioma, CVD chemotherapy, case report, hypoglycemia**

## Introduction

Paragangliomas (PGLs) are rare neuroendocrine tumors with high heritability (1). Around half of PGLs are linked to mutations in succinate dehydrogenase subunit x (SDHx) genes (2, 3). Among these, SDHB mutations are the most common (1). SDHB-mutated PGLs present distinct clinical and biochemical features that may guide personalized therapy (1, 4–6). Here, we report a case of SDHB-mutated metastatic PGL, demonstrating significant tumor shrinkage and complete symptom remission following cyclophosphamide-vincristine-dacarbazine (CVD) chemotherapy. This case aims to contribute further evidence to the understanding of SDHB-mutated PGLs.

## Case presentation

In August 2022, a 40-year-old male Asian patient, presented at the emergency department with syncope, diaphoresis, sialorrhea, absence of tic, and urinary and fecal incontinence. He displayed facial edema, a heart rate of 98 beats per minute (bpm), a blood pressure of 193/114 mm Hg, a respiratory rate of 20 breaths per minute, a body mass index of 24.2 kg/m$^2$, and an Eastern Cooperative Oncology Group (ECOG) score of 2. 1 hours later, he gradually regained consciousness. Approximately 7 months prior to this event, he began experiencing recurring hypoglycemia at night. Over the preceding six months, he suffered recurrent headaches and his self-measured systolic blood pressure at onset exceeded 180 mmHg. Besides, there is no significant medical, familial, or psychosocial history.

Routine blood tests, liver and kidney function assessments, ECG, and cranial CT scans revealed no abnormalities. Serum levels of insulin, C-peptide, insulin-like growth factor I (IGF-I), and growth hormone (GH) were normal when blood glucose was 1.5 mmol/L (Table 1). However, thorax-abdomen CT identified a 14.1×9.7 cm left retroperitoneal mass and multiple pulmonary lesions (Figures 1A, D, G, J). Catecholamine, ACTH, and NSE levels were elevated (Table 1), aligning with a diagnosis of metastatic PGL. Although hyperglycemia is common in PPGL due to excessive catecholamine secretion, this patient experienced recurrent hypoglycemia, prompting us to further confirm the diagnosis through pathology. Additionally, imaging showed multiple lung metastases, ruling out curative surgery. Thus, the patient and family opted for a retroperitoneal lesion biopsy after discussing the biopsy risks. Fortunately, no adverse reactions occurred. Immunohistochemical analysis showed positive expression of Synaptophysin (Syn), Chromogranin A (CgA), and SSTR2, but negative for SDHB and S100 (Figure 2), with a Ki67 labeling index of 60%. Next-generation sequencing (NGS) revealed a somatic copy number loss of the SDHB gene. $^{68}$Ga-DOTATATE and $^{18}$F-FDG positron emission tomography (PET-CT) scans were conducted. The results revealed that the metastasis affected the lungs and skeletal sites, including the anterior segment of the left 7th rib, left scapula, and left humerus (Figure 3).

Despite 1 month of symptomatic therapies, including alpha blockade and intravenous fluid replacement, recurrent hypoglycemia and hypertensive crises persisted. The progression of the disease was presumed to be rapid based on the time when the patient became aware of symptoms. Given the patient's unresponsive state and the tumor's rapid growth, chemotherapy was initiated under critical conditions. A combination of cyclophosphamide (1300 mg, day 1, every 4 weeks), vincristine (2 mg, day 1, every 4 weeks), and dacarbazine (1000 mg, day 1-2, every 4 weeks) was started in September 2022.Surprisingly, a CT scan revealed significant regressions of the retroperitoneal mass and lung metastases (Figures 1B, E, H, K) after two treatment cycles. According to the Response Evaluation Criteria in Solid Tumors version 1.1 (RECIST 1.1), a partial response (PR) was achieved. Additionally, a completely

TABLE 1 Levels of serum insulin, C-peptide, IGF-I, GH and β-hydroxybutyrate during episode of hypoglycaemia.

| Test | Value | Normal range | Blood glucose level at the time of measurement | Collection time |
|---|---|---|---|---|
| Insulin | <0.4 | 1.5uU/ml at least | 1.5 mmol/L | during hypoglycaemia |
| C-peptide | 0.031 | 0.3-1.3 nmol/L | 1.5 mmol/L | during hypoglycaemia |
| IGF-I | 39.53 | 107-216 ng/ml | 1.5 mmol/L | during hypoglycaemia |
| Growth hormone (GH) | 0.34 | 0.030-2.47 ng/ml | 1.5 mmol/L | during hypoglycaemia |
| β-hydroxybutyrate | 0.05 | 0.02 - 0.27 mmol/L | 1.5 mmol/L | during hypoglycaemia |
| Norepinephrine | 10.23 | 0-5.17 nmol/L | N/D | morning |
| Normetanephrine | 12.86 | 0-0.71 nmol/L | N/D | morning |
| 3-mexoxytyramine | 25.83 | 0-18.4 pg/ml | N/D | morning |
| Epinephrine | 0.26 | 0-0.34 nmol/L | N/D | morning |
| Dopamine | 0.20 | 0-0.31 nmol/L | N/D | morning |
| ACTH | 110.70 | 5-78 ng/L | N/D | morning |
| Cortisol | 435.00 | 138-690 nmol/L | N/D | morning |
| NSE | 70.30 | 0-20.4 ng/ml | N/D | morning |

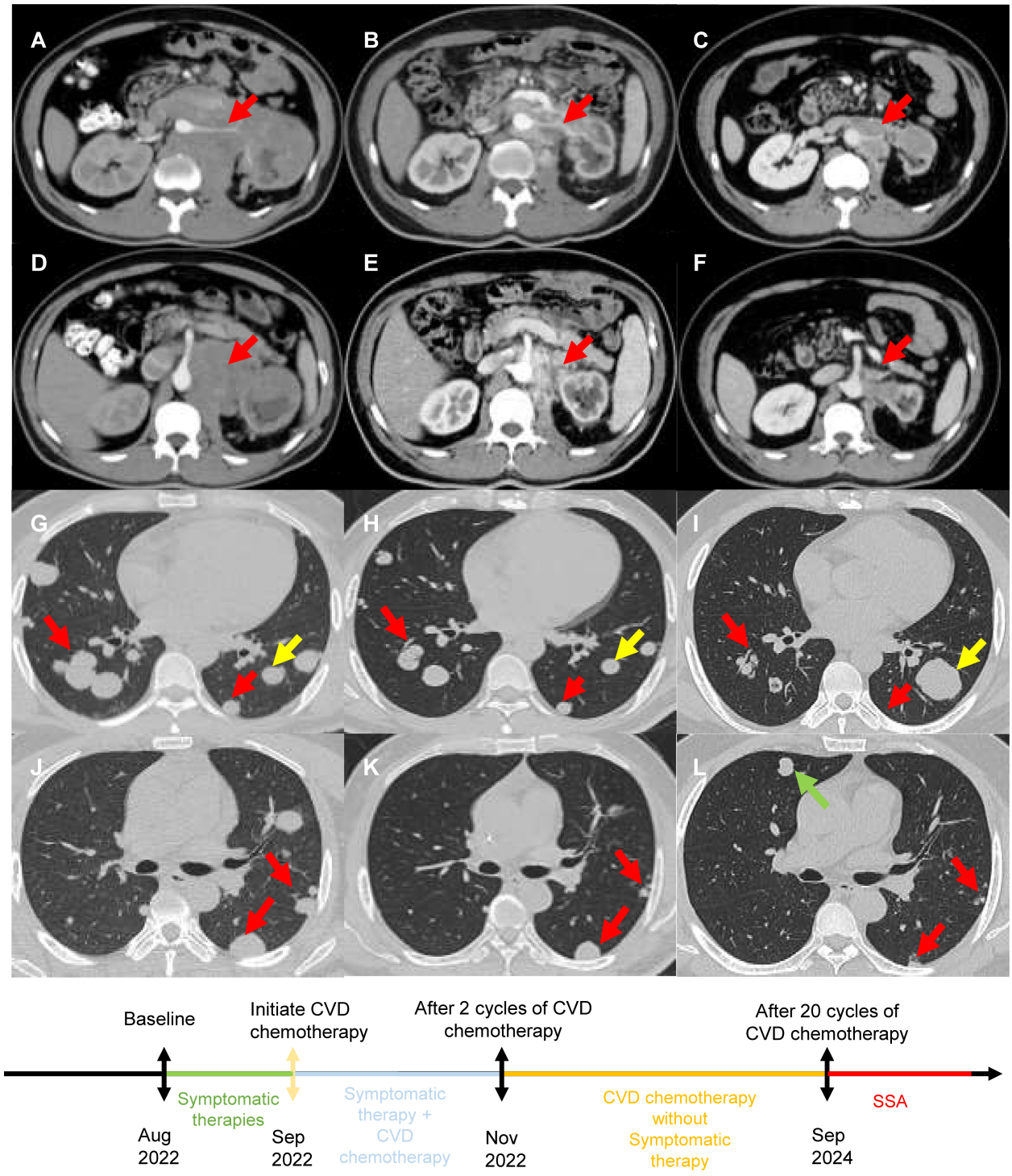


FIGURE 1
**(A, D, G, J)** Prior to CVD chemotherapy, CT revealed retroperitoneal lesions around the pancreas, liver, kidney and multiple diffuse lesions in both lungs. **(B, E, H, K)** After 2 cycles of CVD chemotherapy, CT revealed that retroperitoneal lesions around the pancreas, liver, kidney and multiple diffuse lesions in both lungs reduced in size. **(C, F, I, L)** After 20 cycles of CVD chemotherapy, CT revealed retroperitoneal lesions further reduced in size. Although a small amount of lung lesions enlarged and new lesions appeared, the majority of lung lesions reduced in number and size. [Red arrows indicate shrinking lesions, yellow arrows indicate enlarged lesions, and green arrows indicate new lesions.].

biochemical response with symptom remission was observed, allowing the cessation of symptomatic therapies (Supplementary Figure 1). NSE and catecholamine levels decreased concurrently (Supplementary Figure 1). In September 2024, CT scan revealed new pulmonary lesions and some lung lesion enlarged, suggesting disease progression. However, retroperitoneal lesions and the majority of lung lesions further reduced in size (Figures 1C, F, I, L). The progression-free survival (PFS) of CVD chemotherapy was 24

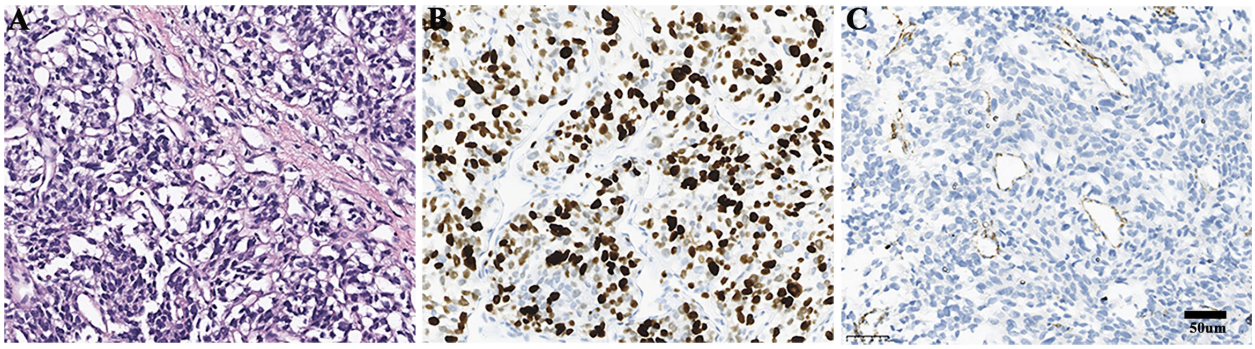


FIGURE 2
Pathological findings of the retroperitoneal lesion. **(A)** Haematoxylin and eosin staining. **(B)** Ki67 positive rate was 60%. **(C)** The expression of SDHB was negative.

months. Given the high SSTR expression, a switch to somatostatin analogue (SSA) therapy is recommended. The patient remains stable without symptoms or treatment-related adverse effects.

## Discussion

In this case, we report a 40-year-old male patient with SDHB-mutated metastatic PGL. A rapid, deep and durable PR, and complete biochemical response were achieved after CVD chemotherapy.

The prevalence of the SDHB mutated PGLs among Chinese patients has been well-documented (7, 8). Compared to others, PGL with SDHB mutation typically exhibit an early onset, noradrenergic or dopaminergic biochemical phenotype, and shorter survival (9, 10). Additionally, precision medicine can be tailored based on the SDHB mutation status. Several studies have proved that CVD chemotherapy was the first-line treatment for PGL individuals with SDHB-mutation (11, 12). Our case reaffirms above points.

Missense mutations and truncating mutations are the most commonly reported types of SDHB mutations in PGLs (13). Compared to missense mutations, truncating mutations in SDHB are typically associated with a higher malignancy potential in PPGLs (14). In our study, the patient had a SDHB mutation characterized by a copy

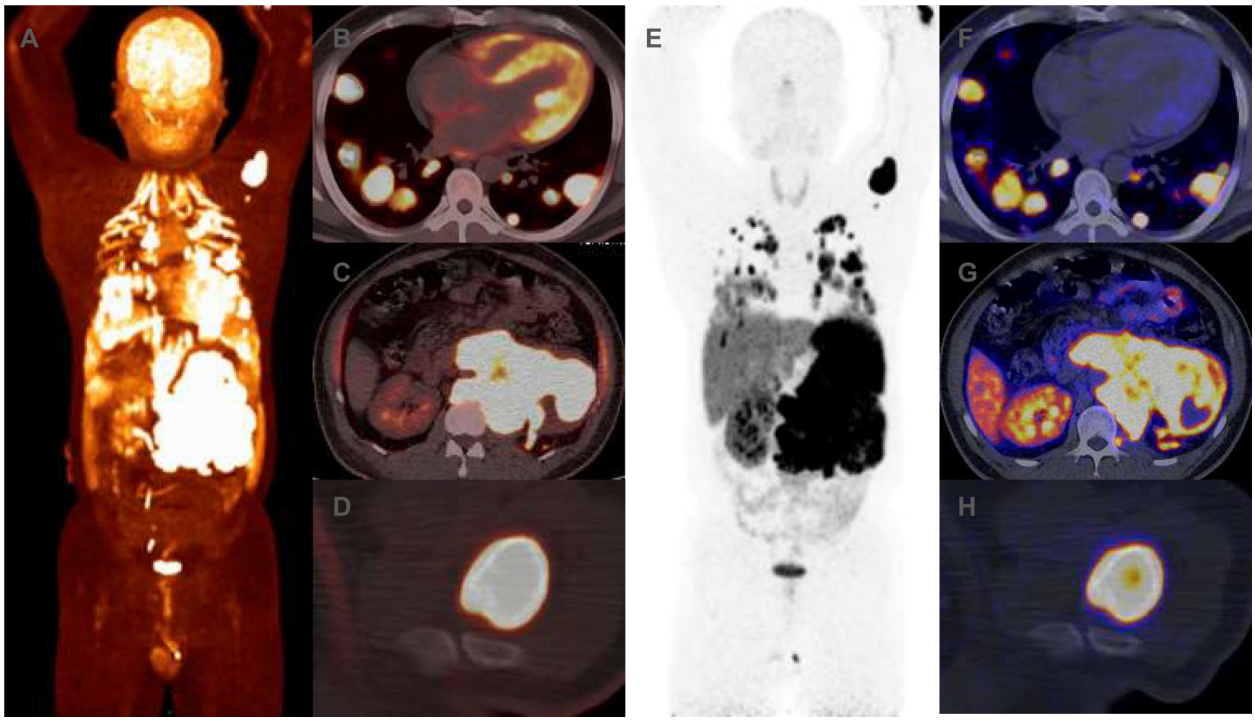


FIGURE 3
**(A–F)** Prior to CVD chemotherapy, 18F-FDG positron emission tomography (PET-CT) revealed increased uptake of 18F-FDG in the left retroperitoneal mass, lung masses and humeral head. The maximum cross-sectional area of the left retroperitoneal mass was approximately 166 × 99mm, with maximum SUV sizes of 21.49. **(G–L)** Prior to CVD chemotherapy, 68Ga-DOTATATE PET-CT revealed increase uptake of 68Ga-DOTATATE in the left retroperitoneal mass, lung masses and humeral head. The maximum SUV sizes of the left retroperitoneal mass was 36. 94.

number loss, a mutation type that has not been widely reported in previous studies. While missense mutations and truncating mutations often lead to a complete loss of the biological function of key proteins, copy number loss typically results in a reduction in gene expression, causing partial functional loss. Whether this mutation type is associated with a better prognosis in patients remains to be confirmed through large-scale clinical studies.

Notably, SDHB mutation differs from the negative immunohistochemical expression of SDHB (15). Consequently, the lack of immunohistochemical expression of SDHB is often utilized as an alternative marker in assessing SDHx gene mutations (15–21). This approach is not only cost-effective but also aids in identifying false negative results from genetic testing. However, we believe that the negative immunohistochemical expression of SDHB cannot replace next-generation sequencing. Many studies have shown that different mutations in the SDHx gene often exhibit different clinical manifestations, which are of great significance for the prognosis and treatment of patients (22, 23). Therefore, we emphasize the significance of incorporating both genetic testing and immunohistochemical analysis in clinical practice for precise diagnosis and prognosis.

Due to the hyperglycemic effect of catecholamines, hypoglycemia directly induced by PGLs is exceedingly rare. We reviewed related profiles and concluded four mechanisms to identify the mechanisms underlying this hypoglycemia (Supplementary Table S1) (24–33). Firstly, tumor autoimmune hypoglycemia, often associated with myeloma and Hodgkin's disease (34, 35). Secondly, liver, adrenal, or pituitary insufficiency also can contribute to hypoglycemia. Thirdly, a massive tumor burden may lead to rapid glucose consumption and subsequent hypoglycemia (29). Furthermore, the production of hypoglycemic substances by tumor, such as IGF-II, IGF-I and GH, can cause hypoglycemia (36). In our case, tumor- autoimmune hypoglycemia antibodies, liver function, adrenal function, and pituitary function were all normal, thus excluding the first two mechanisms. Given the patient's high tumor burden and the improvement of hypoglycemia as the tumor shrank, the latter two mechanisms were assumed to be involved. Rapidly growing tumors consume glucose and release hypoglycemic substances, causing the rare complication of hypoglycemia. However, due to technical limitations and our current understanding, we unfortunately did not measure serum IGF-II levels during hypoglycemia. Therefore, we can only speculate that the causes of this hypoglycemia are likely multifactorial.

## Conclusion

This study presents a rare case of SDHB-mutated metastatic PGLs, demonstrating a rapid, deep and durable response to CVD chemotherapy. It underscored the critical role of SDHB mutations in influencing both prognosis and treatment selection for PGLs.

## Data availability statement

The raw data supporting the conclusions of this article will be made available by the authors, without undue reservation.

## Ethics statement

The studies involving humans were approved by Ethics Committee on Biomedical Research, West China Hospital of Sichuan University. The studies were conducted in accordance with the local legislation and institutional requirements. Written informed consent was obtained from the participant/patient(s) for the publication of this case report.

## Author contributions

CZ: Writing – review & editing, Writing – original draft. YW: Writing – review & editing. KC: Visualization, Methodology, Funding acquisition, Writing – review & editing, Resources. DC: Supervision, Funding acquisition, Writing – review & editing, Resources, Conceptualization, Data curation.

## Funding

The author(s) declare that no financial support was received for the research, authorship, and/or publication of this article.

## Conflict of interest

The authors declare that the research was conducted in the absence of any commercial or financial relationships that could be construed as a potential conflict of interest.

## Generative AI statement

The author(s) declare that no Generative AI was used in the creation of this manuscript.

## Publisher's note

All claims expressed in this article are solely those of the authors and do not necessarily represent those of their affiliated organizations, or those of the publisher, the editors and the reviewers. Any product that may be evaluated in this article, or claim that may be made by its manufacturer, is not guaranteed or endorsed by the publisher.

## Supplementary material

The Supplementary Material for this article can be found online at: https://www.frontiersin.org/articles/10.3389/fendo.2024.1483516/full#supplementary-material

# References

1. Buffet A, Burnichon N, Favier J, Gimenez-Roqueplo AP. An overview of 20 years of genetic studies in pheochromocytoma and paraganglioma. *Best Pract Res Clin Endocrinol Metab*. (2020) 34:101416. doi: 10.1016/j.beem.2020.101416

2. Currás-Freixes M, Piñeiro-Yañez E, Montero-Conde C, Apellániz-Ruiz M, Calsina B, Mancikova V, et al. Pheoseq: A targeted next-generation sequencing assay for pheochromocytoma and paraganglioma diagnostics. *J Mol diagnostics: JMD*. (2017) 19:575–88. doi: 10.1016/j.jmoldx.2017.04.009

3. Ben Aim L, Pigny P, Castro-Vega LJ, Buffet A, Amar L, Bertherat J, et al. Targeted next-generation sequencing detects rare genetic events in pheochromocytoma and paraganglioma. *J Med Genet*. (2019) 56:513–20. doi: 10.1136/jmedgenet-2018-105714

4. Gimenez-Roqueplo AP, Favier J, Rustin P, Rieubland C, Crespin M, Nau V, et al. Mutations in the sdhb gene are associated with extra-adrenal and/or Malignant phaeochromocytomas. *Cancer Res*. (2003) 63:5615–21. Available online at: https://aacrjournals.org/cancerres/article/63/17/5615/510352/Mutations-in-the-SDHB-Gene-Are-Associated-with#related-urls.

5. Amar L, Baudin E, Burnichon N, Peyrard S, Silvera S, Bertherat J, et al. Succinate dehydrogenase B gene mutations predict survival in patients with Malignant pheochromocytomas or paragangliomas. *J Clin Endocrinol Metab*. (2007) 92:3822–8. doi: 10.1210/jc.2007-0709

6. Cui Y, Ma X, Wang F, Wang H, Zhou T, Chen S, et al. Differences in clinical manifestations and tumor features between metastatic pheochromocytoma/paraganglioma patients with and without germline sdhb mutation. *Endocrine practice: Off J Am Coll Endocrinol Am Assoc Clin Endocrinologists*. (2021) 27:348–53. doi: 10.1016/j.eprac.2020.09.015

7. Li C, Li J, Han C, Wang T, Zhang L, Wang Z, et al. Novel and recurrent genetic variants of vhl, sdhb, and ret genes in chinese pheochromocytoma and paraganglioma patients. *Front Genet*. (2023) 14:959989. doi: 10.3389/fgene.2023.959989

8. Ma X, Li M, Tong A, Wang F, Cui Y, Zhang X, et al. Genetic and clinical profiles of pheochromocytoma and paraganglioma: A single center study. *Front Endocrinol*. (2020) 11:574662. doi: 10.3389/fendo.2020.574662

9. Taïeb D, Nölting S, Perrier ND, Fassnacht M, Carrasquillo JA, Grossman AB, et al. Management of phaeochromocytoma and paraganglioma in patients with germline sdhb pathogenic variants: an international expert consensus statement. *Nat Rev Endocrinol*. (2024) 20:168–84. doi: 10.1038/s41574-023-00926-0

10. Crona J, Lamarca A, Ghosal S, Welin S, Skogseid B, Pacak K. Genotype-phenotype correlations in pheochromocytoma and paraganglioma: A systematic review and individual patient meta-analysis. *Endocrine-related Cancer*. (2019) 26:539–50. doi: 10.1530/erc-19-0024

11. Fishbein L, Ben-Maimon S, Keefe S, Cengel K, Pryma DA, Loaiza-Bonilla A, et al. Sdhb mutation carriers with Malignant pheochromocytoma respond better to cvd. *Endocrine-related Cancer*. (2017) 24:L51–l5. doi: 10.1530/erc-17-0086

12. Jawed I, Velarde M, Därr R, Wolf KI, Adams K, Venkatesan AM, et al. Continued tumor reduction of metastatic pheochromocytoma/paraganglioma harboring succinate dehydrogenase subunit B mutations with cyclical chemotherapy. *Cell Mol Neurobiol*. (2018) 38:1099–106. doi: 10.1007/s10571-018-0579-4

13. Liu C, Zhou D, Yang K, Xu N, Peng J, Zhu Z. Research progress on the pathogenesis of the sdhb mutation and related diseases. *Biomedicine pharmacotherapy = Biomedecine pharmacotherapie*. (2023) 167:115500. doi: 10.1016/j.biopha.2023.115500

14. Bayley JP, Bausch B, Jansen JC, Hensen EF, van der Tuin K, Corssmit EP, et al. Sdhb variant type impacts phenotype and Malignancy in pheochromocytoma-paraganglioma. *J Med Genet*. (2023) 60:25–32. doi: 10.1136/jmedgenet-2020-107656

15. Gill AJ. Succinate dehydrogenase (Sdh)-deficient neoplasia. *Histopathology*. (2018) 72:106–16. doi: 10.1111/his.13277

16. Gill AJ, Benn DE, Chou A, Clarkson A, Muljono A, Meyer-Rochow GY, et al. Immunohistochemistry for sdhb triages genetic testing of sdhb, sdhc, and sdhd in paraganglioma-pheochromocytoma syndromes. *Hum Pathol*. (2010) 41:805–14. doi: 10.1016/j.humpath.2009.12.005

17. Castelblanco E, Santacana M, Valls J, de Cubas A, Cascón A, Robledo M, et al. Usefulness of negative and weak-diffuse pattern of sdhb immunostaining in assessment of sdh mutations in paragangliomas and pheochromocytomas. *Endocrine Pathol*. (2013) 24:199–205. doi: 10.1007/s12022-013-9269-4

18. Pai R, Manipadam MT, Singh P, Ebenazer A, Samuel P, Rajaratnam S. Usefulness of succinate dehydrogenase B (Sdhb) immunohistochemistry in guiding mutational screening among patients with pheochromocytoma-paraganglioma syndromes. *APMIS: Acta pathologica microbiologica immunologica Scandinavica*. (2014) 122:1130–5. doi: 10.1111/apm.12269

19. Giubellino A, Lara K, Martucci V, Huynh T, Agarwal P, Pacak K, et al. Urinary bladder paragangliomas: how immunohistochemistry can assist to identify patients with sdhb germline and somatic mutations. *Am J Surg Pathol*. (2015) 39:1488–92. doi: 10.1097/pas.0000000000000534

20. Oudijk L, Gaal J, de Krijger RR. The role of immunohistochemistry and molecular analysis of succinate dehydrogenase in the diagnosis of endocrine and non-endocrine tumors and related syndromes. *Endocrine Pathol*. (2019) 30:64–73. doi: 10.1007/s12022-018-9555-2

21. Su T, Yang Y, Jiang L, Xie J, Zhong X, Wu L, et al. Sdhb immunohistochemistry for prognosis of pheochromocytoma and paraganglioma: A retrospective and prospective analysis. *Front Endocrinol*. (2023) 14:1121397. doi: 10.3389/fendo.2023.1121397

22. Kaplan AI, Dwight T, Luxford C, Benn DE, Clifton-Bligh RJ. Sdha related phaeochromocytoma and paraganglioma: review and clinical management. *Endocrine-related Cancer*. (2024). doi: 10.1530/erc-24-0111

23. Andrews KA, Ascher DB, Pires DEV, Barnes DR, Vialard L, Casey RT, et al. Tumour risks and genotype-phenotype correlations associated with germline variants in succinate dehydrogenase subunit genes sdhb, sdhc and sdhd. *J Med Genet*. (2018) 55:384–94. doi: 10.1136/jmedgenet-2017-105127

24. Mete O, Asa SL, Gill AJ, Kimura N, de Krijger RR, Tischler A. Overview of the 2022 who classification of paragangliomas and pheochromocytomas. *Endocrine Pathol*. (2022) 33:90–114. doi: 10.1007/s12022-022-09704-6

25. Hiramatsu K, Takahashi K, Kanemoto N, Arimori S. A case of pheochromocytoma with transient hyperinsulinemia and reactive hypoglycemia. *Japanese J Med*. (1987) 26:88–90. doi: 10.2169/internalmedicine1962.26.88

26. Fujino K, Yamamoto S, Matsumoto M, Sunada M, Ota T. Paraganglioma associated with hypoglycemia. *Internal Med (Tokyo Japan)*. (1992) 31:1239–41. doi: 10.2169/internalmedicine.31.1239

27. Uysal M, Temiz S, Gul N, Yarman S, Tanakol R, Kapran Y. Hypoglycemia due to ectopic release of insulin from a paraganglioma. *Hormone Res*. (2007) 67:292–5. doi: 10.1159/000099291

28. Frankton S, Baithun S, Husain E, Davis K, Grossman AB. Phaeochromocytoma crisis presenting with profound hypoglycaemia and subsequent hypertension. *Hormones (Athens Greece)*. (2009) 8:65–70. doi: 10.14310/horm.2002.1224

29. Habra MA, Núñez R, Chuang H, Ayala-Ramirez M, Rich T, Kyle K, et al. Fatal hypoglycemia in Malignant pheochromocytoma: direct glucose consumption as suggested by (18)F-2-fluoro-2-deoxy-D-glucose positron emission tomography/computed tomography imaging. *Endocrine*. (2010) 37:209–12. doi: 10.1007/s12020-009-9300-1

30. Altincik A, Ozen S, Celik A, Dokumcu Z, Darcan S, Abaci A, et al. Pediatric bilateral pheochromocytoma and experience of laparoscopic cortical sparing adrenalectomy. *J Pediatr Res*. (2018) 5. doi: 10.4274/jpr.87486

31. Martínez García M, Trincado Aznar P, López Alaminos ME, González Fernández M, Alvarado Rosas A, Laclaustra Gimeno M. Persistent hypoglycemia due to an igf-ii-secreting Malignant pheochromocytoma: A case report and literature review. *Clin Case Rep*. (2020) 8:2433–5. doi: 10.1002/ccr3.3161

32. Abdulhadi B, Anastasopoulou C, Lekprasert P. Tumor-induced hypoglycemia: an unusual case report and review of literature. *AACE Clin Case Rep*. (2021) 7:80–3. doi: 10.1016/j.aace.2020.11.002

33. Alnahas Z, Horani MH. Psun09 an unusual presentation of pheochromocytoma with persistent hypoglycemia, a case report. *J Endocrine Soc*. (2022) 6:A120. doi: 10.1210/jendso/bvac150.244

34. Sorlini M, Benini F, Cravarezza P, Romanelli G. Hypoglycemia, an atypical early sign of hepatocellular carcinoma. *J Gastrointestinal Cancer*. (2010) 41:209–11. doi: 10.1007/s12029-010-9137-0

35. Lau CI, Wang HC, Hsu WC. Hypoglycemic encephalopathy as the initial presentation of hepatic tumor: A case report. *Neurologist*. (2010) 16:206–7. doi: 10.1097/NRL.0b013e3181a6ec56

36. Bodnar TW, Acevedo MJ, Pietropaolo M. Management of non-islet-cell tumor hypoglycemia: A clinical review. *J Clin Endocrinol Metab*. (2014) 99:713–22. doi: 10.1210/jc.2013-3382

frontiers | Frontiers in Endocrinology

TYPE Case Report
PUBLISHED 11 April 2025
DOI 10.3389/fendo.2025.1494783

Check for updates

OPEN ACCESS

EDITED BY
Suja Pillai,
The University of Queensland, Australia

REVIEWED BY
Serena Martinelli,
University of Florence, Italy
Chiara Lopez,
University of Turin, Italy

*CORRESPONDENCE
Jing Xie
xj11559@rjh.com.cn

RECEIVED 12 September 2024
ACCEPTED 24 March 2025
PUBLISHED 11 April 2025

CITATION
Dai D and Xie J (2025) Metastatic pheochromocytoma complicated with Langerhans cell histiocytosis: a case report. *Front. Endocrinol.* 16:1494783. doi: 10.3389/fendo.2025.1494783

COPYRIGHT
© 2025 Dai and Xie. This is an open-access article distributed under the terms of the Creative Commons Attribution License (CC BY). The use, distribution or reproduction in other forums is permitted, provided the original author(s) and the copyright owner(s) are credited and that the original publication in this journal is cited, in accordance with accepted academic practice. No use, distribution or reproduction is permitted which does not comply with these terms.

# Metastatic pheochromocytoma complicated with Langerhans cell histiocytosis: a case report

Dandan Dai and Jing Xie*

Department of Pathology, Ruijin Hospital Affiliated to Shanghai Jiaotong University School of Medicine, Shanghai, China

Pheochromocytoma is a neuroendocrine neoplasm that originates from chromaffin cells of the adrenal medulla. Langerhans cell histiocytosis (LCH) is a proliferative disease of histiocyte-like cells, often associated with activating mutations of the mitogen-activated protein kinase (MAPK) pathway. We present a case of a 49-year-old male with a history of pheochromocytoma, which metastasized to the inferior vena cava eight years after left adrenalectomy. At the same time, it was found that the pheochromocytoma in the metastasis was complicated with LCH, a combination that has not been previously reported. Genetic analysis was carried out by next-generation sequencing (NGS) technology. Somatic mutations of *BRAF* and *RAD54B* were detected in Langerhans cells and *EPAS1* in pheochromocytoma.

KEYWORDS

**Langerhans cell histiocytosis, pheochromocytoma, metastasis, case report, EPAS1 gene**

## 1 Introduction

Pheochromocytomas are rare tumors originating in the adrenal medulla (1) and usually secrete catecholamines leading to hypertension and myocardial degenerative effects (2). Metastatic Pheochromocytoma is most commonly reported in the local lymph nodes, bone, liver and lung (3). Since it is impossible to differentiate non-metastatic and metastatic Pheochromocytoma based upon clinical or even histopathological findings, all Pheochromocytoma are currently considered potentially metastatic tumours (WHO 2022 classification) (4). As a result, all patients with Pheochromocytoma require long and intensive follow up. Pheochromocytoma mostly results from pathogenic variants of predisposing genes, with a genetic contribution that now stands at around 70%. Germline variants account for approximately 40%, while the remaining 30% is attributable to somatic variants (5). Langerhans cell histiocytosis (LCH), the most common histiocytic disorder, encompasses conditions characterized by aberrant function and differentiation or proliferation of cells of the mononuclear phagocyte system (6). LCH is a histiocytic neoplasm characterized by a mass of CD1a + CD207+ histiocytes, exhibiting a diverse range of clinical manifestations from a self-healing rash or single bone destruction to multi-organ disease with potentially fatal consequences (7). In this article, we present a

unique case of metastatic pheochromocytoma complicated with LCH. A 49-year-old male had undergone a left adrenalectomy in 2016 and pathology confirmed pheochromocytoma. In January 2024, the patient presented with intermittent low-grade fever, prompting a comprehensive examination that revealed a mass within the inferior vena cava. Elevated catecholamine levels were detected in both blood and urine. While high resolution CT showed multiple nodules in both lungs. The patient was considered to have multiple metastases of pheochromocytoma and a biopsy of the mass in the inferior vena cava was performed. The pathology confirmed metastatic pheochromocytoma complicated with LCH. Molecular pathology showed *EPAS1* mutation in pheochromocytoma. *BRAF* insertion mutation and *RAD54B* frameshift mutation was detected in in Langerhans cells. This report is, to our knowledge, the first case of pheochromocytoma coexisting with LCH, and also the primary report of detecting *RAD54B* mutation in LCH. It highlights the possibility of intravascular metastasis occurring simultaneously with LCH in patients with a previous history of pheochromocytoma even years after adrenalectomy and emphasizes the need to adopt a comprehensive next-generation sequencing (NGS) panel. According to the latest guidelines, it is mandatory to perform genetic analysis in all pheochromocytoma cases regardless of phenotype. Besides, We propose testing for *RAD54B* gene variants. A possible correlation between *RAD54B* pathogenic variants and LCH clinical course should be considered. For patients diagnosed with pheochromocytoma following surgical intervention, long-term blood pressure monitoring and regular follow-up are recommended to find recurrence or metastasis in time.

## 2 Clinical presentation

A 49-year-old man without specific family history presented with nocturnal episodic headaches in 2016. The headache lasted about 2 hours, accompanied by sweating, no obvious palpitation or dizziness. The patient presented at the local hospital with elevated blood pressure (specific value unknown). Urinary measurements demonstrated elevated level of vanillylmandelic acid at 15.28 mg/24h (normal range, 2-6 mg/24 h), while aldosterone and serum calcium remained within normal limits. Abdominal computed tomography revealed a left adrenal nodule approximately 6.1x4.5cm in size. On the basis of these findings, pheochromocytoma was suspected. In the same year, the patient underwent a left adrenalectomy. The headache and sweating recovered soon after operation. The pathology examination revealed the presence of pheochromocytoma with vascular invasion and capsular invasion(Figures 1A–C). Tumour cells were strongly immunopositive for synaptophysin (Figure 1D), chromogranin A (Figure 1E), SDHB (Figure 1F). Sustentacular cells were immunopositive for S100 protein(Figure 1G). Moreover, immunostains for AE1/AE3, CD56, CD34, Her2, Inhibin and HMB45 were negative (data not shown). Pheochromocytoma of the Adrenal Gland Scaled Score (PASS) of 4 was assigned and the Ki67 proliferation index was 1%. According to the guidelines for genetic

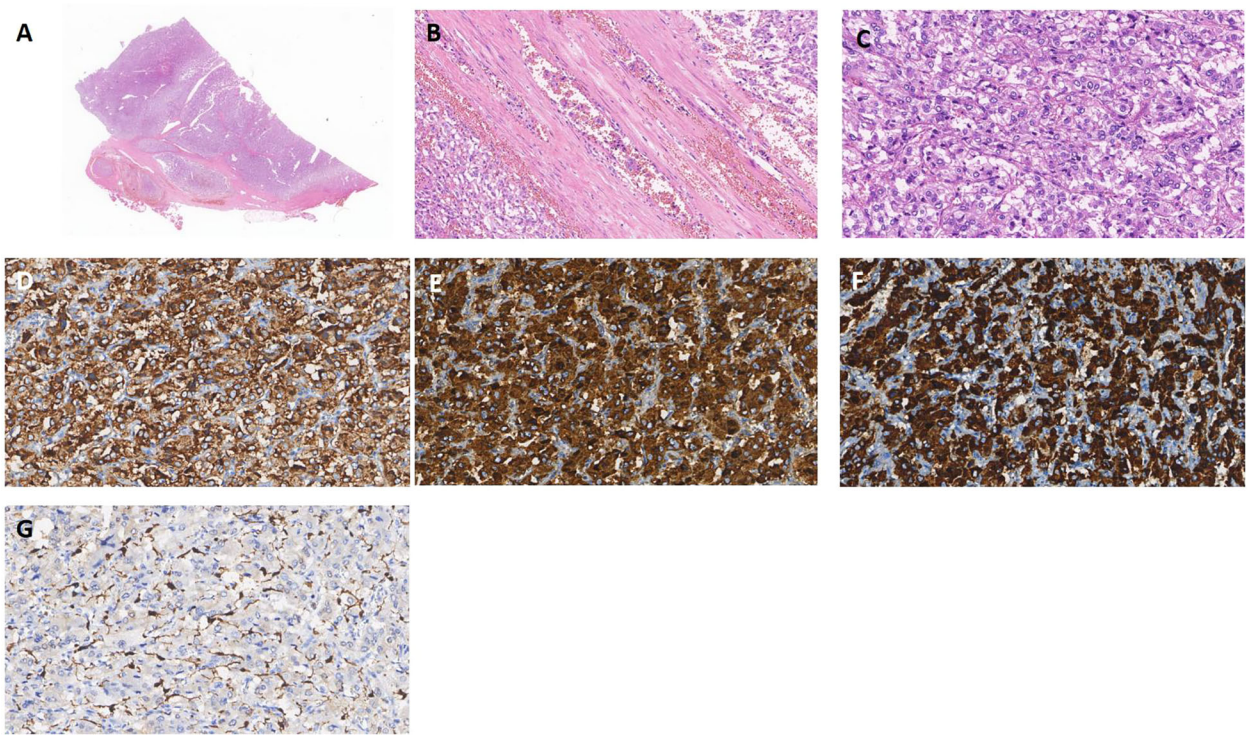


FIGURE 1
Pheochromocytoma **(A)** Pheochromocytoma with vascular invasion (x5 HE). **(B)** Intravascular tumor embolus (x100 HE). **(C)** Classic histoarchitecture with uniform cell nests(Zallballen)(x200 HE). **(D-F)** Syn, CgA and SDHB expression is positive, supporting the diagnosis of pheochromocytoma(x200). **(G)** Immunohistochemical stain for S100 showing classic distribution of sustentacular cells, mostly at the periphery of cell nests(x200).

screening of Pheochromocytomas and paragangliomas (PPGLs), our patient was proposed for next-generation sequencing (NGS) targeting. *EPAS1* mutation was detected in pheochromocytoma. No germline mutations were found. The patient was treated with antihypertensive medication resulting in blood pressure control within the normal range. After discharge, the patient has not been regularly followed up.

In January 2024, the patient developed intermittent low-grade fever. He received treatment at the local hospital for 2 days without improvement (specific details unknown). Abdominal color Doppler ultrasound showed foreign bodies in the inferior vena cava, while high resolution CT showed multiple nodules in both lungs. 68Ga-DOTATATE PET/CT scan(0.59mCi) was performed showing a soft tissue density mass in the left renal vein-inferior vena cava with abnormally high metabolism and multiple solid nodules in both lungs with slightly high metabolism. Combined with the medical history, the patient was considered to have tumor recurrence invading the inferior vena cava, along with multiple metastases in both lungs. The patient's low-grade fever resolved spontaneously after hospitalization and did not recur.

In March 2024, the patient came to the hospital for further examination. Laboratory tests revealed an elevated level of plasma normetanephrine at 5279.1 pg/ml (normal range, 19–121 pg/ml), while metanephrine remained within normal limits. Urinary measurements also revealed elevation levels of epinephrine at 22.57 ug/24h (normal range, <22ug/24h) and norepinephrine at 2290.15 ug/24h (normal range, 7-65ug/24h). Computed tomographic angiography of the abdominal aorta revealed the presence of a mass extending from the left renal vein to the inferior vena cava (Figures 2A–C). No obvious abnormality was found in the right adrenal gland. After two weeks of prophylactic treatment with alpha-blockers, a biopsy of the tumor in the inferior vena cava was conducted under local anesthesia. Pathology confirmed metastatic pheochromocytoma accompanied by LCH. Immunophenotyping of chromaffin cells was consistent with the primary lesion (Figures 2E, F). The pheochromocytoma area was accompanied by an adjacent region comprising of large monocytic cells with reniform-to-oval nuclei and a central horizontal groove, and plentiful of eosinophils (Figures 2D, G). The mononuclear cells revealed positivity for CD1a (Figure 2H), Langerin (Figure 2I) S100 and the Ki67 proliferation index was 10%. Molecular pathology identified the c.1457_1471del; p.N486_P490del mutation in the 12th exon of the *BRAF* gene, and the c.528dupT; p.V177Cfs*9 mutation in the 5th exon of the *RAD54B* gene. The patient underwent a 68Ga-DOTATATE PET/CT scan(0.59mCi). Multiple solid pulmonary nodules were found in both lungs, some of which had slightly higher metabolism. It may suggest the potential pulmonary metastasis from pheochromocytoma. The patient was recommended to undergo further diagnostic tests in order to

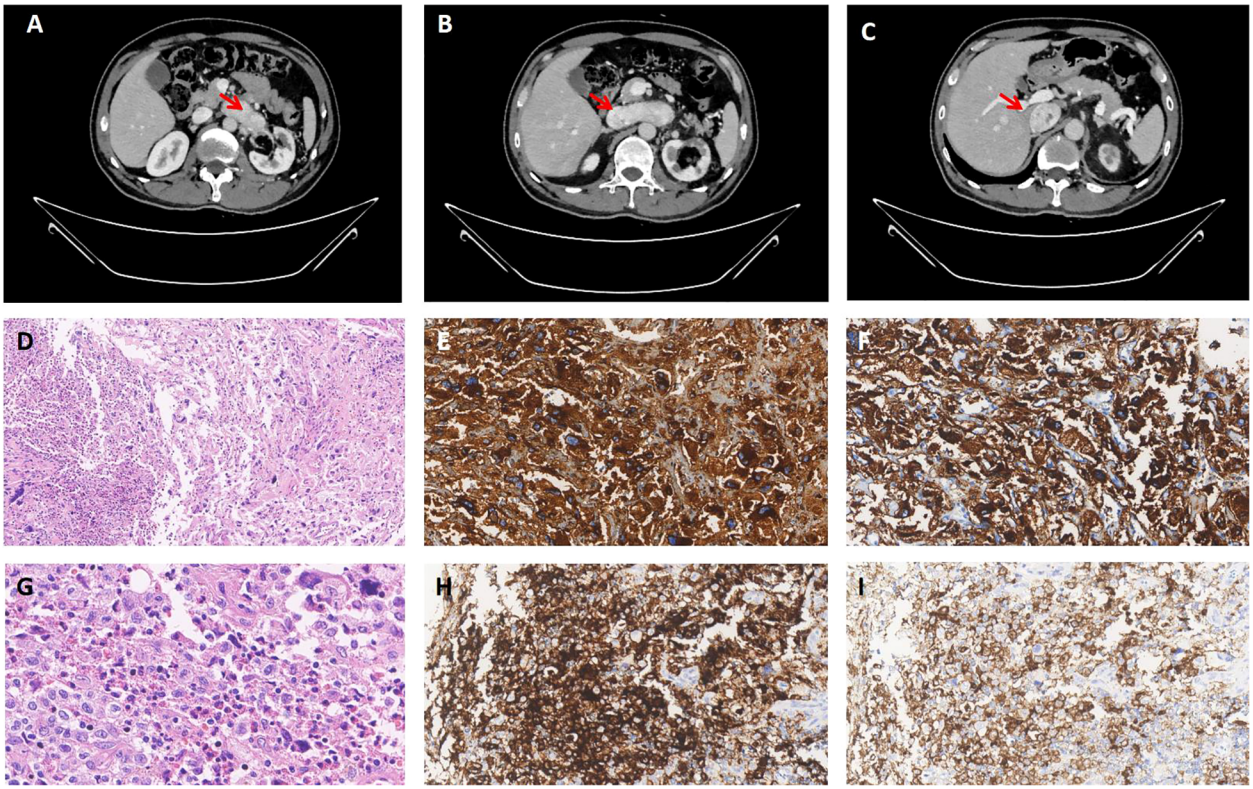


FIGURE 2
Computed tomographic angiography and pathological images. **(A-C)** The lumen of the left renal vein showed a soft tissue mass extending from its junction with the inferior vena cava, along the course of the inferior vena cava. The enhanced scan exhibited significant enhancement. Pheochromocytoma in metastasis. **(D)** The mononuclear cell area on the left side exhibits a significant presence of numerous eosinophils(x100 HE). **(E, F)** Pheochromocytoma expressing CgA and syn (x200). **(G)** The monocytic cells have reniform-to-oval nuclei and a central horizontal groove (x400 HE). **(H, I)** The mononuclear cells are positive for CD1a and Langerin (x200).

confirm the diagnosis. However, the patient expressed no intention to pursue additional investigations. Considering the difficulty of the operation, the patient postponed the operation and took antihypertensive treatment including doxazosin mesylate extended release tablets and arotinolol hydrochloride tablets. The 24-hour ambulatory blood pressure showed that systolic blood pressure and diastolic blood pressure were normal during the day and night after drug use. The circadian rhythm of systolic blood pressure and diastolic blood pressure disappeared. The 24-hour systolic blood pressure and diastolic blood pressure increased (120/77mmHg). After discharge, the patient's blood pressure was monitored and stabilized, and regular follow-up was requested. The clinical course is shown in Table 1.

## 3 Discussion

This case represents a rare complication of pheochromocytoma metastasizing to the inferior vena cava with concomitant LCH. The metastasis of pheochromocytoma to the inferior vena cava has not been reported. In this case *EPAS1*(*HIF2α*) mutation was detected. *EPAS1*has been identified as one of the susceptibility genes associated with Pheochromocytomas (8).

PPGLs are rare neuroendocrine tumors (NETs) derived from adrenomedullary chromaffin cells and from the autonomic paraganglia, respectively. Pheochromocytomas (PCCs) represent about 80–85% of chromaffin-cell neoplasms, whereas paragangliomas (PGLs) account for the remaining 15–20%. Based on transcriptional profile, PPGLs are classified into three clusters. The tree clusters are: 1) hypoxia/pseudohypoxia, 2) kinase signaling group, 3) Wnt signaling pathway (9). Cluster 1 includes PPGLs with variants in genes encoding the hypoxia-inducible factor (HIF) 2α, the Von Hippel–Lindau tumor suppressor (VHL), the prolyl hydroxylase domain (PHD), fumarate hydratase (FH), and succinate dehydrogenase subunits (SDHx) (10). All these mutations promote HIFa stabilization and accumulation resulting in increased angiogenesis via changes in vascular endothelial growth factor-1 and -2 receptors (VEGFR1/2) and platelet-derived growth factor-b receptor (PDGFR) transcription (11). Cluster 2 consists of germline or somatic mutations in RET, NF1, TMEM127, MAX, HRAS and KIF1Bβ which associated with PI3 kinase pathways the "PI3K/AKT/mTOR and MAPK/ERK". Cluster 2 PPGLs are mostly benign exhibiting a mature catecholamine phenotype (12). Cluster 3 PPGLs are due to somatic mutations of the CSDE1 gene or somatic gene fusions of the MAML3 gene (13). Cluster 3 tumors have a more aggressive behavior (5).

LCH is caused by clonal expansion of myeloid precursors that differentiate into CD1a+/CD207+ cells in lesions that leads to a spectrum of organ involvement and dysfunction (14). LCH is often characterized by activating mutations of the mitogen-activated protein kinase (MAPK) pathway with *BRAFV600E* being the most recurrent mutation. The remaining cases of LCH that do not bear the *BRAFV600E* mutation are often characterized by other mutations in the *BRAF* gene (15). *BRAF* mutations have been reported in >50% of patients with LCH (16). BRAF is a core component of the MAPK/ERK1/2 signaling cascade and involves the sequential phosphorylation and activation of RAS-RAF-MEK-ERK (17). In this case, molecular pathology identified the c.1457_1471del; p.N486_P490del mutation in the 12th exon of the *BRAF* gene, which is atypical.

Notably, for the first time, a somatic mutation in the oncogene *RAD54B* was identified in Langerhans cells. RAD54B belongs to the SNF2/SWI2 superfamily, involving in cell cycle regulation after DNA damage and participating in homologous recombinational repair, which ensures the precise repair of the most deleterious DNA lesions, double-stranded breaks (18). *RAD54B* displays oncogene-like characteristics and is amplified or overexpressed in a diverse array of cancer types, including colorectal, lung, prostate and breast (19). It has not been proven yet that *RAD54B* mutation is associated with LCH.

TABLE 1 Clinical timeline.

| Time | Diagnostic Findings | Treatment | Pathological Diagnosis |
|---|---|---|---|
| 2016 | - Elevated blood pressure (value unspecified) | Left adrenalectomy | Pheochromocytoma with intravascular tumor embolus and capsular invasion |
| | - Elevated urinary vanillylmandelic acid (VMA) | | |
| | - Left adrenal nodule (6.1×4.5 cm) on abdominal CT | | |
| January 2024 | - Foreign bodies in inferior vena cava (abdominal ultrasound) | N/A | N/A |
| | - Multiple bilateral lung nodules (high-resolution CT) | | |
| | - 68Ga-DOTATATE PET/CT: High-metabolism mass in left renal vein-IVC; lung nodules | | |
| March 2024 | - Elevated plasma normetanephrine and urinary epinephrine/norepinephrine | - Tumor biopsy | Metastatic pheochromocytoma with LCH (Langerhans cell histiocytosis) |
| | - IVC mass extending from left renal vein (CT angiography) | - Antihypertensive therapy | |

Tumorigenesis is a multiphase process dependent on several modifications at cellular and tissue levels, leading to sustain proliferative signalling, evasion from growth suppressors and from cell death, replicative immortality, and induction of angiogenesis, invasion, and metastasis (20). Beyond genetic alterations, the interplay among cancer cells and tumour microenvironment (TME) components has a central role in tumour initiation and progression (21). Angiogenesis, the development of new blood vessels from established vasculature, provides growth and hematogenous dissemination of the cancer cells. In this case EPAS1 mutation was detected in pheochromocytoma. EPAS1 mutation promotes HIFa stabilization and accumulation resulting in increased angiogenesis, which might enhance the likelihood of the formation and metastasis of other tumors, resulting in the coexistence of the two types of tumors.

More conclusive evidence is still required to ascertain whether there is a definitive correlation between pheochromocytoma and LCH concerning their pathogenesis. Currently, it remains uncertain whether this case represents a simple collision tumor or if it is an instance of LCH triggered by a pheochromocytoma. Due to the presence of multiple nodules in lungs, we were more inclined to suspect that the patient may have systemic LCH and recommended further examination. However, the patient did not cooperate. We recommend regular monitoring of blood pressure and periodic reviews for the patient.

Presently, clinical and hystopatological scoring systems have been studied and validated to assist in predicting the risk of disease recurrence. Parasiliti-Caprino et al. (22) conducted a retrospective multicenter study on 177 PCC patients who underwent radical surgery and proposed a multivariable continuous model for post-surgical PCC recurrence prediction. The model was named the SGAP-model (size, genetic, age, and PASS). It was created on an 8-point scale, by assigning 1 point for tumor size > 50 mm, 3 points for positive genetic testing, 1 point for age ≤ 35 years, and 3 points for PASS ≥ 3. Patients with a SGAP-score of 0-2 showed a virtually absent risk of recurrence; patients with a SGAP-score of 3-4 showed an intermediate risk profile; patients with a SGAP-score of 5-8 showed a markedly elevated risk of recurrence that exceeded 60% after 10 years. An accurate estimation of recurrence risk would be of fundamental importance in clinical practice, as it may allow clinicians to suggest a higher-intensity monitoring when the estimated recurrence risk is high.

## 4 Conclusion

In conclusion, the current case reminds us that pheochromocytoma can metastasize to the inferior vena cava. Due to its rare occurrence and non-specific clinical manifestations, imaging may still be the most valuable method for discovering metastasis. Pheochromocytoma accompanied by LCH has not been reported yet. This rare complication may indicate a potential relationship in the pathogenesis between the two. Whether *RAD54B* gene mutation is a pathogenic mutation of LCH needs to be further explored. Importantly, no pheochromocytoma can be considered fully benign and all patients should be followed for life for recurrence, new primary pheochromocytoma, and metastatic disease.

## Data availability statement

The original contributions presented in the study are included in the article/supplementary material. Further inquiries can be directed to the corresponding author.

## Ethics statement

Written informed consent was obtained from the individual(s) for the publication of any potentially identifiable images or data included in this article.

## Author contributions

DD: Writing – original draft. JX: Writing – review & editing.

## Funding

The author(s) declare that no financial support was received for the research and/or publication of this article.

## Acknowledgments

We are deeply grateful to Dr. Yinchun Jin for his expertise in histological section preparation. Special thanks to Dr. Zhongyu Wang for his insightful interpretation of molecular mechanisms. We also wish to acknowledge Dr. Xu Zhong for his invaluable assistance in clinical data curation.

## Conflict of interest

The authors declare that the research was conducted in the absence of any commercial or financial relationships that could be construed as a potential conflict of interest.

## Publisher's note

All claims expressed in this article are solely those of the authors and do not necessarily represent those of their affiliated organizations, or those of the publisher, the editors and the reviewers. Any product that may be evaluated in this article, or claim that may be made by its manufacturer, is not guaranteed or endorsed by the publisher.

# References


1. Farrugia FA, Charalampopoulos A. Pheochromocytoma. *Endocr Regul*. (2019) 53:191–212. doi: 10.2478/enr-2019-0020

2. Tischler AS, Kimura N, Mcnicol AM. Pathology of pheochromocytoma and extra-adrenal paraganglioma. *Ann New York Acad Sci*. (2006) 1073:557–70. doi: 10.1196/annals.1353.059

3. Angelousi A, Kassi E, Zografos G, Kaltsas G. Metastatic pheochromocytoma and paraganglioma. *Eur J Clin Invest*. (2015) 45:986–97. doi: 10.1111/eci.12495

4. Raleigh DR, Solomon DA, Lloyd SA, Lazar A, Garcia MA, Sneed PK, et al. Histopathologic review of pineal parenchymal tumors identifies novel morphologic subtypes and prognostic factors for outcome. *Neuro Oncol*. (2017) 19:78–88. doi: 10.1093/neuonc/now105

5. Provenzano A, Chetta M, De Filpo G, Cantini G, La Barbera A, Nesi G, et al. Novel germline PHD2 variant in a metastatic pheochromocytoma and chronic myeloid leukemia, but in the absence of polycythemia. *Med (Kaunas)*. (2022) 58:1113. doi: 10.3390/medicina58081113

6. Allen CE, Merad M, McClain KL. Langerhans-cell histiocytosis. *N Engl J Med*. (2018) 379:856–68. doi: 10.1056/NEJMra1607548

7. Li Q. Successful treatment of Langerhans cell histiocytosis in an infant with vemurafenib: a case report and literature review. *J Dermatol Treat*. (2023) 34:2279901. doi: 10.1080/09546634.2023.2279901

8. Buffet A, Burnichon N, Favier J, Gimenez-Roqueplo AP. An overview of 20 years of genetic studies in pheochromocytoma and paraganglioma. *Best Pract Res Clin Endocrinol Metab*. (2020) 34:101416. doi: 10.1016/j.beem.2020.101416

9. Crona J, Taïeb D, Pacak K. New perspectives on pheochromocytoma and paraganglioma: toward a molecular classification. *Endocr Rev*. (2017) 38:489–515. doi: 10.1210/er.2017-00062

10. Pacak K, Wimalawansa SJ. Pheochromocytoma and paraganglioma. *Endocr Pract*. (2015) 21:406–12. doi: 10.4158/EP14481.RA

11. Martinelli S, Amore F, Canu L, Maggi M, Rapizzi E. Tumour microenvironment in pheochromocytoma and paraganglioma. *Front Endocrinol (Lausanne)*. (2023) 14:1137456. doi: 10.3389/fendo.2023.1137456

12. Martinelli S, Maggi M, Rapizzi E. Pheochromocytoma/paraganglioma preclinical models: which to use and why? *Endocr Connect*. (2020) 9:R251–60. doi: 10.1530/EC-20-0472

13. Majewska A, Budny B, Ziemnicka K, Ruchała M, Wierzbicka M. Head and neck paragangliomas-A genetic overview. *Int J Mol Sci*. (2020) 21:7669. doi: 10.3390/ijms21207669

14. Rodriguez-Galindo C, Allen CE. Langerhans cell histiocytosis. *Blood*. (2020) 135:1319–31. doi: 10.1182/blood.2019000934

15. Sconocchia T, Foßelteder J, Sconocchia G, Reinisch A. Langerhans cell histiocytosis: current advances in molecular pathogenesis. *Front Immunol*. (2023) 14:1275085. doi: 10.3389/fimmu.2023.1275085

16. Whitlock JA, Geoerger B, Dunkel IJ, Roughton M, Choi J, Osterloh L. alone or in combination with trametinib, in BRAF V600-mutated pediatric Langerhans cell histiocytosis. *Blood Adv*. (2023) 7:3806–15. doi: 10.1182/bloodadvances.2022008414

17. Zhang W, Liu HT. MAPK signal pathways in the regulation of cell proliferation in mammalian cells. *Cell Res*. (2002) 12:9–18. doi: 10.1038/sj.cr.7290105

18. Mai Y, Lin T, Zhang L, Yang W, Liu S, Wang M, et al. RAD54B inhibits vascular endothelial senescence via suppression of CHK1/p53/p21 pathway. *Can J Physiol Pharmacol*. (2024) 102:137–49. doi: 10.1139/cjpp-2023-0192

19. McAndrew EN, McManus KJ. The enigmatic oncogene and tumor suppressor-like properties of RAD54B: Insights into genome instability and cancer. *Genes Chromosomes Cancer*. (2017) 56:513–23. doi: 10.1002/gcc.22458

20. Hanahan D, Weinberg RA. Hallmarks of cancer: The next generation. *Cell*. (2011) 144:646–74. doi: 10.1016/j.cell.2011.02.013

21. Shoucair I, Weber Mello F, Jabalee J, Maleki S, Garnis C. The role of cancerassociated fibroblasts and extracellular vesicles in tumorigenesis. *Int J Mol Sci*. (2020) 21:6837. doi: 10.3390/ijms21186837

22. Parasiliti-Caprino M, Bioletto F, Lopez C, Maletta F, Caputo M, Gasco V, et al. Development and internal validation of a predictive model for the estimation of pheochromocytoma recurrence risk after radical surgery. *Eur J Endocrinol*. (2022) 186:399–406. doi: 10.1530/EJE-21-0370

# Frontiers in Endocrinology

**Explores the endocrine system to find new therapies for key health issues**

The second most-cited endocrinology and metabolism journal, which advances our understanding of the endocrine system. It uncovers new therapies for prevalent health issues such as obesity, diabetes, reproduction, and aging.

---

## Discover the latest Research Topics

See more →

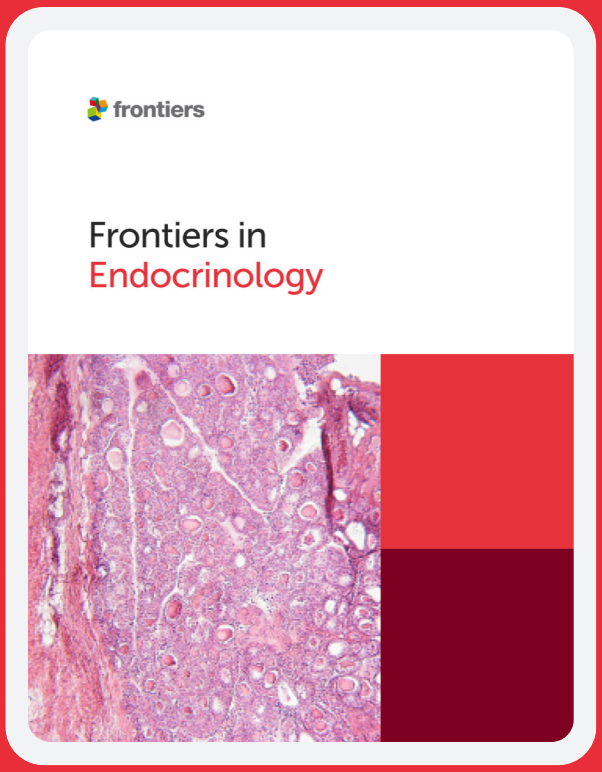


**Frontiers**

Avenue du Tribunal-Fédéral 34
1005 Lausanne, Switzerland
frontiersin.org

**Contact us**

+41 (0)21 510 17 00
frontiersin.org/about/contact